PETROLOGY AND GEOCHEMISTRY OF THE BASAL GABBRO UNIT, UITKOMST COMPLEX

THESIS
Submitted in partial fulfilment of the
requirements for the degree of
MASTER OF SCIENCE (ECONOMIC GEOLOGY)
in the Department of Geology,
Rhodes University

by

TOBY ANTHONY LAVERY STRAUSS

December 1995

The Cu/(Cu+Ni) ratios associated with the Basal Gabbro also display the vertical reverse fractionation trend, supporting the supercooled margin model. The disseminated sulphides in the lowermost units, are regarded as being the result of sulphur saturation induced by contamination from the dolomitic and quartzitic xenoliths. This is supported by isotope data which indicate the high degree of contamination in the lowermost units of the Complex.

The results of this study are used to propose a model for the petrogenesis and metallogenesis of the Uitkomst Complex, whereby the Complex is closely related to the Bushveld Complex. The Basal Gabbro, as supported by its chemistry and style of mineralisation (Cu-rich), represents a supercooled margin to the lowermost units of the Uitkomst Complex, which stoped upwards into the surrounding sediments, assimilating the country rock xenoliths, and precipitating sulphides. Following this was a period in which large quantities of magma moved laterally through the system before the magma flow waned, and closed sytem crystallisation ensued. As the body cooled, the primarily magmatic water was superceded by the hydrothermal magmatic water released from the xenoliths, and later by geothermally driven circulating meteoric water, producing the extensive alteration. This alteration was accompanied by considerable stress and the development of fractures and shears. Finally the Complex was itself intruded by diabase sills and later dolerite dykes.

Acknowledgements

I would like to thank the following people and organisations for their help and time througout the duration of this thesis:

1) The Anglovaal Group for providing the project and the sample material, as well as financing the expenses incurred in collecting the samples and data for this thesis.

2) My supervisor Prof. J.M. Moore, for his time and advice, as well as the interesting discussions throughout my time of study.

3) The geological staff of the Anglovaal Barberton Exploration office, particularly: Dr. Hennie Theart, Anton Lombaard, John Wilton, Tim Livessey, Lourens Erasmus, Kelly Redmond and Mauritz Van Den Berg, all of who provided invaluable geological information as well as a more than hospitable environment.

4) The technical staff of the Geology Department at Rhodes University for their help in sample preparation, particularly: John Hepple; Andre Visagie for XRF sample preparation; and Wilberforce Hashe and Bennet Bongwana for thin section preparations.

5) The geological staff of the Geology Department at Rhodes University for their help regarding the different facets of writing a thesis, particularly: Prof. R. Jacob, Prof. J.S. Marsh, C. Mallinson, and W. Morgan.

6) Dr. Derik De Bruiyne, of the University of the Free State, for his time and patience, whilst using the electron microprobe.

7) Gillian McGregor for the endless hours of work producing the maps.

8) My fellow students Henry Holland, Frans Slabber, Paulo Kerber, and Dave Mooney for help throughout the thesis ranging from discussions to sorting out computer problems.

9) My parents, whose support made this work possible.

Declaration

All work in this thesis is the original work of the author except where specific acknowledgement is made to the work of others.

No portion of this thesis, or the analytical data presented herein, may be reproduced or published without written permission of the author.

Date: 1/3/96

Signed: T. Strauss

T. Strauss

List of Contents

Petrology and Geochemistry of the Basal Gabbro Unit, Uitkomst Complex.

Chapter 1. Introduction

The Uitkomst Complex is situated on the Eastern Transvaal escarpment, 20 km north of Badplaas (Figure 1). The majority of the complex is located on two farms, Uitkomst 541 JT and Slaaihoek 540 JT, with the mineral rights owned by subsidiaries of Anglo American Corporation and the Anglovaal Group respectively. Since the early 1970's the Uitkomst Complex has been the subject of intensive phases of exploration drilling programs by both companies to determine the economic potential of its Ni-Cu-PGE ores. During the course of this study, in July 1995, a joint venture agreement was signed to further investigate and realise its potential.

The objective of this thesis, is to look at the petrology and the geochemistry of the basal unit (the Basal Gabbro), in order to determine its relationship with the rest of the Complex and attempt to gain an understanding of the Cu-Ni mineralisation associated with this unit.

The sample material for this thesis was provided by the Anglovaal Group, from the initial phase of drilling on the farm Slaaihoek 540 JT. This consists of 31 diamond drill boreholes, drilled along six traverses across the complex, approximately 500 metres apart (Figure 2). Within each traverse the borehole spacing was approximately 100 metres. For the purpose of this study, the logging and sampling of material has been limited to these initial boreholes, although observations from other boreholes will not be excluded. Six boreholes have been analysed for either their mineral chemistry (SH3), their whole-rock geochemistry (SH8, SH25, SH26 & SH27), or both (SH10). A further two boreholes (SH18 & SH19) were examined petrographically.

The Uitkomst Complex was first reported by Wagner (1929) as an altered pyroxenitic sill. Wagner (1929) recognised the economic potential of the Uitkomst Complex with respect to the Ni-Cu-PGE mineralisation. Since Wagner's initial report, nothing was published on the Uitkomst Complex until the paper by Kenyon *et al.* (1986), resulting from exploration undertaken on the farm Uitkomst 541 JT by the Anglo American Corporation of South Africa between 1970 and 1976. Unfortunately, the work by Kenyon *et al.* (1986) was limited by a failure to recognise that the stratigraphy encountered on the farm Uitkomst 541 JT is incomplete. Although several other authors (e.g. Sharpe *et al.* (1981) and Schürmann (1992)) have made reference to the Uitkomst Complex since Wagner's initial description, it is only recently that the first complete study of the Complex has been undertaken as the subject of a PhD by Gauert (submitted, 1995) at the University of Pretoria.

The Uitkomst Complex is a narrow elongate mafic - ultramafic body trending in a north-west direction, plunging approximately 8° to the north-west under the Eastern Transvaal escarpment (Figure 1). The exposed length of the Complex is approximately 8 km, and it's width is 1.1 km at its widest point. The north-western extensions of the Complex are as yet still unknown, being beneath the escarpment. Towards the south-east of the Complex, progressively lower litho-stratigraphic units have been exposed due to a combination of the plunge of the body and the local topography. A description of the overall geometry of the Uitkomst Complex is difficult to provide from mapping on the farm Slaaihoek 540 JT, due to limited outcrop. However, mapping by Gauert et al. (1995) of the exposed lower stratigraphic lithologies on the farm Uitkomst 541 JT, combined with borehole information from both properties, indicates that the Complex has a steers-head geometry in cross-section, with the lower part being broadly rectangular in shape, forming the "trough", and the upper part extending laterally in a funnel shape. The Complex has an approximate thickness of 850 metres, excluding later sills, which have increased the thickness of the Complex by approximately 100 metres.

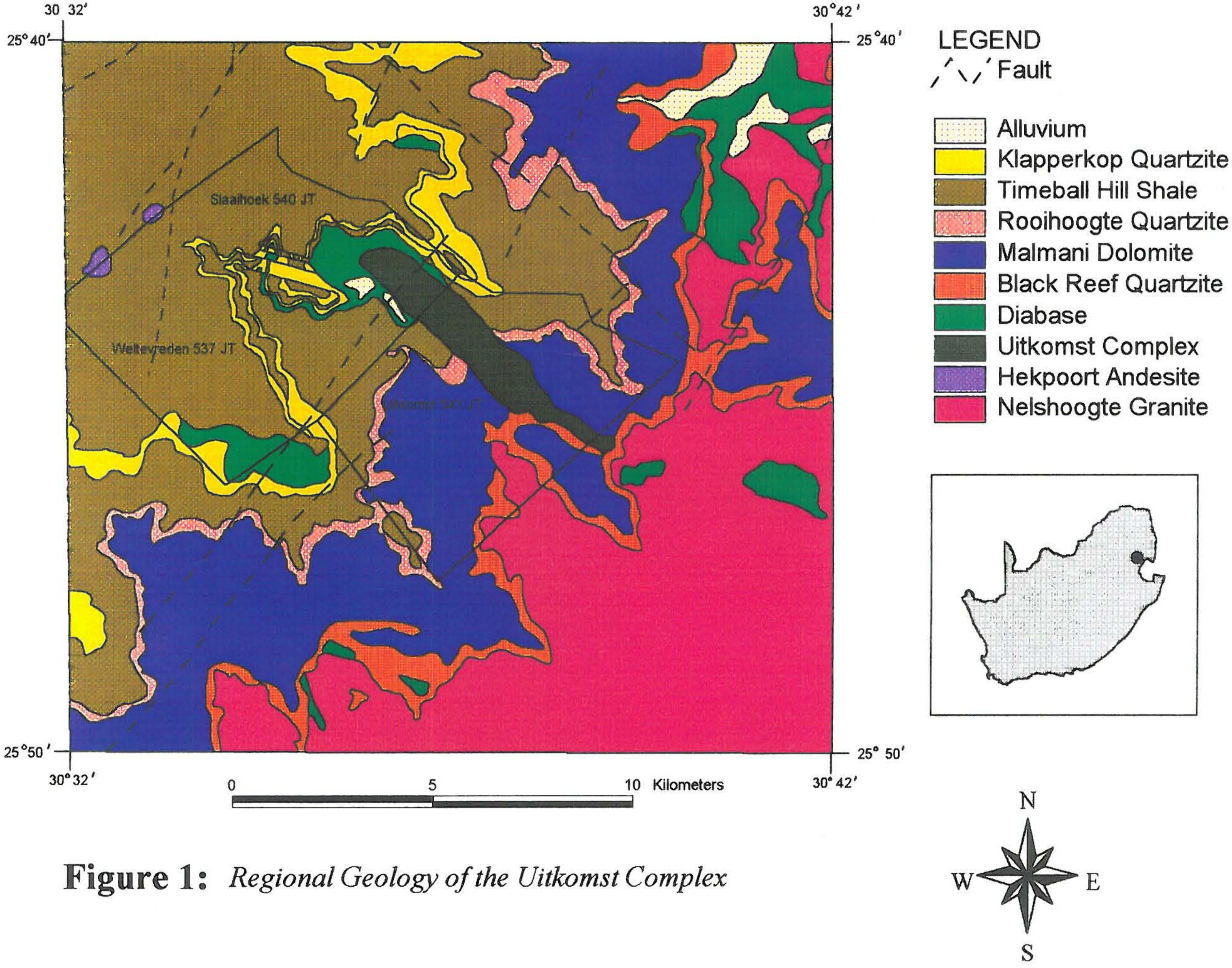

Figure 1: *Regional Geology of the Uitkomst Complex*

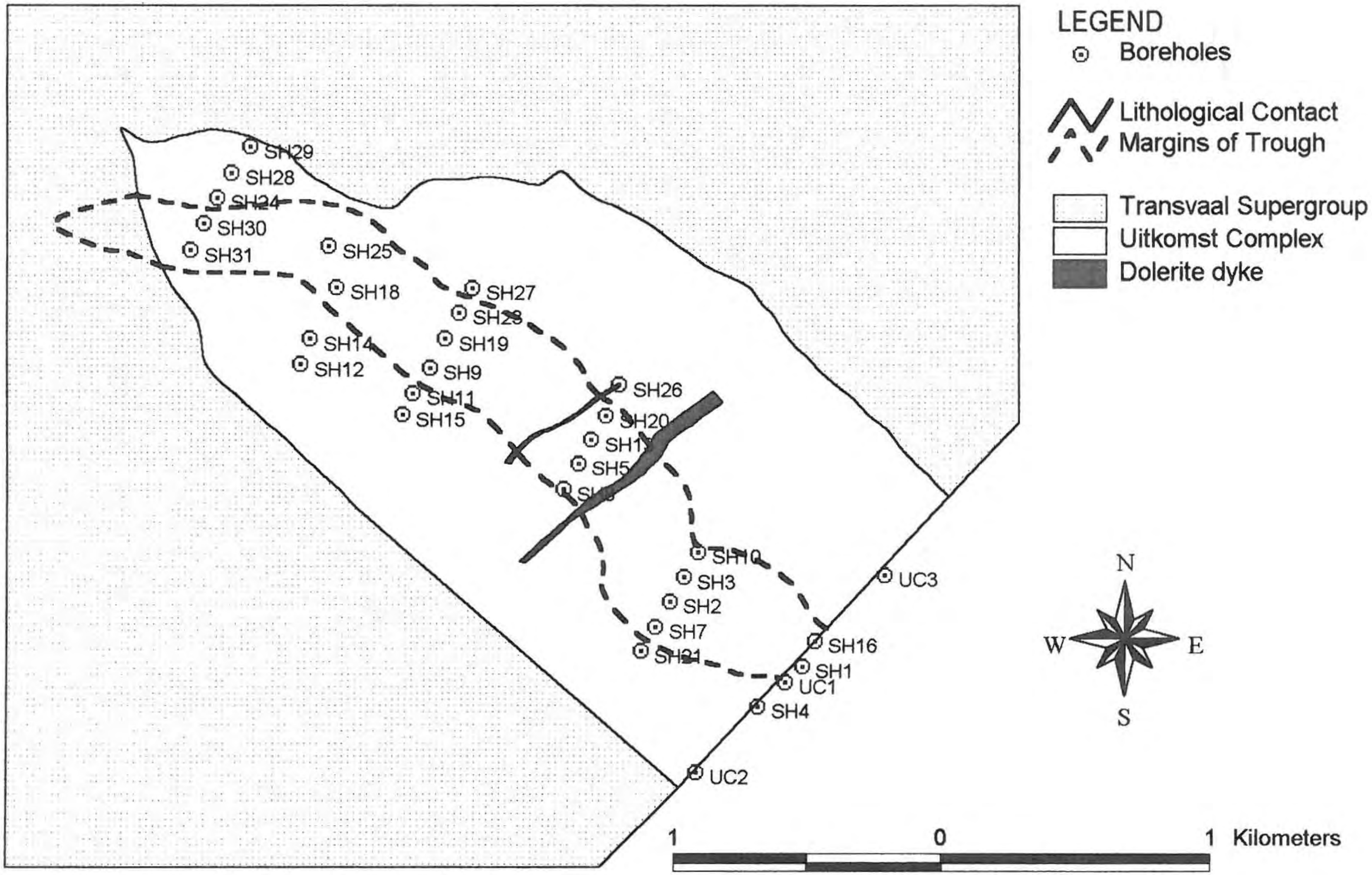

Figure 2: *The Uitkomst Complex on the farm Slaaihoek 540JT, with boreholes from the initial phase of drilling.*

Chapter 2. Regional Geology

The Uitkomst Complex was intruded into the Late Archaean - early Proterozoic sediments of the Transvaal Sequence, transecting quartzites of the Black Reef Formation, dolomites of the Malmani Subgroup, and lower Pretoria Group Shales. The base of the Complex is usually within the quartzitic and dolomitic sediments of the Malmani Subgroup, although related mineralisation is seen below the Complex in quartzites of the Black Reef Formation, and in the basement Nelshoogte Granite. The relevant stratigraphy of the region is shown in Figure 3.

Shale (thick)		**Timeball Hill Formation**	**Pretoria Group**	**Transvaal Supergroup**
Ferruginous quartzite				
Shale (graphitic?) (thin)				
Quartzite	Klapperkop Member			
Shale (thin)				
Quartzite				
Shale (thick)				
Diamictite	Bevets Member	**Rooihoogte Formation**		
Dolomite and chert		**Malmani Subgroup**	**Chuniespoort Group**	
Quartzite		**Black Reef Quartzite Formation**	**Wolkberg Group**	
Conglomerate				
Basement		**Nelshoogte Granite**		

Figure 3 *Stratigraphy of the country rocks in the region of the Uitkomst Complex. From Anglovaal (1993).*

2.1 Country Rocks

2.1.1 Nelshoogte Granite

The Nelshoogte Granite forms the Archaean basement in the region. It has been described as a pluton of biotite tonalitic gneiss, belonging to the Swazian Erathem with an age of older than 2,870 Ma (SACS, 1980).

2.1.2 The Transvaal Sequence

The Transvaal Sequence rests unconformably on the Nelshoogte Granite, with the basal unit being the Black Reef Quartzite Formation of the Wolkberg Group. As its name suggests the Black Reef Quartzite Formation is an arenaceous unit consisting of quartzite with lenses of grit and conglomerate. Within this Formation shale is always present particularly in the upper parts, close to the contact with the overlying dolomite, (SACS, 1980). The Black Reef Formation is preserved around the present day margins of the Transvaal basin, and has thicknesses of between a few metres and 30 m (Eriksson et al., 1993). The upper contact with the overlying dolomite is transitional and conformable (SACS, 1980), although in the region of study the contact appears to be represented by an unconformity.

Unconformably overlying the Wolkberg Group are the chemical sediments of the Chuniespoort Group. These consist of the dolomites and cherts of the Malmani Subgroup, which has been subdivided into five formations on the basis of their chert content as well as the presence or absence of algal structures in the dolomite (SACS, 1980). Overlying the dolomites are the Penge and Duitschland Formations consisting of iron-formations and chemical - clastic deposits respectively (Eriksson *et al.,* 1993). The Penge and Duitschland Formations are apparently absent from the stratigraphy of the Uitkomst region, again being represented by an unconformity.

The Pretoria Group unconformably overlies the chemical sediments of the Chuniespoort Group, the unconformity being angular and karstic (Eriksson *et al.,* 1993). The Pretoria Group consists predominantly of quartzite and shale together with prominent volcanic units (SACS, 1980). The basal Rooihoogte Formation contains the Bevets Conglomerate Member, as recognised in the Pilgrim's Rest goldfields (SACS, 1980). The highest stratigraphic rocks intruded by the Uitkomst Complex are the lower shales and quartzites of the Timeball Hill Formation. Numerous diabase and other basic sills are found at various levels in the Pretoria Group; these have been informally designated the Transvaal diabase (SACS, 1980). Hall (1932) has suggested that these sills are slightly older than the mafic-ultramafic rocks of the Bushveld Complex, which have been dated at approximately 2050 ± 22 Ma (Hamilton, 1977, recalculated by Von Gruenewaldt *et al.,* 1985). An age constraint of approximately 2600/2500 - 2050 Ma may be placed on the Transvaal Sequence (Eriksson *et al.,* 1993).

2.2 Rock Types and Field Relations of the Uitkomst Complex

The Uitkomst Complex is a narrow elongate mafic - ultramafic body trending in a north-west direction, plunging approximately 8° to the north-west under the Eastern Transvaal escarpment (Figure 1). The exposed length of the Complex is approximately 8 km, and it's width is 1.1 km at its widest point. The north-western extensions of the Complex are as yet still unknown, being beneath the escarpment. The cross-section of the Complex is understood to have a steers - head geometry, with the lower part being broadly rectangular in shape, forming the "trough", and the upper part extending laterally in a funnel shape (Figure 4). The Complex has an approximate thickness of 850 metres, excluding later sills, which have increased the thickness of the Complex by approximately 100 metres. Post-intrusive deformation is evident from steeply dipping faults, cutting across the body, causing displacement of tens of metres, and giving rise to graben- and horst-structures (Gauert *et al.*, 1995).

Initial dating of the Complex, carried out at the Bernard Price Institute of Geophysics, at the University of the Witwatersrand, using Rb-Sr techniques on selected biotite grains, gives an age of 2025 Ma (Allsopp, H.L., cited in Kenyon *et al.*, 1986). This can be compared to the Rustenburg Layered Suite of the Bushveld Complex, which has been dated by Rb-Sr techniques to be 2050 ± 22 Ma (Hamilton, 1977. recalculated by Von Gruenewaldt *et al.*, 1985), supporting the view that the Uitkomst Complex may be a satellite intrusion of the Bushveld Complex (Sharpe *et al.*, 1981; Kenyon *et al.*, 1986).

The Complex is generally subdivided into six lithological units, although the names for these vary across the properties. The variation in the names of the units are a result of the heterogeneity of the rock units in terms of their mineralogy and sub-layering, and the fact that intensive alteration has largely obscured their original mineralogy. Therefore for the purpose of this study the unit names used by Anglovaal (1993) will be adopted, although those used by Gauert *et al.* (1994) are shown in Table 1 for reference.

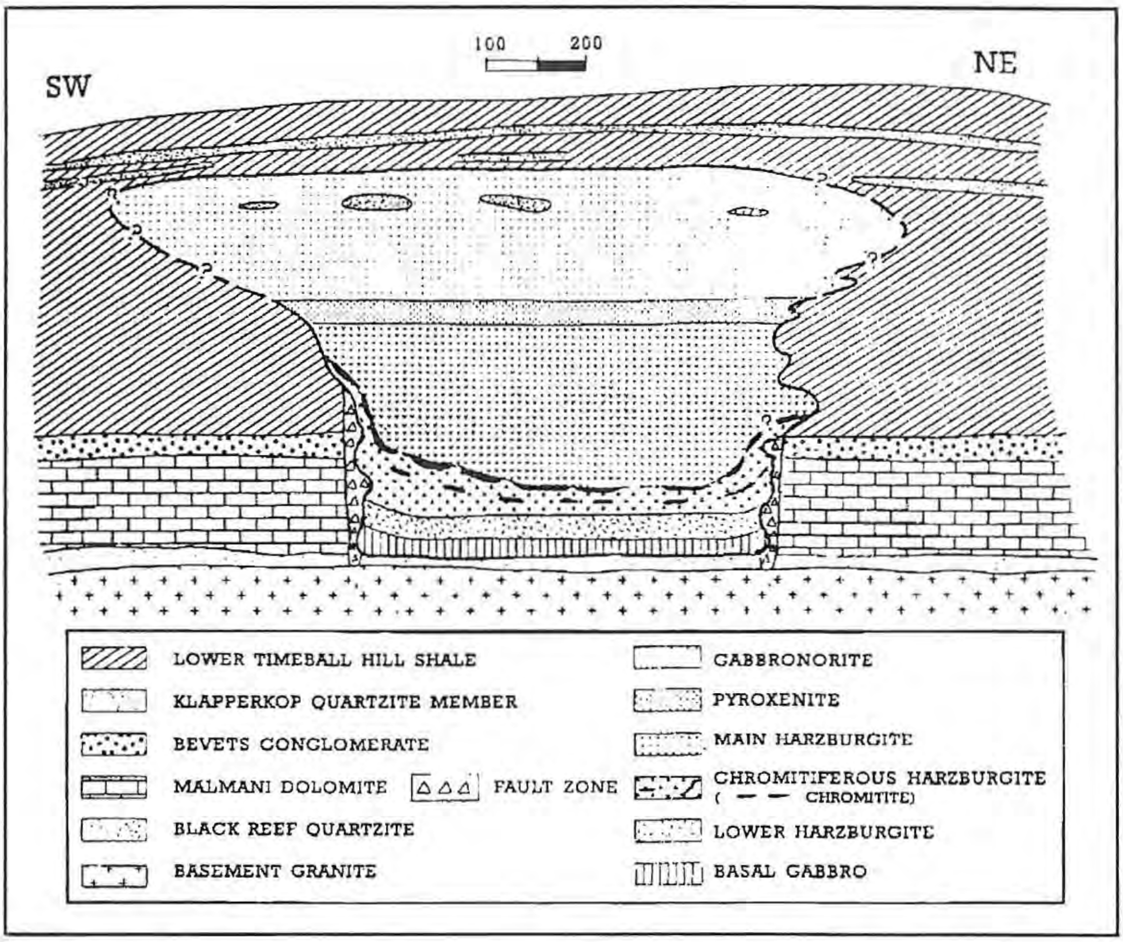

Figure 4 *Schematic cross section through the Uitkomst Complex. From Gauert et al. (1995).*

Slaaihoek (Anglovaal, 1993)	Uitkomst (Gauert *et al.*, 1994)
Norite zone	Gabbronorite
Upper Pyroxenite zone	Pyroxenite
Peridotite zone	Main Harzburgite
Chromititic Pyroxenite zone	Chromitiferous Harzburgite
Lower Pyroxenite zone	Lower Harzburgite
Basal Gabbro zone	Basal Gabbro

Table 1 *A comparison of the unit names for the lithological subdivision of the Uitkomst Complex*

2.2.1 Basal Gabbro

The Basal Gabbro is generally less than 12 metres thick (max. 30 metres) and is thickest and most continuous along the northern margin of the trough, whilst being only sparsely distributed along the southern margin. Initial drilling results from both Slaaihoek and Uitkomst (Kenyon *et al.*, 1986) indicated the lateral continuation of the Basal Gabbro away from the trough. This however, may be a function of the irregular nature of the contact between the rocks of the Complex with the sedimentary wall-rocks. This unit displays a marked basal chill against the floor rocks of the Complex, which are generally quartzitic or dolomitic sediments of the Malmani Subgroup. From underground exploration drives, the basal contact, at least locally, is undulatory and displays a sheared contact with the country rocks The upper contact with the Lower Pyroxenite is of a gradational nature and is frequently obscured by country rock xenoliths or later diabase sills, both of which are not uncommon in the Basal Gabbro. This unit is generally extensively altered and is well mineralised, commonly displaying a finely disseminated to dense net-texture of sulphides with a high copper content (Anglovaal, 1993). The petrology and mineralization will be examined in later sections.

2.2.2 Lower Pyroxenite

The Lower Pyroxenite (Lower Harzburgite) is compositionally and texturally very inhomogeneous, consisting of poorly layered peridotites and pyroxenites with an average thickness of 50 metres (max. 90 metres) (Gauert *et al.*, 1994). This unit has been extensively altered, consisting of remnants of pyroxene and olivine pseudomorphically replaced by large crystals of calcic amphibole (Kenyon *et al.*, 1986; Gauert *et al.*, 1994). Typical alteration minerals include amphibole (tremolite), sericite, chlorite, talc, serpentine and clinozoisite, with tremolite being the dominant mineral phase (Anglovaal, 1993; Gauert *et al.*, 1994). Xenoliths of dolomite and chert are common, displaying varying degrees of assimilation, with pegmatoidal rims of metamorphic-textured diopside and tremolite crystals (Gauert *et al.*, 1994). Gauert (1994) describes variations within this unit including a feldspar-rich lherzolite, grading into olivine-websterite with a high content of interstitial plagioclase, and a pegmatoid comprising feldspar and pyroxene crystals with sulphide filling the interstices.

This unit hosts the bulk of the mineralisation within the Complex, including the Main Mineralized Zone (MMZ). The mineralization has textures ranging from net-textured to large sulphide blebs, and often occurs as concentrations near xenoliths of country rocks (Kenyon *et al.*, 1986; Gauert *et al.*, 1994). The main opaque minerals are ilmenite, magnetite, chromite, pyrrhotite, rutile, chalcopyrite, pentlandite, digenite and pyrite (Gauert *et al.*, 1994).

2.2.3 Chromititic Pyroxenite

The Chromititic Pyroxenite zone (Chromitiferous Harzburgite) has an average thickness of 60 metres and comprises massive to semi-massive or disseminated lenses of chromitite alternating with bands of pyroxenite and peridotite (Gauert *et al.*, 1994; Kenyon *et al.*, 1986). This is a medium- to coarse-grained rock in which the silicates have been extensively altered to an amphibole - serpentine - talc - carbonate assemblage, and the chromitite bands display deformation "schlieren" textures. Carbonate - quartz veins are common in this unit (Gauert *et al.*, 1994).

2.2.4 Peridotite

The Peridotite zone (or Main Harzburgite) is typically 330 metres thick and macroscopically displays a rythmic layering (Gauert *et al.*, 1994). This rock is relatively homogeneous and is composed primarily of olivine chadacrysts (>50%) poikilitically enclosed by coarse-grained orthopyroxene oikocrysts (<40%) (Anglovaal, 1993). Chromite and sulphides (pyrrhotite and pentlandite), as well as intercumulus feldspar and phlogopite are interstitial and make up about 10% of the rock (Gauert *et al.*, 1994). This unit displays varying degrees of alteration, with the olivines being serpentinised, and the pyroxenes being altered to amphibole and chlorite (Anglovaal, 1993).

2.2.5 Upper Pyroxenite

The Upper Pyroxenite zone (or Pyroxenite) is approximately 60 metres thick and has gradational contacts with the Peridotite zone below and the Norite zone above (Gauert *et al.*, 1994). This unit consists of a medium-grained orthopyroxenite interlayered with thin peridotite layers. The contacts between the pyroxenites and peridotites are gradational. The pyroxenite is primarily composed of orthopyroxene (55%), with olivine (35%) and minor amounts of intercumulus feldspar, biotite and clinopyroxene (Anglovaal, 1993).

2.2.6 Norite

The Norite zone (or Gabbronorite) is approximately 250 metres thick and is composed or medium- to coarse-grained plagioclase (labradorite), orthopyroxene and clinopyroxene with interstitial amphibole and biotite. A mesostasis of quartz and feldspar is commonly developed (Gauert *et al.*, 1994; Anglovaal, 1993). This unit has a high content of xenoliths of quartzitic sediments, as well as various autoliths of rock types presumably derived from the layered suite (Anglovaal, 1993).

2.3 Diabase Sills

The Uitkomst Complex has itself been intruded by later diabase sills. Kenyon *et al.* (1986) claim that three major intrusive sills exist, which have spawned numerous secondary sills. The sills are medium- to coarse-grained with characteristic chills on their upper and lower boundaries, and are in sharp contact with the mafic - ultramafic rocks of the Complex. The external appearance of the sills is similar to that of the Basal Gabbro. Mineralogically, the diabases consist of amphibole (tremolite), feldspar, pyroxene, biotite and chlorite (Anglovaal, 1993). The amphibole is a product of the uralitisation of the pyroxenes. Some of the sills contain minor sulphides, probably as contamination from the Complex (Kenyon *et al.*, 1986).

2.4 Xenoliths

The Uitkomst Complex, especially the lower three units, contains a high amount of country rock xenoliths. These usually have characteristic rims of pegmatoid. Two main types of xenolith are encountered in the Complex: one type is dolomitic, frequently showing their original banded nature, whilst the second type consists of fine-grained quartzites or chert. These xenoliths are most likely to be derived from the dolomites of the Malmani Subgroup.

2.5 Massive Sulphides

The country rocks to the Uitkomst Complex are frequently host to massive sulphide mineralisation. This is locally developed and is usually situated in the immediate footwall of the Complex, forming a layer between the Basal Gabbro and the sediments of the Malmani Subgroup. However, significant occurrences of massive sulphides have been found below the Malmani sediments in the Black Reef Quartzite Formation and even within the Nelshoogte Granite. The massive sulphide mineralisation is characterised by a pyrrhotite-rich assemblage.

Chapter 3: Petrography

3.1 Basal Gabbro

The Basal Gabbro, as previously mentioned, has been extensively altered by late- to post-magmatic processes. Of the boreholes available for this study, borehole SH10 is the least altered, and hence best shows the primary magmatic features of this unit. For this reason the bulk of the petrography is taken from borehole SH10, although information from other boreholes is included.

The primary mineralogy of the Basal Gabbro includes plagioclase, orthopyroxene, clinopyroxene, phlogopite, magnetite, ilmenite, and the sulphides pyrrhotite, chalcopyrite and pentlandite. Any estimation of modal proportions will have a strong overprint of the alteration mineralogy, and hence be highly dependent on the extent of the alteration. However, although many of the primary minerals have been altered, those remaining at least give an indication of the relative original proportions. The feldspar, although saussuritized, remains roughly at its original proportion of approximately 40 - 50 % of the rock. The pyroxenes, being highly susceptible to uralitization and chloritization will have greatly reduced proportions. Common values are in the range of 5 - 15 % for both ortho- and clinopyroxenes, although some sections have been so altered that none are identifiable. If it is assumed that all the amphibole is secondary then the pyroxenes could account for 50 - 60 % of the rock in total. Therefore, according to Streckeisen's (1976) classification of igneous rocks (Figure 5), the Basal Gabbro can be classified more correctly as a gabbronorite. However, this classification has been based upon an incomplete mineral assemblage due to the alteration and hence is only an indication of the initial rock type.

As mentioned earlier, the Basal Gabbro displays a marked chill towards the base of the unit, where it is in contact with the sediments of the Malmani Subgroup. This chill zone in thin section SH10-9 (409.40 m) is a fine-grained rock with grain sizes averaging 0.5 mm (Plate 1). The pyroxenes (both clino- and orthopyroxene) show euhedral to subhedral crystal shapes (Plate 2). Biotite and apatite occur as late-stage phases filling the voids between the plagioclase laths and the pyroxenes. The brown colour of the biotite suggests a high Ti content (Deer *et al*, 1992). The pyroxenes are with the exception of opaques, inclusion free (Plate 3). This section, presumably because of its fine grain size is only mildly altered. From this essentially aphanitic hornfelsic base the grain size increases upwards until it attains average sizes of 1 mm in thin section SH10-8 (408.60 m). This section is at the uppermost part of the "quench" zone. Alteration (saussuritisation and uralitisation) of the rock is more extensive than in thin section SH10-9, although some patches are more altered than others. The pyroxenes are subhedral and often surrounded by a rim of carbonate. One clinopyroxene grain is seen to have an inclusion of orthopyroxene (Plate 4), suggesting that fractional crystallisation, rather than rapid quenching is commencing. Frequently a rim of small opaque crystals is seen around biotite grains (Plate 5), especially along the contact with amphiboles (altered pyroxenes). This basal chill is about 1 metre thick, and shows increasing alteration upwards.

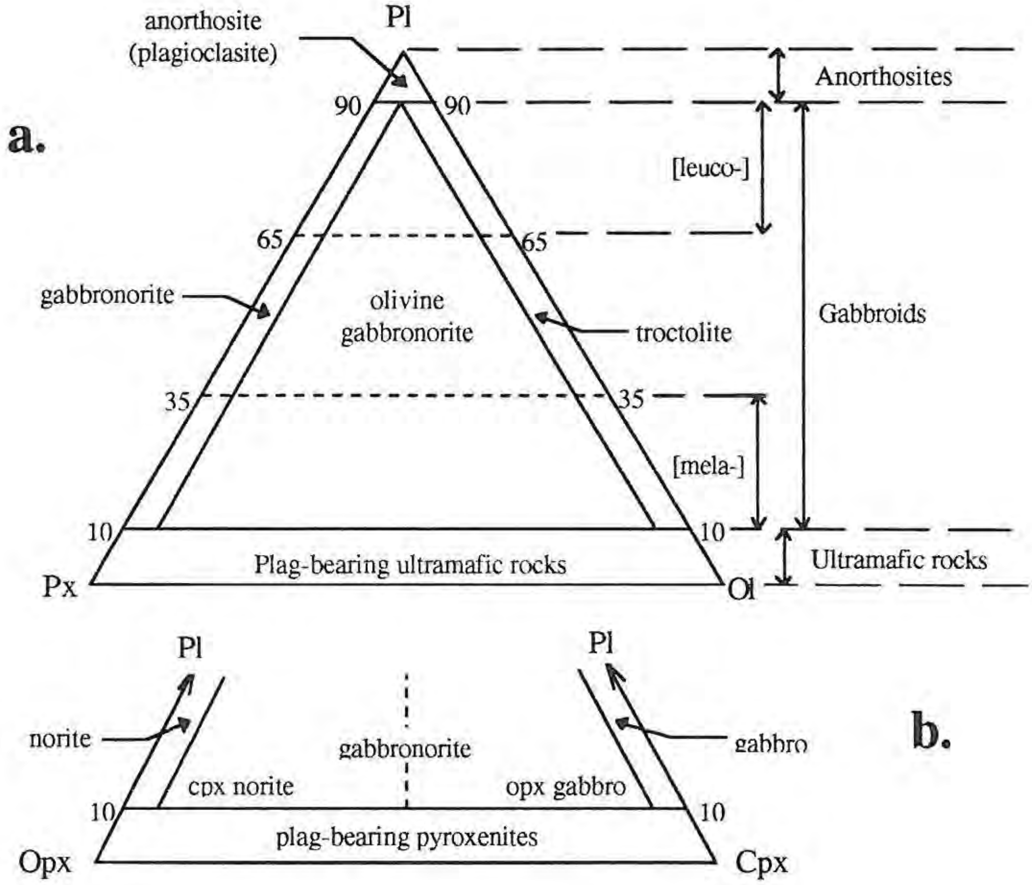

Figure 5. *Classification and nomenclature of gabbroic rocks.*
a. *Gabbroic rocks composed of plagioclase, pyroxene, and olivine.*
b. *Subdivision of gabbroic rocks into gabbro, gabbronorite (opx gabbro and cpx norite), and norite*
From Streckeisen (1976).

Thin sections SH10-7 (407.20 m), SH10-6 (405.50 m) and SH10-5 (404.80 m) show a progressive increase in the opaque content. This increase in proportion is also matched by an increase in the grain size of the opaques from a maximum of 0.5 mm in thin section SH10-7 to over 1 mm in thin section SH10-5. The opaques are frequently associated with biotites (Plate 6), suggesting that they have precipitated together in the interstices between the pyroxenes and feldspars. The alteration in these sections is more pervasive than in the basal chill, often with the total replacement (uralitisation) of pyroxenes by amphiboles. Two types of amphibole can be recognised in thin section, one being a hornblende and the other having an acicular tremolitic or actinolitic appearance. The Basal Gabbro displays a well developed intergranular texture, frequently with a mesostasis of quartz and feldspar (Gauert *et al.*, 1995) (Plates 7 & 8). The ophitic texture described by Gauert *et al.* (1995), is not seen in the sections examined, with no optical continuity between adjacent interstitial grains.

In thin section 10-4 (404.07 m) which is 6 cm beneath a dolomite xenolith, the texture and mineralogy of the rock is markedly different, and represents an alteration rim around the xenolith (Plate 9). This will be discussed in more detail in a later section. Above the xenolith in thin section 10-3 (403.43 m), which is below a quartzite xenolith on the Lower Pyroxenite contact, the rock is highly altered (Plate 10). The major mineral components are amphiboles, feldspars and carbonate, with net-textured blebs of opaques. Thin section 10-2 (403.20 m) displays the effects of highly intensive alteration with the development of clinozoisite (Plate 11), produced by the breakdown of plagioclase and mica.

3.2 Alteration

As mentioned previously the Basal Gabbro has been extensively altered by late- to post-magmatic processes. The alteration products include amphiboles, saussurite, and chlorite. Uralitisation is the most obvious of the alteration processes with the formation of amphibole from the breakdown of pyroxenes. Two main amphiboles are recognisable in thin section, hornblende and an acicular tremolitic or actinolitic variety (Plate 11). The amphiboles can be seen to pseudomorphically replace the pyroxenes, most frequently resulting in total replacement. However in sections where the alteration is less pervasive, various stages of this process can be seen, with the preservation of relicts of pyroxene (Plates 12 to 16). Uralitisation is the process whereby anhydrous pyroxenes are hydrated during deuteric alteration, to form amphiboles, proceeding first as follows (Deer *et al.*, 1978):

$$\underbrace{3(Mg,Fe)SiO_3}_{\text{orthopyroxene}} + \underbrace{Ca(Mg,Fe)Si_2O_6}_{\text{diopside}} + \underbrace{NaAlSi_3O_8 + CaAl_2Si_2O_8}_{\text{plagioclase}} + H_2O$$

$$\Leftrightarrow \underbrace{NaCa_2(Mg,Fe)_4Al_3Si_6O_{22}(OH)_2}_{\text{hornblende}} + \underbrace{4SiO_2}_{\text{quartz}}$$

This reaction is responsible for producing the hornblende-type amphiboles. Another reaction produces the acicular actinolitic amphiboles as follows (Deer *et al.*, 1978):

$$\underset{\text{pyroxene}}{10Ca(Mg,Fe)Si_2O_6} + \underset{\text{anorthite}}{CaAl_2Si_2O_8} + 5H_2O \Leftrightarrow \underset{\text{actinolite}}{(OH)_2Ca_2(Mg,Fe)_5Si_8O_{22}}$$

$$+ \underset{\text{chlorite}}{(OH)_8(Mg,Fe)_5Al_2Si_3O_{10}} + 9CaO + \underset{\text{quartz}}{11SiO_2}$$

Saussuritisation is the term given to the deuteric alteration of plagioclase feldspar. It is characterised by the replacement of plagioclase by a fine-grained aggregate of zoisite, epidote, albite, calcite, sericite and zeolites (Bates & Jackson, 1980). In the Basal Gabbro, and indeed in the whole Complex, this is a very common alteration process, resulting in the murky appearance of feldspars in thin section (Plates 10, 12 & 13). Several of the reactions involved in the saussuritisation of plagioclase are given below (Colvine *et al.*, 1988):

$$\underset{\text{plagioclase}}{3(Ca,Na)Al_2Si_2O_8} + CO_2 + \tfrac{1}{2}H_2O \rightarrow \underset{\text{epidote}}{Ca_2Al_3Si_3O_{12}(OH)} + \underset{\text{albite}}{3NaAlSi_3O_8} + \underset{\text{calcite}}{CaCO_3} + 2\tfrac{1}{2}O_2$$

$$\underset{\text{albitc}}{NaAlSi_3O_8} + K^+ + 2H^+ \rightarrow \underset{\text{scricitc}}{KAl_3Si_3O_{10}(OH)_2} + \underset{\text{quartz}}{6SiO_2} + 3Na^+$$

The effect of the numerous dolomite xenoliths is economically of significance, as they may have played a large role in the generation of the base metal sulphides. Thin section 10-4 (404.07 m) is situated 6 cm beneath a xenolith of Malmani dolomite. Mineralogically the pyroxenes in this section have a different composition to typical pyroxenes within the Basal Gabbro (see chapter 4), being diopsidic (clinopyroxenes) and having higher enstatite contents (orthopyroxenes). In thin section the pyroxenes are larger, and where unaltered have a fresher appearance (Plate 17). However, they have been intensely serpentinised, with serpentinisation consisting of an anastomosing network of veinlets of serpentine and magnetite being concentrated along fractures (Plate 18). The orthopyroxenes alter to serpentine as follows (Winkler, 1976):

$$\underset{\text{orthopyroxene}}{6MgFeSi_2O_6} + 2H_2O \rightarrow \underset{\text{serpentine}}{Mg_3Si_2O_5(OH)_4} + \underset{\text{magnetite}}{Fe_3O_4} + \underset{\text{quartz}}{SiO_2}$$

The mineral assemblage of pyroxene (esp. diopside), quartz, calcite, phlogopite, talc, and serpentine associated with the proximity of dolomite xenoliths (Plates 19 & 20), is also commonly associated with the development of magnesian skarns (Meinert, 1992). In many skarns there is a transition from early/distal metamorphism resulting in hornfels, reaction skarn, and skarnoid, to later/proximal metasomatism resulting in relatively coarse-grained, ore-bearing skarn (Meinert, 1992). In the case of the interaction between dolomite xenoliths and the magma, one would expect to see the products of proximal metasomatism, with the fluids and volatiles being derived largely from the xenolith. This is indeed the case with the development of the characteristic pegmatoid rim around the dolomite xenolith consisting of coarse-grained pyroxenes, plagioclase and phlogopite. Elsewhere in the stratigraphy, in proximity to xenoliths, the author has logged the presence of red vesuvianite. Typical reactions which may be expected to take place include the following (Winkler, 1976):

3 dolomite + 4 quartz + 1 H_2O —> 1 talc + 3 calcite + 3 CO_2
5 dolomite + 8 quartz + 1 H_2O —> 1 tremolite + 3 calcite + 7 CO_2
1 dolomite + 2 quartz —> 1 diopside + 2 CO_2

Although these are only a few of the many reactions taking place in a skarn environment, they show how diopside, tremolite, calcite and CO_2 are produced. These reactions also show that the source of the calcite which is ubiquitous in the rocks with a high xenolith component (e.g. Lower Pyroxenite) is from reaction with the dolomite xenoliths. The effect of the magma - xenolith reactions on sulphide precipitation will be discussed in a later section.

The presence of the sulphides in the skarn zone (Plate 21), although only minor, is further evidence for the importance of the xenoliths in ore formation. These skarn zones also display evidence of retrograde alteration (as discussed above), with the production of hydrous phases such as amphibole and chlorite. A more detailed examination of the effect of the xenoliths on the magma, in terms of mineralogy and sulphide precipitation is beyond the scope of this project, requiring detailed microscopy as well as microprobe, isotope and fluid inclusion analyses of the skarn minerals.

The most plausible explanation for the extensive alteration of the Basal Gabbro, is that with the cooling of the Complex, meteoric water from the surrounding country rocks began to circulate and invade the intrusion, being driven by the heat of the complex. This was combined with the high water and volatile content of the magma itself derived from the assimilation of xenoliths and wall rocks whilst being transported and emplaced into its present position.

3.3 Mineralisation

The mineralisation of the Basal Gabbro consists primarily of the sulphides pyrrhotite, chalcopyrite and pentlandite, and the oxides magnetite and ilmenite. Noticeably absent from the Basal Gabbro are grains of chromite. The relative proportions of the various sulphides are:

pyrrhotite > chalcopyrite > pentlandite

The sulphides are interstitial to the silicate phases and vary from being disseminated, accounting for less than 1% of the rock, to being net-textured (Plate 22) and locally constituting over and above 20% of the rock. Pentlandite is an exsolution product from the pyrrhotite, and commonly occurs as flame-like exsolution bodies (Plate 23), extending from fractures and grain boundaries into the pyrrhotite parallel to {0001} (Ramdohr, 1980). Other occurrences of pentlandite are as aggregates occurring along fractures in pyrrhotite and at grain boundaries, especially between pyrrhotite and chalcopyrite (Plate 24). These aggregates are frequently up to 0.2 mm in size. Chalcopyrite is commonly seen both as inclusions in pyrrhotite (Plates 25 & 27), as well as replacing pyrrhotite (Plate 26). The inclusion of chalcopyrite in pyrrhotite is a feature reportedly only occurring in high-temperature magmatic rocks which have been cooled fast (Ramdohr, 1980).

Magnetite is present in two forms, firstly as a primary mineral of "titanomagnetite" usually forming discrete grains with ilmenite exsolution lamellae in a magnetite host (Plate 28). It is also present as a secondary product, enclosing all the other opaque minerals, pyrrhotite, chalcopyrite, pentlandite and ilmenite (Plate 29). Ilmenite also occurs as discrete grains, probably produced from the exsolution from magnetite, but possibly also occurring as a primary crystallising phase from the magma. The "pseudo-exsolution" of ilmenite in chalcopyrite (Plate 24) is most likely caused by the ilmenite exsolving from a titanomagnetite, whose magnetite portion has been totally replaced by chalcopyrite (Ramdohr, 1980). In the more altered rocks ilmenite also remains as skeletal rods with the magnetite having been totally replaced. (Plates 30 & 31). The volume formerly occupied by the magnetite, is often rendered semi-opaque by the presence of an extremely fine-grained brown substance, which is probably a hydrated Fe-oxide (Elsdon, 1982). Ilmenite also occurs with inclusions of pyrrhotite and chalcopyrite, suggesting that it is replacing these minerals (Plates 32 & 33). The paragenesis of the various opaques is shown below in Figure 6.

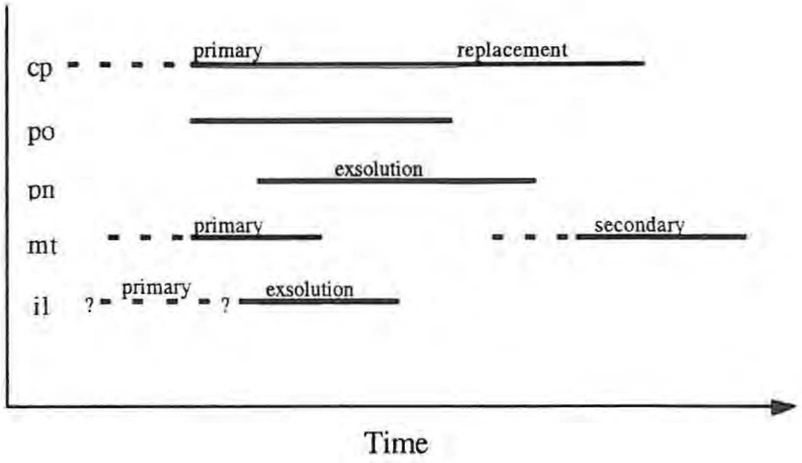

Figure 6. *The paragenetic sequence for the opaque minerals from the Basal Gabbro. cp = chalcopyrite, po = pyrrhotite, pn = pentlandite, mt = magnetite, il = ilmenite*

3.4 Lower Pyroxenite

The Lower Pyroxenite is a highly variable and inhomogeneous unit, and a complete petrographic description is beyond the requirements and the scope of this project. However, for completeness the basal part of the Lower Pyroxenite in borehole SH10, above the dolomitic and quartzitic xenoliths, will be briefly examined. Thin section 10-1 (401.10 m) which is situated above the quartzite xenolith on the contact with the Basal Gabbro, is extensively altered, with intense uralitisation, serpentinisation and chloritisation. This section is also characterised by the development of corona textures (Plates 34 & 35). These consist of pseudomorphs of pyroxene (or olivine) that have been totally replaced by talc, and surrounded by a rim of chlorite. The pseudomorphs themselves are separated by bands of serpentine.

3.5 Diabase Sills

The diabase sills are medium-fine grained rocks (Plate 36), with the majority of minerals being less than 1 mm in size, although plagioclase laths occur with lengths up to 2 mm. The main minerals are plagioclase, amphibole (hornblende), biotite and opaque minerals, with minor amounts of quartz, chlorite, epidote and carbonate. Although having an external appearance similar to the Basal Gabbro, they generally have a higher biotite (phlogopite?) content, with up to 12 % biotite. They also display the alteration seen throughout the Complex, suggesting they were intruded shortly after the Complex was emplaced, and before the late- to post-magmatic alteration attained its zenith.

Chapter 4: Mineral Chemistry of the Basal Gabbro

4.1 Technique

All mineral analyses were performed on an automated Cameca electron microprobe analyser at the University of the Free State, using a variety of international and in-house standards. The analyses were done using a focused electron beam with an approximate beam diameter of 1 μm. The accelerating voltage used was 20kV, with a beam current of 20mA.

4.2 Orthopyroxene Compositions

Orthopyroxene is only found in abundance in boreholes SH10 and SH3, and even in these cases often displays a certain degree of amphibolitisation, and only remains as relicts within amphiboles. From these two boreholes a total 136 analyses of 75 grains were analysed from 13 different stratigraphic levels (Appendix C). In order to monitor any zonation in the grains, either caused during crystallisation or by post-crystallisation amphibolitisation, both the cores and rims were measured wherever possible. The effects of zoning between the core and rim domains is illustrated with respect to $Mg\#_{opx}$, Al_2O_3, CaO and TiO_2 for selected microprobe analyses in Figure 7, and a few selected core-rim couplets are shown in Table 2.

The majority of orthopyroxenes have compositions classifying them as enstatites in terms of the new nomenclature (Morimoto, 1989). The orthopyroxenes show a wide variation in enstatite contents from approximately $En_{43.4}$ to En_{72}. The ranges of the cation % are:

	Mg	Fe + Mn	Ca
Cumulus opx	44.63 - 71.97	25.61 - 55.48	1.30 - 6.28

When the core compositions of the orthopyroxenes from borehole SH10 are plotted (Figure 8), two discrete clusters are distinguishable. The bulk of the analyses form a well defined cluster with compositions of between $En_{45.9}$ and $En_{56.7}$. A smaller cluster consisting of 10 core analyses forms another well defined range, with compositions of between $En_{63.5}$ and $En_{72.0}$. This more Mg-rich cluster consists of samples from probe section SH10-4 (404.07 m), which is 6 cm beneath a dolomite xenolith. The variation in orthopyroxene compositions (i.e. Mg-rich and Mg-poor) can be explained by two alternative models.

Firstly, it is possible that the magnesian population of orthopyroxenes in probe section SH10-4 (404.07 m) resulted by simple crystallisation of the magma. Evidence for this theory includes the fact that the basal chill (probe section SH10-9 (409.40 m)), which supposedly represents the parental magma, has several orthopyroxenes which have more magnesian compositions (Figure 7) than those in probe section SH10-4 (404.07 m). Furthermore, the element variation diagrams (Figure 9) show that the Mg-rich data from SH10-9 are within the range of SH10-4 for all elements with the possible exception of Ti. Therefore, it is possible that the compositional gap between the Mg-rich orthopyroxenes from SH10-4 and the less magnesian compositions from other samples (Figure 9), is a result of a shortage of data, and that there is a continuum resulting from simple fractionation.

The alternative theory recognises that there are two populations of orthopyroxenes, being produced by two different processes. The bulk of the orthopyroxenes have very similar compositions resulting from normal processes of crystallisation of the magma. However, it is postulated that the population consisting of Mg-rich orthopyroxenes from SH10-4 were produced by a process of Mg-enrichment due to skarnification associated with the assimilation of the nearby dolomite xenolith into the melt (as discussed in Chapter 3). The Mg-rich data from the basal chill in section SH10-9 are envisaged to represent slightly altered (skarnified) compositions, resulting from either the assimilation of mini-xenoliths, or from direct interaction with the country rocks during the transport and emplacement of the magma into the dolomites.

It is suggested that the latter theory of skarnification best explains the orthopyroxene compositions of the Basal Gabbro. This theory is supported by a number of other observations. Firstly, the supposedly "skarnified" section (SH10-4) displays textures very different to the surrounding rock sections, such as coarse grain size, fresh appearance of grains (where unaltered), and serpentinisation of the rock. All of these textures are characteristic of skarns. Secondly, the mineral assemblage of the "skarnified" section, being pyroxene (especially diopside), quartz, calcite, phlogopite, talc and serpentine, is also typically characteristic of magnesian skarns. Finally, the proximity (6 cm) of the "skarnified" section to a dolomite xenolith is further support for the process of skarnification in explaining the Mg-enrichment of the orthopyroxenes in this section.

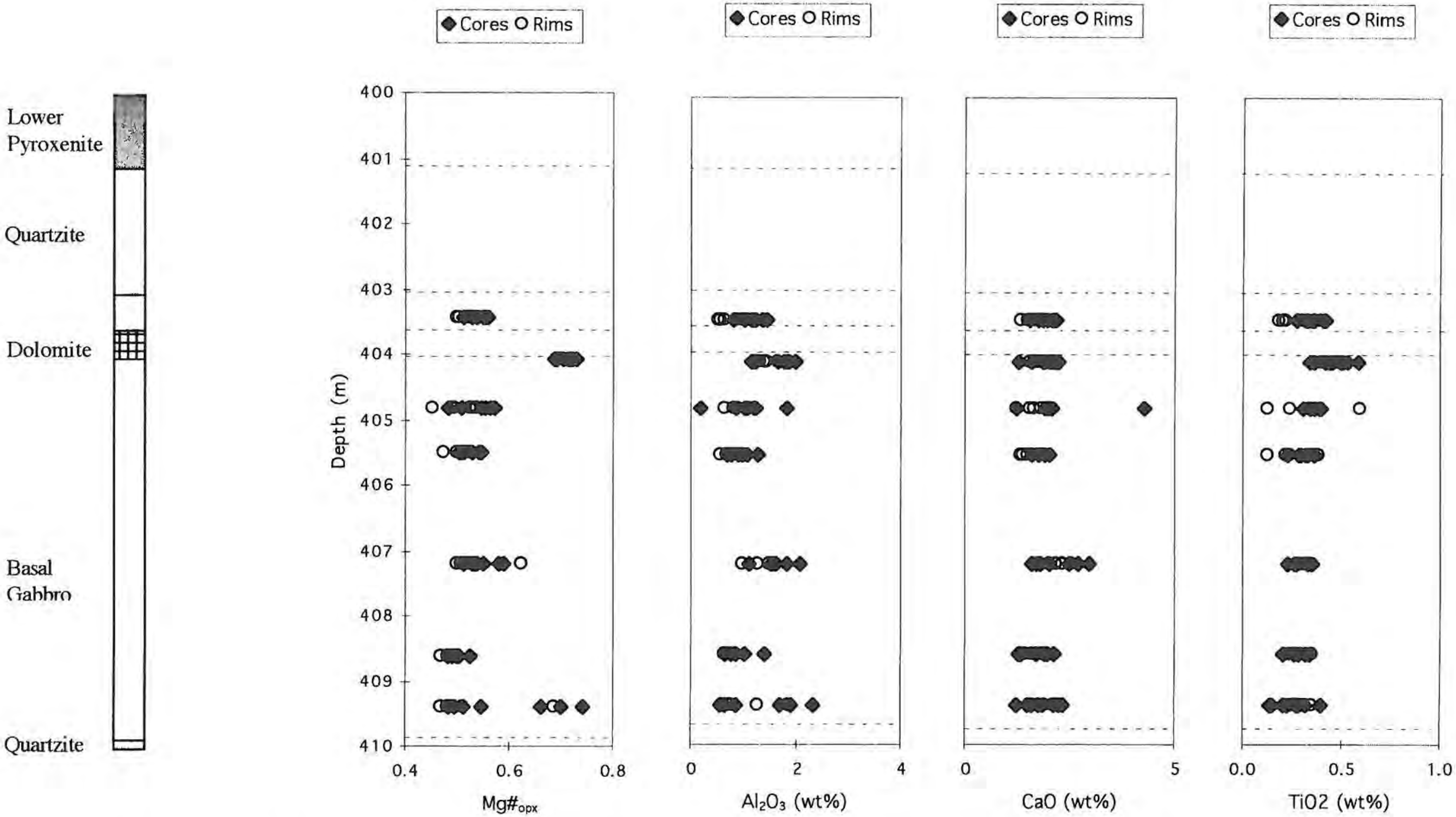

Figure 7 *Variation in core and rim compositions of orthopyroxenes from borehole SH10, plotted against stratigraphic height.*

Analysis #	153	154	88	89	7	8	27	29	40	41	58	59	76	77
Section	10-9	10-9	10-8	10-8	10-7	10-7	10-6	10-6	10-5	10-5	10-4	10-4	10-3	10-3
Label	*OPX 1C*	*OPX 1R*	*OPX 1C*	*OPX 1R*	*OPX 5C*	*OPX 5R*	*OPX 7C*	*OPX 7R*	*OPX 5C*	*OPX 5R*	*OPX 5C*	*OPX 5R*	*OPX 3C*	*OPX 3R*
SiO_2	51.09	50.12	49.57	49.78	51.16	50.34	49.98	49.83	50.85	50.47	53.80	53.27	50.21	50.08
TiO_2	0.39	0.35	0.28	0.29	0.35	0.31	0.36	0.24	0.36	0.37	0.50	0.48	0.36	0.18
Al_2O_3	2.31	1.26	0.85	0.73	1.83	1.49	0.98	0.84	1.18	0.88	1.98	1.28	1.13	0.50
FeO	25.79	29.01	30.86	30.14	25.55	28.28	29.49	29.98	26.58	27.84	16.71	18.47	28.73	29.15
Cr_2O_3	0.12	0.02	0.00	0.01	0.04	0.05	0.01	0.00	0.00	0.00	0.05	0.03	0.06	0.12
MnO	0.37	0.58	0.55	0.58	0.51	0.53	0.61	0.77	0.56	0.54	0.28	0.21	0.52	0.61
NiO	0.04	0.04	0.00	0.06	0.04	0.05	0.09	0.02	0.07	0.08	0.06	0.09	0.03	0.07
MgO	17.35	15.62	16.05	16.66	17.55	16.24	17.22	17.80	17.86	17.62	25.03	23.54	16.86	16.51
CaO	2.11	2.25	1.33	1.67	2.49	1.75	1.60	1.30	1.91	1.80	2.22	1.77	1.93	1.31
Na_2O	0.05	0.05	0.00	0.08	0.07	0.03	0.11	0.00	0.04	0.06	0.05	0.13	0.10	0.00
K_2O	0.01	0.00	0.01	0.01	0.02	0.01	0.00	0.00	0.00	0.00	0.01	0.03	0.00	0.01
Total	99.64	99.31	99.50	100.00	99.60	99.08	100.46	100.78	99.42	99.65	100.69	99.29	99.92	98.55
Cations based on 6 oxygens														
Si	1.9513	1.9585	1.9478	1.9429	1.9569	1.9601	1.9348	1.9268	1.9583	1.9526	1.9456	1.9685	1.9459	1.9713
Ti	0.0113	0.0102	0.0082	0.0084	0.0099	0.0092	0.0104	0.0070	0.0105	0.0107	0.0135	0.0134	0.0105	0.0053
Al	0.1038	0.0581	0.0394	0.0334	0.0825	0.0681	0.0447	0.0382	0.0536	0.0401	0.0843	0.0555	0.0516	0.0233
Fe^{2+}	0.8237	0.9478	1.0141	0.9837	0.8172	0.9209	0.9546	0.9693	0.8560	0.9004	0.5053	0.5707	0.9312	0.9593
Cr	0.0036	0.0008	0.0000	0.0002	0.0011	0.0015	0.0004	0.0000	0.0000	0.0000	0.0013	0.0008	0.0017	0.0039
Mn	0.0121	0.0193	0.0184	0.0192	0.0166	0.0174	0.0199	0.0252	0.0184	0.0176	0.0085	0.0065	0.0169	0.0204
Ni	0.0014	0.0011	0.0000	0.0018	0.0013	0.0016	0.0029	0.0006	0.0021	0.0023	0.0018	0.0026	0.0010	0.0021
Mg	0.9879	0.9099	0.9402	0.9693	1.0010	0.9427	0.9938	1.0261	1.0254	1.0162	1.3497	1.2969	0.9742	0.9688
Ca	0.0863	0.0942	0.0562	0.0699	0.1019	0.0730	0.0666	0.0538	0.0787	0.0744	0.0861	0.0699	0.0800	0.0552
Na	0.0040	0.0040	0.0000	0.0058	0.0050	0.0026	0.0084	0.0000	0.0028	0.0045	0.0035	0.0090	0.0074	0.0000
K	0.0007	0.0000	0.0003	0.0003	0.0008	0.0003	0.0001	0.0000	0.0002	0.0000	0.0007	0.0014	0.0001	0.0006
Mg#	0.55	0.49	0.48	0.50	0.55	0.51	0.51	0.51	0.55	0.53	0.73	0.69	0.51	0.50
En content	51.72	46.16	46.34	47.47	51.69	48.25	48.84	49.46	51.83	50.59	69.23	66.72	48.65	48.35
Fs content	43.76	49.06	50.89	49.11	43.05	48.02	47.89	47.95	44.20	45.70	26.35	29.69	47.35	48.90
Wo content	4.52	4.78	2.77	3.42	5.26	3.74	3.27	2.59	3.98	3.71	4.42	3.59	4.00	2.75

Table 2 *Selected electron microprobe analyses of orthopyroxene core and rim pairs from borehole SH10.*

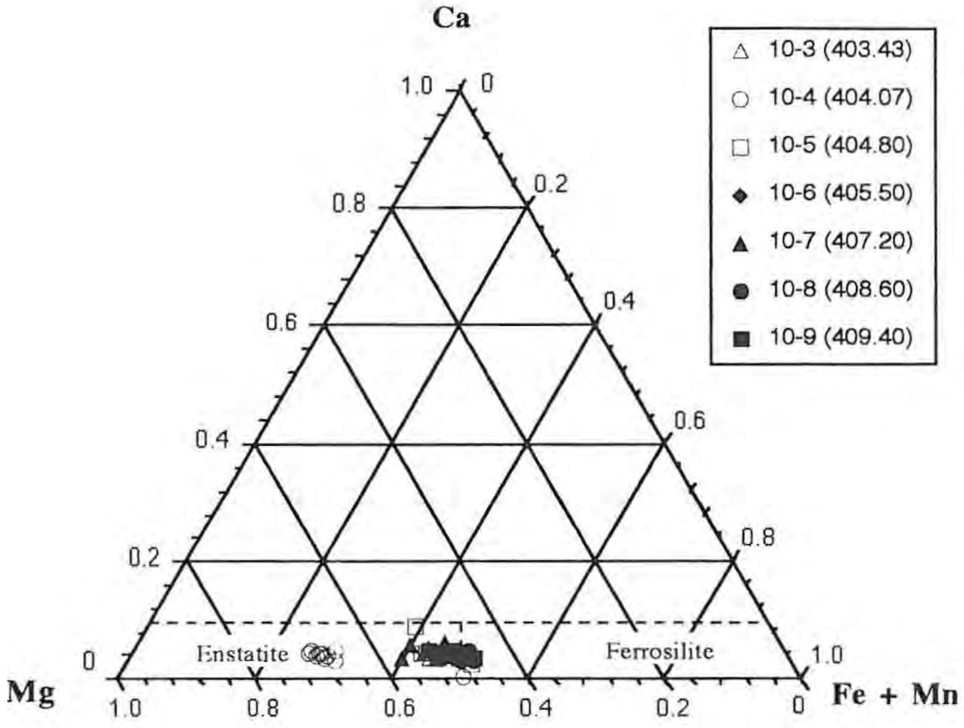

Figure 8 *Compositional range of orthopyroxene cores from borehole SH10.*

Figure 9 shows some element concentrations and ratios plotted against the Mg#$_{opx}$. Three populations of orthopyroxenes have been classified from the Basal Gabbro. These are firstly, orthopyroxenes from borehole SH10 excluding those from section SH10-4, secondly the Mg-rich orthopyroxenes from borehole SH10 (i.e. section SH10-4), and finally all the orthopyroxenes from borehole SH3. From Figure 9 it can be seen that the three different categories plot in different fields according to the Mg#$_{opx}$. These three fields form a continuum from the least altered rocks of borehole SH10 at one end (lower Mg#$_{opx}$), to the "skarnified" rock of section SH10-4 at the other end (high Mg#$_{opx}$). Borehole SH3 forms a field between these two extremes, suggesting that the chemistry of the orthopyroxenes is being controlled by the degree of alteration. Borehole SH3 has a high xenolith content (borehole logs in Appendix B) and is therefore likely to be displaying a varying degree of skarnification, depending on the proximity of a xenolith to the probe sections.

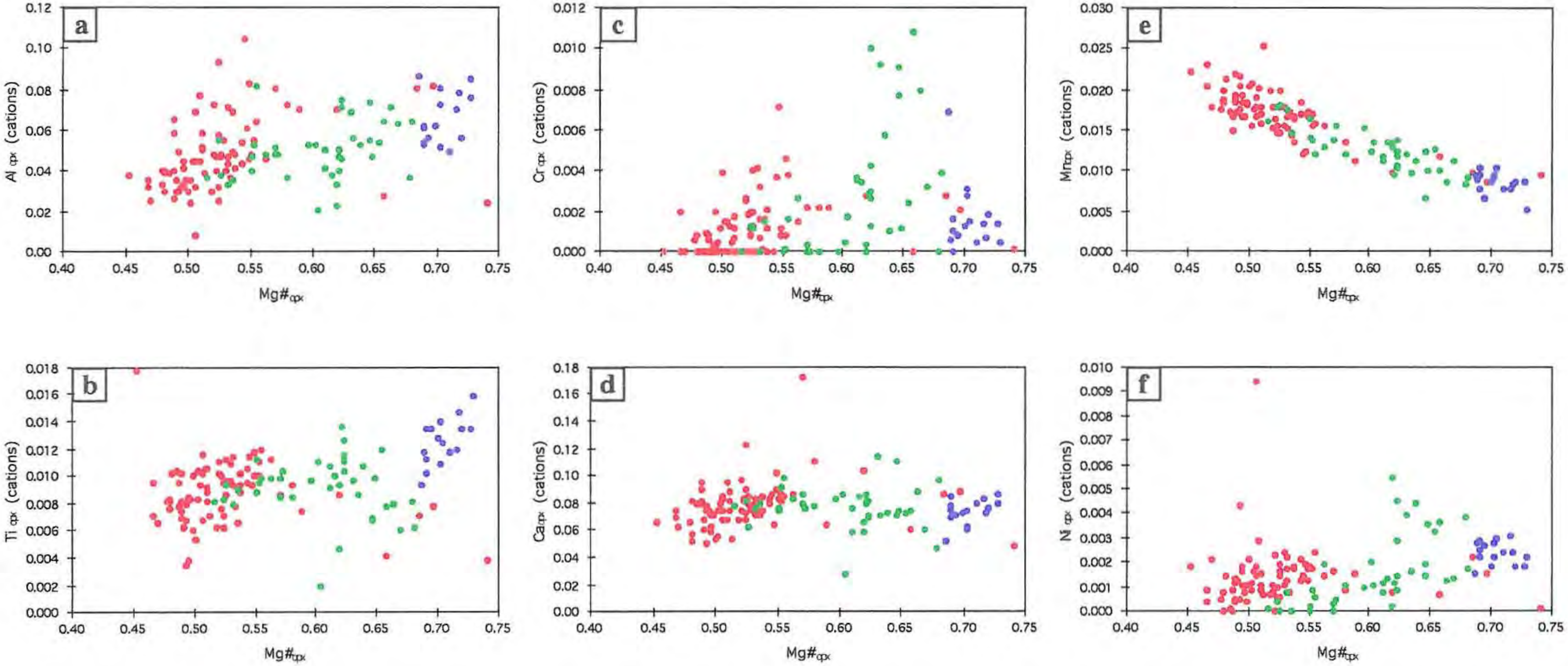

Figure 9 *Plot against* $Mg\#_{opx}$ *of (a) Al, (b) Ti, (c) Cr, (d) Ca, (e) Mn and (f) Ni cations in orthopyroxene. (●) SH10 Basal Gabbro, (●) SH3 Basal Gabbro, and (●) skarn-type orthopyroxenes from thin section SH10-4*

For the relatively unaltered sections from borehole SH10 only Mn displays a well defined trend, which follows the expected fractional crystallisation path, correlating negatively with the Mg$\#_{opx}$ and hence positively with Fe. All the other elements show only very weak correlations with the Mg$\#_{opx}$. In general, the interelement relationships are not particularly well defined for the orthopyroxene population. Possible reasons for the observed poor correlations might be:

a) that the limited stratigraphic thickness being measured is too small, so that any variations in element concentration may be overshadowed by the measuring error associated with the analyses.

b) elements are partitioning into other co-precipitating phases, such as magnetite, ilmenite and plagioclase, which are controlling the element distribution i.e. magnetite and ilmenite are removing Fe, whilst orthopyroxene removes Mg, therefore the Mg$\#_{opx}$ is not representing fractional crystallisation. However, the good inverse correlation of the Mg$\#_{opx}$ with Mn, suggests that the Mg$\#_{opx}$ does indicate fractional crystallisation.

c) variable degrees of late- to post-magmatic alteration of the pyroxenes may have obscured any underlying trends.

d) certain elements may be close to detection limits, and hence no trends can be observed, this is especially likely for Ni and Cr.

4.3 Clinopyroxene Compositions

Cumulus clinopyroxene is an important primary magmatic constituent of the Basal Gabbro, and although being very susceptible to amphibolitisation, primary grains and remnants remain, again largely in boreholes SH10 and SH3. Figure 10 shows the compositions of the clinopyroxenes on the Ca-Mg-Fe ternary diagram. Clearly, these are poorly constrained covering the ranges of diopside and augite. This wide range of compositions is most likely explained by a combination of exsolution resulting in an inaccurate analysis of the mineral, and post-magmatic alteration. However, it can be seen that the bulk of the diopsides are from thin section SH10-4 (404.07 m) which is 6 cm below the dolomite xenolith. These compositions represent typical skarn mineralogies and are therefore most likely caused by the skarnification processes around the carbonate xenolith. The clinopyroxenes from thin sections SH10-3 and SH10-7 occur on the edge of the pyroxene miscibility gap (Deer *et al.*, 1978), and hence can not be original compositions. These compositions may be a result of either measuring undetected low-Ca exsolution lamellae, or post-magmatic alteration. The remaining clinopyroxenes are mainly high-Ca augites from thin sections SH10-5, SH10-6 and SH10-9, which are thought to represent original compositions. Selected electron microprobe analyses for clinopyroxene core-rim pairs are shown in Table 3.

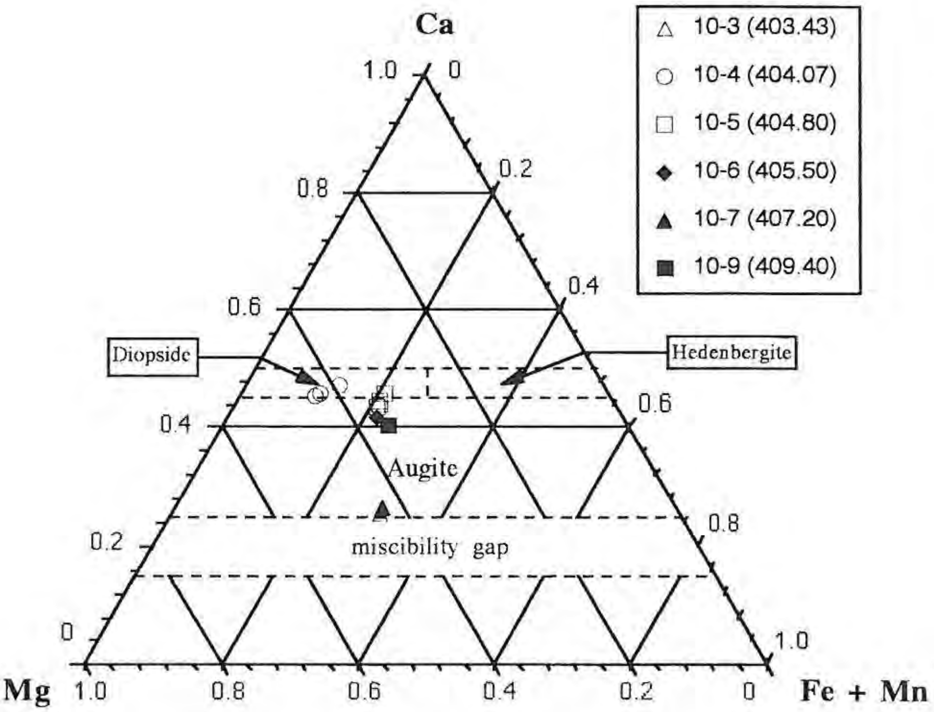

Figure 10 *Compositional range of clinopyroxenes from borehole SH10*

Analysis #	44	45	68	70	78	79
Section	10-5	10-5	10-4	10-4	10-3	10-3
Label	*CPX 1C*	*CPX 1R*	*CPX 2C*	*CPX 2R*	*CPX 4C*	*CPX 4R*
SiO_2	52.33	51.94	52.78	52.83	51.62	52.02
TiO_2	0.63	0.23	0.46	0.34	0.60	0.56
Al_2O_3	2.02	1.00	1.92	1.85	3.95	3.84
FeO	12.62	12.89	7.35	7.51	17.94	17.21
Cr_2O_3	0.06	0.01	0.40	0.15	0.06	0.00
MnO	0.30	0.32	0.17	0.09	0.18	0.18
NiO	0.02	0.01	0.05	0.04	0.07	0.06
MgO	11.80	11.84	15.39	15.08	14.12	13.48
CaO	20.53	21.64	22.39	22.87	11.56	11.47
Na_2O	0.55	0.41	0.42	0.49	1.34	1.39
K_2O	0.06	0.02	0.00	0.00	0.51	0.53
Total	100.93	100.32	101.34	101.25	101.95	100.74
Cations based on 6 oxygens						
Si	1.9595	1.9684	1.9333	1.9391	1.9183	1.9467
Ti	0.0177	0.0066	0.0127	0.0095	0.0167	0.0156
Al	0.0892	0.0448	0.0830	0.0801	0.1729	0.1695
Fe^{2+}	0.3952	0.4085	0.2253	0.2305	0.5573	0.5385
Cr	0.0018	0.0004	0.0117	0.0042	0.0016	0.0000
Mn	0.0095	0.0102	0.0051	0.0026	0.0057	0.0058
Ni	0.0007	0.0004	0.0013	0.0013	0.0022	0.0019
Mg	0.6587	0.6689	0.8404	0.8252	0.7823	0.7521
Ca	0.8237	0.8788	0.8788	0.8992	0.4604	0.4600
Na	0.0396	0.0298	0.0299	0.0349	0.0965	0.1005
K	0.0031	0.0011	0.0000	0.0000	0.0242	0.0253
Mg#	0.63	0.62	0.79	0.78	0.58	0.58
En content	34.91	34.02	43.11	42.15	43.32	42.82
Fs content	21.45	21.29	11.82	11.91	31.18	30.99
Wo content	43.65	44.69	45.07	45.93	25.50	26.19

Table 3 *Selected core and rim electron microprobe analyses of clinopyroxenes. Note that section 10-4 is close to a dolomite xenolith and represents a skarn-type mineralogy.*

4.4 Amphibole Compositions

The high degree of amphibolitisation of the lower units in the Uitkomst Complex, is indicated by the paucity of sections with primary pyroxenes. However, where they are found the pyroxenes are often found as remnants within amphiboles, which are pseudomorphically replacing pyroxenes. In thin section, two main amphiboles were recognised on the basis of their textures: a hornblende and an acicular tremolite / actinolite.

A total of 28 core domains were analysed from boreholes SH10 and SH3. The microprobe data were processed using "Emp-Amph" a computer program written by Mogessie *et al.* (1988) which converts the weight percent oxides into cations on the basis of 23 oxygens. The program then classifies the amphibole according to the International Mineralogical Association amphibole nomenclature scheme, set out Leake (1978) and Rock and Leake (1984). After this classification all analysed amphibole grains are calcic amphiboles, and plot in the fields of actinolite, actinolitic hornblende and magnesio-hornblende depending upon their Si concentration (Figure 11). Selected amphibole compositions as determined by the electron microprobe are shown in Table 4.

Point	2	12	19	8	9	5	16	23
Section	10-7	10-3	3-10	10-5	10-4	10-6	10-2	3-8
Label	*magnesio-hornblende*	*magnesio-hornblende*	*magnesio-hornblende*	*actinolitic hornblende*	*actinolitic hornblende*	*actinolite*	*actinolite*	*actinolite*
SiO_2	47.12	51.52	48.34	50.81	52.01	55.78	54.99	54.03
TiO_2	1.41	0.60	1.19	0.43	0.04	0.02	0.05	0.04
Al_2O_3	7.00	4.09	5.18	1.56	0.50	0.62	0.23	0.58
Cr_2O_3	0.04	0.05	0.30	0.05	0.17	0.00	0.07	0.02
FeO	18.73	17.79	10.59	13.29	5.75	16.28	14.58	17.58
MnO	0.18	0.20	0.17	0.36	0.09	0.27	0.27	0.36
MgO	11.71	13.83	17.20	12.18	16.73	15.32	16.35	15.09
CaO	10.96	10.36	12.87	21.54	24.71	12.43	13.47	12.52
Na_2O	1.93	1.42	1.21	0.32	0.06	0.04	0.13	0.29
K_2O	1.25	0.51	0.39	0.00	0.00	0.01	0.03	0.03
Total	100.34	100.37	97.43	100.54	100.05	100.76	100.16	100.54
Cations based on 23 oxygens (after Mogessie et al., 1988)								
Si	6.813	7.231	6.963	7.396	7.405	7.785	7.742	7.613
Ti	0.157	0.068	0.130	0.043	0.008	0.000	0.008	0.008
Al	1.190	0.675	0.883	0.271	0.086	0.101	0.042	0.093
Cr	0.009	0.008	0.035	0.008	0.017	0.000	0.008	0.000
Fe^{3+}	0.712	1.126	0.542	0.000	0.000	0.571	0.372	0.812
Fe^{2+}	1.557	0.968	0.730	1.617	0.684	1.334	1.346	1.263
Mn	0.026	0.025	0.017	0.043	0.008	0.034	0.034	0.042
Mg	2.529	2.894	3.694	2.640	3.549	3.188	3.435	3.166
Ca	1.695	1.561	1.981	3.357	3.770	1.863	2.031	1.889
K	0.235	0.093	0.069	0.000	0.000	0.000	0.008	0.008
Na	0.539	0.388	0.338	0.088	0.017	0.008	0.034	0.076
Total	15.462	15.036	15.381	15.463	15.544	14.884	15.060	14.970
Al^{IV}	1.187	0.675	0.883	0.271	0.086	0.101	0.042	0.093
Al^{VI}	0.003	0.000	0.000	0.000	0.000	0.000	0.000	0.000
(Ca + Na)Σ	2.000	1.949	2.000	3.357	3.770	1.871	2.031	1.965
NaB	0.305	0.388	0.019	0.000	0.000	0.008	0.000	0.076
(Na + K)A	0.469	0.093	0.388	0.088	0.017	0.000	0.042	0.008

Table 4 *Selected electron microprobe analyses for the main types of amphibole.*

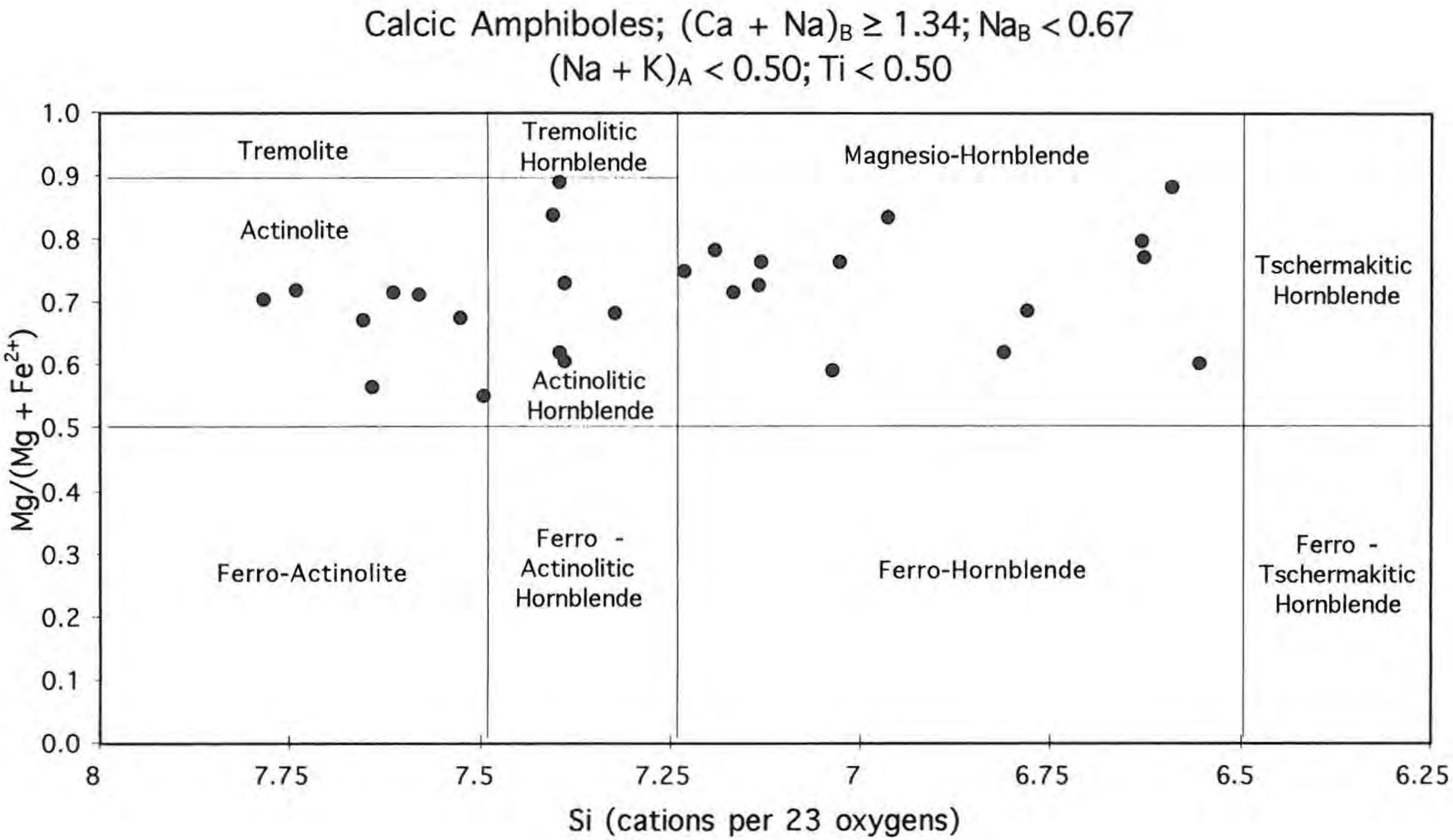
Calcic Amphiboles; (Ca + Na)B ≥ 1.34; NaB < 0.67
(Na + K)A < 0.50; Ti < 0.50
Tremolite
Tremolitic Hornblende
Magnesio-Hornblende
Actinolite
Tschermakitic Hornblende
Actinolitic Hornblende
Ferro-Actinolite
Ferro - Actinolitic Hornblende
Ferro-Hornblende
Ferro - Tschermakitic Hornblende
1.0
0.9
0.8
0.7
0.6
0.5
0.4
0.3
0.2
0.1
0.0
8
7.75
7.5
7.25
7
6.75
6.5
6.25
Mg/(Mg + Fe2+)
Si (cations per 23 oxygens)

Figure 11

4.5 Two-Pyroxene Geothermometry

Compositional data for co-existing orthopyroxene and clinopyroxene from the Basal Gabbro, were used to estimate the equilibration temperature of the pyroxenes, using the two pyroxene geothermometer after Mori and Green (1978). This geothermometer is based on the temperature dependent activity ratio (*K*) of Fe and Mg between co-existing Ca-poor and Ca-rich pyroxenes. The Mori and Green (1978) equation is shown below for T° kelvin:

$$\ln K = \frac{1500}{T^{\circ}\mathrm{K}} - 1.07$$

where the activity ratio (*K*) is defined as:

$$K = \frac{(\mathrm{Fe/Mg})_{opx}}{(\mathrm{Fe/Mg})_{cpx}}$$

Therefore for the pyroxene equilibration temperature in T°C the equation is as follows:

$$\mathrm{T^{\circ}C} = \left(\frac{1500}{\mathrm{Ln}K + 1.07}\right) - 273.15$$

The wide range of compositional values exhibited by both the orthopyroxenes and the clinopyroxenes (Figures 8 and 10), even from the same stratigraphic level, creates problems in regards to which grains should be used for the calculations. In order to address this problem, yet still achieve a reasonably accurate "answer", two procedures were followed. Firstly, core compositions of grains were used for calculations, and secondly, temperatures were calculated for each orthopyroxene grain in a section being measured against every clinopyroxene grain in the section, thereby calculating temperatures for all the various combinations of pyroxene pairs. These temperatures can then be summarised using standard statistical methods.

Section	Depth m	OPX $_{Fe}$	OPX $_{Mg}$	CPX $_{Fe}$	CPX $_{Mg}$	T °C
10-9	409.4	0.994	0.915	0.4767	0.6828	719
10-9	409.4	0.9907	0.9645	0.4767	0.6828	757
10-9	409.4	0.9746	0.9453	0.4767	0.6828	754
10-9	409.4	0.9239	0.9659	0.4767	0.6828	810
10-9	409.4	0.8237	0.9879	0.4767	0.6828	929
10-6	405.5	0.8489	0.9937	0.4221	0.6868	799
10-6	405.5	0.9659	0.993	0.4221	0.6868	708
10-6	405.5	0.9546	0.9938	0.4221	0.6868	716
10-6	405.5	0.9038	1.0071	0.4221	0.6868	762
10-6	405.5	0.8573	1.0228	0.4221	0.6868	814
10-6	405.5	0.951	0.9636	0.4221	0.6868	699
10-5	404.8	0.7718	1.0291	0.3952	0.6587	887
10-5	404.8	1.0104	0.9423	0.3952	0.6587	636
10-5	404.8	0.7718	1.0291	0.4154	0.6735	912
10-5	404.8	1.0104	0.9423	0.4154	0.6735	651
10-5	404.8	0.8355	1.039	0.3952	0.6587	827
10-5	404.8	0.856	1.0254	0.3952	0.6587	798
10-5	404.8	0.8206	1.0591	0.3952	0.6587	858
10-5	404.8	0.9481	0.9743	0.3952	0.6587	692
10-5	404.8	0.8418	1.0353	0.3952	0.6587	819
10-5	404.8	0.8355	1.039	0.4154	0.6735	850
10-5	404.8	0.856	1.0254	0.4154	0.6735	820
10-5	404.8	0.8206	1.0591	0.4154	0.6735	882
10-5	404.8	0.9481	0.9743	0.4154	0.6735	710
10-5	404.8	0.8418	1.0353	0.4154	0.6735	841
		min=	636		n=	25
		max=	929		mean=	786
					S.D.=	80
					95% conf. ±	31

Table 5 *Combinations of pyroxene pairs used to calculate the equilibration temperatures according to the two pyroxene geothermometer after Mori and Green (1978).*

Table 5 shows the 25 combinations of pyroxene pairs and their calculated temperatures. These range from 636°C to 929°C, with a mean of 786°C ± 31° at the 95% confidence level. When the calculated temperatures are plotted against depth (Figure 12), it can be seen that the variation in calculated temperatures is such, that no discernible trend can be recognised in the Basal Gabbro.

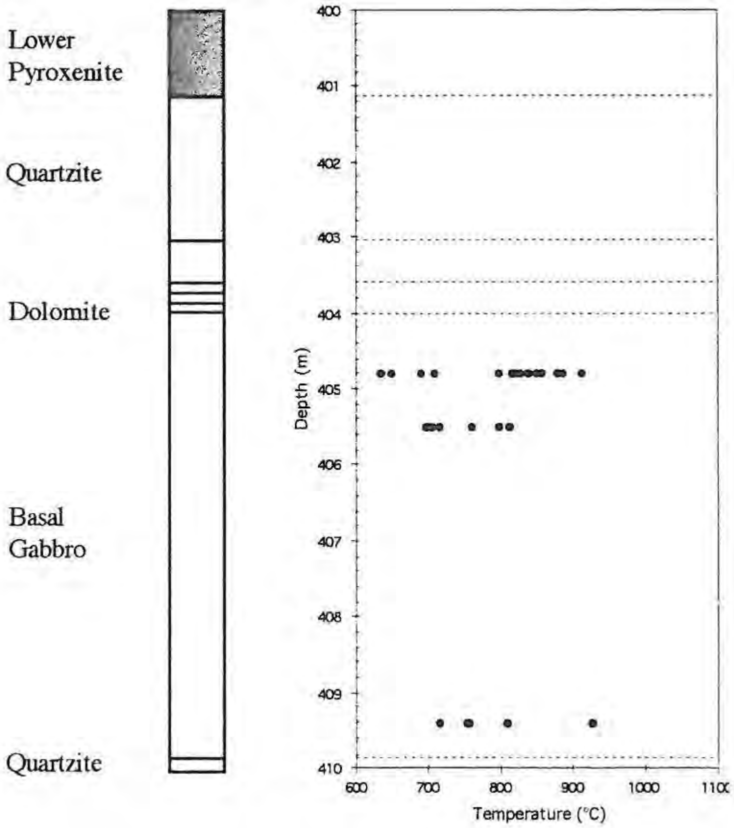

Figure 12 *Stratigraphic variation of calculated temperatures by two-pyroxene thermometry for borehole SH10.*

4.6 Ca-amphibole Geobarometer

The Ca-amphibole geobarometer is based on the correlation of the crossite content (NaM_4) in Ca-amphibole with the pressure of metamorphism. Ca-amphibole, where it coexists with iron oxide, albite and chlorite, should have fixed NaM_4, at any given *T* and *P*. In high pressure amphiboles NaM_4 varies inversely with Al^{iv} as a function of the pressure (Brown, 1976). Figure 13 shows a plot of the NaM_4 versus Al^{iv} components of the amphiboles as well as the empirical pressure ranges estimated by Brown (1977) for the various compositions. From this it can be seen that the maximum pressure of amphibole equilibration is in the vicinity of 5 - 6 kilobars. If the assumption is made that the "retrograde" amphibolitisation is caused in the latter stages of crystallisation by the increasing activity of meteoric water, then this pressure can be assumed to represent a maximum pressure of emplacement. Two populations of amphiboles can be distinguished, firstly the high pressure magnesio-hornblendes, and secondly the lower pressure actinolitic hornblendes and actinolites.

A possible mechanism by which these two populations can coexist, is outlined below. As uralitisation commenced, the high pressure magnesio-hornblendes would have been produced. During this process, the Complex and surrounding rocks would have been subjected to considerable stress due to the volume increases associated with the hydration of pyroxenes and other minerals. These stresses would have been released by fracturing and shearing, lowering the pressure, and creating an environment whereby the lower pressure actinolites could have formed.

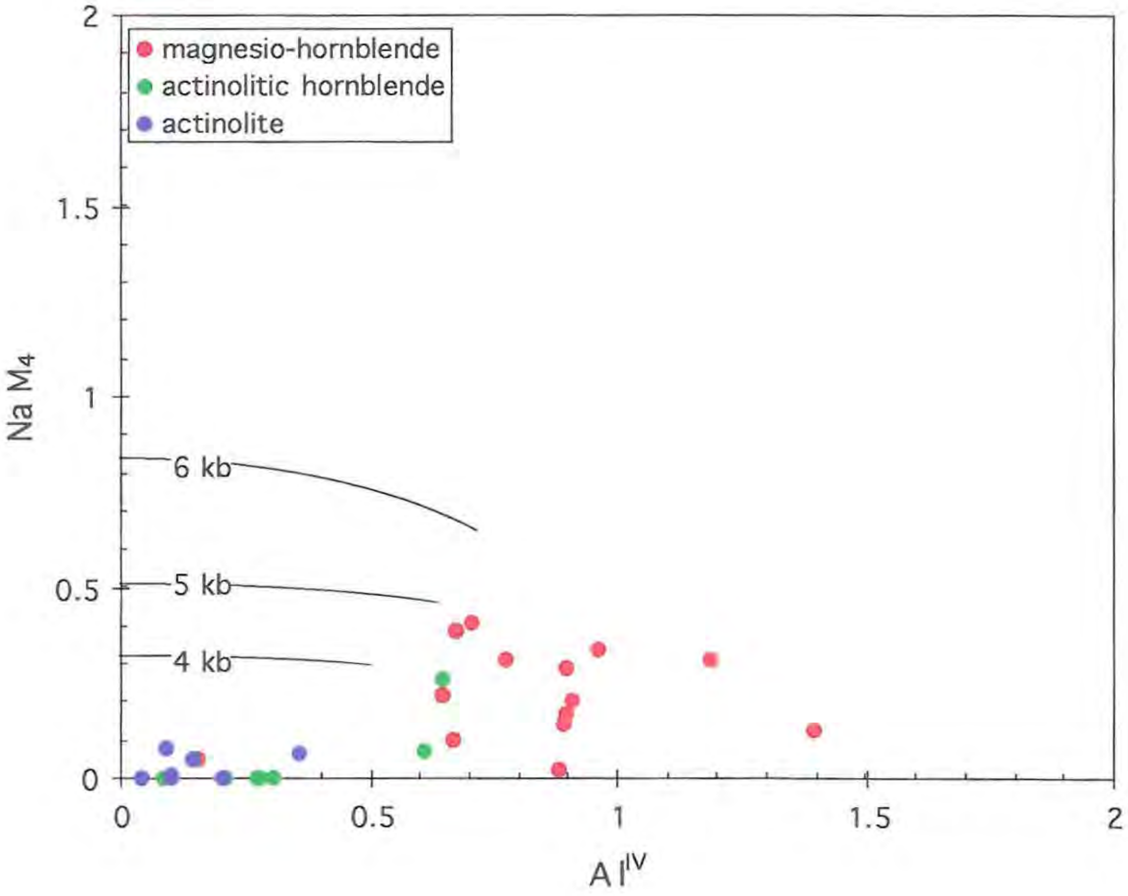

Figure 13 *Plot of the NaM$_4$ versus the Al^{IV} components of the different amphiboles with the empirical pressure ranges estimated by Brown (1977).*

Chapter 5: Whole-Rock Geochemistry

5.1 Introduction

All samples were analysed by the XRF-method of Norrish and Hutton (1969) as used in the Geology Department, Rhodes University by Marsh (1979). Details of analytical techniques are attached in Appendix D. Seventy samples were taken from boreholes SH8, SH10, SH25, SH26 and SH27 (Figure 2). These boreholes were chosen on the basis of a) geographical spread, and b) presence of adequate Basal Gabbro. This selection of boreholes reflects well the distribution of the Basal Gabbro as being concentrated along the northern margin of the Complex. Sulphide-rich boreholes and samples were, if possible, avoided due to problems encountered during the preparation of fusion discs. For this reason three samples have trace element data, but no corresponding major element data. For these three data points sulphide values have been estimated, by using the measured sulphur counts obtained from the powder pellets (details in Appendix D). Within each borehole, samples were taken more or less equidistantly where the lithology appeared homogeneous. Otherwise, representative samples were taken of the various lithological changes, including xenoliths, pegmatoids, diabases, and alteration products.

Whole rock analyses were carried out on the five boreholes previously mentioned. Of these analyses, 40 were of the Basal Gabbro, 17 were of the Lower Pyroxenite, 7 were of diabase sills and 6 were of dolomite and quartzite xenoliths. A detailed study of the xenoliths is not within the context of this study, although they have been analysed and included for comparative purposes.

Readers should be aware that the numbering of the XRF samples does **not** correlate with the same numbers from the thin sections and the microprobe sections. For example, the XRF sample SH10-9 comes from a depth of 404.07 m, whereas the microprobe and thin section SH10-9 comes from a depth of 409.40 m.

5.2 Assessment of Alteration

The alteration of the Uitkomst Complex is recognised as an important factor in the genesis of the Complex and it's economic potential. It is thus essential to differentiate between the geochemical effects of alteration, as opposed to the primary magmatic processes, on the compositional variation within the Complex.

5.2.1 Volatile Content

The increase in the volatile component of a rock is characteristic of amphibolitisation and deuteric alteration. The volatile content was measured as loss on ignition (L.O.I) by ashing the samples at 1000°C for about eight hours. During the ashing process, the samples lose weight by releasing volatiles (mainly H_2O^+ and CO_2), but gain weight by oxidation of FeO to Fe_2O_3. Therefore the L.O.I. content is only a rough estimate of the volatile content of the rock. About 80% of the analyses have L.O.I values of between 1% and 4%, although values up to 22.1% were recorded for carbonate samples (Figure 14). These values can be seen to be high when compared to those of Maier (1991), who measured more typical L.O.I. values of less than 1% for the ultramafic rocks in the UG2 - Merensky unit interval of the Upper Critical Zone in the Western Bushveld Complex. However, it is not uncommon for Karoo basalts to attain values in the vicinity of 3% - 4% (Marsh, pers. comm. 1995) The high L.O.I values seen in the Uitkomst samples are caused by a combination of factors, including: a) the initial volatile content of the magma b) the addition of volatiles released from the assimilation of xenoliths and wall rocks, and c) the hydration associated with the late- to post-magmatic amphibolitisation and alteration. As the high L.O.I values can be accounted for, none of the analyses have been rejected, and the major elements have therefore been recalculated to 100% L.O.I. and H_2O^- free.

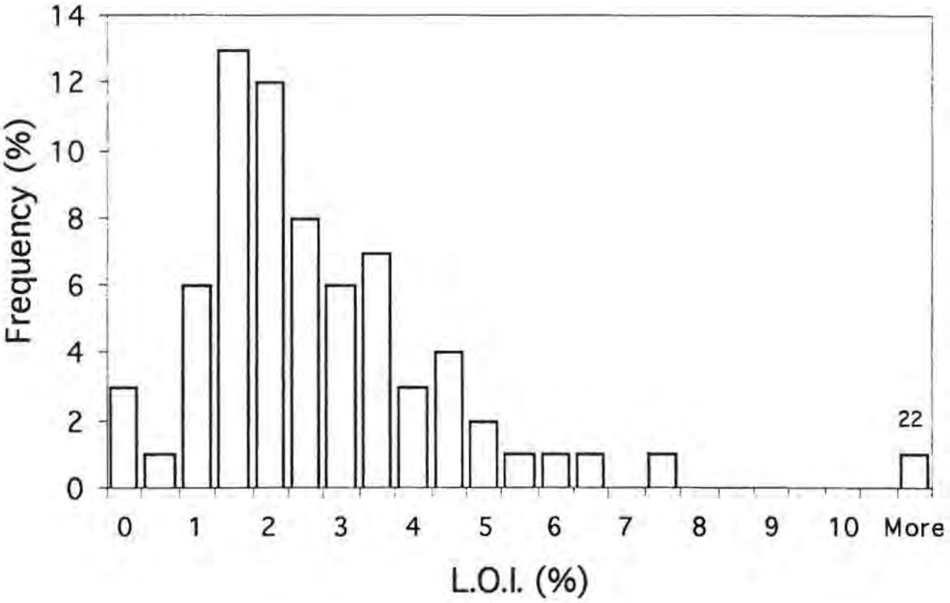

Figure 1 4 *Frequency histogram illustrating the range in L.O.I. of the 70 samples analysed by XRF (including sills and xenoliths).*

5.2.2 Indexing the Mobility of trace and major elements

In order to resolve whether geochemical trends are the result of primary or secondary chemical variations, it is necessary to determine the relative mobility of the trace and major elements. Incompatible elements (e.g zirconium (Zr), uranium (U) and phosphorous (P)) are well known as sensitive indicators of igneous processes such as fractional crystalisation, crustal contamination, magma mixing and partial melting (e.g. Henderson, 1968; Campbell, 1987). Furthermore, Zr has been shown to be relatively immobile during the alteration and metamorphism of the basaltic rocks of the Dordabis Formation (Williams-Jones, 1984), which was of a higher grade than the late- to post-magmatic alteration of the Uitkomst Complex (lower greenschist facies). For this reason, the assumption has been made that Zr is likely to have remained unaffected by the alteration of the Uitkomst Complex.

Figure 15 shows the vertical variation of Zr concentration for the boreholes analysed (these are shown in greater detail and with corresponding lithologies in Figures 30 - 34). All of these plots show a well defined trend, of decreasing Zr concentration upwards through the borehole. This trend is the opposite of what is expected with fractional crystallisation and represents a reverse fractionation trend, which will be discussed in detail in a later chapter. In almost all cases where there is a major deviation from the trend,the values of Zr correlate with diabase sills (higher values) or contamination from the country rocks (lower values). The well defined trends in Zr concentration can thus be used as tangible evidence for the assumption that Zr has remained immobile.

Figures 16 and 17 show variations in major and trace element concentrations in relation to the Zr content. Incompatible elements that have remained immobile during subsequent alteration are expected to correlate closely with Zr, whereas immobile compatible elements can be expected to show an inverse correlation with Zr. Elements which show a large variation when plotted against Zr, can be accounted for by several means. Firstly, certain elements may be unaffected by the process of fractional crystallisation and hence show poor correlations with Zr even in the unaltered rock. Secondly, certain elements which may have originally shown a close correlation with Zr, have since been mobilised by late- to post-magmatic alteration. Finally certain elements (e.g. Pb) may be at such low concentrations, that they are close to the lower limit of detection by XRF analysis, and hence no pattern can be detected.

In attempting to determine the primary geochemical processes of the basal portion of the Uitkomst Complex, it is important to avoid the use of elements which have subsequently been mobilised. Therefore only elements which one can be fairly certain have remained immobile should be used. These elements will have well defined trends with respect to Zr. The elements with poorly defined trends are possibly (among other causes) the result of mobilisation, and hence should be avoided.

From the element-Zr plots (Figures 16 - 17), it is clear that there are a couple of points with "abnormally" high Zr contents. These samples contain pegmatoidal patches possibly related to the presence of nearby xenoliths. The major element variation diagram (Figure 16) shows fairly well defined trends for the oxides SiO_2, TiO_2, Al_2O_3, Na_2O, K_2O and P_2O_5, suggesting that these may have remained immobile during subsequent alteration. The trace element variation diagrams (Figure 17) indicate that the incompatible elements Nb, Y, Ce, Nd and La have well defined trends with respect to Zr, suggesting that they have been unaffected by later alteration and have remained immobile.

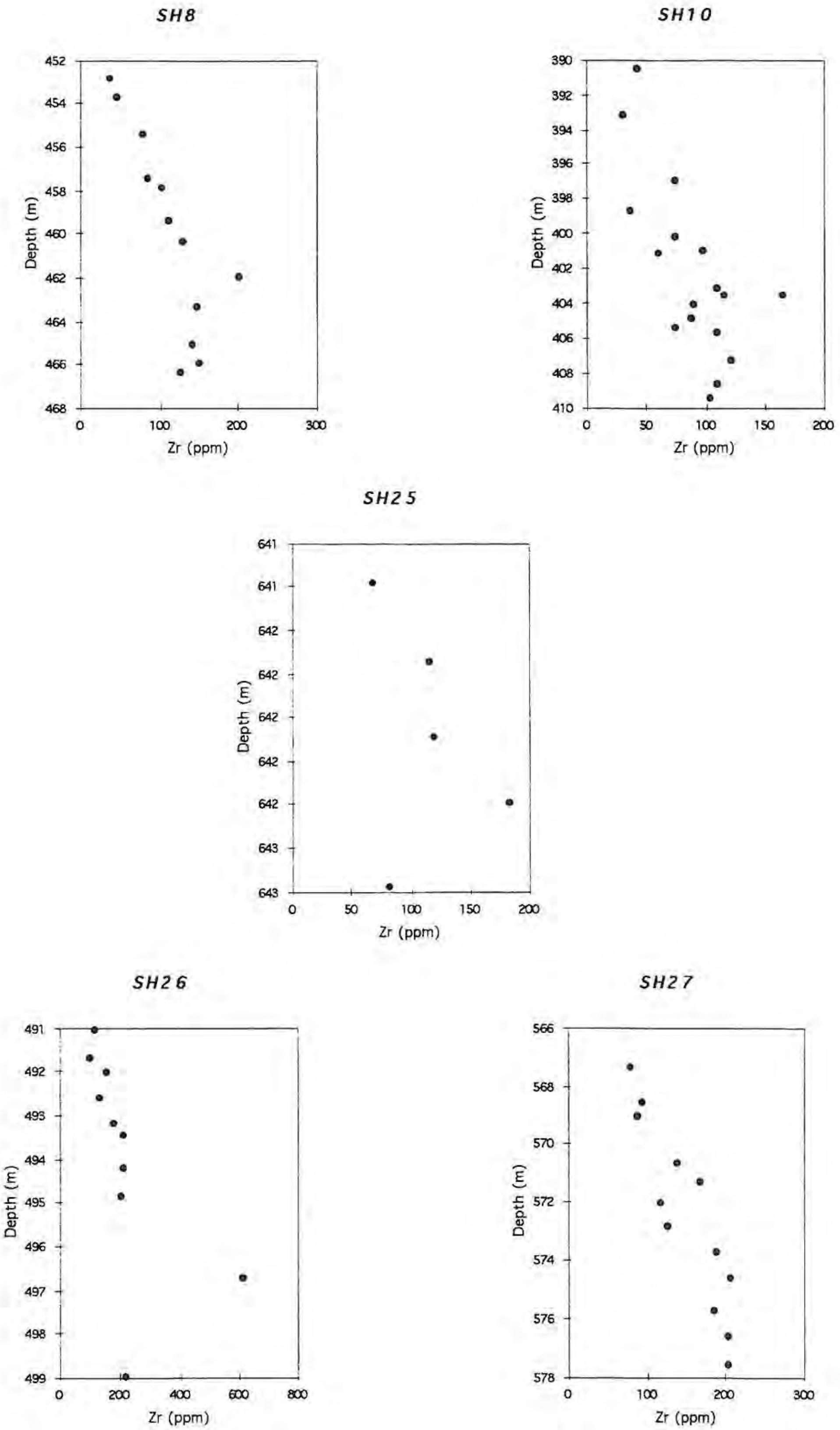

Figure 15 *Plots of the Zr concentration (ppm) of samples from the Basal Gabbro and the Lower Pyroxenite against depth, for various boreholes.*

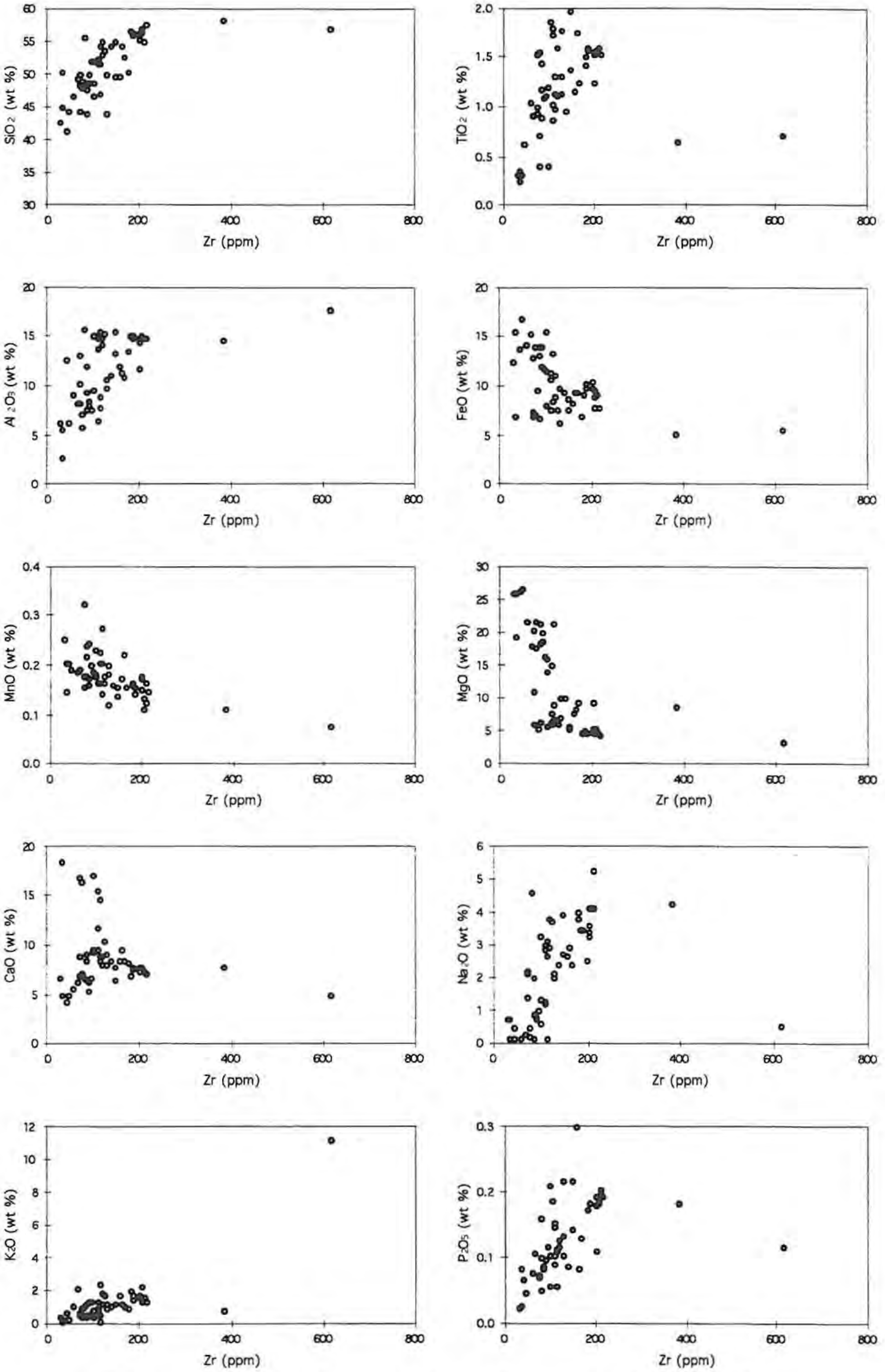

Figure 16 *Major element variation diagrams (weight % oxides) using Zr as the abscissa*

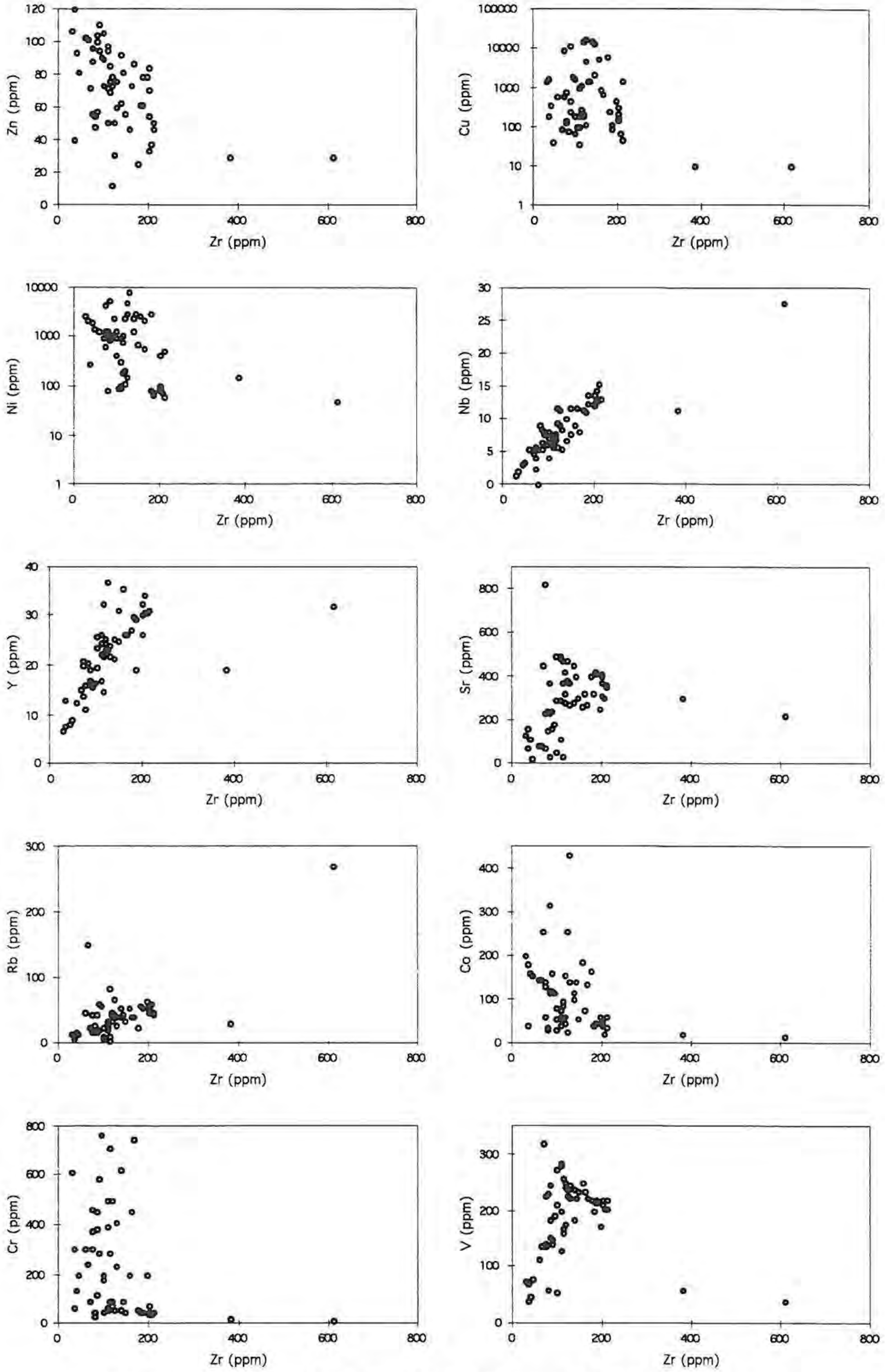

Figure 17 *Trace element variation diagrams (in parts per million) using Zr as the abscissa. Note log scales for Cu & Ni*

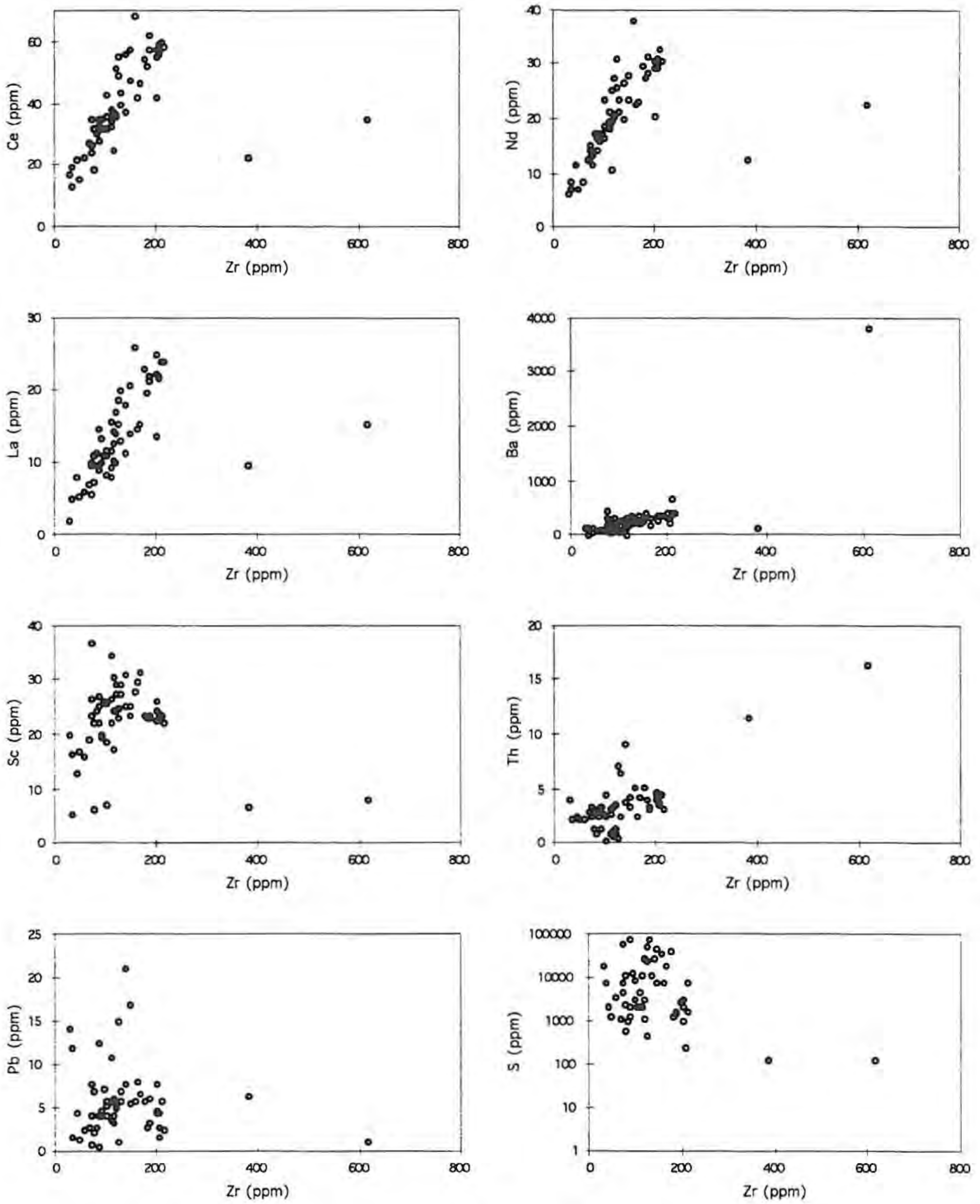

Figure 17 (cont) *Trace element variation diagrams (in parts per million) using Zr as the abscissa.Note log scale for sulphur.*

5.3 Tectonic Classification of the Basal Gabbro

In order to classify the Basal Gabbro it is necessary to select a classification scheme which is based on immobile elements, which are unlikely to have been affected by late- to post-magmatic alteration. The Zr-Nb-Y scheme of Meschede (1986) discriminates between four main basalt fields: within-plate alkali basalts, within-plate tholeiitic basalts, N-type MORB (depleted in incompaptibles) and E-type MORB (enriched in incompatibles). Figure 18 shows these fields with the data from the Basal Gabbro superimposed. The Basal Gabbro of the Uitkomst Complex can therefore be seen to represent a within-plate tholeiite. However, it should be noted that the use of geochemical discrimination diagrams, in particular the Ti-Zr-Y diagram of Pearce and Cann (1973) and the F_1-F_2 diagram of Pearce (1976) has been shown by Duncan (1987) to be subject to error. Duncan (1987) concluded that the composition of a basalt is a function of its source composition, degree of partial melting, and the various fractionation and contamination processes it may have undergone prior to crystallisation, and will only be indicative of a certain tectonic environment when at least some of these functions are unique to that environment. In the case of the Basal Gabbro, it is suggested that in using the incompatible elements Zr, Nb, and Y, they will have at least behaved in a similar fashion to each other, and hence been relatively unaffected by the degree of partial melting, fractionation and contamination. Thus, it is hoped that these elements retain their original ratios and hence represent their source compositions. Whether this is the case or not is unclear, although the compositions appear to plot (Figure 18) in the expected field of within-plate tholeiite.

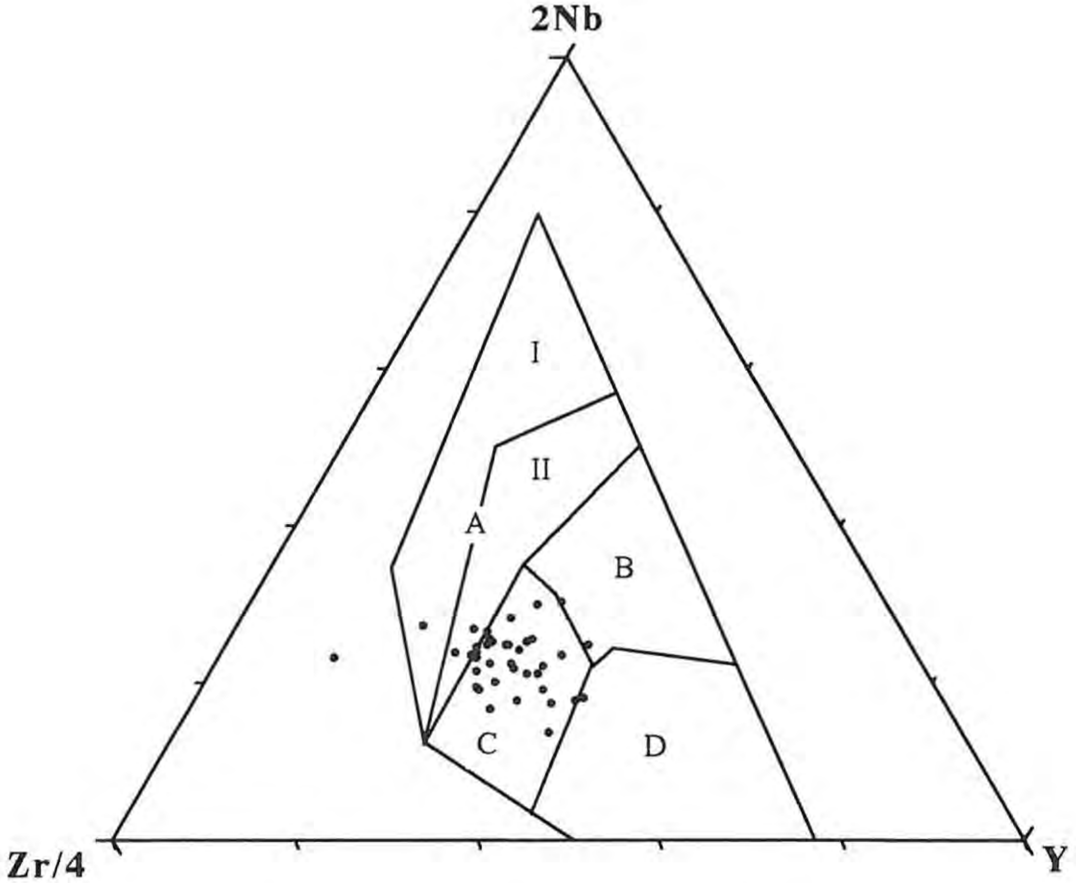

Figure 18 *The classification of the Basal Gabbro on the Zr-Nb-Y discrimination diagram for basalts (after Meschede, 1986). The fields are defined as follows:* ***AI****, within-plate alkali basalts;* ***AII****, within-plate alkali basalts and within-plate tholeiites;* ***B****, E-type MORB;* ***C****, within-plate tholeiites and volcanic-arc basalts;* ***D****, N-type MORB and volcanic-arc basalts.*

5.4 Major Elements

Due to the limitations of XRF analysis not being able to differentiate between Fe^{2+} and Fe^{3+}, all measured Fe is reported as Fe_2O_3. However, this is clearly not how the Fe is distributed throughout the rock, as it is also present in sulphides as FeS, and silicate minerals as FeO. In the case of this study, the presence of a high quantity of sulphides in the rock, both adds to and dominates the Fe content, such that any sample with sulphide mineralisation masks any underlying cryptic variation in the Fe content of the silicates. When trying to determine the evolution of the Complex, one is primarily looking at the chemical behaviour of the silicate phases, so it is necessary to account for the effect of the sulphides. This has been done by analysing for sulphur. As previously mentioned the three main sulphides are pyrrhotite [$Fe_{1-x}S$], chalcopyrite [$CuFeS_2$] and pentlandite [$(Ni,Fe)_8S_9$], all of which have the basic characteristic of having one sulphur atom for each Fe, Cu and Ni atom. Therefore if the assumption is made that all of the Cu and Ni detected by XRF is in sulphide form, the sulphur associated with the Cu and Ni can be removed leaving a value for sulphur that corresponds with the amount of pyrrhotite present. This assumption is made with the recognition that Ni does exist in the silicate phases, but in concentrations that make it inconsequential when compared to total values of Ni in the rock. Another simple calculation determines the amount of Fe required for the pyrrhotite, leaving the amount of Fe in the silicate and oxide phases. This has been recalculated to FeO even though it is known Fe_2O_3 is present as oxides (in magnetite and ilmenite) and as Fe^{3+} substituting for Al in amphibole. The absence of the Fe_2O_3 component is one of the reasons that the major element totals are less than 100%. These calculations are shown in Appendix D.

The removal of FeS from the total Fe in order to determine the geochemistry of the silicates is based on an initial assumption that the sulphides were formed as a primary magmatic product and not by the secondary alteration of silicate minerals. If this assumption is wrong, and the sulphides are secondary and utilising Fe from the alteration of silicates, then the use of parameters such as the Mg# [Mg/(Mg + Fe)] will also be erroneous, as only a portion of the Fe content is being used, the rest having been assigned to the sulphide phase. An example of the effect of using "sulphide corrected Fe" as opposed to total Fe is shown with respect to the Mg# of borehole SH10 (Figure 19). The trends of the Mg#'s show two very different trends within the Basal Gabbro when plotted against depth, and it is necessary to decide which is the "correct" method for displaying the primary characteristics of the silicate phases. Despite these uncertainties, the "sulphide corrected" Mg# trend supports the trends displayed by other elements such as Zr and P_2O_5, and hence has some validity. Therefore the hypothesis that the sulphides are a primary (albeit possibly remobilised) feature has been assumed, and "sulphide corrected" data will be used with the intention of either confirming or rejecting this hypothesis.

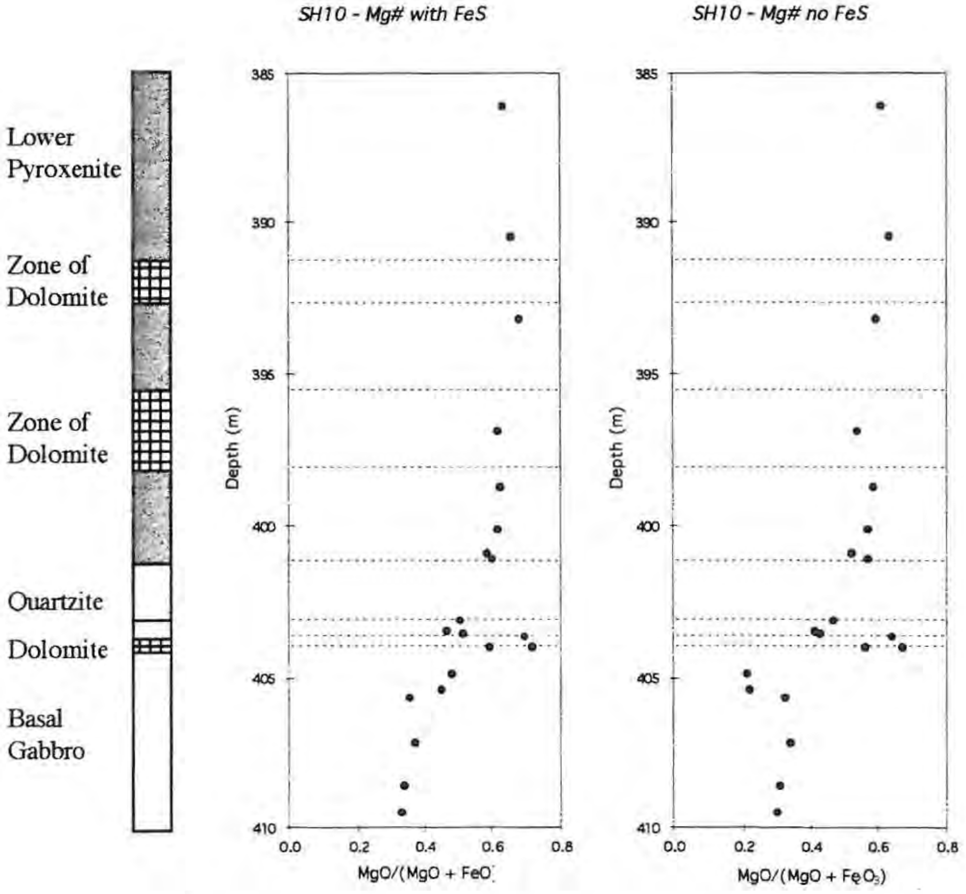

Figure 19 *Plots comparing the different Mg# obtained by using FeO (sulphide corrected) and Fe_2O_3 (total Fe) for borehole SH10. Note - all values normalised for H_2O and LOI*

The stratigraphic variations of selected major elements for the five boreholes are shown in Figures 20 - 24. These have been plotted using the data which has been normalised for H_2O^- and LOI. The variation in the Mg# (calculated as the weight ratio MgO/(MgO + FeO)) reflects the fractionation trend of the magma, *viz.* the relative increase in the Fe content of the magma with respect to Mg, as Mg is removed and preferentially incorporated into the pyroxenes. In all of the boreholes it can be seen that the Mg# increases upwards through the Basal Gabbro and into the Lower Pyroxenite. In boreholes with analyses from higher stratigraphic levels (SH8, SH10 and SH27) the trend of the Mg# becomes more constant with increasing height, and may tentatively begin to decrease through the Lower Pyroxenite. The irregularities in the trend are either caused by the proximity to xenoliths, or by variations in mineral proportions.

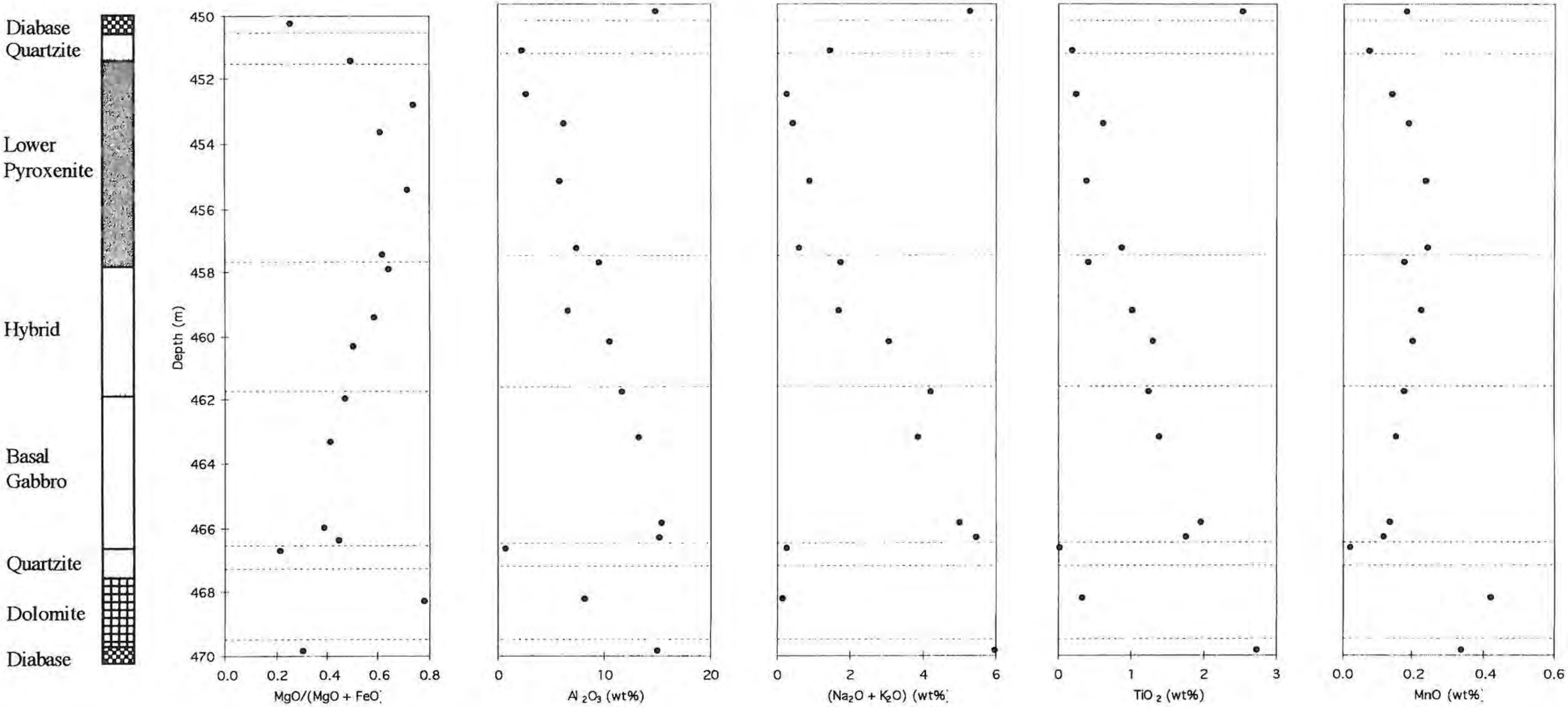

Figure 20 *Selected whole-rock major element data plotted against stratigraphic height for borehole SH8.*

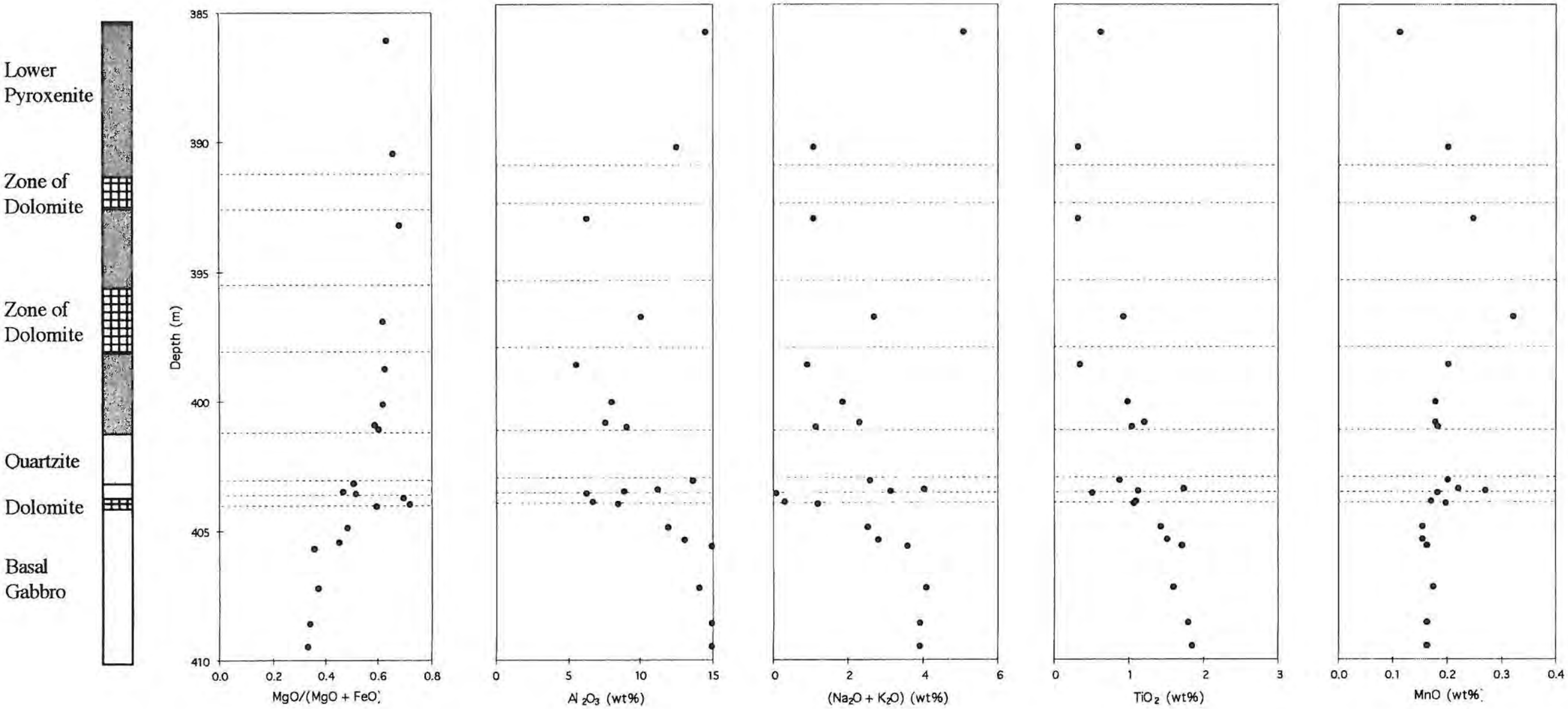

Figure 21 *Selected whole-rock major element data plotted against stratigraphic height for borehole SH10.*

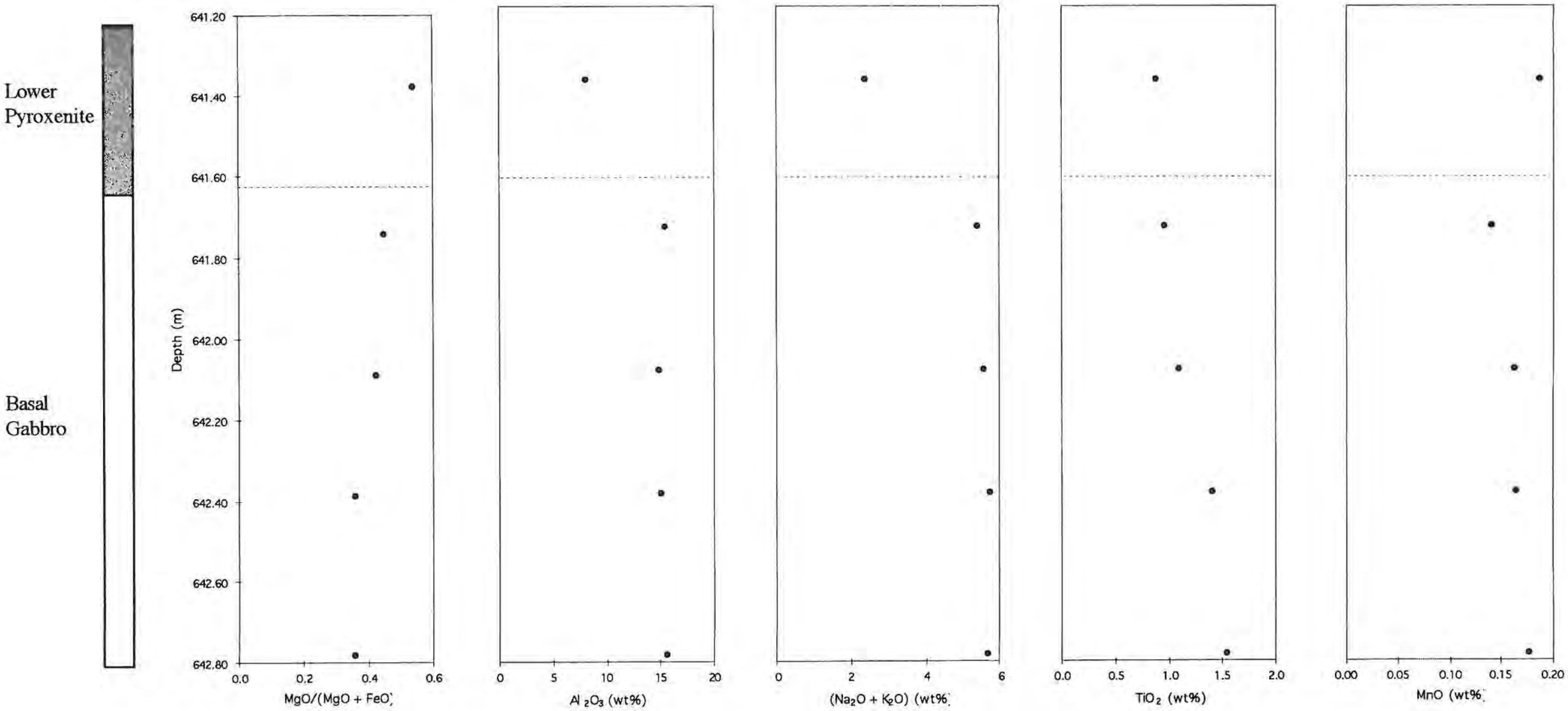

Figure 22 *Selected whole-rock major element data plotted against stratigraphic height for borehole SH25.*

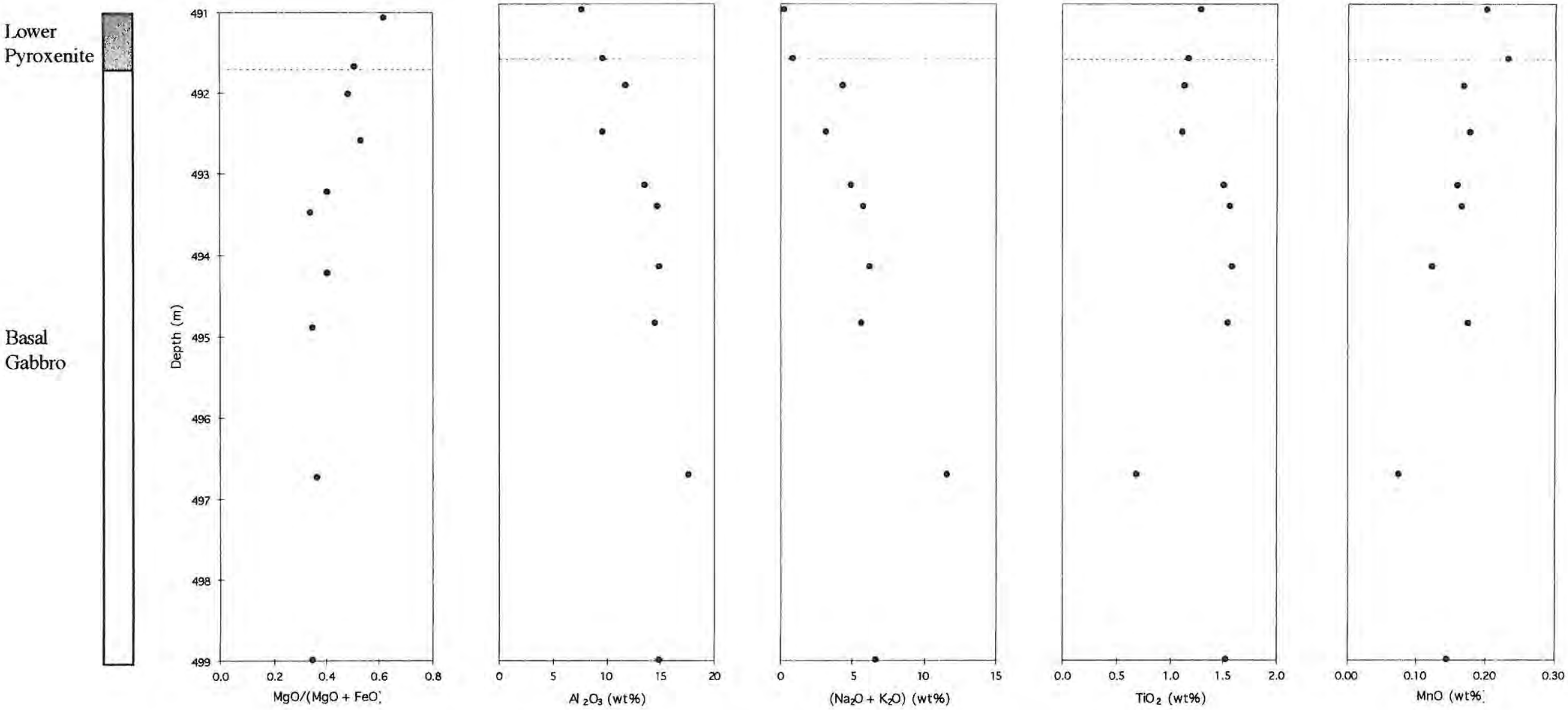

Figure 23 *Selected whole-rock major element data plotted against stratigraphic height for borehole SH26.*

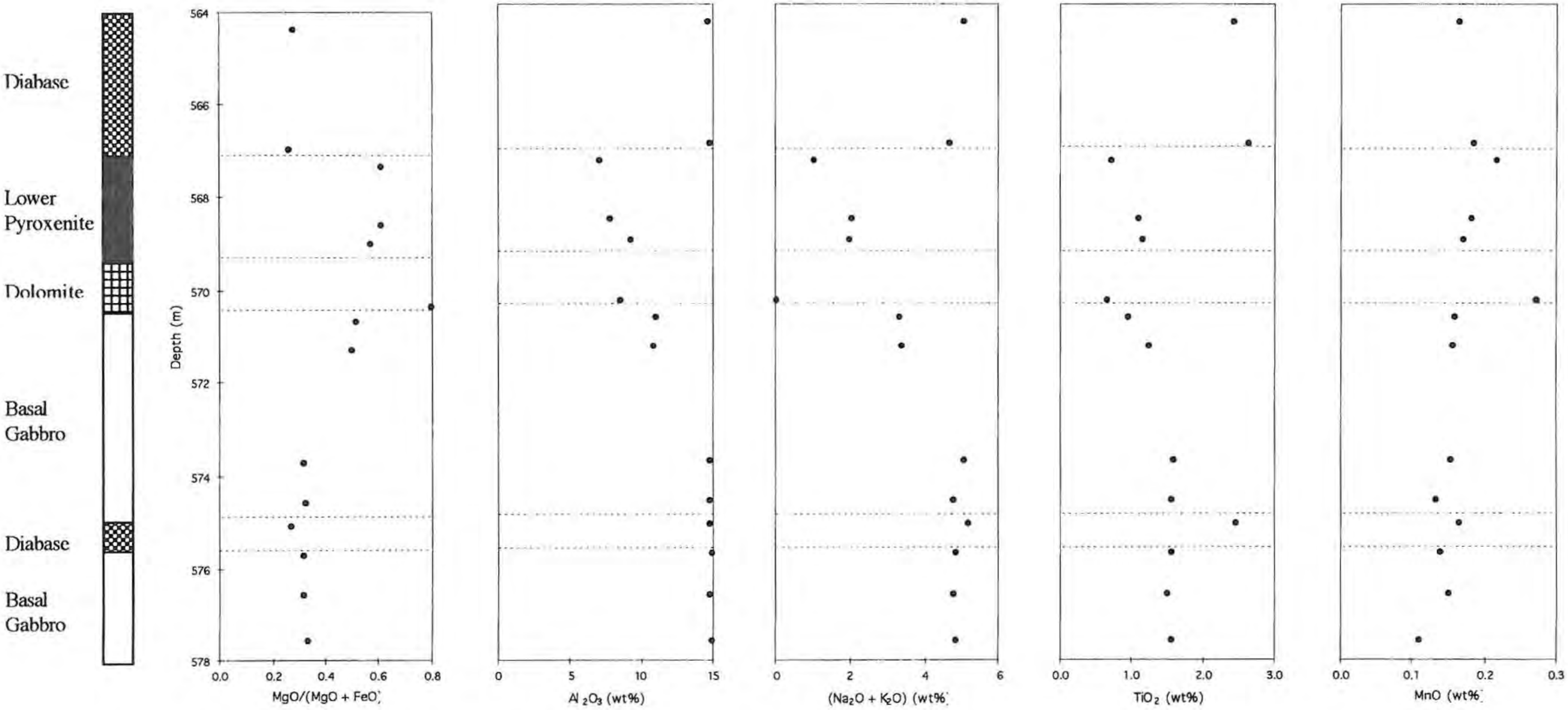

Figure 24 *Selected whole-rock major element data plotted against stratigraphic height for borehole SH27.*

The upwardly increasing trend in Mg# is a reverse fractionation trend, and is thus not what would be expected if the unit(s) were undergoing fractional crystallisation. Rather, this trend is what would be expected in the chilled margin of an intruded body of magma. The absence of any significant inflection or break in the trend of the Mg#, especially at the level of the Basal Gabbro - Lower Pyroxenite contact, is further evidence of this representing a chill of one intrusion rather than separate intrusions.

The behaviour of Al and the total alkalis ($Na_2O + K_2O$) is less well defined than the Mg#, and is controlled by the variation in plagioclase content with stratigraphic height. All the boreholes show a broad antipathetic trend to the Mg#, although in SH10 in particular (Figure 21) there is a large amount of variation, caused by the presence of the dolomite xenolith and the feldspathic "pegmatoidal" phases mentioned earlier. The lower plagioclase content of the Lower Pyroxenite in relation to the Basal Gabbro is apparent from all the plots of Al_2O_3 and ($Na_2O + K_2O$).

Titanium shows a well defined trend similar to Al_2O_3 and the total alkalis. Concentrations decrease upwards through the Basal Gabbro and lower Lower Pyroxenite and display an increase thereafter. The titanium is mainly controlled by the presence of ilmenite and magnetite, although minerals such as phlogopite and pyroxene contain a certain amount. This pattern is again consistent with a reverse fractionation trend associated with a chilled margin..

5.5 Trace Elements

Whole rock trace element analyses were carried out on all seventy samples. The results are shown in Appendix D. The elements of significance which will be discussed are S, the base metals Cu, Ni, Co, and Zn, and the incompatible elements Zr and P as well as the Cr/V and Cr/Ti ratios.

5.5.1 Sulphur

Figures 25 - 29 shows plots of weight % sulphide against stratigraphic height for the analysed boreholes, in order to display zones of sulphide mineralisation. The amount of sulphide was determined by the summation of the calculated values of FeS, NiS and CuS (as discussed earlier and in Appendix D).

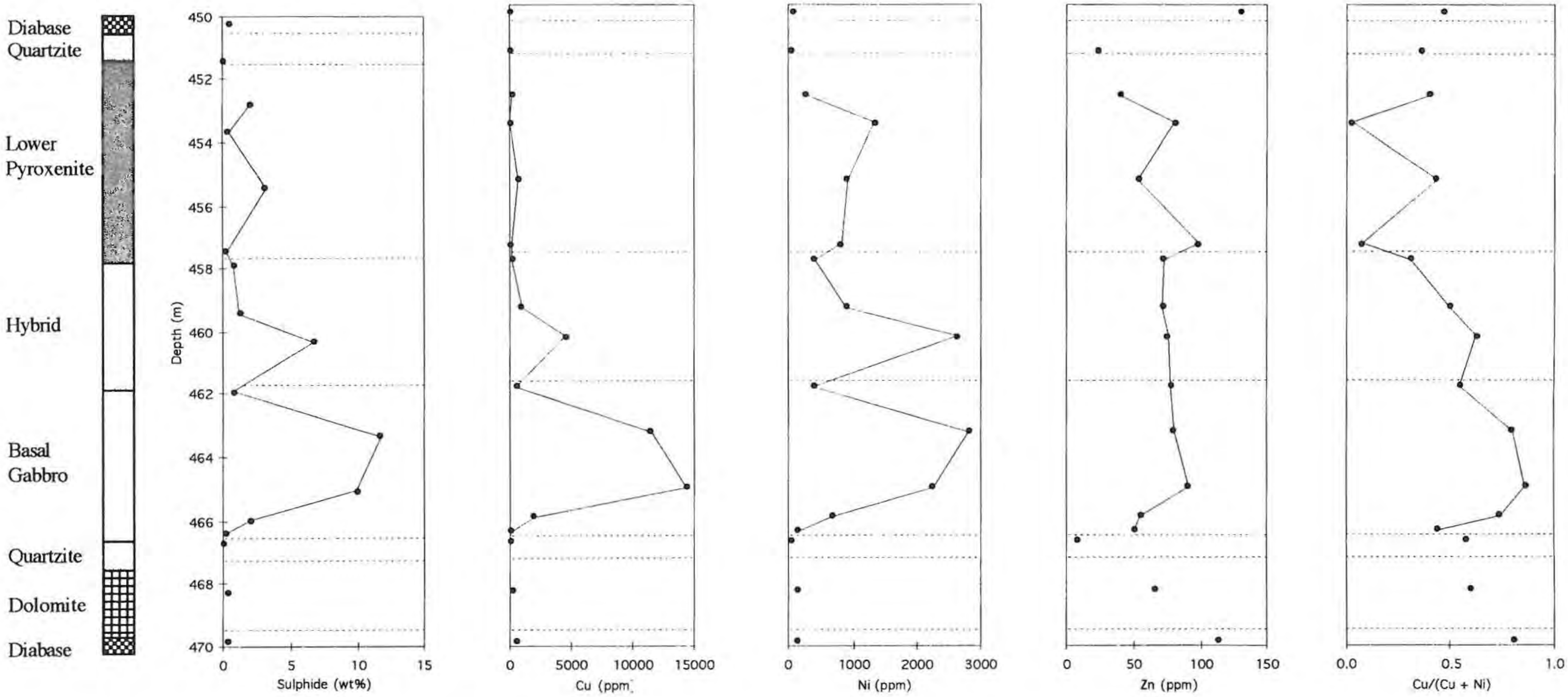

Figure 25 *Stratigraphic distribution of the base metals Cu, Ni, and Zn, as related to that of sulphide and the Cu/(Cu + Ni) ratio for borehole SH8.*

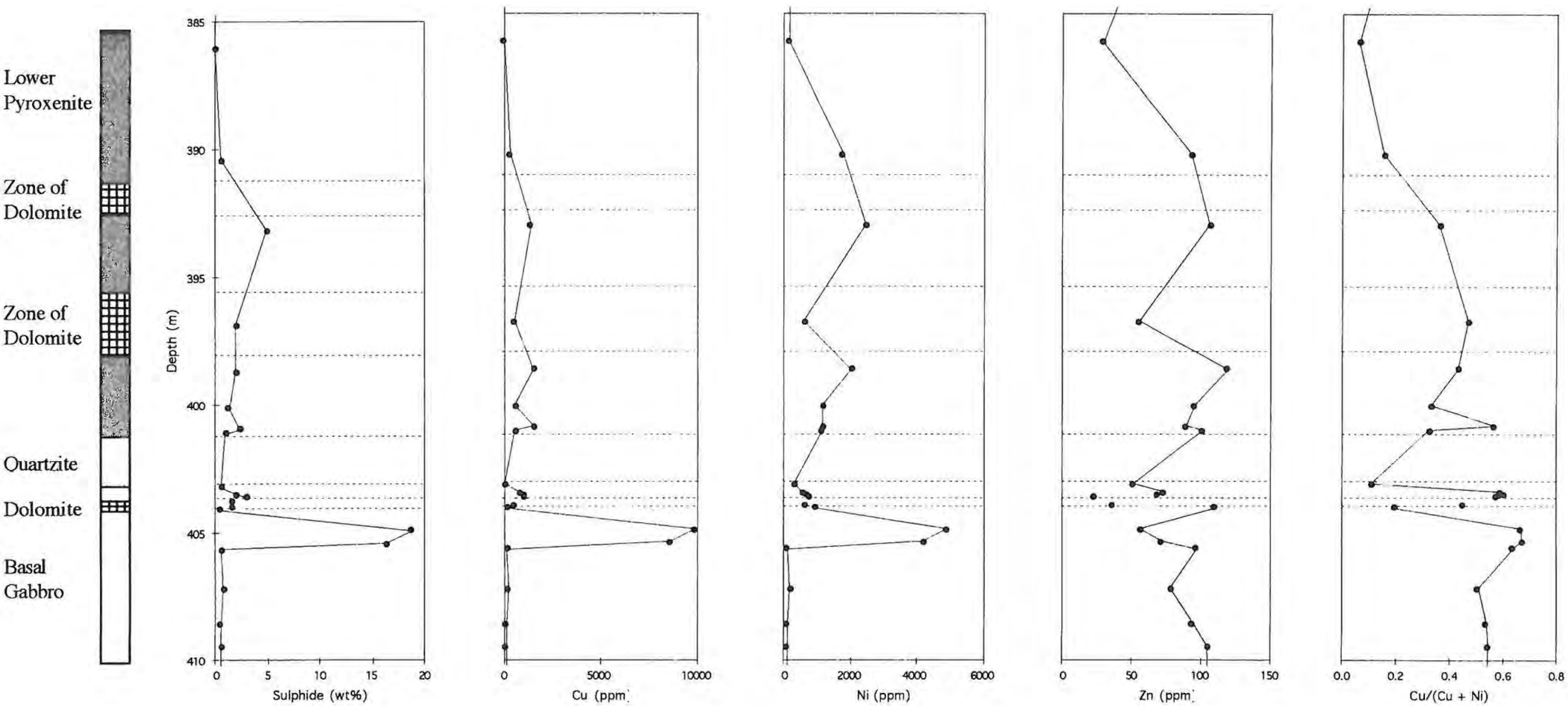

Figure 26 *Stratigraphic distribution of the base metals Cu, Ni, and Zn, as related to that of sulphide and the Cu/(Cu + Ni) ratio for borehole SH10.*

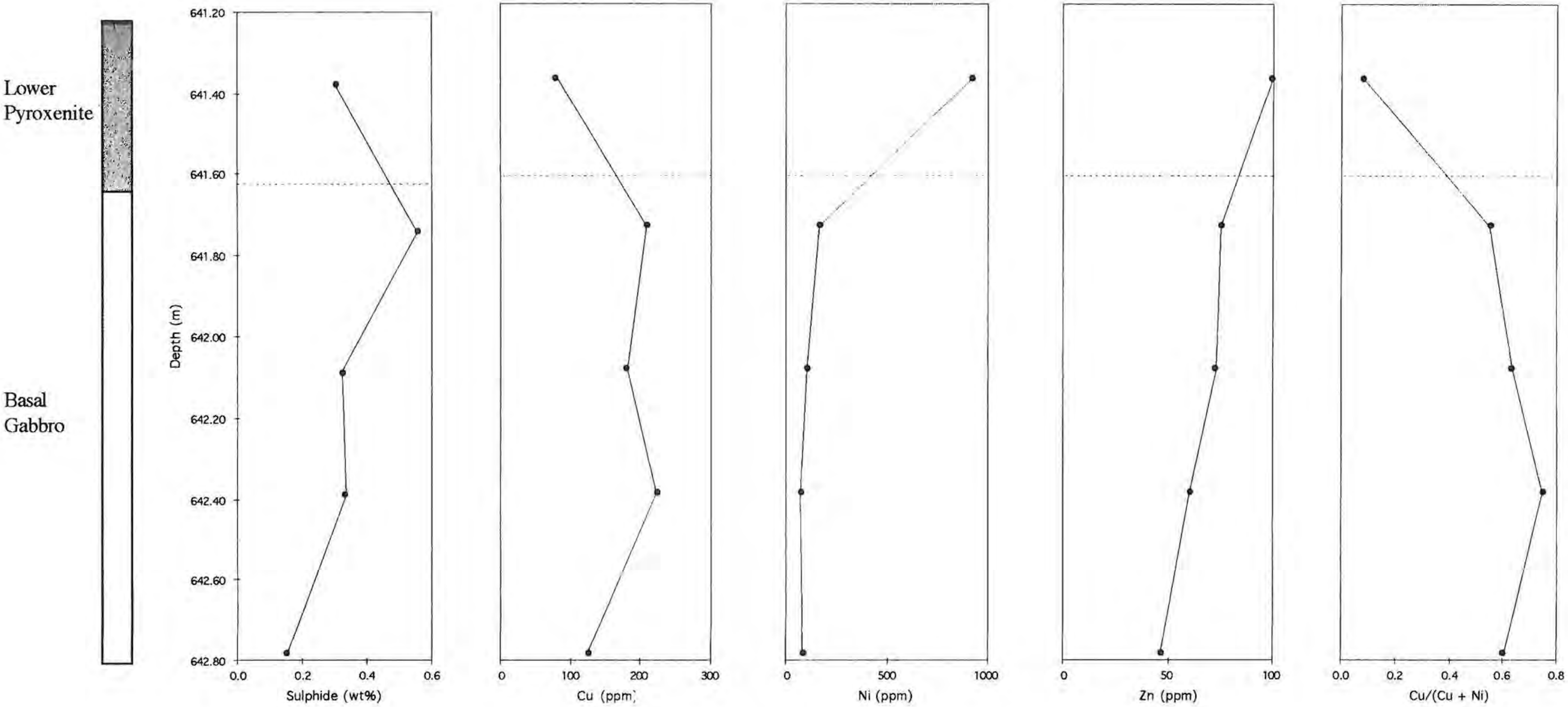

Figure 27 *Stratigraphic distribution of the base metals Cu, Ni, and Zn, as related to that of sulphide and the Cu/(Cu + Ni) ratio for borehole SH25.*

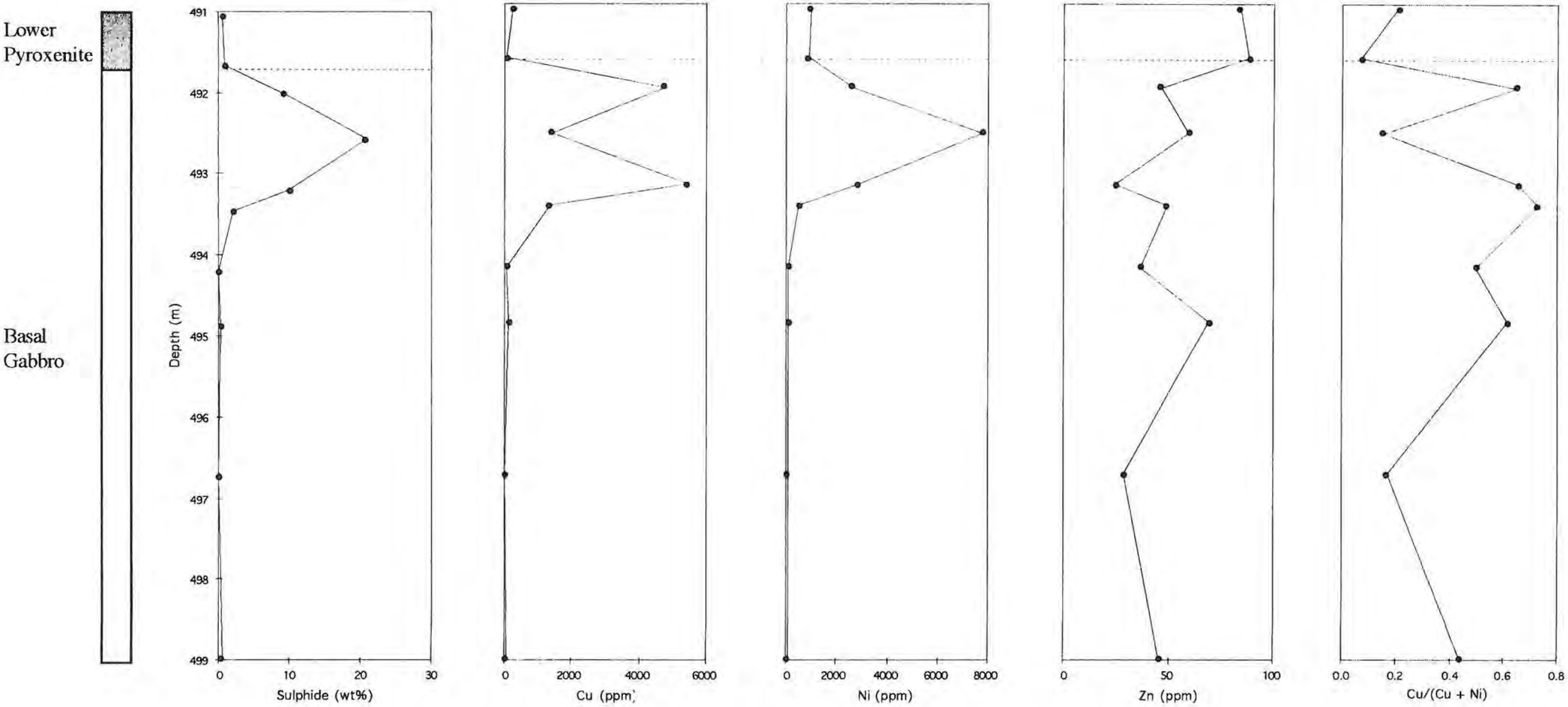

Figure 28 *Stratigraphic distribution of the base metals Cu, Ni, and Zn, as related to that of sulphide and the Cu/(Cu + Ni) ratio for borehole SH26.*

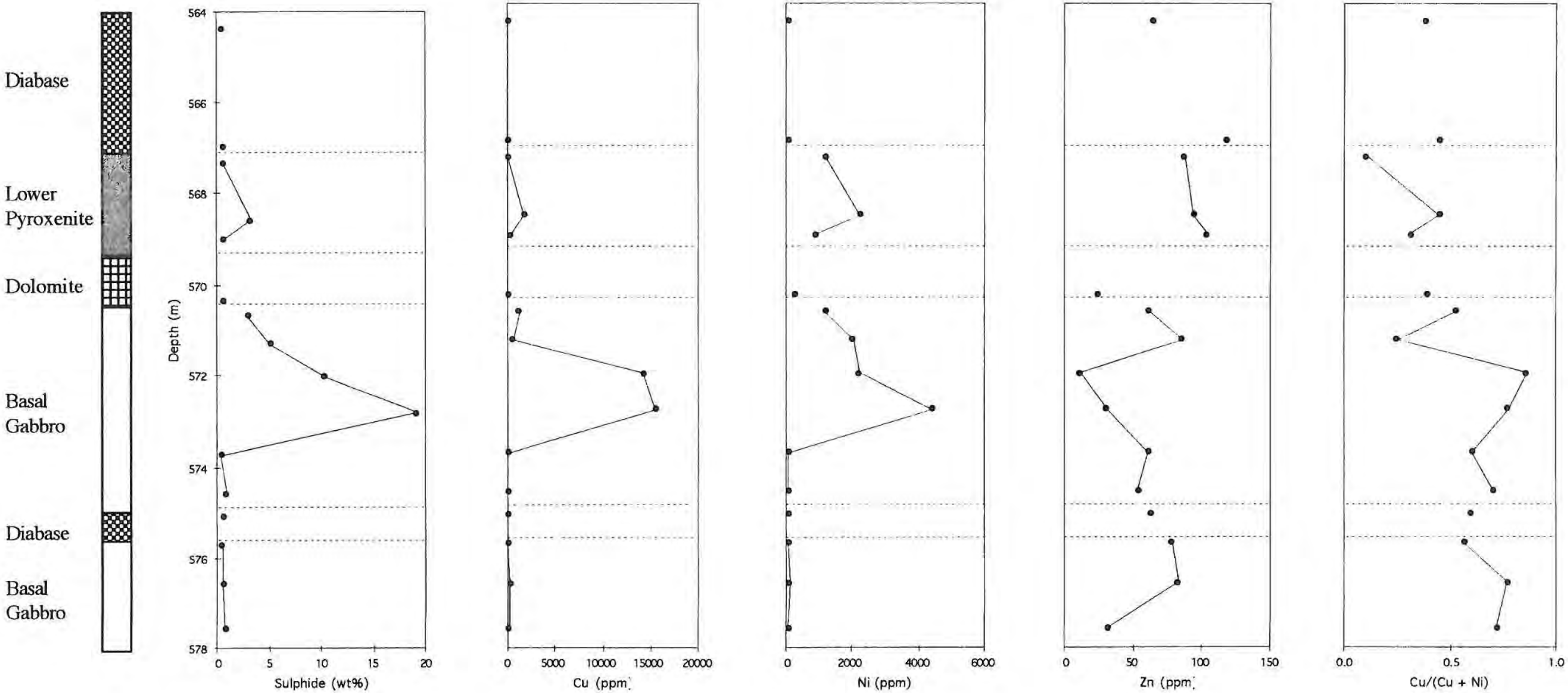

Figure 29 *Stratigraphic distribution of the base metals Cu, Ni, and Zn, as related to that of sulphide and the Cu/(Cu + Ni) ratio for borehole SH27.*

Sulphide values in SH8 (Figure 25) are elevated over the stratigraphic interval between about 460 m and 465 m below collar elevation, in which the maximum value is 11.74 %. Within this sulphide peak is a sample with very low values of sulphide, Cu and Ni, which is located at the logged contact between the Basal Gabbro below and the Lower Pyroxenite hybrid zone above. However, although the sulphide, Cu and Ni contents show a severe depletion at this point, the Zn content remains constant. This suggests that Zn is not hosted by the sulphides but is included in the silicate phases. Therefore this depletion represents the later remobilisation and removal of the sulphides. The relatively minor variations in sulphide content (< 5%) within the Lower Pyroxenite proper can be explained by the clustering nature of the sulphides which have been remobilised and concentrated in veins and fractures.

In boreholes SH10 and SH27 (Figures 26 & 29) there is a dolomite xenolith either at, or just below the contact between the Lower Pyroxenite and the Basal Gabbro. In both cases there is a large sulphide peak located about 1 m beneath the xenolith, with sulphide values up to 18.73 % (SH10) and 19.16 % (SH27). Above the dolomite xenolith in SH27 there is another sulphide peak in the Lower Pyroxenite, this is situated half a metre above the xenolith. In the case of borehole SH26 (Figure 28) where there is a less complicated section of Lower Pyroxenite above Basal Gabbro, a sulphide peak with a maximum value of 20.77 % sulphide occurs about 1 metre beneath the logged contact. Borehole SH25 (Figure 27) which was logged as unmineralised has sulphide values of less than 1 %, and thus displays no sulphide peak. However, it does show the same trend of increasing sulphide content upwards through the Basal Gabbro, followed by a decrease in the overlying Lower Pyroxenite.

The main points that can be made about the sulphide distribution, are:

1) there is a trend of increasing sulphide content upwards through the Basal Gabbro, followed by a decrease in the overlying Lower Pyroxenite.

2) Beneath dolomite xenoliths is a large sulphide peak, which is separated from the xenolith by a zone of low sulphide content.

3) Above the dolomite xenolith, is another smaller, displaced sulphide peak.

4) Where no xenolith is present the sulphide peak is situated at least 1 metre beneath the Lower Pyroxenite contact.

5.5.2 Base Metals

The stratigraphic distribution of the base metals Cu, Ni and Zn, as well as the Cu/(Cu + Ni) ratio, are shown in Figures 25 - 29. The extremely close correlation of Cu and Ni content with sulphur content, is evidence that these elements occur primarily as the sulphides chalcopyrite and pentlandite respectively. The base metal Co (not shown) has a very close correlation with Ni, and closely mimics the pattern displayed by Ni. This can be explained by the fact that Co readily substitutes for Ni in pentlandite (Ramdohr, 1980). Borehole SH25, which has low concentrations of sulphide (< 1%), and is unmineralised in the Basal Gabbro, shows the expected close correlation between Cu and sulphur content. However, the Ni content shows a trend more closely relating to that of Zn, suggesting that both Zn and Ni are hosted in silicate phases.

A selection of distribution coefficients for various silicate and oxide minerals is shown in Table 6. Values of 5, 1.5 - 5, and 3 are the distribution coefficients of Ni for spinel, orthopyroxene and clinopyroxene respectively, being the most likely phases containing the Ni. Concentrations of Zn in the Basal Gabbro and Lower Pyroxenite are in the order of approximately 100 ppm for all the analysed boreholes. Zn will largely substitute for Mn^{2+} and is therefore likely to be in any of the ferromagnesian minerals. Experimental results by MacLean and Shimazaki (1976) show that when there are coexisting silicate and sulphide liquids, Ni and Cu are strongly partitioned into the sulphide liquid, with Co being weakly partitioned into the sulphide liquid. Zn however shows a slight preference for the silicate liquid.

The relationship between Cu and Ni as shown by the Cu/(Cu + Ni) ratio in Figures 25 - 29, shows a broadly decreasing trend upwards through the Basal Gabbro. This is similar to the pattern displayed by the Mg#, and can therefore represents a reverse fractionation trend. The Cu/(Cu + Ni) ratio can be used to demonstrate remobilisation of the sulphides, based upon the higher mobility of Cu compared to Ni. This can be used as one of the possible means for explaining deviations from the broadly decreasing upward trend. Depletions in the Cu/(Cu + Ni) ratio relative to the trend, suggests that copper has been remobilised, whereas an increase relative to the general trend may be a result of the precipitation of coarse-grained chalcopyrite in fractures or interstitial spaces. At the contact between the Basal Gabbro and the "hybrid" Lower Pyroxenite in borehole SH8 where there is a depletion in sulphide content but no variation in Zn content, there is a corresponding decrease in the Cu/(Cu + Ni) ratio, further suggesting that remobilisation of sulphides occurred at this point.

	Olivine	Orthopyroxene	Clinopyroxene	Plagioclase	Spinel
Ni	10 (2) 3.5 - 3.8 (3) 3.4 - 4.8 (6) 5 - 20 (22)	1.1 - 3.1 (1) 4 (2) 3 - 5 (3)	2 (2) 2 - 4 (3) 6.5 (5)	0.01 (2) 0.2 (4)	5 (2)
Cr	0.2 (2) 2.7 (9) 3.1 - 10 (13) 0.25 - 25 (22)	2 (2)	10 (2) 20 (9) 40 (12)	0.01 (2) 0.1 (11)	
V	0.04 (1) 0.09 (3) 0.05 (9)	0.06 - 3.4 (1) 0.3 (3) 0.5 - 2.3 (8)	1.5 (3) 1.3 (9) 0.94 - 4.1 (12) 0.06 - 3.4 (14)		38 (1)
Co	1 - 7 (1) 3.1 (9) 4.8 (17) 3.6 (22)	1.2 (7)	0.5 - 2 (10) 1.7 - 4.9 (5) 1.2 (7) 1.2 (9)	0.1 (8) 0.026 (7) 0.01 - 0.09 (22)	3.4 (7)
Sc	0.37 (1) 0.33 (7) 0.25 (3) 0.15 - 0.02 (22)	0.53 - 1.4 (1) 3.3 (7) 1.1 (3)	3.1 (3)	0.017 - 0.065 (1) 0.08 (7) 0.01 (20) 0.01 - 0.08 (22)	0.048 (1)
Sr	0.003 (1) 0.001 (2) 0.1 (18) 0.01 - 0.02 (22)	0.018 (1) 0.01 (2)	0.07 (2) 0.1 (17)	2.2 (2) 3.06 (16) 1.75 (21)	0.01 (2)
Rb	0.001 (2) 0.01 (3)	0.004 (1) 0.0006 (15)	0.017 (1) 0.001 (2) 0.03 (17)	0.94 - 3.3 (18) 0.07 (2)	
Zr	0.01 (19) 0.015 - 0.1 (22)	0.03 (19)	0.12 (1) 0.2 - 0.7 (22)	0.01 (19)	
Cu	0.27 - 0.47 (1) 0.023 (7)	0.071 (7)	2.4 - 1.5 (1)	0.004 (7) 0.24 (5)	
Zn	1.8 (7)	0.49 (2)		0.13 (7)	

(1) Irving (1978), (2) Cox *et al.* (1979), (3) Frey *et al.* (1978), (4) De Long (1974),

(5) Ewart *et al.* (1973), (6) Leeman & Lindstrom (1978), (7) Paster *et al.* (1974),

(8) Jensen (1973), (9) Duke (1976), (10) Lindstrom & Weill (1978), (11) Walker (1970),

(12) Campbell & Borley (1974), (13) Flower (1973), (14) Ringwood (1970),

(15) Hanson (1977), (16) Drake & Weill (1975), (17) Hart & Brooks (1974),

(18) Phillpots & Schnetzler (1970), (19) Pearce & Norry (1979), (20) Salpas *et al.* (1983)

(21) Morse (1982), (22) Lemarchand *et al.* (1987).

Table 6 *A selection of information on distribution coefficients, taken from the literature. After Maier (1991).*

5.5.3 Incompatible Trace Elements

Trace (and minor) element geochemistry is a particularly valuable tool for examining the evolution of an igneous body. They are by their nature limited in concentration (<1000 ppm) and sensitive to processes such as fractional crystallisation, crustal contamination and magma mixing. Furthermore their low concentrations have permitted the accurate determination of partition coefficients for certain minerals (Table 6), allowing behavioural predictions to be made from various elements. The use of trace elements in this study are for two main purposes: firstly, to help confirm or reject the hypothesis that the sulphides in the Basal Gabbro are a magmatic feature, and have not been produced as a result of the alteration of Fe-rich silicates. Secondly, trace elements can help in further interpreting the evolution of the basal part of the Complex.

One of the characteristics that differentiate layered mafic intrusions from other types of igneous rock, is that cumulus minerals accumulate at the floor and expel the intercumulus (residual) magma. It is this characteristic that makes fractional crystallisation possible. Incompatible elements are those with low bulk distribution coefficients for the observed cumulus phases, and are thus fractionated into the residual magma. Therefore the concentration of incompatible elements can indicate the degree of fractionation of the rock, so that with increasing fractionation, the concentration of the incompatible elements will increase in the rock so long as the elements are not compatible with a cumulus phase (e.g. P with cumulus apatite). However, the concentration of the incompatible element is not solely controlled by the degree of fractionation, but also by the porosity of the rock in which the intercumulus liquid may crystallise (e.g.Wager, 1963; Henderson, 1968; Campbell, 1987). Furthermore, as the porosity of the cumulate rock increases the efficiency of fractional crystallisation decreases (Henderson, 1975). Therefore any trend in incompatible concentration is a function of the initial porosity of the cumulate rock and the degree of fractionation.

Five trace elements (Zr, P, Cr, V and Ti) have been selected to address the points outlined above. Zirconium (Zr) is an incompatible element which has extremely low partition coefficients for the primary cumulate minerals (Table 6). It thus becomes concentrated in the reidual melt, finally crystallising in the intercumulus spaces as zircon. In a normal fractionation trend the Zr content could therefore be expected to show an increase into the more fractionated rocks . Phosphorus (P) is typically found in higher concentrations than Zr, and may more correctly be classified as a minor element (0.1 - 1 wt%). Like Zr it is incompatible with respect to the cumulus minerals, and will concentrate and finally crystallise as intercumulus apatite. Therefore like Zr, in a normal fractionation trend there will be an increase in the P_2O_5 content in the more fractionated rocks. Chromium (Cr) is an element which is often enriched in the cumulus minerals of fractionated mafic-ultramafic bodies. As can be seen from Table 6 Cr is highly compatible with respect to olivine, orthopyroxene, clinopyroxene, and (not shown) spinel (chromite, magnetite, etc.). Therefore in a normal fractionation sequence Cr is rapidly depleted in the more fractionated rocks. Both vanadium (V) and titanium (Ti) are incompatible with respect to the major cumulate minerals. However, as can be seen from Table 6, they are highly compatible with spinels (V and Ti) and ilmenite (Ti). The Cr/V and Cr/Ti ratios have been used, as firstly, the ratio will be more sensitive to a change than the single elements, and secondly the effect of spinels (chromite and magnetite) on the trend will to some extent be balanced.

Figures 30 - 34 show the stratigraphic variation in the Zr and P_2O_5 content and the Cr/V and Cr/Ti ratios for the five boreholes. The Zr content shows a general trend which decreases upwards through the Basal Gabbro and into the Lower Pyroxenite in all the boreholes. This is the opposite to the expected trend for a normally fractionating magma body and suggests a reverse fractionation trend. Both SH25 and SH26 (Figures 32 and 33) show a slight increase in the Zr content near the base of the Basal Gabbro before displaying the reverse fractionation trend.

The P_2O_5 content also shows a reverse fractionation trend for boreholes SH10, SH8, SH25 and SH27. In borehole SH10 (Figure 31) this trend reverts to a normal fractionation trend (i.e. increasing P_2O_5 content) from about midway through the Lower Pyroxenite at a depth of approximately 393 m below collar elevation. The trend in borehole SH26 is more cryptic, with a decrease in P_2O_5 content corresponding with the increase in Zr near the base of the Basal Gabbro. There is also an erratic pattern in the vicinity of the Lower Pyroxenite - Basal Gabbro contact.

All the boreholes display an upwards increase in the Cr/V and Cr/Ti ratios, and thus display more evidence for a reverse fractionation pattern. In borehole SH10 (Figure 31), there is a peak in both the ratios, and then a decrease in ratios upwards. This suggests the onset of a normal fractionation pattern, corresponding with that shown by P_2O_5. There is a very distinct zone of elevated Cr/V and Cr/Ti ratios in borehole SH27 (Figure 34), which may be caused by the presence of chromite grains.

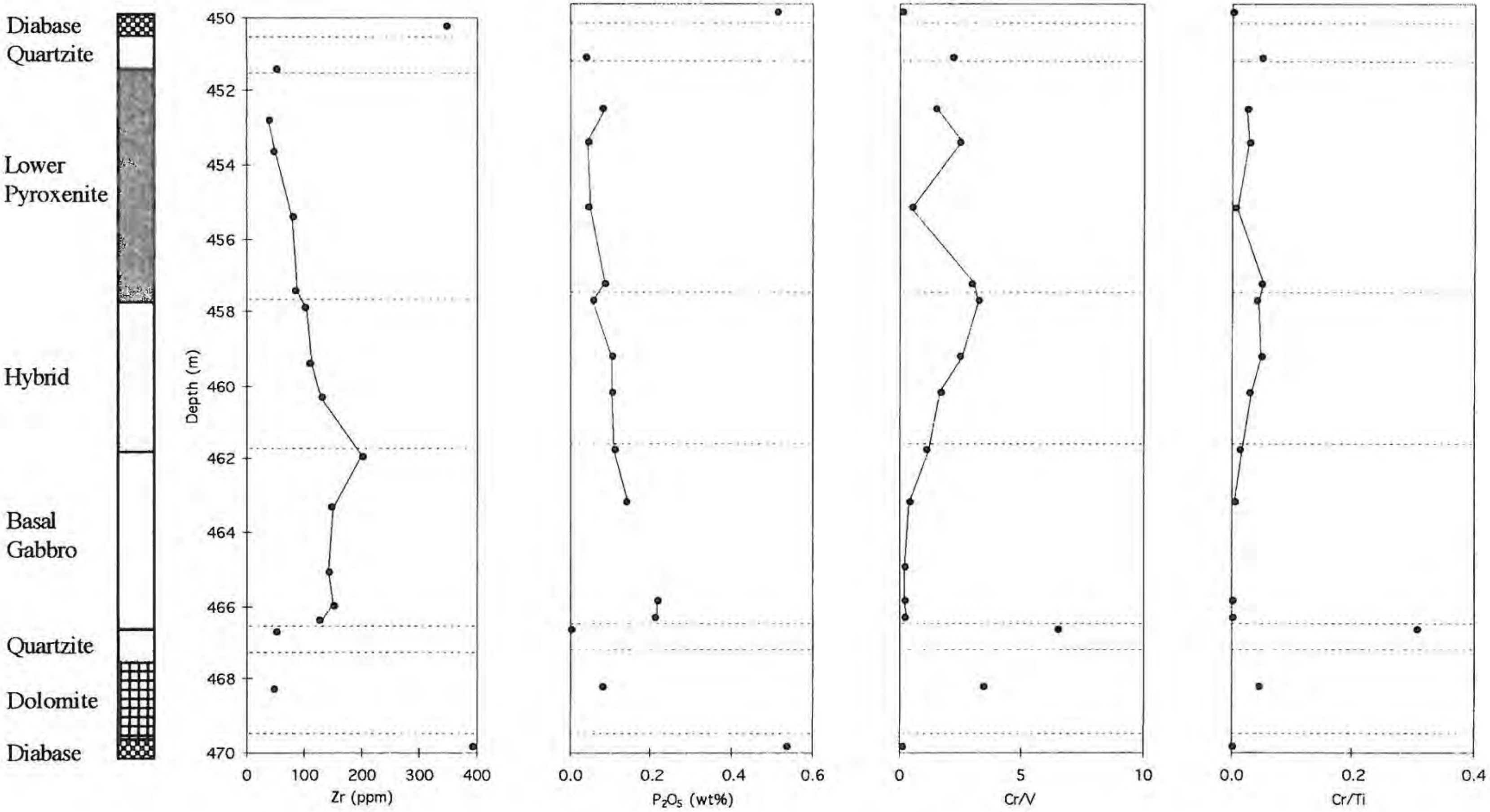

Figure 30 *Stratigraphic distribution of the trace elements Zr and P_2O_5 and the variation in the Cr/V and Cr/Ti ratios for borehole SH8.*

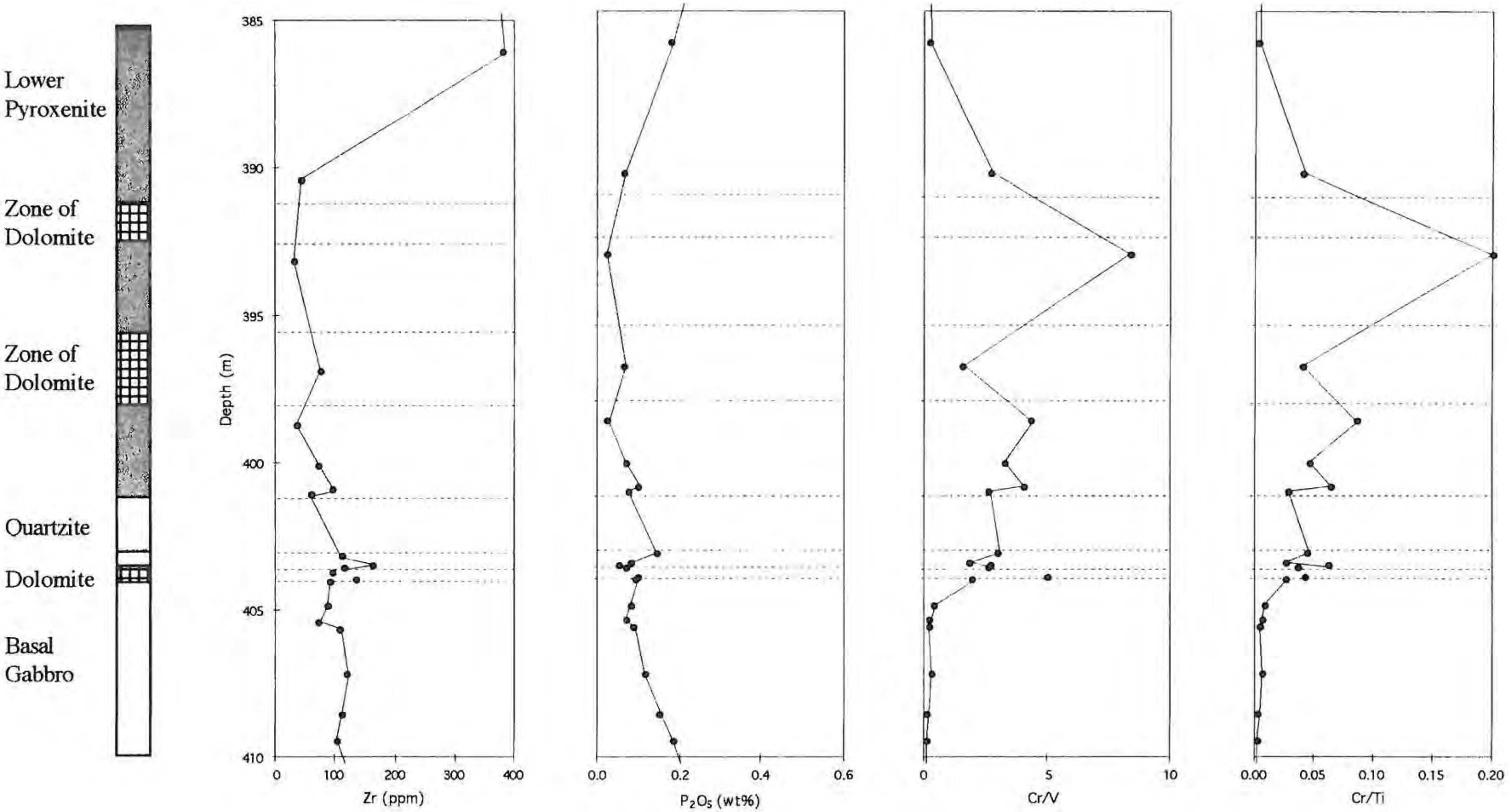

Figure 31 *Stratigraphic distribution of the trace elements Zr and P_2O_5 and the variation in the Cr/V and Cr/Ti ratios for borehole SH10.*

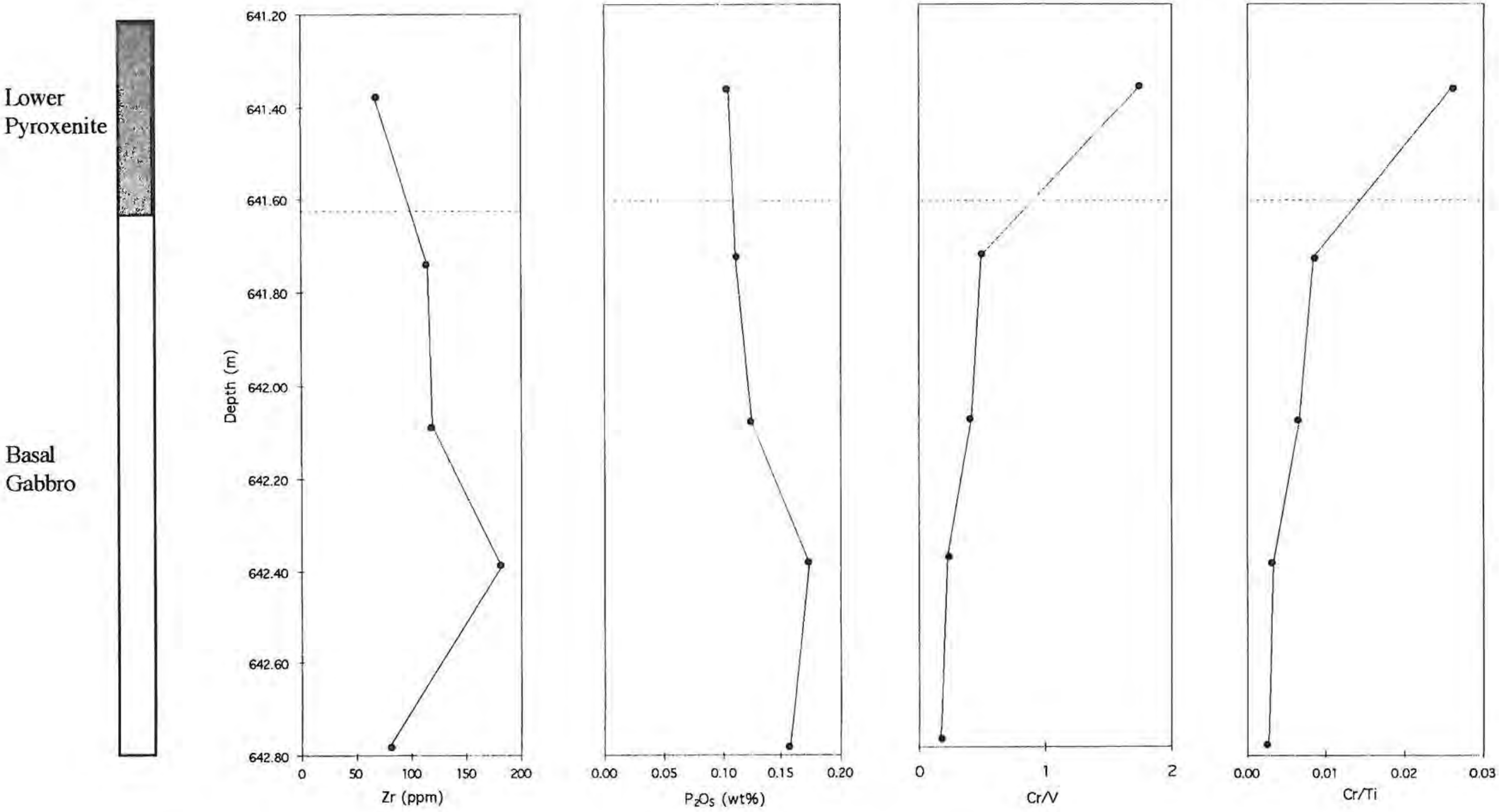

Figure 32 *Stratigraphic distribution of the trace elements Zr and* P_2O_5 *and the variation in the Cr/V and Cr/Ti ratios for borehole SH25.*

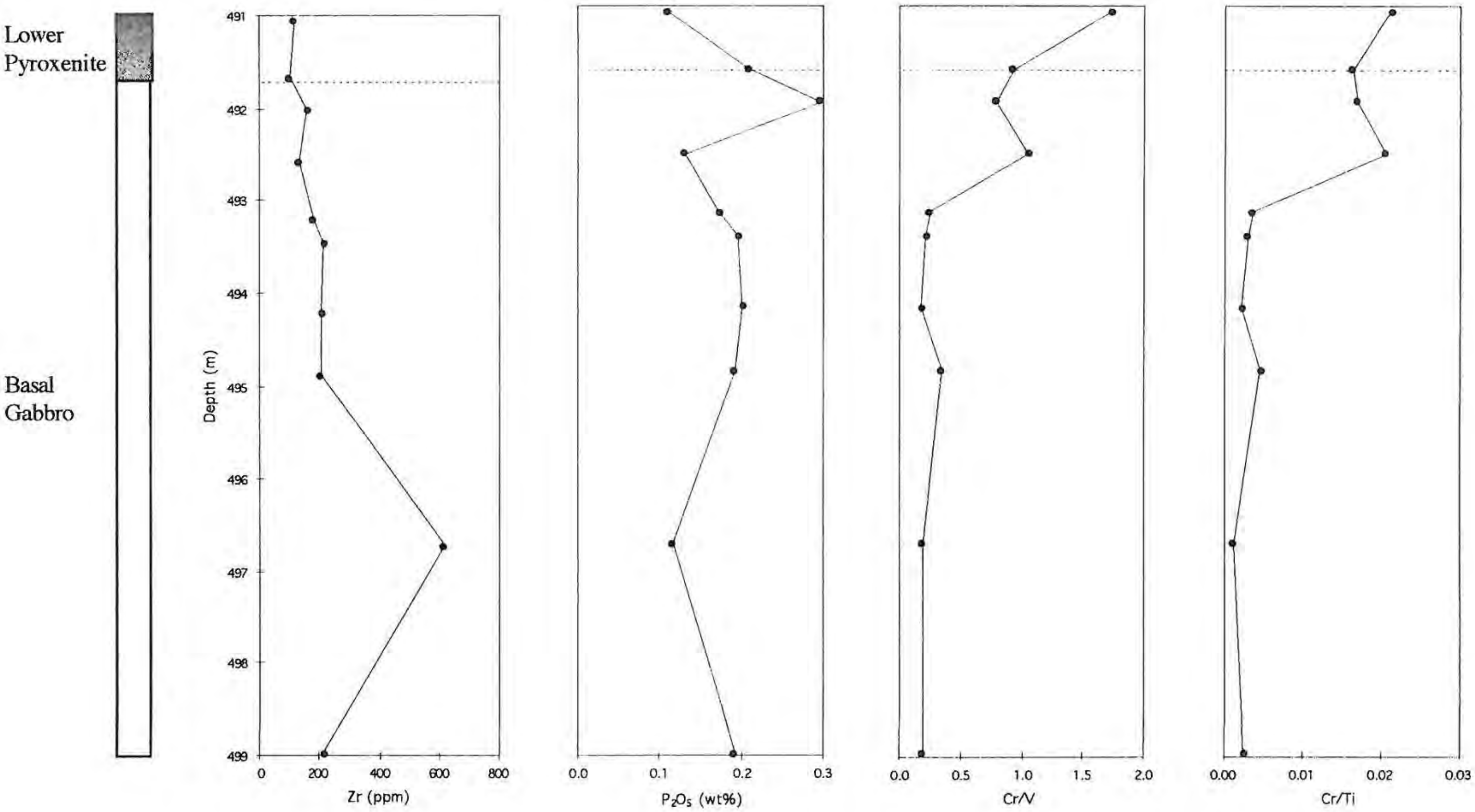

Figure 33 *Stratigraphic distribution of the trace elements Zr and P_2O_5 and the variation in the Cr/V and Cr/Ti ratios for borehole SH26.*

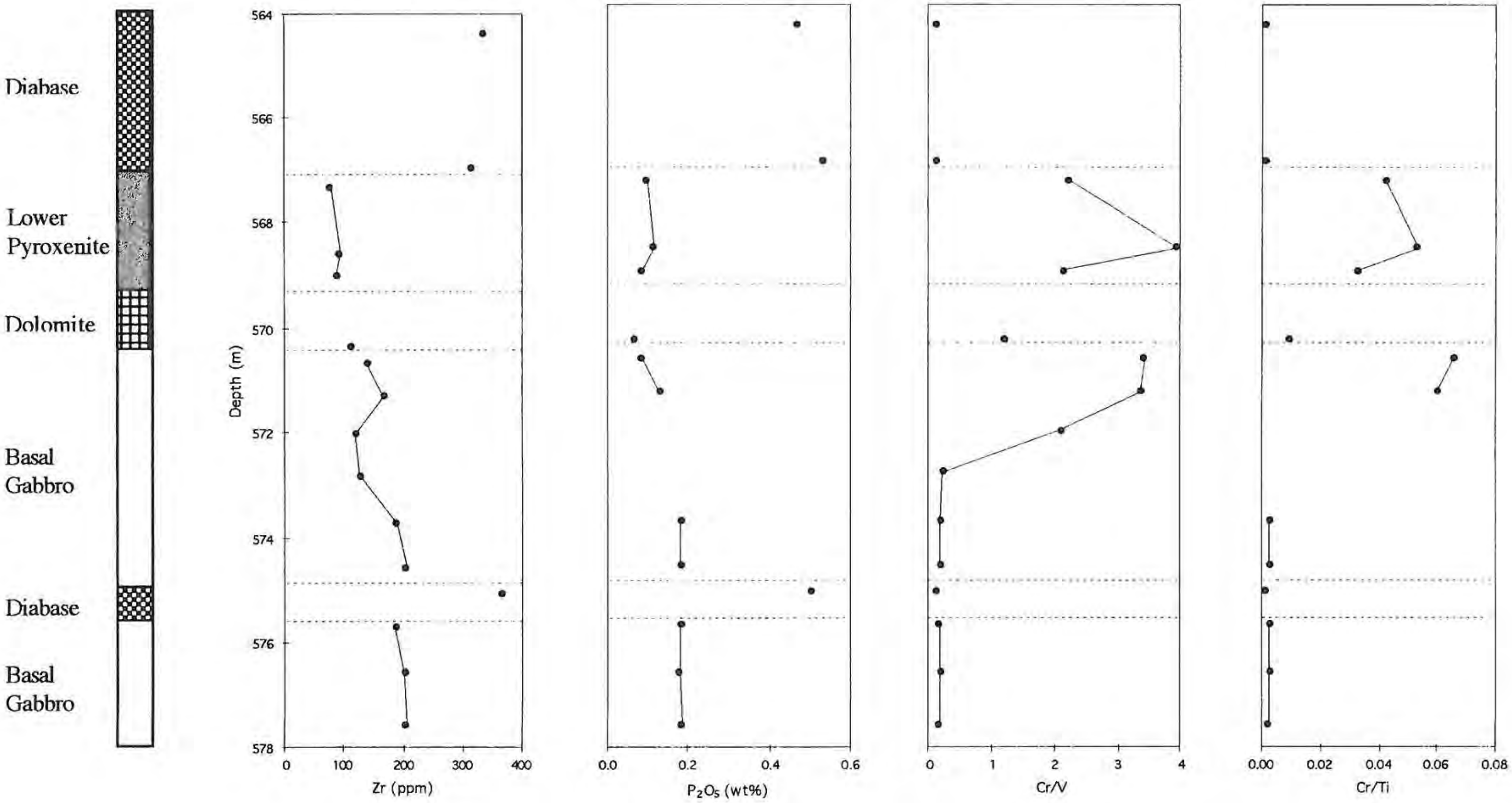

Figure 34 *Stratigraphic distribution of the trace elements Zr and P_2O_5 and the variation in the Cr/V and Cr/Ti ratios for borehole SH27.*

5.6 Discussion

The whole-rock geochemical trends that have been observed with respect to both major and trace elements, have consistently shown what has been referred to as a "reverse fractionation" trend. These trends all show either an upwards enrichment or depletion which contrasts against the expected trend produced by fractional crystallisation. However, there are several other ways in which these "reverse" trends can be produced. Firstly, they may represent the continual influx of magma from a fractionated magma chamber, so that the earliest influxes of magma are more evolved than the later influxes. This mechanism will be discussed in a later section.

An alternative process whereby the reverse trend can be produced is related to the intensive alteration of the Complex. The uralitisation of pyroxenes results in the increase of Mg, and hence a relative decrease in the Fe content. The effect of this is to increase the Mg#. When this process is combined with the fact that the alteration becomes more pervasive upwards through the Basal Gabbro, a mechanism is produced whereby the Mg# increases upwards as a direct result of the increased alteration. However, two problems exist with this mechanism being responsible for the observed trend. Firstly, the extent of alteration, if anything, becomes more pronounced upwards into the Lower Pyroxenite, but the Mg# begins to decrease. The second problem relates to the behaviour of the trace elements. Pyroxenes commonly contain between 3 - 5 % TiO_2, 2.5 - 4 % Al_2O_3 and 0.5 - 0.8 % alkalis, whereas hornblende commonly contains 10 % Al_2O_3, 2 % alkalis and rarely more than 2.5 % TiO_2 (Deer *et al.*, 1963).The uralitisation process therefore mobilises and disperses the incompatibles such as Ti, and scavenges elements such as Al and the alkalis. However, elements such as P_2O_5 and Zr, are not accommodated in the crystal lattices of either pyroxenes or amphiboles and hence uralitisation will have no affect on their distribution. This is evident by the fact that both P_2O_5 and Zr show reverse trends, which can only be a result of primary magmatic processes. Therefore, a hypothesis whereby the reverse geochemical trends are a product of the intense alteration can be rejected. Finally, as is suggested by this study, the "reverse fractionation" trend can be produced in the "chilling" of the magma. This will be discussed in more detail in a later section. A summary of the whole-rock compositions of the Basal Gabbro is shown in Table 7.

	Basal Gabbro					Chills	
	max	*min*	*median*	*Average*	*S.D.*	*Average*	*S.D.*
SiO_2	57.41	43.82	53.55	52.56	3.76	55.00	2.32
TiO_2	1.96	0.40	1.50	1.37	0.34	1.65	0.14
Al_2O_3	17.54	6.44	14.39	13.10	2.53	15.07	0.28
FeO	15.50	5.44	9.01	9.13	1.99	8.97	1.61
MnO	0.27	0.08	0.16	0.17	0.04	0.14	0.03
MgO	19.96	3.09	5.99	7.24	3.65	5.11	0.78
CaO	16.94	4.80	8.23	8.68	2.45	8.18	1.58
Na_2O	5.25	0.49	2.93	2.84	1.13	4.05	0.84
K_2O	11.11	0.31	1.13	1.46	1.71	1.23	0.38
P_2O_5	0.30	0.06	0.14	0.15	0.05	0.19	0.02
FeS	19.30	0.03	0.69	2.91	4.85	0.38	0.29
CuS	1.76	0.00	0.03	0.24	0.44	0.02	0.01
NiS	1.25	0.01	0.05	0.17	0.27	0.01	0.01
TOTAL	100.00	100.00	100.00	100.00		100.00	
Zn	110.20	11.40	69.05	64.60	22.44	55.92	28.07
Cu	15491.60	9.50	224.85	2536.02	4462.38	114.54	54.02
Ni	7790.10	47.20	389.15	1191.21	1711.66	86.56	30.15
Nb	27.45	3.76	8.83	9.69	4.17	10.73	2.36
Zr	615.08	74.28	134.99	156.51	85.32	146.50	60.11
Y	36.36	16.30	25.36	25.79	5.13	28.69	6.08
Sr	485.77	46.99	354.46	336.99	97.04	364.45	87.88
Rb	268.40	6.90	40.29	43.92	40.02	39.94	16.87
Co	426.70	12.00	57.20	93.68	87.16	37.06	11.97
Cr	742.10	6.90	70.90	173.63	201.45	41.30	6.48
V	317.50	36.90	217.00	210.37	52.60	227.74	26.00
Ce	67.80	29.86	42.73	45.25	10.67	46.81	11.37
Nd	37.68	14.89	23.29	24.13	5.52	26.29	5.94
La	25.66	5.45	15.21	15.90	5.45	17.24	6.00
Ba	3787.50	54.90	258.40	356.99	566.40	285.66	93.31
Sc	34.30	6.90	24.30	24.38	5.12	23.82	1.47
Th	16.21	0.13	3.35	3.52	2.78	1.75	1.84
Pb	20.86	0.74	5.45	5.97	4.14	2.56	1.06
S	73042.96	0.00	2320.56	10812.93	18762.62	1461.27	1024.42

Table 7 *Maximum, minimum, median, and the mean and standard deviation of the normalised compositions of the 40 samples of the Basal Gabbro. Also shown is the average and standard deviation of the five chilled margins*

5.7 Chemical Affinity to the Bushveld Complex

Many authors have suggested a relationship exists between the rocks of the Bushveld Complex and the Uitkomst Complex (Sharpe *et al.*, 1981; Kenyon *et al.*, 1986; Gauert *et al.*, 1995). Hatton and Sharpe (1989) analysed several types of sills in the vicinity of the Bushveld Complex, and concluded that the B1-micropyroxenite sills represent the parental magmas of the Bushveld Complex. On the assumption that the chill of the Basal Gabbro represents an approximation of the parental magmas of the Uitkomst Complex, Gauert *et al.* (1995) examined the relationship with the Bushveld Complex by comparing the rocks of the Basal Gabbro to the B1-micropyroxenite sills analysed by Hatton and Sharpe (1989). This initial comparison was based on nine samples of Basal Gabbro. Figure 35 shows a multi-element plot of the Basal Gabbro, based on 40 samples, which has been normalised to the compositions of the B1-micropyroxenite.

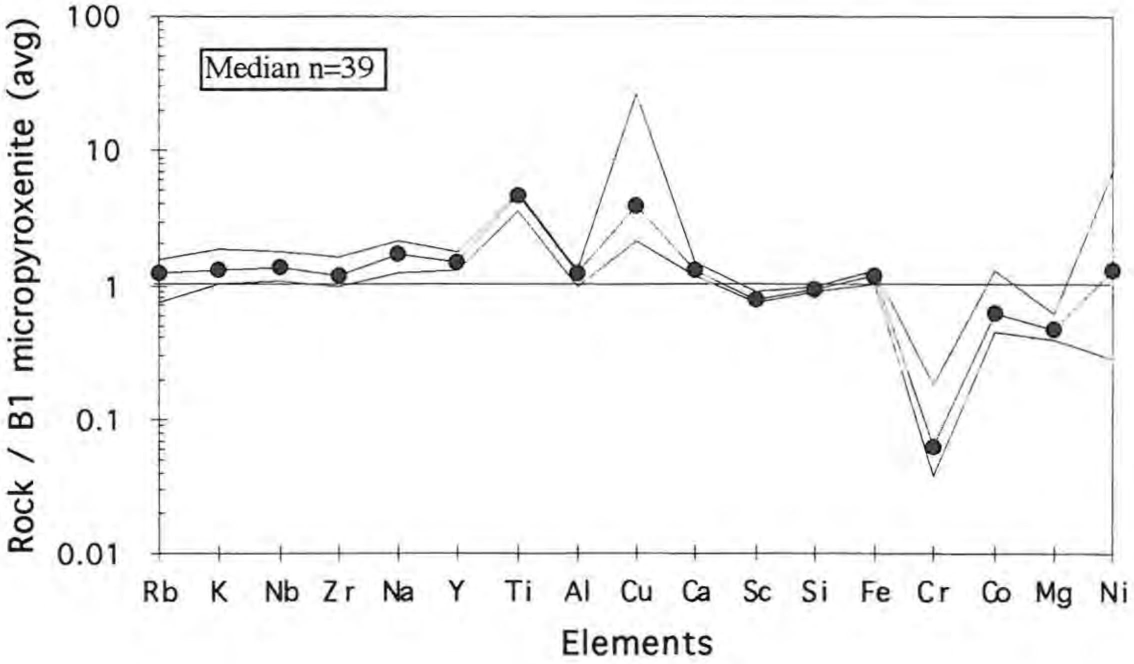

Figure 35 *Chemical composition of the Basal Gabbro normalised against the B1-micropyroxenite after Hatton and Sharpe (1989). Note the dots indicate median values and the lines on either side are the 25th and 75th percentile. The elements have been plotted to show a general pattern of increasing compatibility to the right of the diagram*

This plot shows a similar pattern to that produced by Gauert *et al.* (1995), and shows that the Basal Gabbro has very similar compositions to the parental magmas of the Bushveld Complex. However, the Basal Gabbro shows a very marked enrichment in Ti and Cu, and a strong depletion in the Cr and Mg content of the magma in relation to the B1-micropyroxenites.Therefore, the magma which crystallised the Basal Gabbro (thereby possibly being the parental magma the Uitkomst Complex) was a slightly more evolved magma than that from which the Bushveld Complex crystallised. However, on the basis of the close correlation for the bulk of the elements plotted in Figure 35, one can support a genetic link postulated by Gauert *et al.* (1995) between the Uitkomst Complex and the Bushveld Complex.

5.8 Diabase Sills.

Although the diabase sills are not part of the Uitkomst Suite, as they both intrude the igneous rocks of the Complex as well as the surrounding country rocks, they do have a similar macroscopic appearance to the Basal Gabbro, and will hence be examined briefly below. Seven samples of diabase sills were analysed for their composition. Of these, one sample was taken from the chilled margin of the sill. The results of these analyses are shown in Table 8, with their calculated average and standard deviation. When the sample from the chilled margin is compared to the average compositions of chills from the Basal Gabbro (Figure 36) it can be seen that the diabases show a marked enrichment in incompatible elements, and a depletion in compatible elements, as well as for Cu, Ni and Cr. The diabase sills therefore represent an even more evolved magma than the Basal Gabbro.

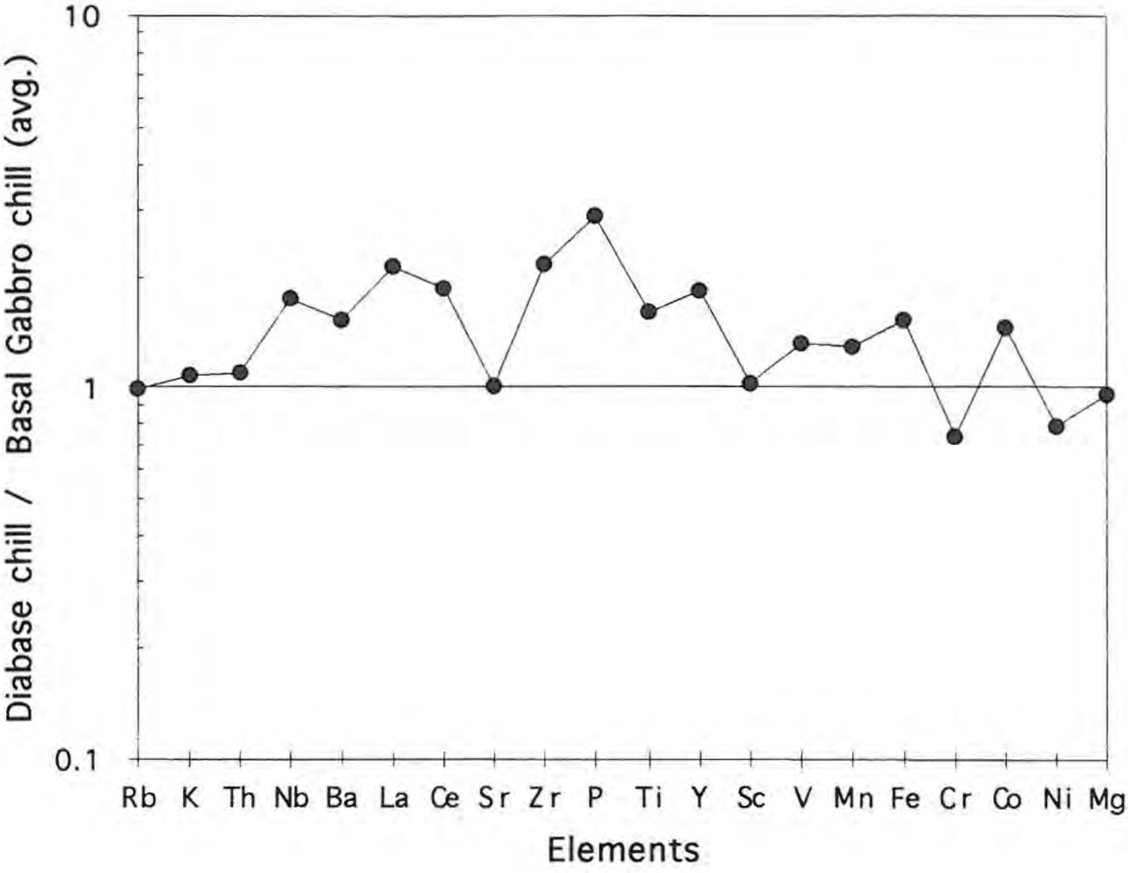

Figure 36 *Multi-element plot showing the relative enrichment in elements of the chill of the diabase in relation to the average chill of the Basal Gabbro. Note - there is a general increase in compatibility to the right.*

SAMPLE	SH8-12	SH8-17	SH10-16	SH10-17	SH27-13	SH27-14	SH27-16	AVERAGE	SD
Depth m	*450.24*	*469.86*	*422.40*	*371.70*	*564.40*	*566.98*	*575.07*		
						Chill			
SiO_2	50.68	51.68	52.10	50.24	50.72	49.90	51.78	51.02	0.84
TiO_2	2.51	2.71	2.48	2.45	2.43	2.63	2.48	2.53	0.10
Al_2O_3	14.74	14.99	14.76	14.81	14.61	14.70	14.68	14.76	0.12
FeO	13.25	11.30	12.64	13.39	13.25	13.73	12.04	12.80	0.86
MnO	0.18	0.34	0.17	0.19	0.16	0.18	0.17	0.20	0.06
MgO	4.63	5.06	4.26	5.20	5.05	4.91	4.53	4.81	0.34
CaO	7.66	7.06	7.56	7.94	7.75	8.17	8.09	7.75	0.38
Na_2O	3.61	3.82	3.36	3.24	3.39	3.35	3.68	3.49	0.21
K_2O	1.68	2.12	1.65	1.52	1.66	1.33	1.48	1.63	0.25
P_2O_5	0.52	0.54	0.53	0.47	0.47	0.54	0.51	0.51	0.03
FeS	0.516	0.250	0.478	0.522	0.473	0.537	0.536	0.473	0.102
CuS	0.009	0.096	0.008	0.011	0.009	0.009	0.015	0.022	0.033
NiS	0.010	0.024	0.009	0.015	0.014	0.011	0.010	0.013	0.005
TOTAL	100.00	100.00	100.00	100.00	100.00	100.00	100.00	100.00	
Zn	130.90	113.00	112.20	132.00	65.20	118.30	62.50	104.87	29.11
Cu	58.90	617.40	54.00	72.90	54.70	56.80	94.30	144.14	209.19
Ni	64.70	147.00	54.90	94.90	86.60	67.80	63.40	82.76	31.60
Nb	18.89	20.02	18.58	16.29	17.42	18.57	18.61	18.34	1.18
Zr	348.53	394.68	349.94	329.40	336.36	315.27	367.92	348.87	26.23
Y	52.25	51.84	52.56	46.76	48.82	52.49	52.64	51.05	2.32
Sr	347.29	378.70	354.64	412.79	370.56	368.69	358.13	370.11	21.61
Rb	51.03	80.37	56.06	47.34	57.96	39.64	53.52	55.13	12.69
Co	50.60	31.70	46.90	56.50	53.20	54.10	46.80	48.54	8.26
Cr	30.10	31.90	25.70	32.80	31.30	30.60	29.90	30.33	2.28
V	277.70	278.20	263.80	275.30	281.50	296.80	276.60	278.56	9.79
Ce	91.68	90.82	91.44	74.34	78.96	86.36	85.12	85.53	6.71
Nd	51.48	47.93	49.49	44.06	45.08	49.30	46.73	47.72	2.62
La	33.22	35.55	33.56	32.66	32.64	36.39	34.51	34.08	1.46
Ba	446.70	328.50	457.20	439.70	483.10	434.50	467.60	436.76	50.58
Sc	23.30	24.50	21.50	22.60	23.10	24.40	23.50	23.27	1.04
Th	3.94	4.14	4.75	2.29	2.91	1.93	3.30	3.32	1.02
Pb	3.14	17.74	5.30	8.89	2.47	2.09	2.30	5.99	5.72
S	1887.39	1269.83	1734.40	1925.65	1740.95	1962.66	1979.60	1785.78	248.19

Table 8 *Normalised compositions of diabase sills, showing the average and standard deviation of the values.*

Chapter 6: Petrogenesis and Metallogenesis of the Uitkomst Complex

6.1 Previous Work and Existing Models

The first report on the Uitkomst Complex was by Wagner (1929) who recorded a "big sill of highly altered pyroxenite carrying platinum in association with magmatic nickel-copper-iron sulphide. The occurrence in some respects bears a close analogy to those of Sudbury in Canada. The precise nature of the intrusion is not at present known". Wagner, however, regarded the Complex as being part of the Archaean Swaziland System.

Since Wagner's initial report, nothing was published on the Uitkomst Complex until the paper by Kenyon *et al.* (1986), resulting from exploration undertaken on the farm Uitkomst 541 JT by the Anglo American Corporation of South Africa between 1970 and 1976. On the basis of four main factors, Kenyon *et al.* (1986) interpreted the Uitkomst Complex as representing an inverted fractionation sequence. This model is now no longer valid, primarily due to the incomplete stratigraphy that was encountered on the farm Uitkomst. However, Kenyon *et al.* (1986) completed the first geochemical examination of the Complex, concentrating on the chromitites from the Ultramafic Chromitite zone (Chromititic Pyroxenite zone). Kenyon *et al.* (1986) interpreted the increasing $(Mg^{2+} \text{ x } 100)/(Mg^{2+} + Fe^{2+})$ ratio of chromite upwards through various chromitites as evidence for the inverted nature of the sequence. However, Arculus *et al.* (1974) show that the MgO content in chromite can be increased by either increasing the temperature, or more significantly, by increasing the oxygen fugacity of the magma, which could be achieved by contamination from volatiles released by the alteration of the numerous dolomitic and silicic xenoliths. In Figure 37 the ratios $(Cr^{3+} \text{ x } 100)/(Cr^{3+} + Al^{3+} + Fe^{3+})$ against $(Mg^{2+} \text{ x } 100)/(Mg^{2+} + Fe^{2+})$ have been plotted for the chromites from the Uitkomst Complex. Also depicted are the fields of values for the Upper and Lower Critical Zones of the Bushveld Complex, as well as the average composition of the Steelpoort and Leader chromitites (Kenyon *et al.*, 1986). From this diagram it is evident that the compositions of the Uitkomst chromitites are most similar to those of the Lower Critical Zone, although having slightly higher Fe^{3+} and MgO contents (Kenyon *et al.*, 1986). This suggests an affinity to the Bushveld Complex magmas responsible for the production of the Lower Critical Zone.

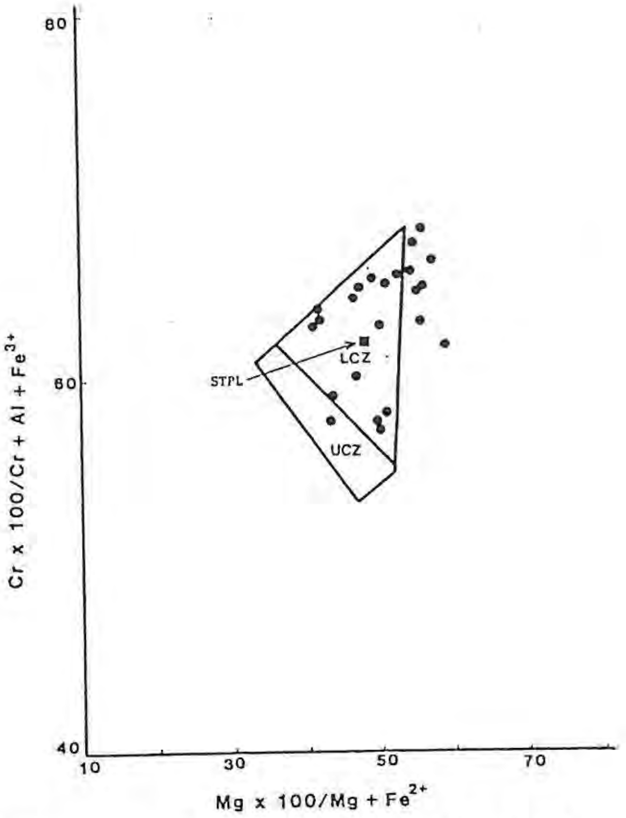

Figure 37 *Plots of Cr x 100/Cr + Al + Fe^{3+} against Mg x 100/Mg + Fe^{2+} for Uitkomst chromites as compared to Cameron's (1977) data for the Lower (LCZ) and Upper Critical Zone (UCZ) of the Bushveld Igneous Complex. Point "STPL" represents the average for the Steelpoort and Leader Seam Chromite. From Kenyon et al. (1986).*

The supposed genetic link with the Bushveld Complex was further supported by Sharpe *et al.* (1981), who proposed that the Uitkomst Complex represented one of several satellite bodies to the Bushveld Complex arranged concentrically around the Bushveld Complex. In this model, Sharpe *et al.* (1981) suggested that the seven feeders of the Bushveld Complex and its various satellite bodies lie on two elliptical traces (Figure 38) which represent two inverted conical fractures, produced by fracturing of the crust associated with mantle diapirism (Figure 39). These concentric ellipses are themselves broadly concentric to the assumed margins of the Transvaal basin, and their locus lies on the Great Dyke - Bushveld trend, with the feeders lying along, and being controlled by, regional basement lineaments (Sharpe *et al.*, 1981).

The geographical location, and the spatial orientation of the Uitkomst Complex in relation to the Bushveld Complex is also evidence for this relationship. The maximum predicted depth of the Rustenburg Layered Suite of the Bushveld Complex is 9 km. If the Uitkomst Complex, plunging at 8°, is projected back along its axis, it is calculated that it will attain a depth of 9 km at a horizontal distance of 65 km from where it plunges beneath the escarpment. Perhaps not so coincidentally, the measured horizontal distance between the Uitkomst Complex and the closest outcrop of the layered rocks of the Bushveld Complex is 65 km.

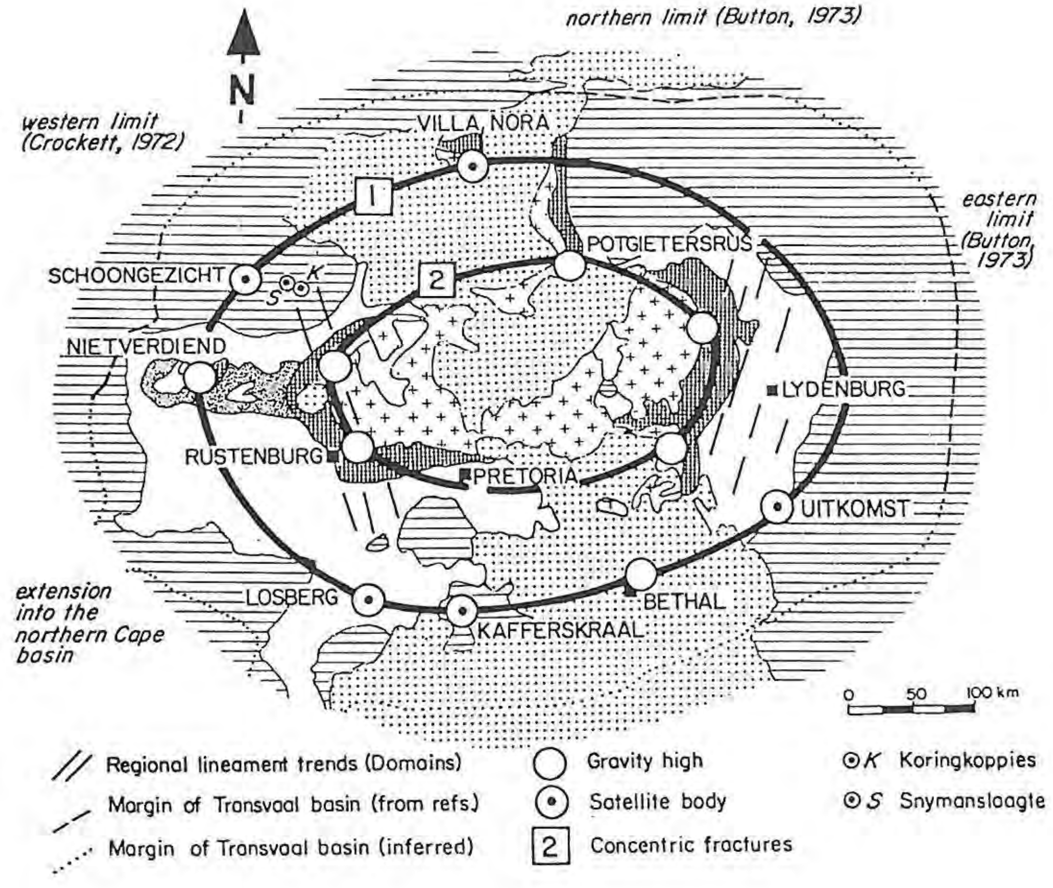

Figure 38 *The elliptical arrangement of feeder sites, satellite bodies and the supposed original concentric margin of the Transvaal basin. After Sharpe et al. (1981).*

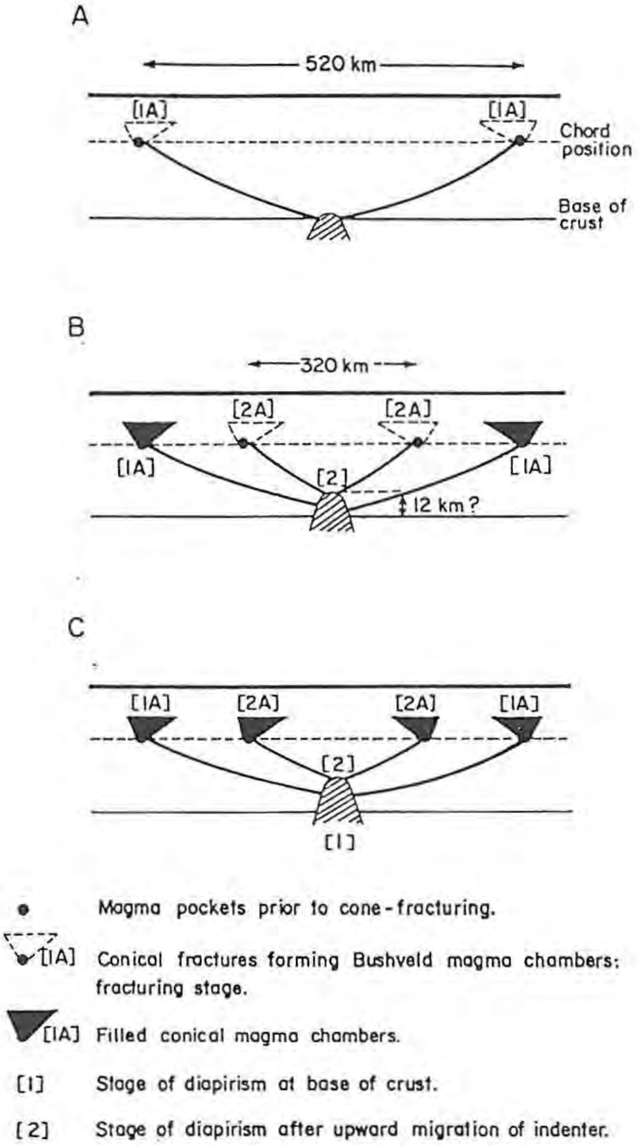

Figure 39 *A cartoon of the mechanism envisaged whereby two concentric fractures were formed in the crust by mantle diapirism. After Sharpe et al. (1981).*

The first complete study of the Uitkomst Complex has been the subject of a PhD by Gauert (submitted, 1995) at the University of Pretoria. Gauert *et al.* (1994) has suggested that the Uitkomst Complex represents a magma conduit intruded between two NW-SE-striking fracture systems. From a combination of whole-rock chemistry and the mineral chemistry of pyroxene, olivine and plagioclase, Gauert *et al.* (1995) suggest that an early contaminated pulse of magma formed the chilled Basal Gabbro, with the overlying Lower Pyroxenite representing a dense, sulphide-rich highly contaminated cumulate rock. Later pulses of uncontaminated magma precipitated the Peridotite zone, which on account of its almost constant composition, implied the existence of an "infinite" magma source and hence the movement of large quantities of magma through a conduit, rather than a large finite pool of magma from which it crystallised (Gauert *et al.,* 1995). Finally, near the top of the Peridotite zone, the flow of magma abated and gave rise to the closed-system conditions that produced the normal fractionating sequence of the Upper Pyroxenite and Norite units (Gauert *et al.,* 1995), complete with the abundant xenoliths from the roof rocks in the uppermost unit.

Gauert *et al.* (1995) have undertaken both S and Sr isotope studies of the Complex. The sulphur isotope studies were based on sixty-five samples of disseminated pyrrhotite, chalcopyrite, and pyrite from the Basal Gabbro, Lower Pyroxenite and Peridotite zones. The results of this study are shown in Figure 40, suggesting that magmatic sulphur ($\delta^{34}S$ close to 0 per mil) has been contaminated by sedimentary sulphur ($\delta^{34}S$ less than -10 per mil), with the chilled Basal Gabbro displaying a wide variation of sulphur sources (Gauert *et al.,* 1995). Gauert *et al.* (1995) postulated that one of the sources for the sedimentary sulphur may be pyrite from the shales of the Timeball Hill Formation.

The strontium isotope studies were based on 10 plagioclase separates from various rock units, and display a range of initial Sr-isotope ratios (R_0) at a model age 2,050 Ma, of between 0.704 to 0.715, and Rb/Sr ratios between 0.03 and 0.35 (Gauert *et al.,* 1994). The Basal Gabbro has variable to high R_0 values, as a result of contamination by the country rocks (Gauert *et al.,* 1995).

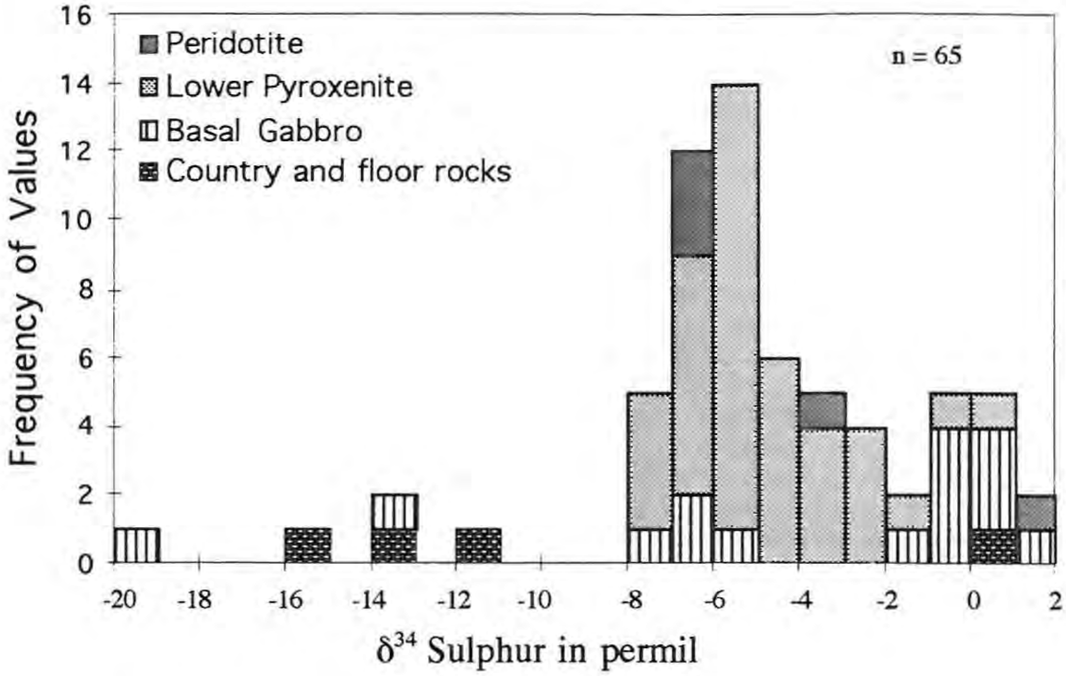

Figure 40 *Sulphur isotope ratios (in per mil $\delta^{34}S$) of pyrrhotite, chalcopyrite and pyrite separates from the Uitkomst Complex. Modified from Gauert et al. (1995).*

6.2 Evolution of the Uitkomst Complex

6.2.1 Basal Gabbro unit

The Basal Gabbro has been extensively examined in this study with respect to its petrology, mineral and whole rock geochemistry, all of which consistently indicate that it represents the chilled margin to the Uitkomst Complex. The various evidence for this conclusion will be discussed below.

The very nature of there being a "basal" gabbro is a common occurrence in layered intrusions world-wide. Gabbroic chilled margins have been reported from many mafic-ultramafic intrusions including: Insizwa in South Africa (Tischler *et al.*, 1981; Lightfoot and Naldrett, 1983, 1984; Lightfoot *et al.*, 1987), the Bushveld Complex (Frick, 1973), the Mt. Sholl-type intrusions in the Pilbara region of Australia (Mathison and Marshall, 1989), the Jimberlana Intrusion in Autsralia (Campbell, 1987), the Muskox Complex in Canada (Irvine and Smith, 1969), the St. Stephen Intrusion in Canada (Paktunc, 1989), and the Sudbury Irruptive (Naldrett, 1989). Tischler *et al.* (1981) and Lightfoot and Naldrett (1984) have suggested that the formation of a more evolved basal unit is the result of supercooling, whereby the viscosity of the magma is increased towards the contact. The gravitational settling of the higher temperature more mafic minerals such as olivine and pyroxene is thus impeded by the increasing viscosity (due to increased cooling) encountered with proximity to the margin.

The model outlined above relies on gravitational crystal settling as the fundamental process. An alternative model of compositional convection in the intercumulus material has been suggested by Tait *et al.* (1984) and Campbell (1987). This model utilises supercooling at the base of the intrusion with high heat loss through the floor. This causes the rapid cooling of the intercumulus magma and the early crystallisation of the intercumulus minerals with the cumulus minerals to form a fine-grained chilled margin. As one gets further away from the basal contact of the intrusion and the zone of crystallisation, the degree of supercooling is diminished, and the process of compositional convection in the intercumulus liquid becomes more dominant. The zone of crystallisation caused by the supercooling causes a lighter depleted fluid above, which convects upwards through the intercumulus melt, and is replaced by a denser undepleted melt from the overlying magma. Further into the intrusion, compositional convection ceases to be the main process operating within the body, as it requires crystallisation and high heat loss as a driving force, which becomes less readily available further into the body, as crystallisation releases latent heat, thereby reducing heat loss.

A "basal" gabbro can therefore be seen to represent an extended "chill zone", with a gradational upper contact to a more primitive, cumulate lithology. This gradational nature with the overlying unit is clearly seen between the Basal Gabbro and the Lower Pyroxenite, and is exemplified by borehole SH8, where the contact is of such a gradational nature, and the primary mineralogy has been obscured by alteration, that it is impossible to pinpoint a contact, and has been necessary to log the contact as a "hybrid" zone. This gradational nature of the contact is difficult to explain by any other mechanism, such as the Basal Gabbro being an earlier forerunner of the main intrusion, or alternatively, being a later sill.

The chilled margin theory is further supported by the petrology of the Basal Gabbro. Most obvious is the decreasing grain size observed towards the contact with the country rocks, suggesting that nucleation of crystals and the rates of crystallisation were increasing. Other textural evidence includes the presence of the mesostasis of quartz and feldspar suggesting a granophyric nature, and hence a rapid cooling and crystallisation of the melt. The paragenesis of the sulphides, with pyrrhotite containing possible inclusions of chalcopyrite is also indicative of a rapidly quenched magma (Ramdohr, 1980).

The geochemistry of the lower part of the Complex is strong evidence for the interpretation of the Basal Gabbro as representing a chilled margin. If the Basal Gabbro represented an earlier, independent intrusion, one would expect to see the effects of fractional crystallisation, such as an upwards decrease in the $Mg\#_{opx}$ in the mineral chemistry of the pyroxenes, as the crystallising magma was depleted in Mg and other compatible elements. However, the mineral chemistry of the pyroxenes shows virtually no variation upwards through the Basal Gabbro, and if anything a progressive increase in the $Mg\#_{opx}$ (Figure 7) , suggesting that the Basal Gabbro represents only a small part of a much larger intrusion of magma, with the Basal Gabbro being too small a section to display any coherent fractionation trend.

In general the whole-rock geochemistry, having been corrected for the presence of primary sulphides, shows smooth curves through the Basal Gabbro - Lower Pyroxenite contact zone, with no inflections or deviations, suggesting there is a continuity in the chemistry, and that the two units are in fact from the same original magma. The data from this study consistently show that for both major and trace elements, there is a reversed fractionation trend through the Basal Gabbro and into the overlying Lower Pyroxenite. The change in nature of the fractionation sequence seen near the base of the Lower Pyroxenite in the case of this study, to that of a normally fractionating body, is supported by Gauert (*pers. comm.*, 1995), who reports that the whole-rock Mg# of the Lower Pyroxenite decreases from 86 at the base, to 60 at the top of the unit. This pattern of a reversed fractionation trend at the base of the Complex reverting to a normal fractionating trend some distance above, is a feature described in many mafic-ultramafic intrusions, including Insizwa (Tischler *et al*, 1981; Lightfoot and Naldrett, 1983, 1984; Lightfoot *et al.,* 1984, 1987), Jimberalana (Campbell, 1987) Sudbury (Naldrett, 1989), and the Platreef in the Potgietersrus Limb of the Bushveld Complex (Buchanan *et al.*, 1981; Gain and Mostert, 1982; Hulbert and Von Gruenewaldt, 1982).

This geochemical pattern of a basal reversed fractionation trend can be explained by numerous models. Lightfoot and Naldrett (1984) proposed a model for the Insizwa Complex, whereby supercooling and subsequent increase in the viscosity inhibited the gravitative settling of cumulus minerals. A problem with this model was highlighted by Lightfoot *et al.* (1984), who recognised that at Insizwa the compositional variations in the basal gabbro are controlled by the settling of olivine into a low-Mg parent magma. Lightfoot *et al.* (1984) found that the olivine mineral chemistry was in contradiction to the model. If the model were correct then the first olivines to crystallise out would be expected to be the most Mg-rich, and would then display a normal fractionation trend. Their data, however, showed that the olivine mineral chemistry represented a reverse fractionation trend. A further problem with this model is that it relies on gravitative settling as the primary mechanism operational at the base of the intrusion. However it is now widely recognised that other mechanisms are at work within intrusions, including convection and compaction.

An alternative model was proposed for the Insizwa Complex by Lightfoot *et al.* (1984) whereby the olivine and associated minerals (such as orthopyroxene) crystallised and settled under equilibrium conditions in a vertical or subvertical feeder dyke, producing an upper fractionated zone depleted in olivine, and a lower zone enriched in Mg-rich olivine. Intrusion of this liquid along the bedding of the sediment would produce an initial coating of a more fractionated liquid, which with continued influx would become progressively less fractionated. There are however several problems with applying this model to the Uitkomst Complex, firstly, the basal gabbro in the Insizwa Complex is an olivine gabbro (e.g. Tischler *et al.*, 1981), whereas in the Uitkomst Complex the Basal Gabbro is dominated by orthopyroxenes. If these pyroxenes are assumed to have behaved in a similar fashion to the olivines at Insizwa, and been fractionated in a feeder dyke, then one would expect there to be a paucity of pyroxenes in the lower parts of the Basal Gabbro and for them to display a variation in composition. However, what is actually seen is that orthopyroxenes are common throughout (including the chilled margin) and show little to no compositional variation with height. Another problem with the feeder dyke model, is that unlike in the Insizwa Complex (Lightfoot and Naldrett, 1983) there is no evidence for a vertical or subvertical feeder nearby the Uitkomst Complex, but rather that it is a lateral conduit (Gauert *et al.*, 1995).

An alternative model invokes compaction of the crystal pile (Irvine, 1980; McKenzie 1984, 1985; Richter and McKenzie, 1984), whereby the lower density of the intercumulus melt in relation to the cumulus grains, creates an imbalance between the hydrostatic and lithostatic pressure gradients, resulting in compaction and an upward flow of the melt. However, Sparks *et al.* (1985) calculated that this mechanism should be an important factor in the evolution of large layered intrusions, but not in the evolution of small intrusions.

Considering the above discussions on mechanisms for generating reverse fractionation trends, it appears that the model of supercooling and compositional convection best satisfies what is observed within the Basal Gabbro in terms of petrology and geochemistry.

6.2.2 Ore Genesis

The presence of the large quantities of sulphides within the Basal Gabbro, is a not uncommon feature of basal gabbros in other intrusions such as the Insizwa Complex, Sudbury, etc.(e.g. Tischler *et al.*, 1981; Naldrett, 1989). However, the high Cu/(Cu + Ni) ratio that is associated with the Basal Gabbro relative to the Lower Pyroxenite, is somewhat unusual and seems to contradict the predicted sequence of Ni > Cu > Co > Fe > Zn, based on partition coefficients for the metals into the sulphide phase (MacLean and Shimazaki, 1976). However, this can be explained by examining the evolution of an immiscible sulphide in the Fe-Cu-Ni-S system. At high temperatures and depending on the oxygen fugacity (fo_2), magnetite is the first phase to crystallise out of the magma with a drop in temperature, this is followed closely by the separation of an immiscible sulphide liquid. The various mechanisms by which a magma can be induced to become saturated with respect to sulphur, and hence separate an immiscible sulphide liquid will be examined later. With a further drop in temperature, the immiscible sulphide liquid crystallises into a monosulphide solid solution (MSS) which at high temperatures is capable of containing all of the Ni, Cu and Co in solution (Craig and Kullerud, 1969). This MSS typically begins to crystallise from the liquid at 1150 °C, and is fully crystallised by 1100 °C, however the presence of magnetite can lower this temperature by 85 °C (Craig and Kullerud, 1969). As the temperature decreases the amount of Cu the MSS can carry decreases and by 850 °C an intermediate solid solution (ISS) Cu-rich phase may segregate from the MSS (Figure 41). By 970 °C chalcopyrite can first occur in a stable form. As temperatures continue to decrease, the MSS field shrinks and all the Cu is forced into the ISS, where it moves to the grain boundaries and forms crystals. Eventually as temperatures keep decreasing the Ni is driven out of the MSS and forms as pentlandite stringers and rims around grains (Craig and Kullerud, 1969). Finally by 150 °C , pentlandite forms flame-like exsolution textures in the MSS which crystallises as pyrrhotite. Kullerud *et al.* (1969) have shown that for the average compositions of Sudbury sulphide ores, over a temperature range extending from about 1150° to 865 °C, a mechanism exists in the Cu-Fe-S system whereby a relatively Cu-rich liquid may be segregated from a pyrrhotite-type phase. Furthermore their study suggested that a similar segregation of a Ni-rich liquid will only occur at temperatures above 1120 °C (Kullerud *et al.*, 1969).

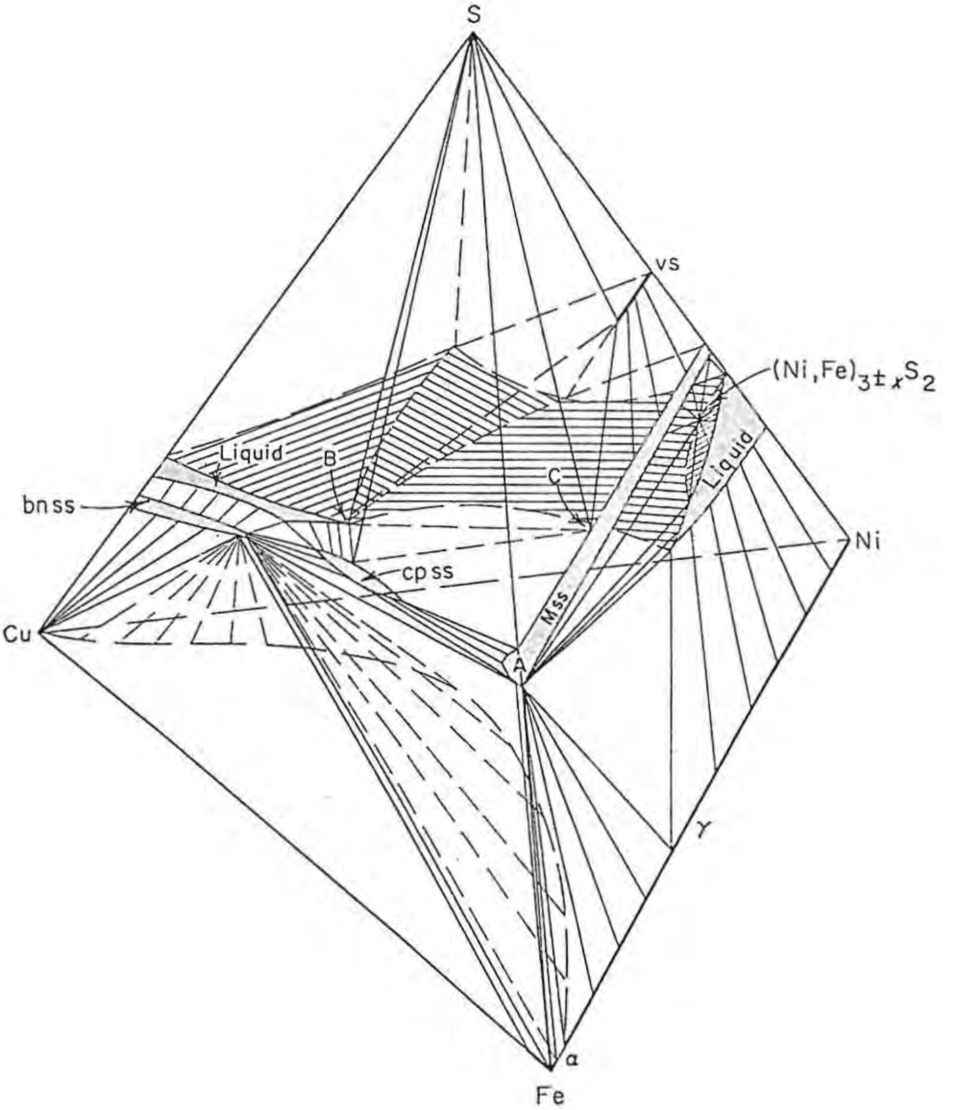

Figure 41 *Schematic 850° C isothermal diagram of the Cu-Fe-Ni-S system in the presence of vapour. Most tie lines to sulphur are omitted for clarity. Note that MSS spans the entire Fe-Ni-S face of the system, and that chalcopyrite is a stable phase. (After Craig and Kullerud, 1969).*

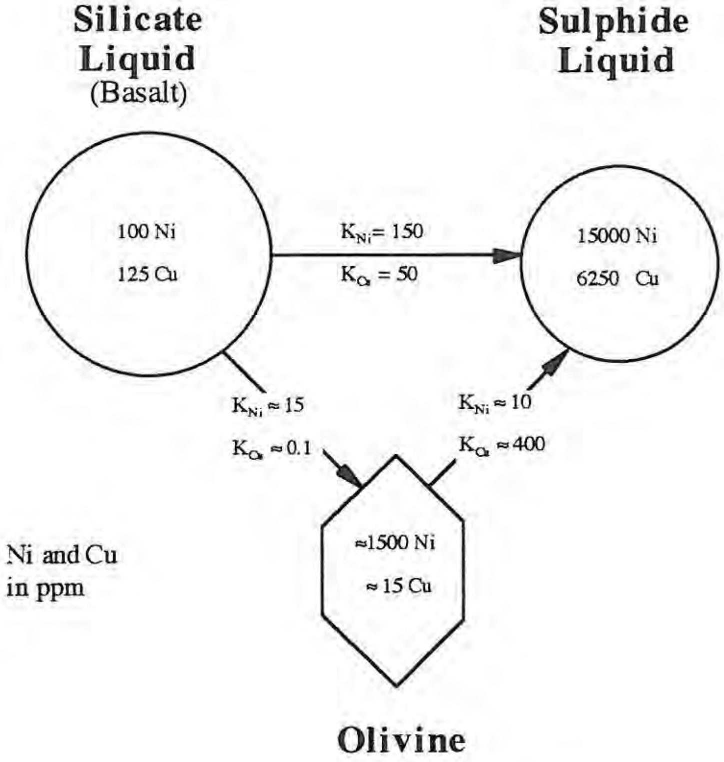

Figure 42 *Diagram showing the partitioning of elements between phases under equilibrium conditions. The presence of olivine does not affect partitioning between the liquids, but the precipitation of olivine may rapidly deplete the liquids in Ni and slowly enrich them in Cu. After MacLean and Shimazaki (1976).*

However, if the Basal Gabbro represents a chill, it may be expected that the Ni content should also be reflected in the whole rock compositions, as the MSS is capable of carrying all the Ni until the low temperature exsolution of pentlandite (Kullerud *et al.*, 1969). This problem can be explained by examining the partitioning of the metals with respect to different phases. MacLean and Shimazaki (1976) have shown that Ni partitions very strongly into olivine (Figure 42), and hence can be expected to have higher values in rocks with a high olivine content, which most usually are cumulate rocks. This will result in Ni being depleted relative to Cu in the residual silicate melt and hence also in any sulphide liquid formed at a later time. Rajamani and Naldrett (1978) showed that this is the case and that the more evolved rocks (as measured by the MgO content) show a decrease in Ni content with concomitant increase in the Cu content (Figure 43).

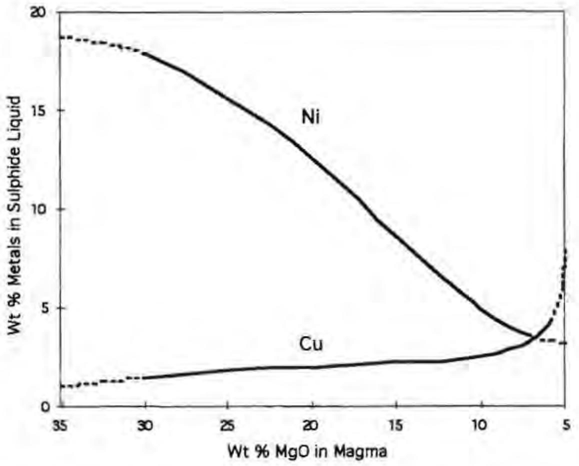

Figure 43 *Variation in the Ni and Cu contents of the sulphide liquid segregating from successive liquids of a fractionally crystallising komatiitic magma with weight percent MgO of these liquids. After Rajamani and Naldrett (1978).*

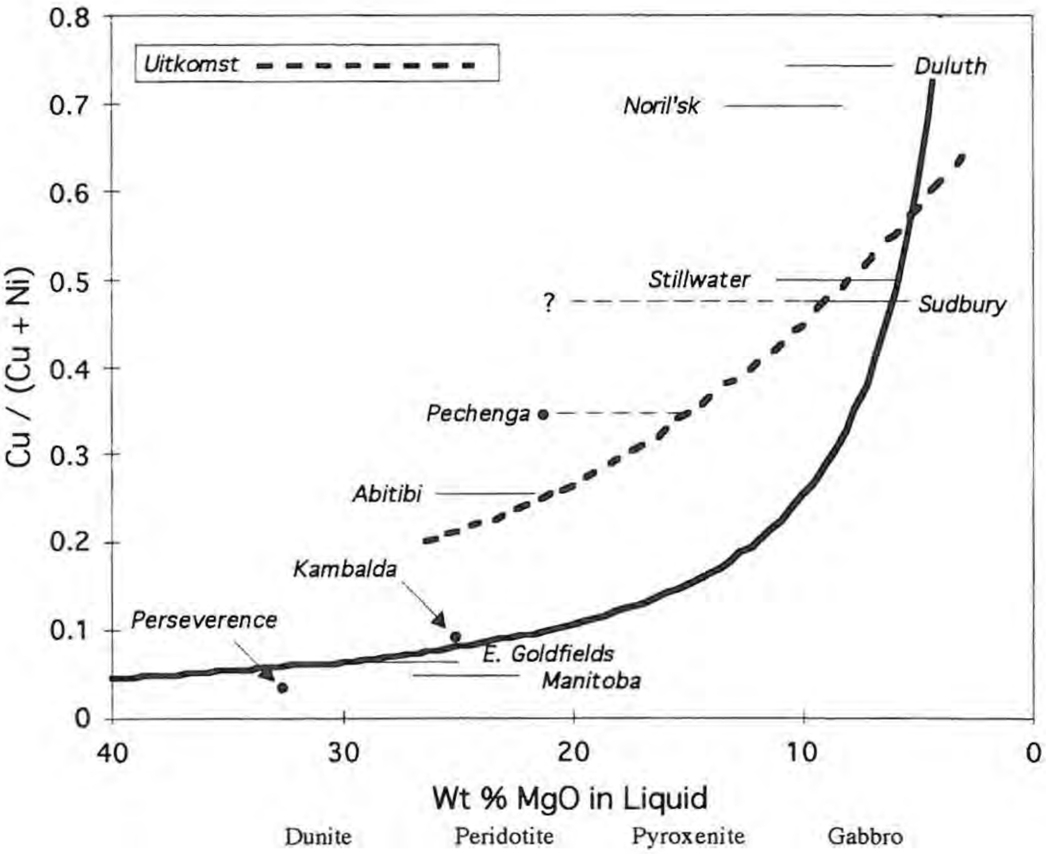

Figure 44 *Calculated relationship between the Cu/(Cu + Ni) ratios of sulphide liquids and weight percent MgO of komatiitic magma (Rajamani and Naldrett, 1978). The Cu/(Cu + Ni) ratio versus weight percent MgO of the lowermost units of the Uitkomst Complex has also been plotted. Superimposed on the diagram are the estimates of the relationship between Cu/(Cu + Ni) and weight percent MgO for several other ore bodies (Naldrett and Cabri, 1976).*

Therefore Rajamani and Naldrett (1978) predict that ore deposits in more evolved rocks will have a higher Cu/(Cu + Ni) ratio than those with more primitive rocks (Figure 44). With regard to the lowermost units of the Uitkomst Complex it can be seen that when the Cu/(Cu + Ni) ratio is plotted against MgO (wt%) (Figure 45), there is an inverse relationship between the degree of basicity and the Cu/(Cu + Ni) content of the rock, suggesting that it is the rock type which is controlling the Cu/(Cu + Ni) ratio.

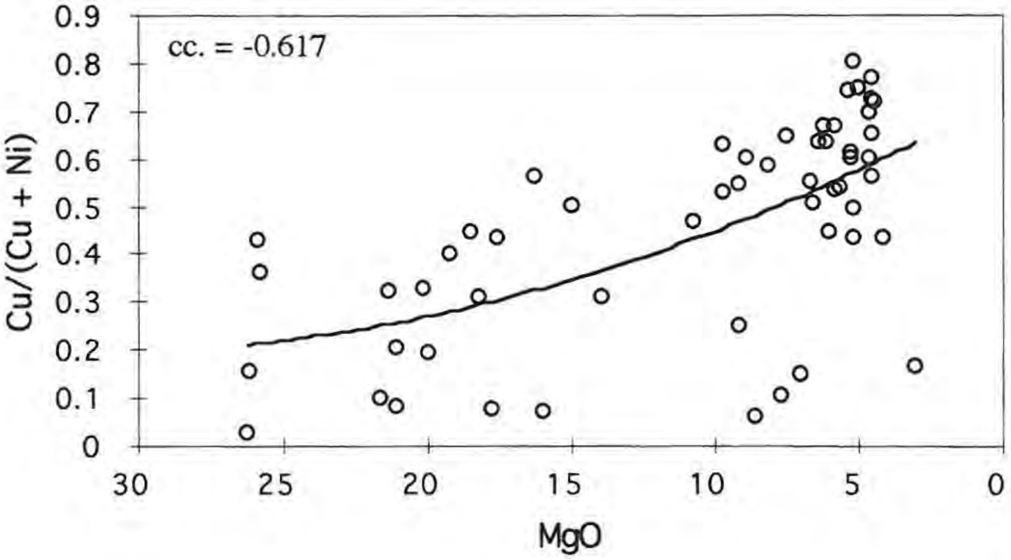

Figure 45 *Plot showing the correlation between the Cu/(Cu + Ni) ratio and the MgO content of the magma. This inverse relationship is what is predicted by Rajamani and Naldrett (1978).*

Figure 42 also indicates that Ni has a higher partition coefficient for the sulphide liquid than Cu, suggesting that when a sulphide liquid forms, the early sulphides will be enriched in Ni relative to Cu. Therefore Ni can be seen to be more compatible with respect to sulphides than Cu, and hence the Cu rich Basal Gabbro, in itself represents a reverse fractionation sequence. This "reverse fractionation sequence" with a decreasing Cu/(Cu + Ni) ratio in the Basal Gabbro is likely to be a result of the combination of two processes. Firstly it is a result of the inhibited settling, due to the increased viscosity, of Ni-rich sulphides from higher in the sequence. Secondly, it can be seen that the high Cu/(Cu + Ni) ratio in the Basal Gabbro is largely a function of the evolved nature of the rock, which itself is a result of the supercooling of an evolved parental magma for the lower part of the Complex. Therefore, the patterns seen in the metal and sulphide distribution within the Basal Gabbro further support the model that the Basal Gabbro represents a supercooled chilled margin.

Although this model explains the development of a Cu-rich base, it doesn't explain what causes the immiscible sulphides to segregate initially and scavenge certain chalcophile elements such as Cu and Ni from the silicate magma, forming concentrations of these metals as potentially economic sulphide deposits. There are a number of possible ways an immiscible sulphide liquid can be induced to separate from the silicate magma, all of which require sulphur to become saturated in the melt with respect to the sulphur-carrying capacity of the melt. Firstly, sulphur saturation can be attained by simply a decrease in temperature. Haughton *et al.* (1974) suggest that falling temperature also decreases the capacity of a basaltic liquid to dissolve sulphur by five to seven times assuming a constant ratio of oxygen fugacity (fo_2) to sulphide fugacity (fs_2). A second process whereby an immiscible sulphide liquid can be produced is by increasing the partial pressure of sulphur (fs_2) in the melt. Sulphur saturation can be exceeded and an immiscible sulphide liquid will be produced. The most usual way this can be achieved is by the addition of sulphur to the magma from an external source such as sediments rich in sulphur, like evaporites, or by the assimilation of sulphides.

Another mechanism which induces sulphide saturation is by either increasing the oxygen fugacity, thereby decreasing the ferrous iron (Fe^{2+}) content of the magma, and hence the sulphur-carrying capacity. The oxygen fugacity can be increased by means such as assimilation of water, diffusion of H_2 out from a magma, foundering of cooled, oxidised roof rocks from a magma chamber, and direct assimilation of oxygen (Haughton *et al.*, 1974). An alternative method of producing sulphur saturation is by the assimilation of SiO_2-rich material, for which sulphur solubility is lower than for mafic rocks, thereby reducing the sulphur solubility (Irvine, 1975). Finally, sulphide immiscibility may occur as a result of the fractional crystallisation of a silicate melt. This is due to the relative increase in sulphur in the melt, as it is not incorporated into any silicate mineral. Therefore by a combination of increasing the partial pressure of sulphur (fs_2) and the natural decrease in temperature, sulphide saturation will eventually occur. The fractional crystallisation of minerals such as pyroxene and feldspar, both of which are less iron-rich than the parent magma, will cause a relative increase in the Fe^{2+} content of the remaining magma, and hence shift the magma away from the point of sulphide saturation (Haughton *et al.*, 1974). By a similar process, the crystallisation of opaque oxides such as magnetite, chromite or ilmenite, will locally produce a zone of decreased FeO and hence push the magma beyond the sulphur saturation point (Haughton *et al.*, 1974).

There are two main possibilities which will be discussed below. The first possibility is that the sulphides in the Basal Gabbro are simply produced by a decrease in temperature, forcing sulphur saturation (Haughton *et al.*, 1974). The evidence for this is the very nature of the Basal Gabbro representing a chilled margin. The second possibility is that sulphide immiscibility was induced by contamination from the wall rocks and, more importantly, the numerous xenoliths. This has been proposed as the mechanism of formation for both the Platreef in the Potgietersrus Limb of the Bushveld Complex (Buchanan *et al.*, 1981; Gain and Mostert, 1982; Cawthorn *et al.*, 1985; Barton *et al.*, 1986) as well as many of the sulphide deposits within the Sudbury Irruptive (Irvine, 1975; Naldrett, 1989). As mentioned earlier the xenoliths and country rocks in the immediate vicinity of the basal portions of the Complex, consist primarily of Malmani dolomites, quartzites and chert. By the assimilation of quartzites and chert the carrying capacity of the magma for sulphur will be considerably reduced, prompting immiscibility (Irvine, 1975). The assimilation and alteration of the dolomite give rise to reactions producing carbon dioxide and water, thereby increasing the oxygen fugacity, causing a reduction in the FeO content, and thus precipitating sulphide (de Waal, 1977). Furthermore, de Waal (1977) has suggested that this may also involve the dissolution of silicates still close to their crystallisation temperatures, due to a slight increase in volatile constituents, and thus create spaces in which the sulphide can accumulate as well as permit the development of pegmatoids. The abundance of xenoliths combined with the high variability in the sulphur isotope ratios attained by Gauert *et al.* (1995), suggests that contamination was extensive in the Basal Gabbro, and hence favours a contamination model for the prime cause of sulphide saturation. The source of the sedimentary sulphur component may have been the pyritic shales of the Timeball Hill Formation as suggested by Gauert *et al.*, (1995). A model for the genesis of the sulphides in the lower part of the Uitkomst Complex is outlined below.

With the emplacement of the highly contaminated basal portion of the Uitkomst Complex, supercooling began around the margins. The supercooling associated with the chilled margin initiated the precipitation of magnetite and ilmenite, which in turn, combined with temperature and contamination induced sulphurisation, locally lowered the sulphur solubility and precipitated sulphides (Haughton *et al.*, 1974), thus accounting for the small minor disseminations of sulphide seen in the chill. However, due to the rapid crystallisation and increased viscosity, sulphides were unable to settle into the chill zone. Higher up in the Basal Gabbro, where crystallisation was taking place at a slower rate, reaction of the magma with the dolomitic and SiO_2-rich xenoliths created an oversaturation of sulphur, and the segregation of an immiscible sulphide. In the rims around the xenoliths, silicates were partially resorbed, creating spaces in which pegmatoids and skarn mineralogy developed. These spaces also enabled the gravitational settling of sulphides, accounting for the zones of sulphide depletion seen around the xenoliths. As the sulphide formed near the base of the intrusion, it could not chemically process the entire magma column and only depleted the lowermost layer in Cu and Ni (Tischler *et al.*, 1981). Further up in the more mafic Lower Pyroxenite, fractional crystallisation commenced, and the magma continued to assimilate the xenoliths, keeping the sulphur saturation high, and continuing to precipitate sulphides.

An alternative model that an immiscible sulphide had formed prior to the emplacement of the lower portion of the Complex, such as has been suggested for the Insizwa Complex (Lightfoot *et al.*, 1984), can be rejected on the grounds that within the chilled margin of the Basal Gabbro, there is an extremely low sulphide content.

6.3 General

6.3.1 Alteration

One major characteristic of the Uitkomst Complex is the extensive alteration of the primary mineralogy. The types of alteration seen (uralitisation, saussuritsation etc.) are all indicative of large quantities of water permeating through the rock. The source of the waters are likely in part to be magmatic, but the Sr-isotope data (Gauert *et al.*, 1995) suggest a high amount of contamination. Therefore the water can be from two external sources; firstly the assimilation of sedimentary xenoliths. Gain and Mostert (1982) postulated that in the Platreef of the Potgietersrus Limb of the Bushveld Complex, the numerous dolomitic xenoliths were initially subjected to prograde metamorphism which released CO_2 and H_2O into the magma, and possibly sulphur. They considered that the CO_2 was more readily absorbed into the magma, and the H_2O remained and subsequently caused the retrogressive alteration. The second external source of the water could be circulating meteoric water. Harrigan and MacLean (1976) have suggested that the alteration of gabbro dykes in Matagami, Quebec, is due to the thermal gradient caused by the intrusion, driving hydrothermal convection systems, and hence introducing large quantities of meteoric water into the body causing the alteration. The same mechanism is postulated to have been partially responsible for the alteration in the Uitkomst Complex, being complemented by water released from the assimilation of sedimentary xenoliths, and possibly a minor magmatic component. The likely sequence of alteration is as follows. Firstly, with intrusion of the Complex water would be primarily of magmatic origin. As xenoliths were assimilated, sedimentary water would have been released into the system, mixing with the magmatic water and generating a magmatic-hydrothermal system. This stage of alteration would have been responsible for the skarnification and serpentinisation seen in proximity to the xenoliths. As the Complex cooled, it would have been invaded by circulating meteoric water, being driven by the thermal gradient. This meteoric water would have been responsible for the second, pervasive stage of alteration responsible for the large scale uralitisation and saussuritisation seen throughout the Complex. Therefore, the alteration seen in the Uitkomst Complex is a result of a continual process whereby an early, localised skarnification phase was gradually replaced by a later, pervasive meteoric phase.

The large scale introduction of water will have had extensive effects on the stress regime both within and outside the cooling body. The hydration of anhydrous minerals is accompanied by a significant volume increase, generating considerable stress, which would have been accommodated by fracturing and shearing within the Complex and the surrounding rocks. Evidence for this is the numerous faults seen within the Complex, as well as the presence of the sheared contact between the Basal Gabbro and the country rocks seen underground in exploration drives. These fractures will have served as conduits for the transportation and remobilisation of sulphides and explain the sulphide-filled veins and fractures seen in drill core, as well as the development of massive sulphide bodies within the footwall and the country rocks.

6.3.2 Relationship to the Bushveld Complex

A relationship between the Uitkomst Complex and the Bushveld Complex has been suggested by several authors (Sharpe *et al.*, 1981; Kenyon *et al.*, 1986; Gauert *et al.*, 1995). Geochemical evidence has been produced by Gauert *et al.* (1995), and supported by this study (Figure 35), suggesting that the parental magma of the Uitkomst Complex, represented by the chilled margin of the Basal Gabbro, is similar in composition to the B1-micropyroxenites of Hatton and Sharpe (1989) which are widely regarded as representing the parental magma of the Bushveld Complex. Therefore on account of the age, geographical location, and geochemistry of the Uitkomst Complex, there is strong evidence to support a close genetic relationship with the Bushveld Complex.

6.4 Implications and Final Comment

On the basis of this study and on the work by Gauert *et al.* (1995), a petrogenetic model is suggested for the Uitkomst Complex. The first magma to be introduced was emplaced between two faults in a NW-SE striking direction, being controlled by regional lineaments. The magma exploited the unconformable contact between the Black Reef Quartzite Formation and the Malmani Subgroup, stoping upwards and assimilating the overlying dolomite and shale. The first magma was of an evolved composition (low MgO and high SiO_2 content) and is represented by the chilled Basal Gabbro, being the supercooled, Cu-rich margin of the lower units of the Complex. The assimilation of the dolomitic and quartzitic sediments increased the oxygen fugacity (fO_2) and prompted sulphur saturation and the precipitation of sulphides and chromite in the Lower Pyroxenite and Chromititic Pyroxenite units. Further pulses of uncontaminated magma gave rise to the sulphide-poor Peridotite zone. The constant and ultramafic compositions in the Peridotite Zone, indicate the existence of an "infinite" magma source which Gauert *et al.* (1995) interpreted as indicating the movement of large quantities of magma through the system in a magma conduit. Towards the top of the Peridotite zone, normal fractionation commences, representing the onset of closed system conditions and the generation of the Upper Pyroxenite and Norite zones.

As the Complex cooled, the magmatic convection system gave way to a hydrothermal convection system, introducing large quantities of meteoric water into the system. Accompanying the subsequent hydration of the mineral assemblage was the development of faults and shears, resulting from stress induced by the volume increase of the minerals. Hydrothermal fluids utilised these fractures for the remobilisation of the sulphides, producing the massive sulphides and the large blebs of remobilised sulphides. At some period whilst the Complex was undergoing alteration, the even more evolved diabase sills were emplaced and altered. At a later date the whole package was itself intruded by the regional dolerite dykes.

References

Anglovaal (1993). *Logging instructions for geologists on the Slaaihoek Project.* Anglovaal Internal Memorandum (unpubl.). 44 pp.

Arculus, R.J., Gillberg, M.E. and Osborn, E.F. (1974). The system Mg-iron ore oxide-Cr_2O_3-SiO_2: Phase relations among olivine, pyroxene, silica and spinel in air at 1 atm: *Carnegie Inst.Washington Year Book*, **73**, p. 317-322.

Barton Jr, J.M., Cawthorn, R.G., and White, J. (1986). The role of contamination in the evolution of the Platreef of the Bushveld Complex. *Economic Geology*, **81**, 1096 - 1104.

Bates, R.L. and Jackson, J.A (Eds.) (1980). *Glossary of Geology - second edition.* American Geological Institute, Falls Church, Virginia, 751 pp.

Brown, E.H. (1977). The crossite content of Ca-amphibole as a guide to pressure of metamorphism. *Journal of Petrology*, **18**, 53 - 72.

Buchanan, D.L., Nolan, J., Suddaby, P., Rouse, J.E., Viljoen, M.J., and Davenport, J.W.J. (1981). The genesis of the sulphide mineralisation in a portion of the Potgietersrus Limb of the Bushveld Complex. *Economic Geology*, **76**, 568 - 579.

Campbell, I. (1987). Distribution of orthocumulate textures in the Jimberlana Intrusion. *Journal of Geology*, **95**, 35 - 54.

Campbell, I.H. and Borley, G.D. (1974). The geochemistry of pyroxenes from the Lower Layered Series of the Jimberlana Intrusion, Western Australia. *Cont. Min. Petrol.*, **47**, 281-297.

Cawthorn, R.G., Barton Jr, J.M., and Viljoen, M.J. (1985). Interaction of floor rocks with the Platreef on Overysel, Potgietersrus, Northern Transvaal. *Economic Geology*, **80**, 988 - 1006.

Coghill, B.M. (1994). *Aspects of the ultramafic rocks and PGE mineralization of the Selukwe Subchamber, Great Dyke.* Ph.D thesis (unpubl.), University of Natal, Pietermaritzburg, 264 pp.

Colvine, A.C., Fyon, J.A, Heather, K.B., Marmont, S., Smith, P.M. and Troop, D.G. (1988). Archaean lode gold deposits in Ontario. *Ontario Geological Survey, Miscellaneous paper* **139**, 108 pp.

Cox, K.G., Bell, J.D. and Pankhurst, R.H. (1979). *The interpretation of igneous rocks.* George, Allen and Unwin, London, 450 pp.

Craig, J.R. and Kullerud, G. (1969). Phase relations in the Cu-Fe-Ni-S system and their application to magmatic ore deposits. In *Magmatic ore deposits* Wilson H.D.B. (ed.) *Econ. Geol. Monograph 4*, 344 - 358.

Deer, W.A., Howie, R.A., and Zussman, J. (1963). *Rock-forming minerals. Volume 2: Chain silicates. 2nd edition.* Longman Group Ltd., England. 379 pp.

Deer, W.A., Howie, R.A., and Zussman, J. (1978). *Rock-forming minerals. Volume 2A: Single chain silicates.* Longman Group Ltd., England. 668 pp.

Deer, W.A., Howie, R.A., and Zussman, J. (1992). *An introduction to the rock-forming minerals.* Longman Scientific and Technical, England. 696 pp.

DeLong, S.E. (1974). Distribution of Rb, Sr and Ni in igneous rocks, central and western Aleutian Islands, Alaska. *Geochim. Cosmochim. Acta*, **38**. 245-266.

De Waal, S.A. (1977). Carbon dioxide and water from metamorphic reactions as agents for sulphide and spinel precipitation in mafic magmas. *Trans. Geol. Soc. S. Afr.*, **80**, 193 - 196.

Drake, M.J. and Weill, D.F. (1975). Partition of Sr, Ba, Ca, Y, Eu^{2+}, Eu^{3+} and other REE between plagioclase feldspar and magmatic liquid: an experimental study. *Geochim. Cosmochim. Acta*, **39**, 689- 712.

Duke, J.M. (1976). Distribution of the Period Four transition elements among olivine, calcic clinopyroxene and mafic silicate liquid: experimental results.*Journal of Petrology*, **17**, 499-521.

Duncan, A.R. (1987). The Karoo Igneous Province - A problem area for inferring tectonic setting from basalt geochemistry. *Journal of Volcanology and Geothermal Research*, **32**, 13 - 34.

Elsdon, R. (1982). Autometasomatic alteration of gabbro, Kap Edvard Holm intrusive complex, East Greenland. *Mineralogical Magazine*, **45**, 219 - 225.

Eriksson, P.G., Sweitzer, J.K., Bosch, P.J.A., Schereiber, U.M., Van Deventer, J.L., and Hatton, C.J. (1993). The Transvaal Sequence: an overview. *Journal of African Earth Sciences,* **16**, 25 - 51.

Ewart, A., Bryan, W.B. and Gill, J.B. (1973). Mineralogy and geochemistry of the younger volcanic islands of Tonga, S.W. Pacific.*Journal of Petrology*, **14**, 429-465.

Flower, M.F.J. (1973). Trace-element distribution in lava flows from Anjouan and Grande Comore, western Indian Ocean. *Chemical Geology*, **12**, 81-98.

Frey, F.A., Green, D.H. and Roy, S.D. (1978). Intergrated Models for Basalt Petrogenesis: A study of quartz tholeiites to olivine melilitites from South Eastern Australia, utlizing geochemical and experimental petrological data. *Journal of Petrology*, **19**, 463-513.

Frick, C. (1973). The "sill phase" and the "chill zone" of the Bushveld Igneous Complex. *Trans. Geol. Soc. S. Afr.*, **76**, 7 - 14.

Gain, S.B. and Mostert, A.B. (1982). The geological setting of the platinoid and base metal sulphide mineralisation in the Platreef of the Bushveld Complex in Drenthe, north of Potgietersrus. *Economic Geology*, **77**, 1395 - 1404.

Gauert, C.D.K., de Waal, S.A., and Wallmach, T. (1994). The geology of the Uitkomst Complex, Eastern Transvaal - evidence for a magma conduit. *Ext. Abst. Centennial Geocongress 1995*. Geol. Soc. of South Africa, Johannesburg. 512 - 515.

Gauert, C.D.K., de Waal, S.A., and Wallmach, T. (1995). The geology of the Uitkomst Complex, a stratiform basic to ultrabasic intrusion in Eastern Transvaal, South Africa. *Journal of African Earth Sciences*. (In press).

Gribble, C.D. and Hall, A.J. (1992). *Optical mineralogy - principles and practice*. UCL press, London, 303 pp.

Hall, A.L. (1932) The Bushveld Igneous Complex of the Central Transvaal. *Mem. Geol. Surv. S. Afr.*, **28**, 554 p.

Hamilton, J. (1977). Isotope and trace element studies of the Great Dyke and Bushveld mafic phase and their relation to early Proterozoic magma genesis in Southern Africa. *Journal of Petrology*, **18**, 24 - 52.

Hanson, G.N. (1977). Geochemical evaluation of the suboceanic mantle.*J. Geol. Soc. Lond.*, **134**, 235-253.

Harrigan, D.B. and MacLean, W.H. (1976). Petrography and geochemistry of alteration patches in gabbro dykes at Matagami, Quebec. *Can. J. Earth Sci.*, **13**, 500 - 511.

Hart, S.R. and Brooks, C. (1974). Clinopyroxene - matrix partitioning of K, Rb, Cs, Sr, and Ba. *Geochim. Cosmochim. Acta*, **38**, 1799-1806.

Hatton, C.J. and Sharpe, M.R. (1989) *Significance and origin of boninite-like rocks associated with the Bushveld Complex.* In: Crawford A.J., (Ed.) *Boninites*, Unwin-Hyman, London, 465 pp.

Haughton, D.R., Roeder, P.L., and Skinner, B.J. (1974). Solubility of sulphur in mafic magmas. *Economic Geology*, **69**, 451 - 467.

Henderson, P. (1968). The distribution of phosphorous in the early and middle stages of fractionation of some basic layered intrusions. *Geochimica et Cosmochimica Acta*, **32**, 897 - 911.

Henderson, P. (1975). Geochemical indicator of the efficiency of fractionation of the Skaergaard intrusion, east Greenland. *Mineralogical Magazine,* **40**, 285 - 291.

Hulbert, L.J. and Von Gruenewaldt, G. (1982). Nickel, copper, and platinum mineralisation in the Lower Zone of the Bushveld Complex, South of Potgietersrus. *Economic Geology*, **77**, 1296 - 1306.

Irvine, T.N. (1975). Crystallisation sequences in the Muskox intrusion and other layered intrusions. II. Origin of chromitite layers and similar deposits of other magmatic ores. *Geochim. Cosmochim. Acta*, **39**, 991 - 1020.

Irving, A.J. (1978). A review of experimental studies of crystal/liquid trace element partitioning. *Geochim. Cosmochim. Acta*, **42**, 743-770.

Irvine, T.N. (1980). *Infiltration metasomatism, adcumulus growth, and double-diffusive fractional crystallisation in the Muskox intrusion and other layered intrusions.* In: Hargraves, R.B., (ed.) *Physics of Magmatic Processes,* Princeton University Press, Princeton, 325 - 383.

Irvine, T.N. and Smith, C.H. (1969). Primary oxide minerals in the layered series of the Muskox intrusion. In *Magmatic ore deposits* Wilson H.D.B. (ed.) *Econ. Geol. Monograph 4*, 76 - 94.

Jensen, B.B. (1973). Patterns of trace element partitioning.*Geochim. Cosmochim. Acta*, **37**, 2227-2242.

Kenyon, A.K., Attridge, R.L., and Coetzee, G.L. (1986) The Uitkomst nickel - copper deposit, Eastern Transvaal. In: *Anhaeusser, C.R. & Maske, S., (eds.) Mineral Deposits of Southern Africa* **2**, Geol. Soc. of South Africa, 1009 - 1017.

Kullerud, G., Yund, R.A., and Moh, G.H. (1969). Phase relations in the Cu-Fe-S, Cu-Ni-S, and Fe-Ni-S systems. In *Magmatic ore deposits* Wilson H.D.B. (ed.) *Econ. Geol. Monograph 4*, 323 - 343.

Leake, B.E. (1978). Nomenclature of amphiboles. *Canadian Mineralogist,* **16**, 501 - 520.

Leeman , W.P. and Lindstrom, D.J. (1978). Partitioning of Ni^{2+} between basaltic and synthetic melts and loivines - an experimental study. *Geochim. Cosmochim. Acta*, **42**, 801-816.

Lemarchand, F., Villemant, B. and Calas, G. (1987). Trace element distribution coeffieients in alkaline series. *Geochim. Cosmochim. Acta*, **51**, 1071-1081.

Lightfoot, P.C. and Naldrett, A.J. (1983). The geology of the Tabankulu section of the Insizwa Complex, Transkei, southern Africa, with reference to the nickel sulphide potential. *Trans. geol. Soc. S. Afr.*, **86**, 169 - 187.

Lightfoot, P.C. and Naldrett, A.J. (1984). Chemical variation in the Insizwa Complex, Transkei, and the nature of the parent magma. *Canadian Mineralogist*, **22**, 111 - 123.

Lightfoot, P.C., Naldrett, A.J., and Hawkesworth, C.J. (1984) The geology and geochemistry of the Waterfall Gorge section of the Insizwa Complex with particular reference to the origin of the nickel sulphide deposits. *Economic Geology*, **79**, 1857 - 1879.

Lightfoot, P.C., Naldrett, A.J., and Hawkesworth, C.J. (1987). Re-evaluation of chemical variation in the Insizwa Complex, Transkei. *Canadian Mineralogist*, **25**, 79 - 90.

Lindstrom, D.J. and Weill, D.F. (1978). Partitioning of transition metals between diopside and coexisting silicate liquids: I. Nickel, cobalt, and manganese. *Geochim. Cosmochim. Acta*, **42**, 817- 831.

MacLean, W.H. and Shimazaki, H. (1976). The partition of Co, Ni, Cu, and Zn between sulphide and silicate liquids. *Economic Geology*, **71**, 1049 - 1057.

Maier, W.D. (1991). *Geochemical and petrological trends in the UG2 - Merensky unit interval of the Upper Critical Zone in the Western Bushveld Complex*. Ph.D. thesis (unpubl.), Rhodes University, 253 pp.

Mathison, C.I. and Marshall, A.E. (1981). Ni-Cu sulphides and their host mafic-ultramafic rocks in the Mt. Sholl intrusion, Pilbara region, Western Australia. *Economic Geology*, **76**, 1581 - 1596.

McKenzie, D.P. (1984). The generation and compaction of partially molten rock. *Journal of Petrology*, **25**, 713 - 765.

McKenzie, D.P. (1985). The extraxtion of magma from the crust and mantle. *Earth and Planetary Science Letters*, **74**, 81 - 91.

Meinert, L.D. (1992). Skarns and skarn deposits. *Geoscience Canada*, **19** (**4**), 145 - 162.

Meschede, M. (1986). A method of discriminating between different types of mid-ocean ridge basaslts and continental tholeiites with the Nb-Zr-Y diagram. *Chemical Geology,* **56**, 207 - 218.

Mogessie, A., Tessadri, R., and Veltman, C.B. (1988). "Emp-Amph". An interactive program written in hypertalk to calculate the structural formulae and tabulate the names of electron microprobe analyses of amphiboles according to the IMA-/scheme.

Mori, T. and Green, D.H. (1978). Laboratory duplication of phase equilibria in natural garnet lherzolites. *Journal of Geology*, **86**, 83 - 97.

Morimoto, N. (1989). Nomenclature of pyroxenes. *Canadian Mineralogist,* **27**, 143 - 156.

Morse, S.A. and Nolan, K.M. (1984). Origin of strongly reversed rims on plagioclase in cumulates. *Earth. Plan. Sci. Lett.*, **68**, 485- 498.

Naldrett, A.J. (1989). Contamination and the origin of the Sudbury structure and its ores. In: *Ore deposition associated with magmas* Whitney, J.A. and Naldrett, A.J. (eds.) *Reviews in Economic Geology, volume 4*, 119 - 134.

Norrish, K. and Hutton, J.T. (1969). An accurate X-ray spectrographic method for the analysis of a wide range of geological samples. *Geochimica et Cosmochimica Acta*, **33**, 431 - 453.

Paktunc, A.D. (1989). Petrology of the St. Stephen Intrusion and the genesis of related nickel-copper sulphide deposits. *Economic Geology*, **84**, 817 - 840.

Paster, T.P., Schauwecker, D.S. and Haskin, L.A. (1974). The behaviour of some trace elements during solidification of the Skaergaard layered series.*Geochim. Cosmochim. Acta*, **38**, 1549 - 1577.

Pearce, J.A. and Norry, M.J. (1979). Petrogenetic implications of Ti, Zr, Y and Nb variations in volcanic rocks. *Contr. Min. Petrol.*, **69**, 33-47.

Philpotts, J.A. and Schnetzler, C.C. (1970). Phenocryst - matrix partition coefficients for K, Rb, Sr and Ba, with applications to anorthosite and basalt genesis.*Geochim. Cosmochim. Acta.*, **34**, 307 - 322.

Rajamani, V. and Naldrett, A.J. (1978). Partitioning of Fe, Co, Ni, and Cu, between sulphide liquid and basaltic melts and the composition of Ni-Cu sulphide deposits. *Economic Geology*, **73**, 82 - 93.

Ramdohr, P. (1980). *The ore minerals and their intergrowths - 2nd edition.*. Pergamon Press ltd., Oxford, England. 1205 pp.

Richter, F.M. and McKenzie, D.P. (1984). Dynamical models for melt segregation from a deformable matrix. *Journal of Geology,* **92**, 739 - 740.

Ringwood, A.E. (1970). Petrogenesis of Apollo 11 basalts and implications for lunar origin.*Journal of Geophysical Research,* **75**, 6453-6479.

Rock, N.M.S. and Leake, B.E. (1984). The International Mineralogical Association amphibole nomenclature scheme: computerisation and its consequences. *Mineralogical Magazine,* **48**, 211 - 217.

SACS (South African Committee for Stratigraphy) 1980. *Stratigraphy of South Africa. Part 1(Comp. L.E. Kent). Lithostratigraphy of the Republic of South Africa, South West Africa / Namibia, and the republics of Bophuthatswana, Transkei and Venda.* Geol. Surv. South Africa, Handbook **8**, 690 pp.

Salpas, P.A., Haskin, L.A. and McCallum, I.S. (1983). Stillwater anorthosites: a lunar analogue? *Journal of Geophysical Research,* **88**, b27-b39.

Schürmann, L.W. (1992). The geochemistry of the Wanhoop multiple intrusion: a preliminary interpretation of the origin of the Uitkomst Complex. *Abstracts Geocongress 1992,* Geol. Soc. South Africa, Bloemfontein.

Sharpe, M.R., Bahat, D., and Von Gruenewaldt, G. (1981). The concentric elliptical structure of feeder sites to the Bushveld Complex and possible economic implications. *Trans. Geol. Soc. S. Afr.,* **84**, 239 - 244.

Sparks, R.S.J., Huppert, H.E., Kerr, R.C., McKenzie, D.P., and Tait, S.R. (1985). Postcumulus processes in layered intrusions. *Geological Magazine,* **122**, 469 - 484.

Streckeisen, A. (1976). To each plutonic rock its proper name. *Earth Science Reviews,* **12**, 1 - 33.

Tait, S.R., Huppert, H.E., and Sparks, R.S.J. (1984). The role of compositional convection in the formation of adcumulate rocks. *Lithos,* **17**, 139 - 146.

Tischler, S.E., Cawthorn, R.G., Kingston, G.A., and Maske, S. (1981). Magmatic Cu-Ni-PGE mineralisation at Waterfall Gorge, Insizwa, Pondoland, Transkei. *Canadian Mineralogist*, **19**, 607 - 618.

Van Der Merwe, M.J. (1976). The layered sequence of the Potgietersrus Limb of the Bushveld Complex. *Economic Geology*, **71**, 1337 - 1351.

Von Gruenewaldt, G., Sharpe, M.R., and Hatton, C.J. (1985). The Bushveld Complex: Introduction and review. *Economic Geology,* **80**, 803 - 812.

Wager, L.R. (1963). The mechanism of adcumulus growth in the layered deries of the Skaergaard intrusion. *Min. Soc. America Special Paper 1*, 1 - 9.

Wagner, P.A. (1929). *The platinum deposits and mines of South Africa.* Oliver and Boyd, Edinburgh. 326 pp.

Walker, K.R. (1970). The Palisade Sill, New Jersey. A reinvestigation. *Geol. Soc. America Special Paper 111*, 178.

Willemse, J. and Bensch, J.J. (1964). Inclusions of original carbonate rocks in Gabbro and Norite of the eastern part of the Bushveld Complex. *Trans. geol. Soc. S. Afr.,* **67**, 1 - 88.

Williams-Jones, I.E. (1984). *The petrology of the basalts of the Dordabis Formation, in the vicinity of Dordabis in Central S.W.A./Namibia.* Msc thesis. (Unpubl.), Rhodes University. 114 pp.

Winkler, H.G.F. (1976). *Petrogenesis of metamorphic rocks - fourth edition.* Springer-Verlag, New York, USA, 334 pp.

Appendix A

Plates of Photomicrographs

Plate 1. *Chill zone of Basal Gabbro, showing fine grain size and distribution of pyroxenes, feldspar, mica and opaques. Note minor uralitisation Section SH10-9 (409.40) Field of view = 4.4 mm*

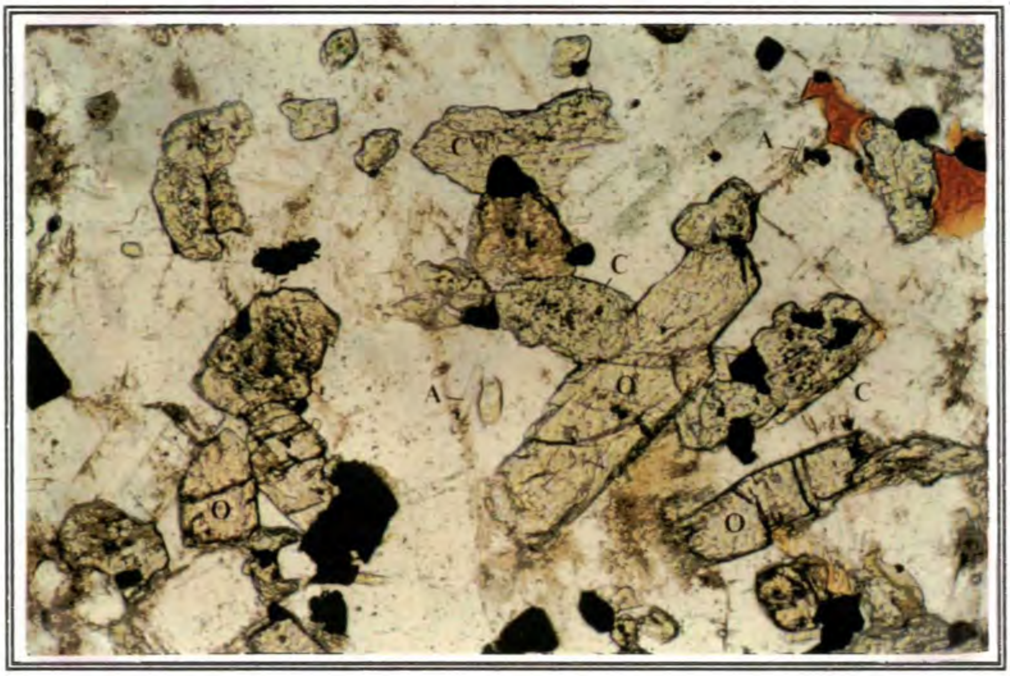

Plate 2. *Chill zone of Basal Gabbro, showing euhedral to subhedral crystals of orthopyroxene(O) and clinopyroxene(C). Note the intercumulus nature of the mica and the presence of laths of apatite(A), as well as the opaques. Section SH10-9 (409.40). Field of view = 1.1 mm*

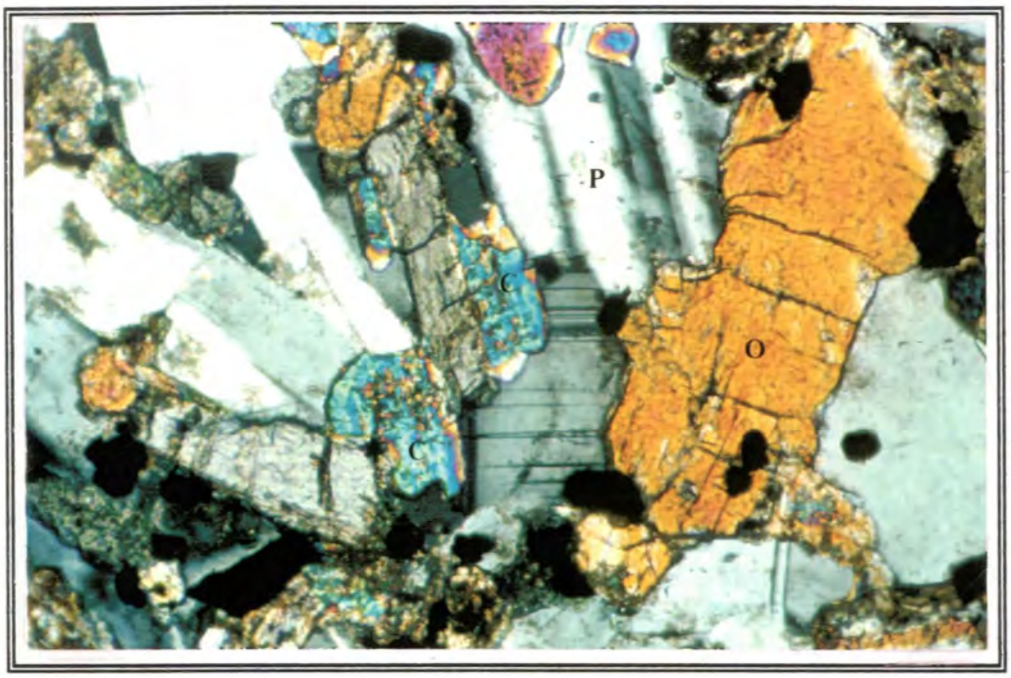

Plate 3. *Chill zone of Basal Gabbro, showing inclusions of opaques in orthopyroxene(O). Also present is plagioclase(P) and clinopyroxene(C). Section SH10-9 (409.40) Field of view = 1.1 mm*

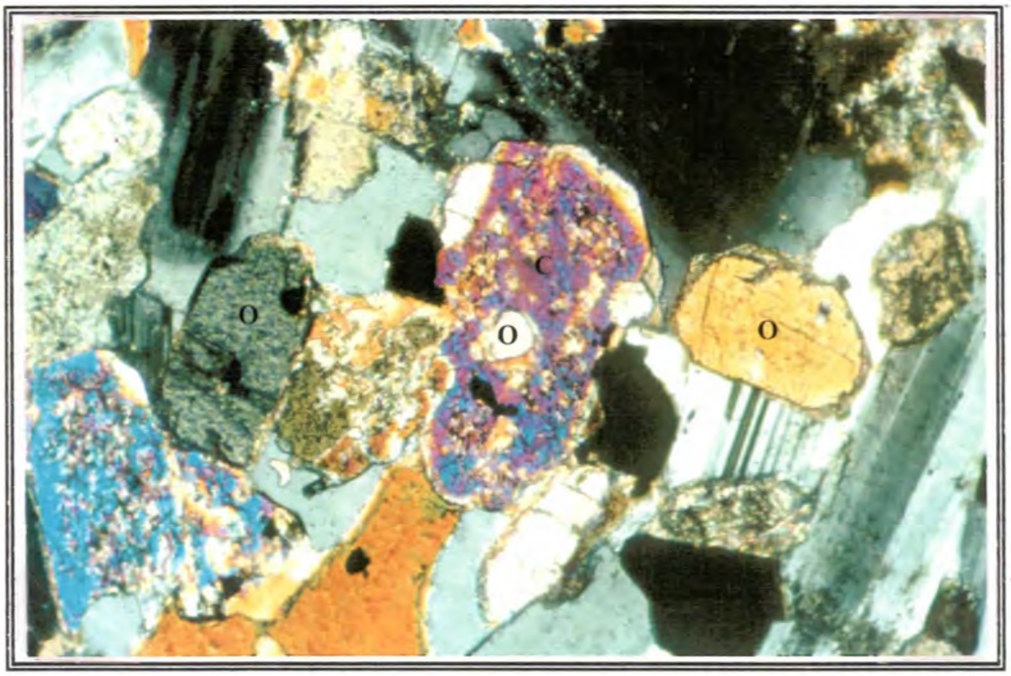

Plate 4. *Chill zone of Basal Gabbro, showing clinopyroxene(C) with an inclusion of orthopyroxene(O). Note the slight uralitisation of the clinopyroxene. Section SH10-8 (408.60). Field of view = 1.1 mm*

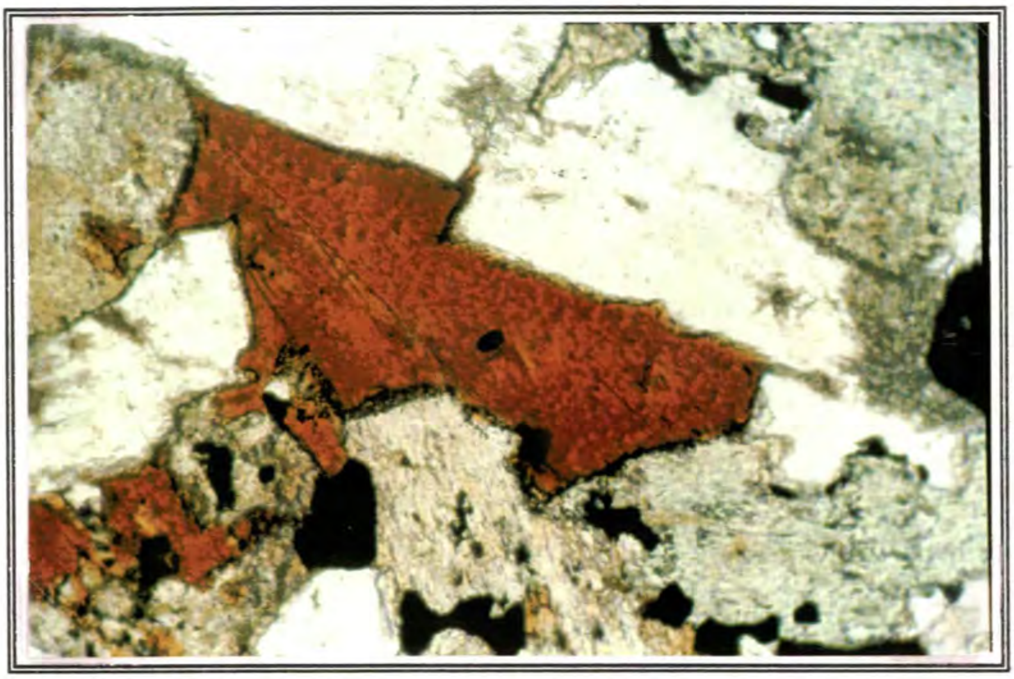

Plate 5. *Intercumulus mica (phlogopite), with a rim of opaques along the contact with the pyroxene grains. Note the brown colour of the mica suggesting high Ti content. Section SH10-8 (408.60) Field of view = 1.1 mm*

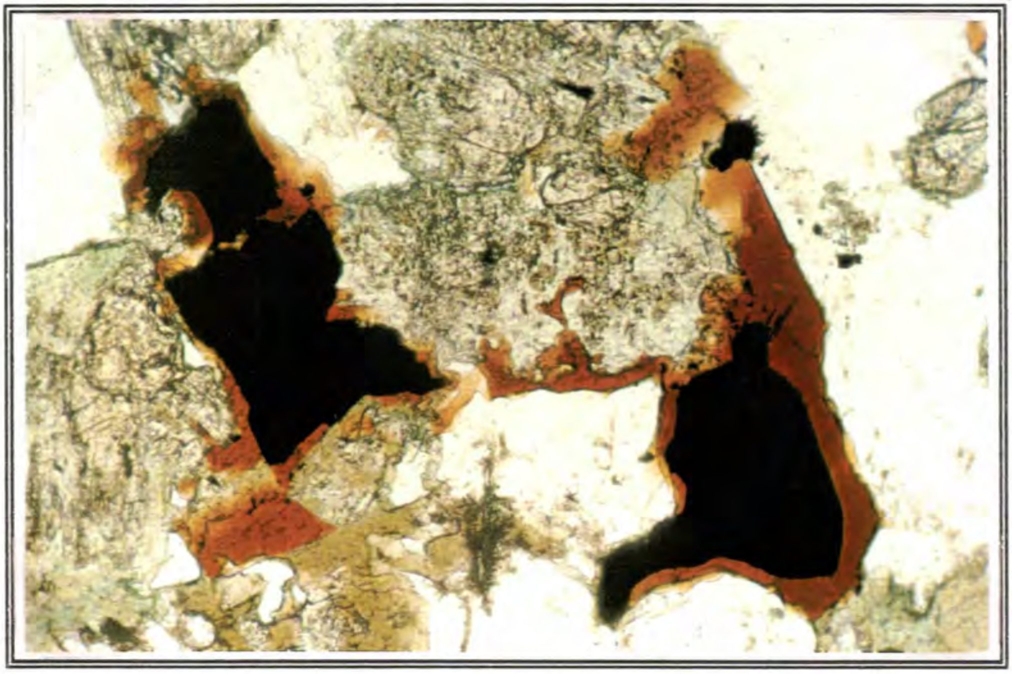

Plate 6. *Close association of the mica (phlogopite) with opaques, suggesting the later crystallisation of these minerals. Note the uralitisation of the pyroxenes, and saussuritisation of feldspar in the lower centre of the photograph. Section SH10-6 (405.50). Field of view = 1.1 mm*

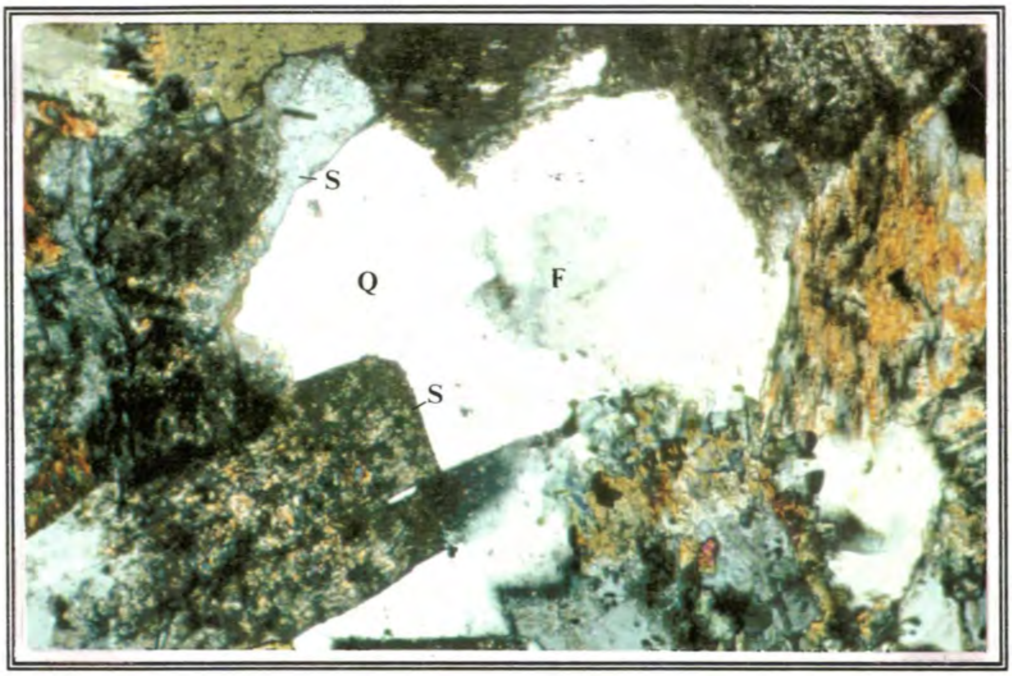

Plate 7. *Mesostasis of quartz(Q) and feldspar(F). Note the saussuritisation(S) of the feldspars surrounding the quartz, and the uralitisation of the pyroxenes. Section SH10-7 (407.20) Field of view = 1.1 mm*

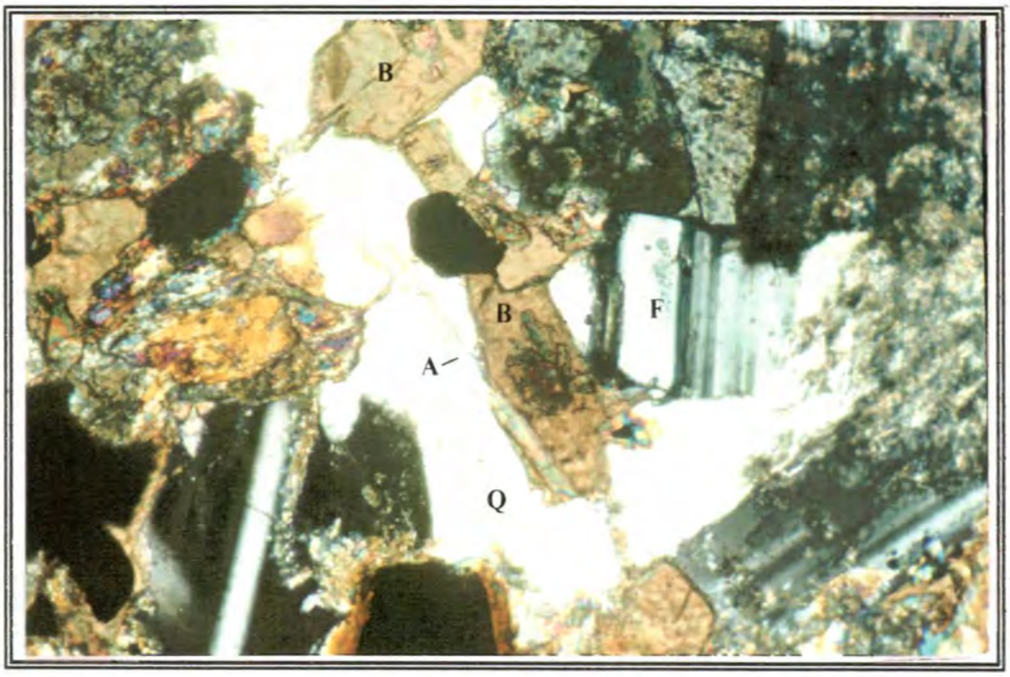

Plate 8. *Mesostasis of quartz(Q) and feldspar(F) with biotite(B) and apatite(A), indicating that this is a late stage product in the crystallisation sequence. Section SH10-6 (405.50). Field of view = 1.1 mm*

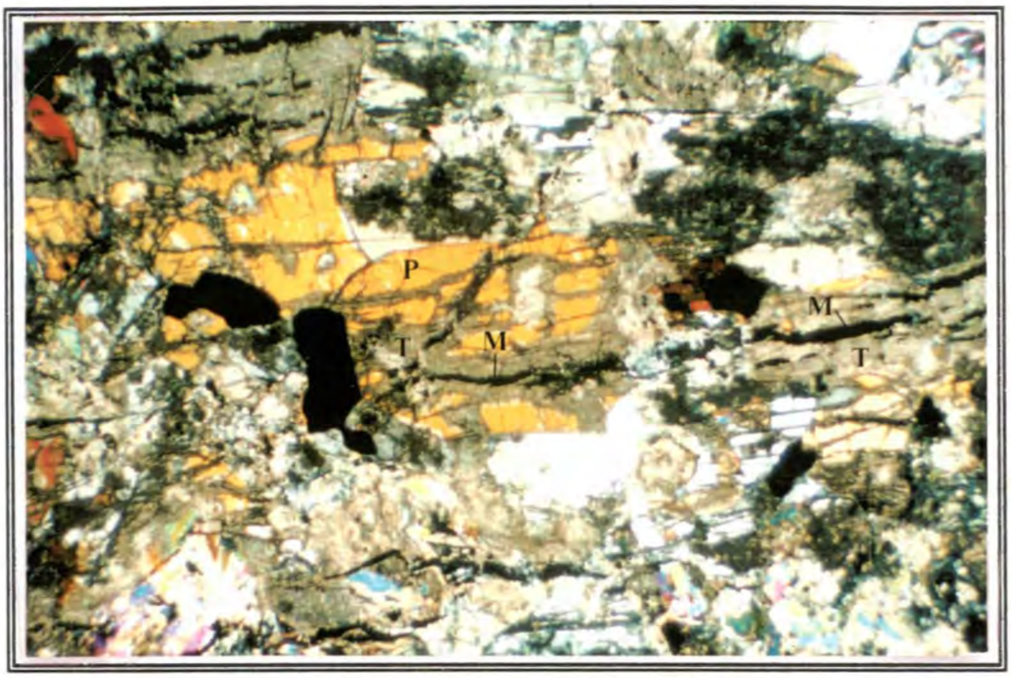

Plate 9. *The markedly different nature of the rock below a xenolith, showing a fractured and altered pyroxene(P). Note the"seams" of magnetite(M) and talc(T). Section SH10-4 (404.07) Field of view =4.4 mm*

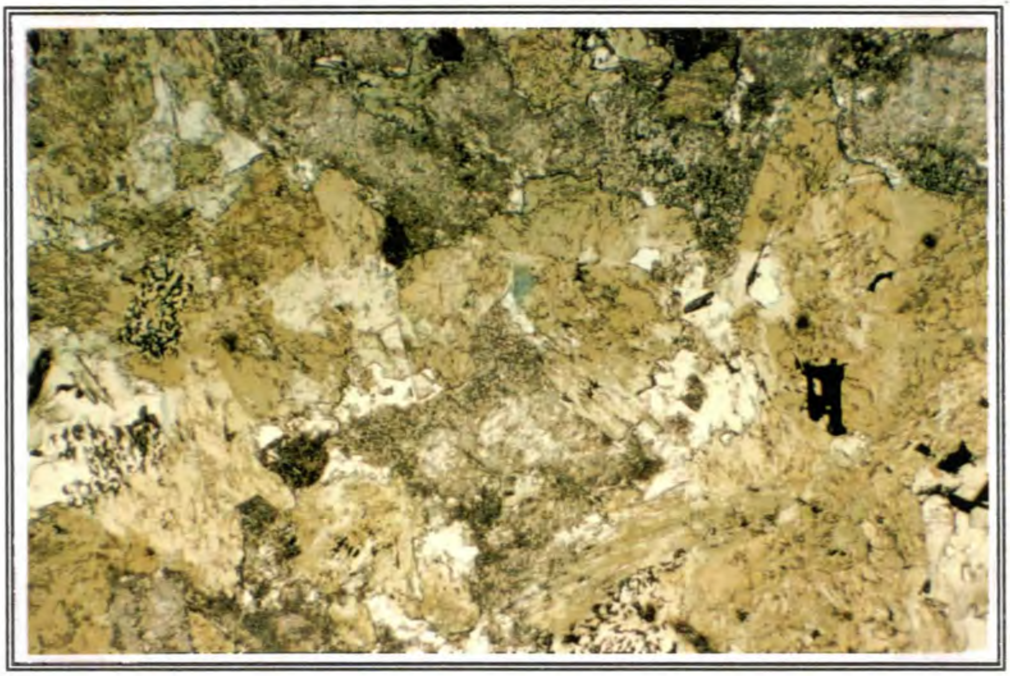

Plate 10. *Highly altered Basal Gabbro situated between a dolomitic and quartzitic xenolith. Note the almost total uralitisation, the saussuritisation, and the chlorite. Section SH10-3 (403.43). Field of view = 4.4 mm*

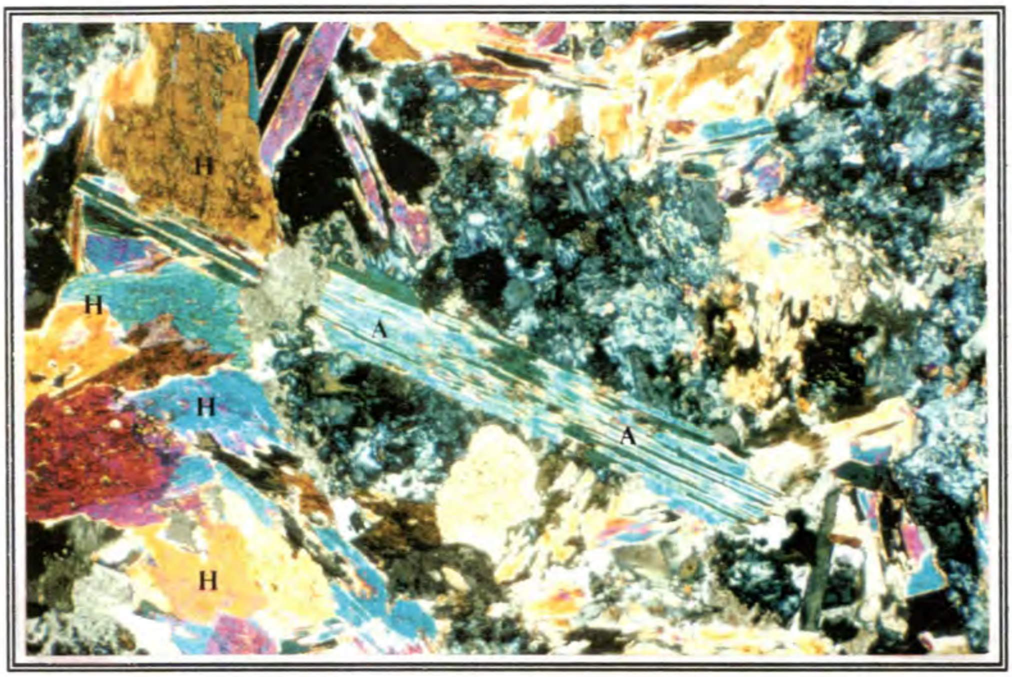

Plate 11. *Basal Gabbro with two types of amphibole: the acicular tremolitic / actinolitic type(A) and the hornblende type(H). Also the development of the blue-grey coloured clinozoisite. Section SH10-2 (403.20) Field of view = 4.4 mm*

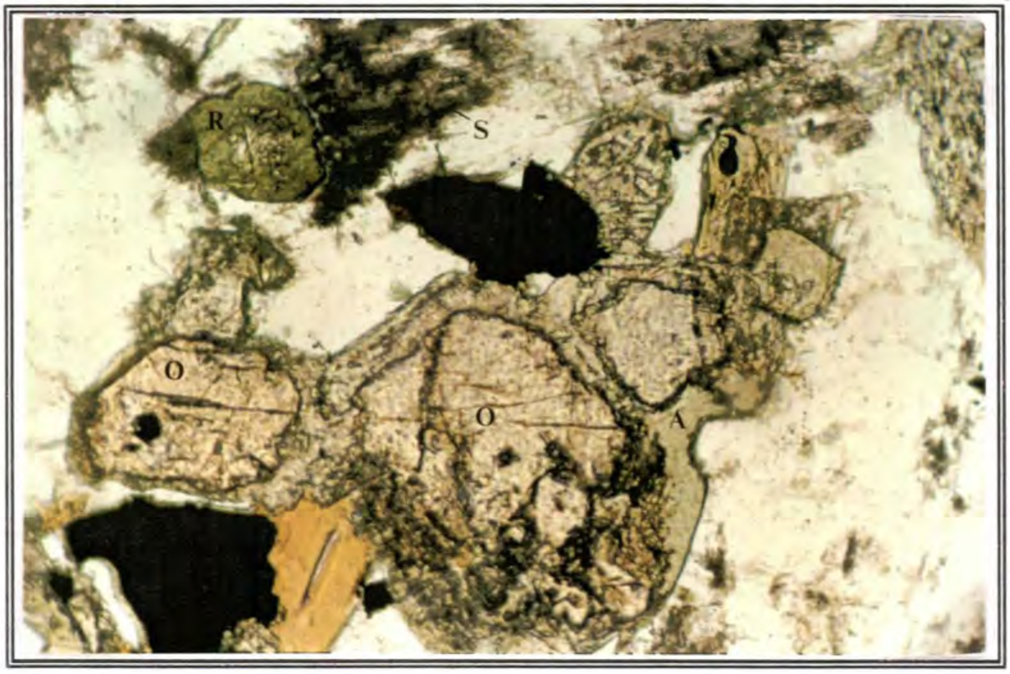

Plate 12. *Basal Gabbro showing the early stages of uralitisation of orthopyroxene. The amphibole forms a rim around the pyroxene. Note the totally replaced pyroxene in the top left of the photograph, with the saussuritised plagioclase beside it. Section SH10-7 (407.20). Field of view = 1.1 mm*

Plate 13. *Basal Gabbro showing the further development of uralitisation(U) of pyroxene(O), as well as the advanced saussuritisation of plagioclase(P). Section SH19-5 (511.05) Field of view = 1.1 mm*

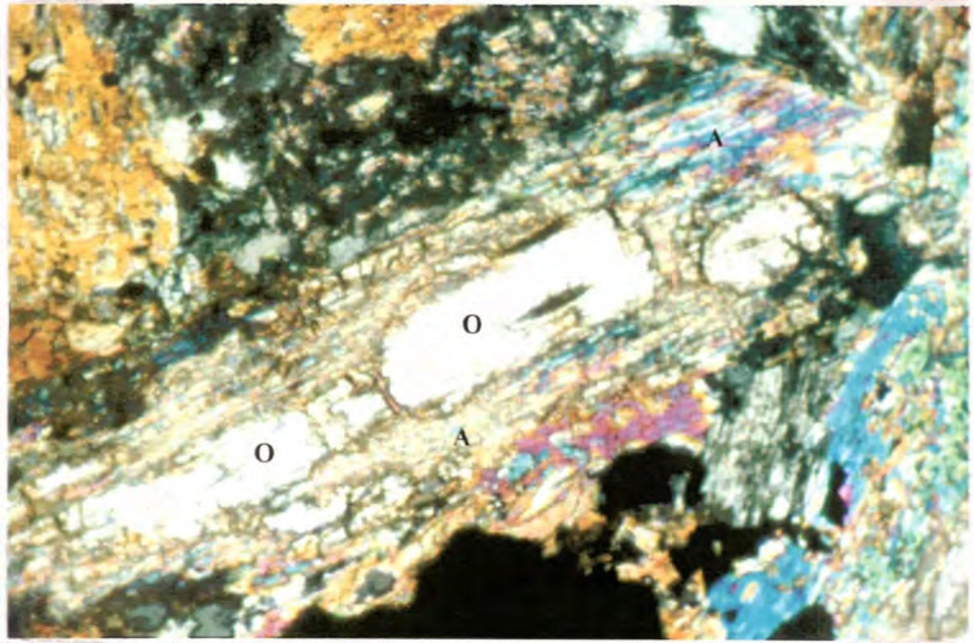

Plate 14. *Basal Gabbro showing more advanced stages of uralitisation of pyroxene, leaving only a relict of the original orthopyroxene grain(O). The amphibole(A) can be seen to be pseudomorphing the pyroxene. Section SH19-5 (511.05). Field of view = 1.1 mm*

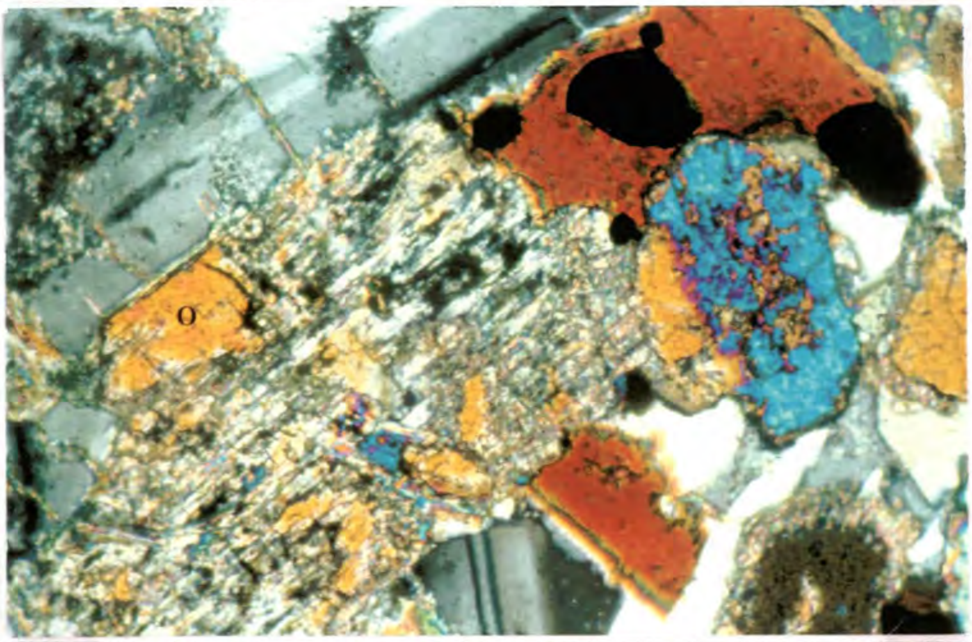

Plate 15. *Basal Gabbro showing a highly advanced stage of uralitisation of pyroxene,leaving only minor relicts of the original pyroxene(O). Section SH10-7 (407.20) Field of view = 1.1 mm*

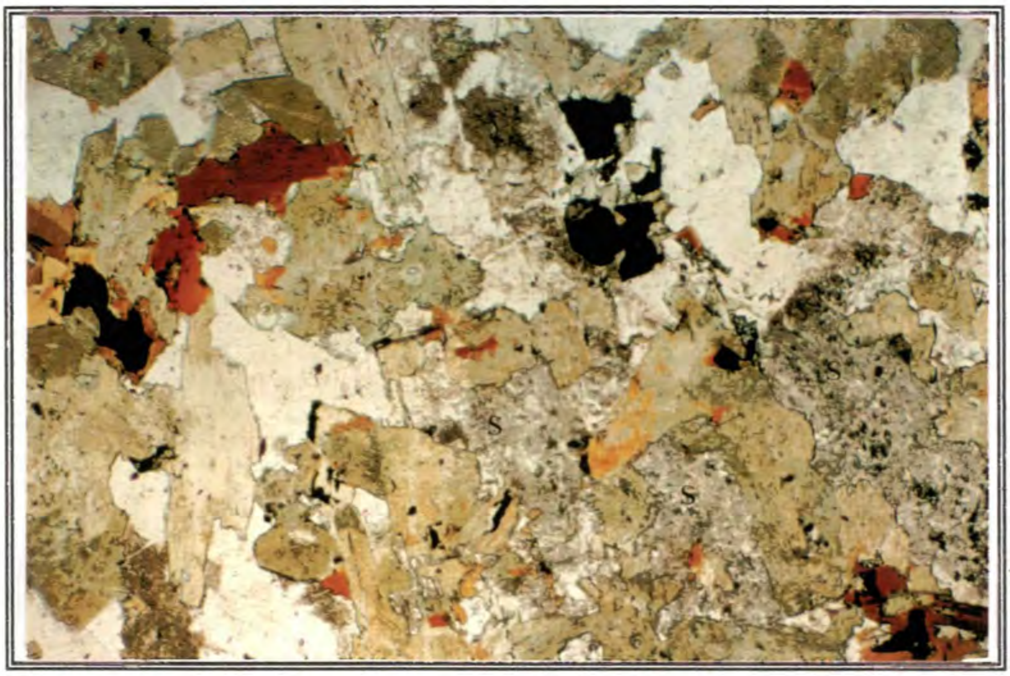

Plate 16. *Basal Gabbro showing total uralitisation and extensive saussuritisation(S) of plagioclase. This is a typical section of Basal Gabbro not from SH10. Section SH18-7 (583.45). Field of view = 4.4 mm*

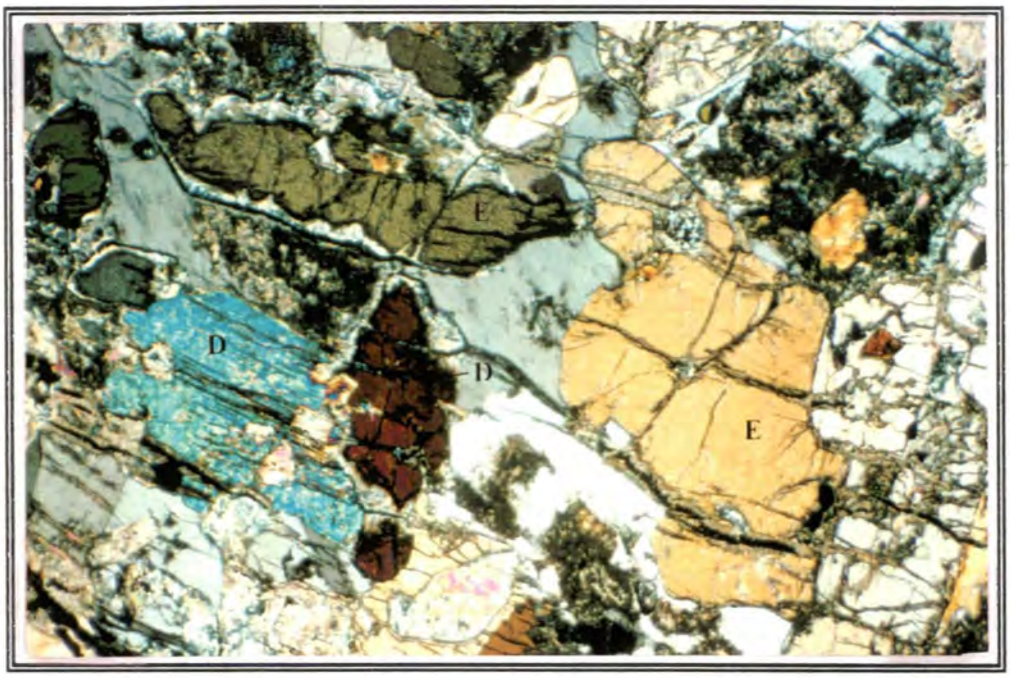

Plate 17. *Diopsides(D) and Mg-rich enstatites(E) in proximity to a dolomite xenolith, Note the larger and fresher appearance of the pyroxenes. Section SH10-4 (404.07) Field of view = 4.4 mm*

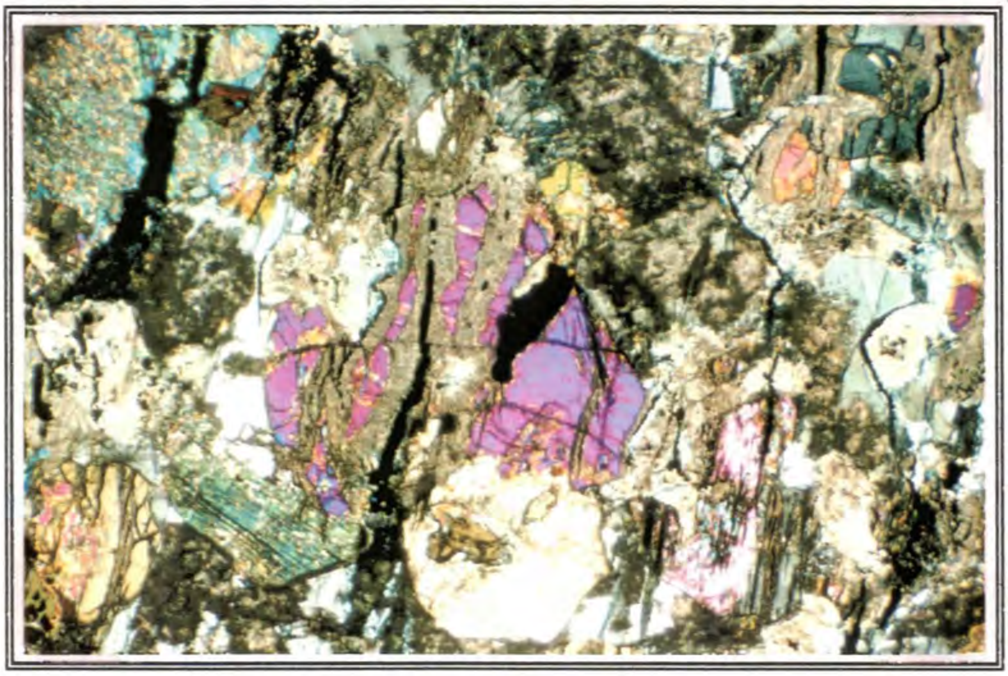

Plate 18. *Basal Gabbro in proximity to a dolomite xenolith, with a pyroxene showing serpentinisation and the formation of anastomosing veinlets of serpentine, talc and magnetite. Note that the photograph is from a thicker electron microprobe section. Section SH10-4 (404.07). Field of view = 4.4 mm*

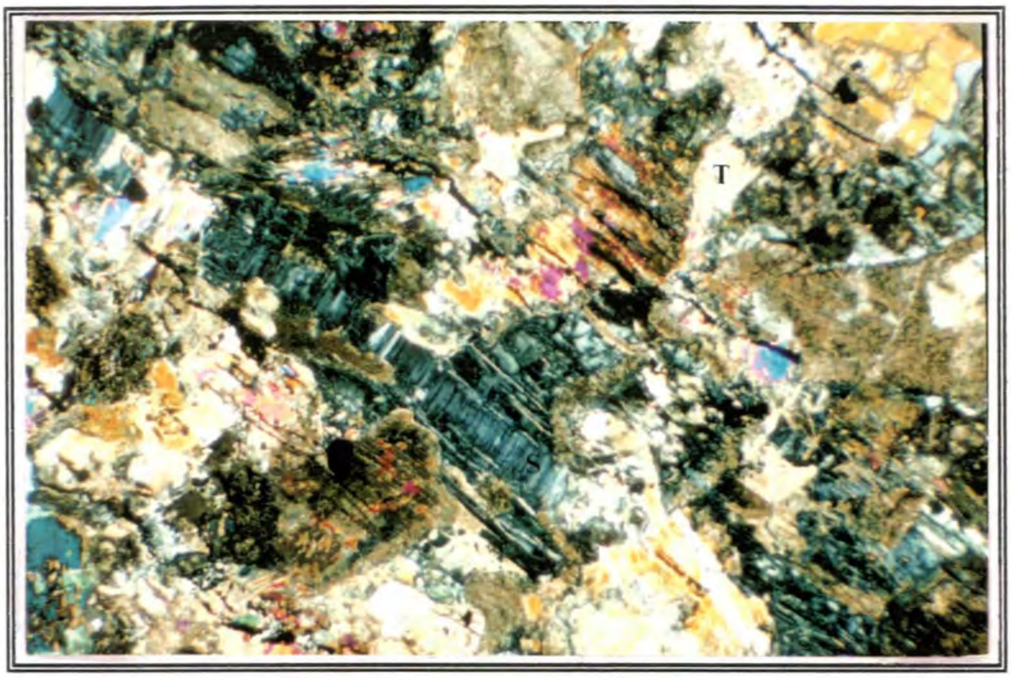

Plate 19. *Basal Gabbro in proximity to a dolomite xenolith, showing the intense alteration and development of talc(T) and serpentine(S). Section SH10-4 (404.07) Field of view = 4.4 mm*

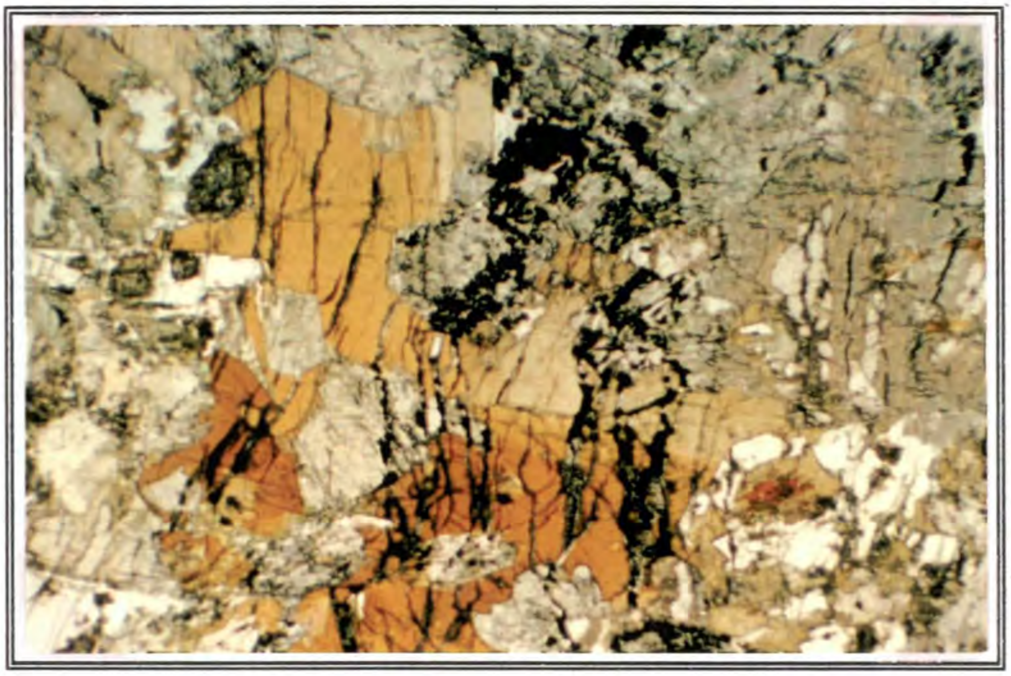

Plate 20. *Basal Gabbro in proximity to a dolomite xenolith,showing the development of coarse-grained mica, and its association with opaques. Section SH10-4 (404.07). Field of view = 4.4 mm*

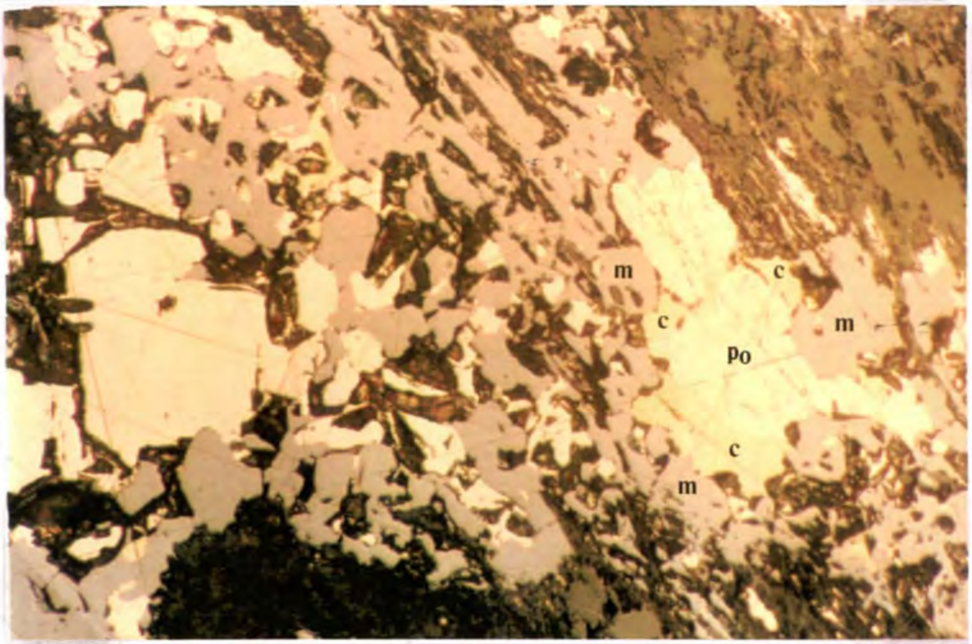

Plate 21. *Basal Gabbro in proximity to a dolomite xenolith, showing sulphides in the skarn zone. Chalcopyrite(c) is replacing pyrrhotite(po), with both being enclosed (replaced) by magnetite(m). Note this is an electron microprobe section. Section SH10-4 (404.07) Field of view = 0.625 mm*

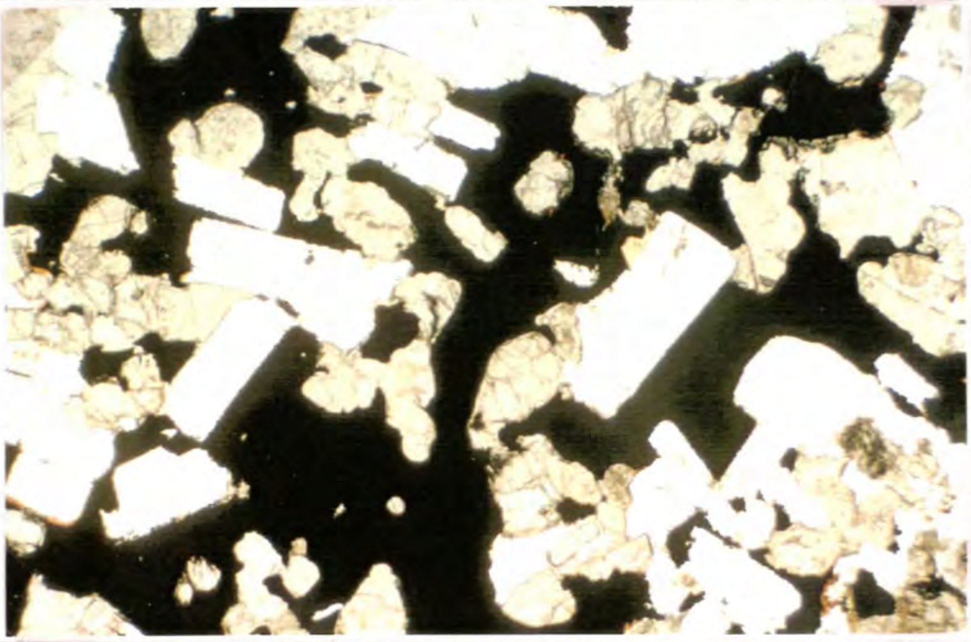

Plate 22. *Basal Gabbro showing the net-textured nature of the sulphides. Section SH10-5 (404.80). Field of view = 4.4 mm*

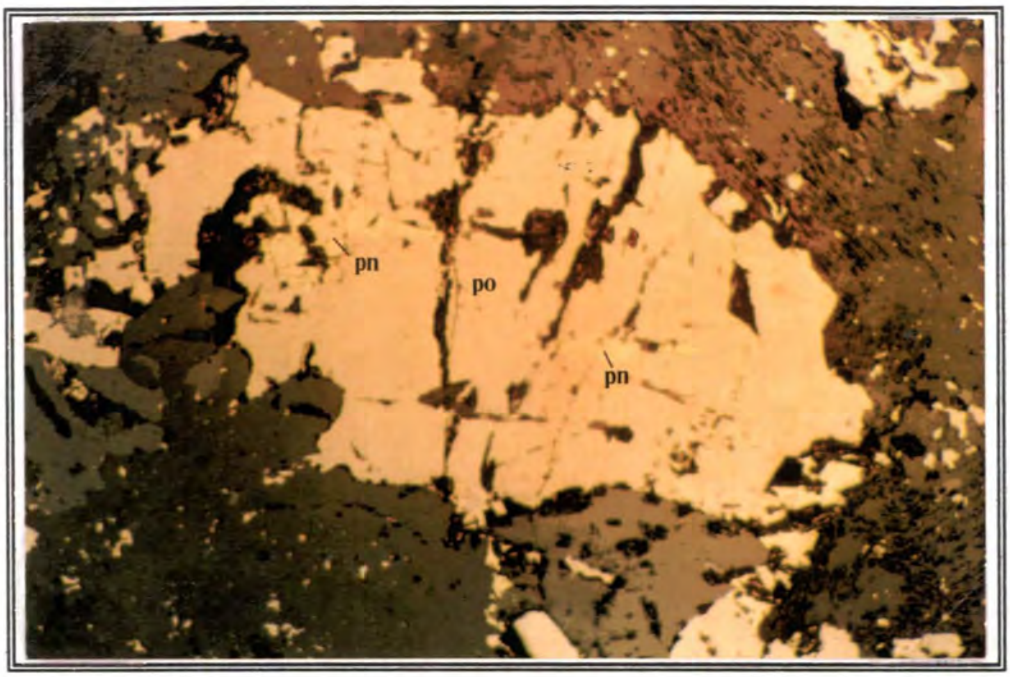

Plate 23. *Basal Gabbro showing the flame-like exsolution bodies of pentlandite(pn) parallel to {0001} in pyrrhotite(po). Note this is an electron microprobe section. Section SH26-5 (492.47) Field of view = 1.25 mm*

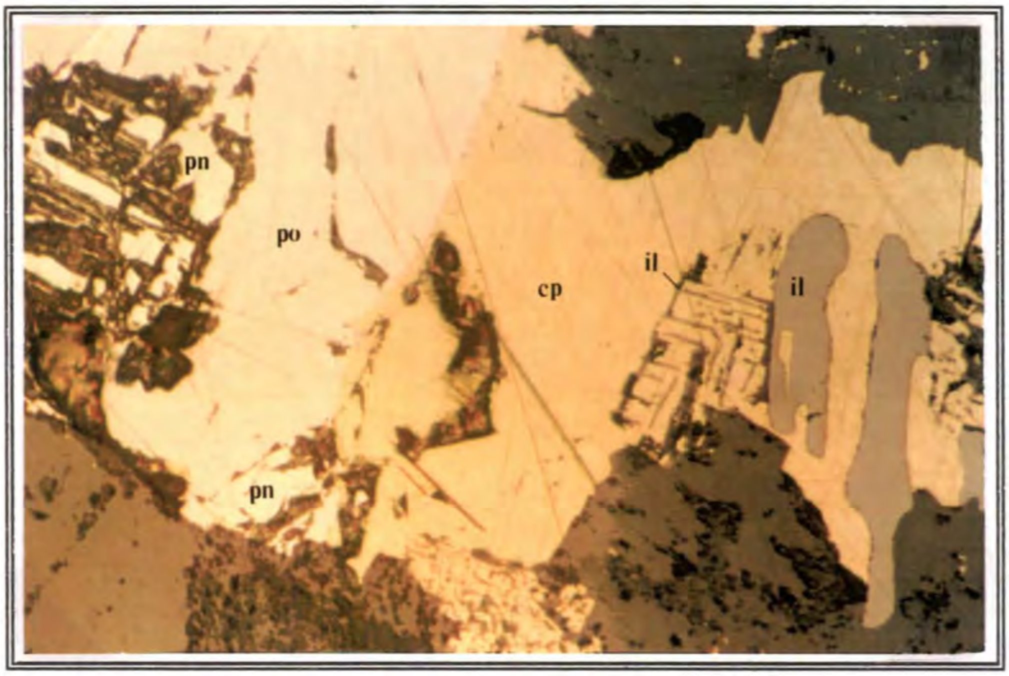

Plate 24. *Basal Gabbro aggregates of pentlandite(pn) occurring along fractures and at grain boundaries, especially between pyrrhotite(po) and chalcopyrite(cp). Note also the ilmenite(il) exsolved from magnetite which has been totally replaced by chalcopyrite. Note this is an electron microprobe section Section SH10-6 (405.50). Field of view = 0.625 mm*

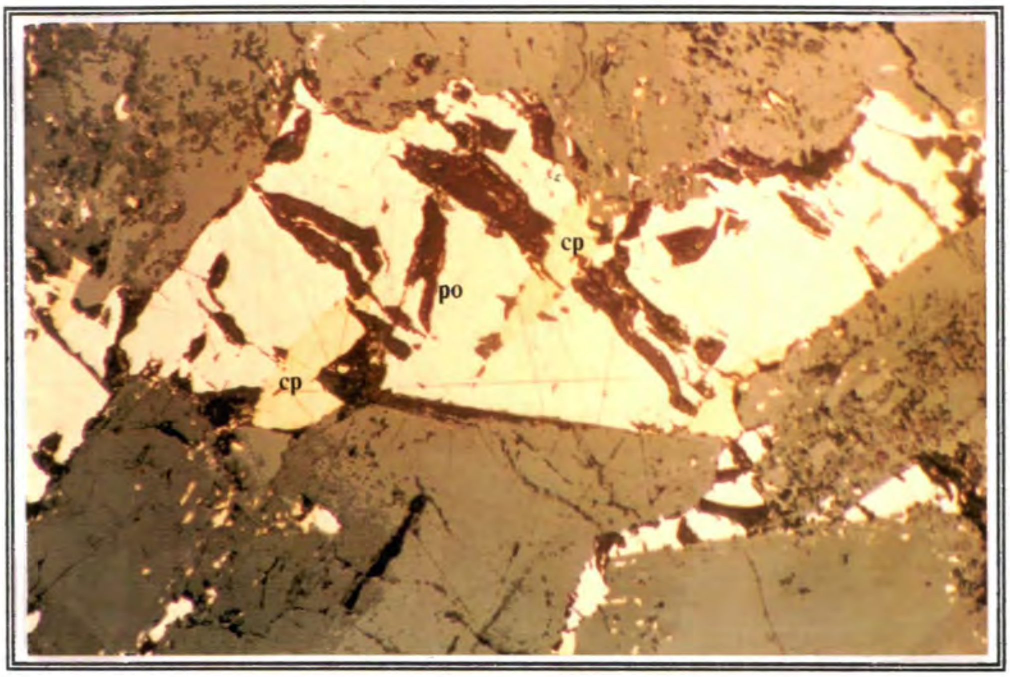

Plate 25. *Basal Gabbro showing chalcopyrite(cp) being enclosed (replaced) by pyrrhotite(po). Note this is an electron microprobe section. Section SH10-6 (405.50) Field of view = 1.25 mm*

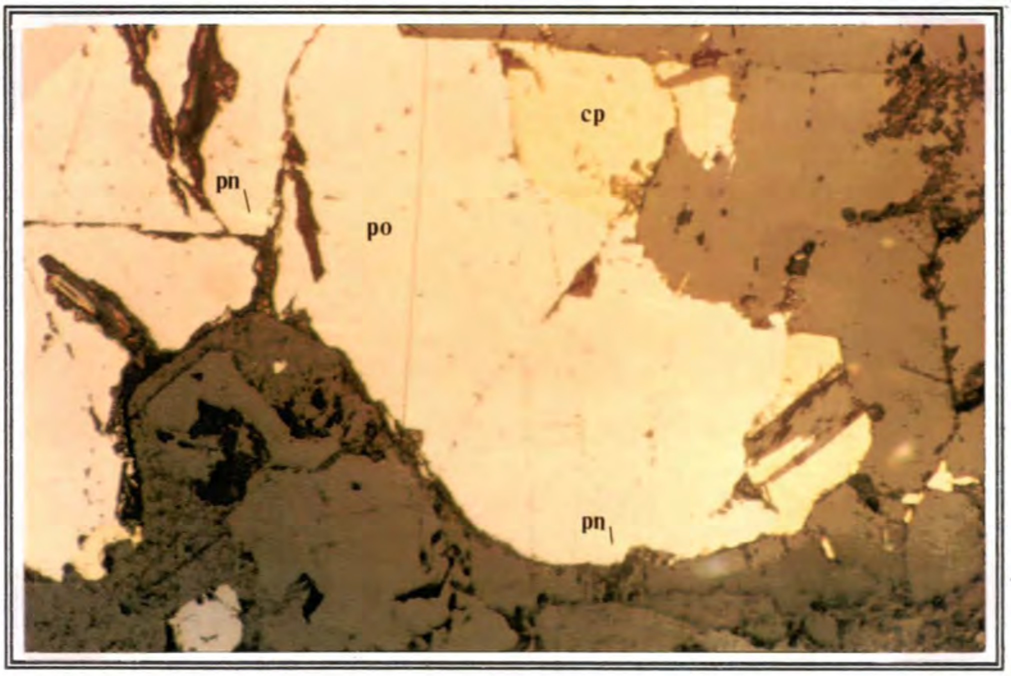

Plate 26. *Basal Gabbro showing chalcopyrite(cp) replacing pyrrhotite(po). Flame-like exsolution bodies of pentlandite(pn) are also visible commonly in association with fractures and grain boundaries. Note this is an electron microprobe section. Section SH10-5 (404.80). Field of view = 0.625 mm*

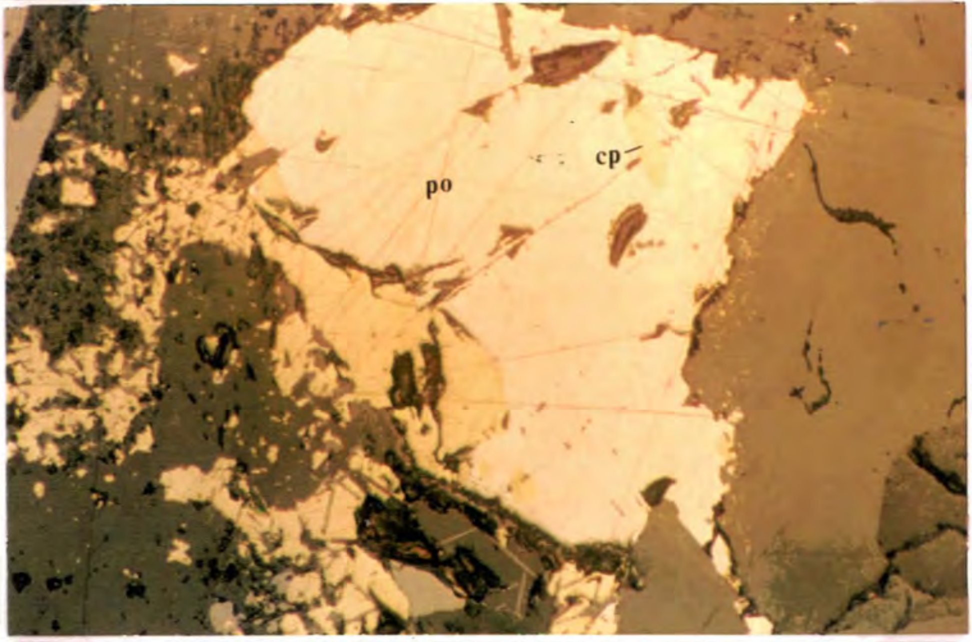

Plate 27. *Basal Gabbro showing pyrrhotite(po) enclosing (replacing) chalcopyrite(cp). Note this is an electron microprobe section. Section SH10-6 (405.50) Field of view =0.625 mm*

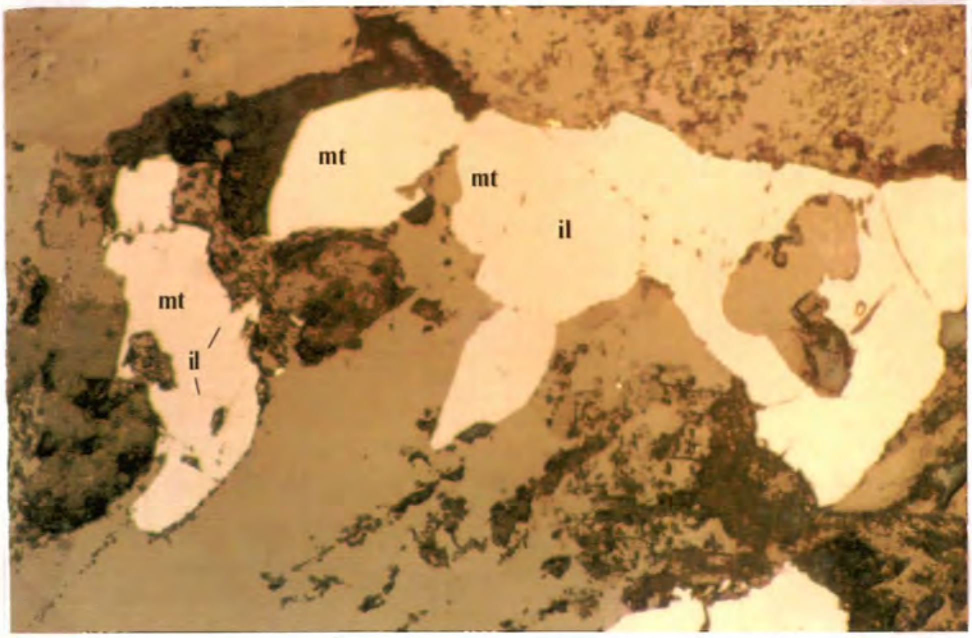

Plate 28. *Basal Gabbro showing magnetite(mt) as a discrete grain with exsolution lamellae of ilmenite(il). Also visible is the (possible?) replacement of ilmenite by magnetite. Note this is an electron microprobe section. Section SH10-7 (407.20). Field of view = 0.625 mm*

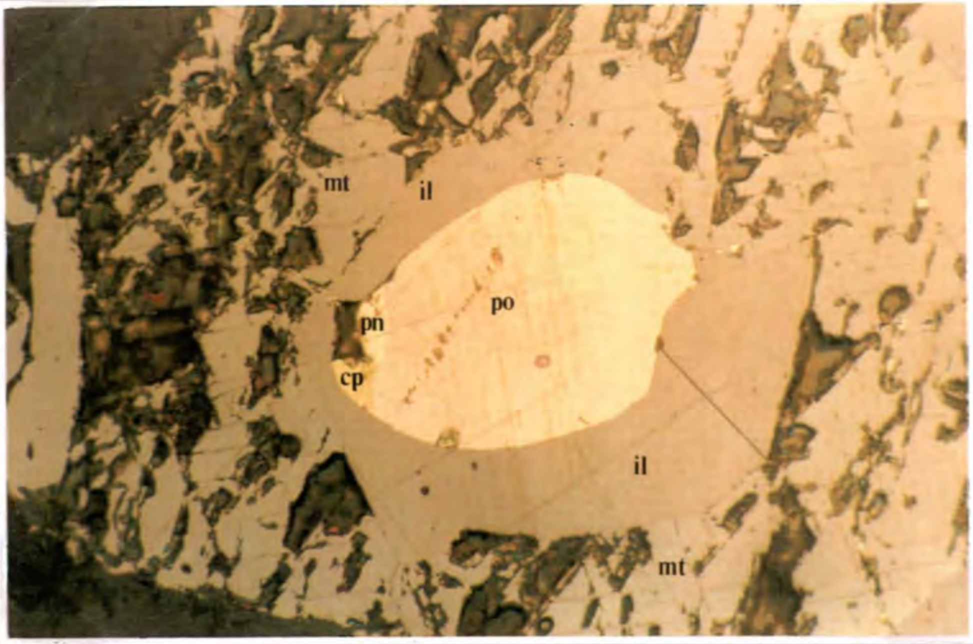

Plate 29. *Basal Gabbro showing secondary magnetite(mt) surrounding ilmenite(il) which in turn is enclosing pyrrhotite(po), chalcopyrite(cp) and pentlandite(pn). Note this is an electron microprobe section. Section SH10-5 (404.80) Field of view =0.25 mm*

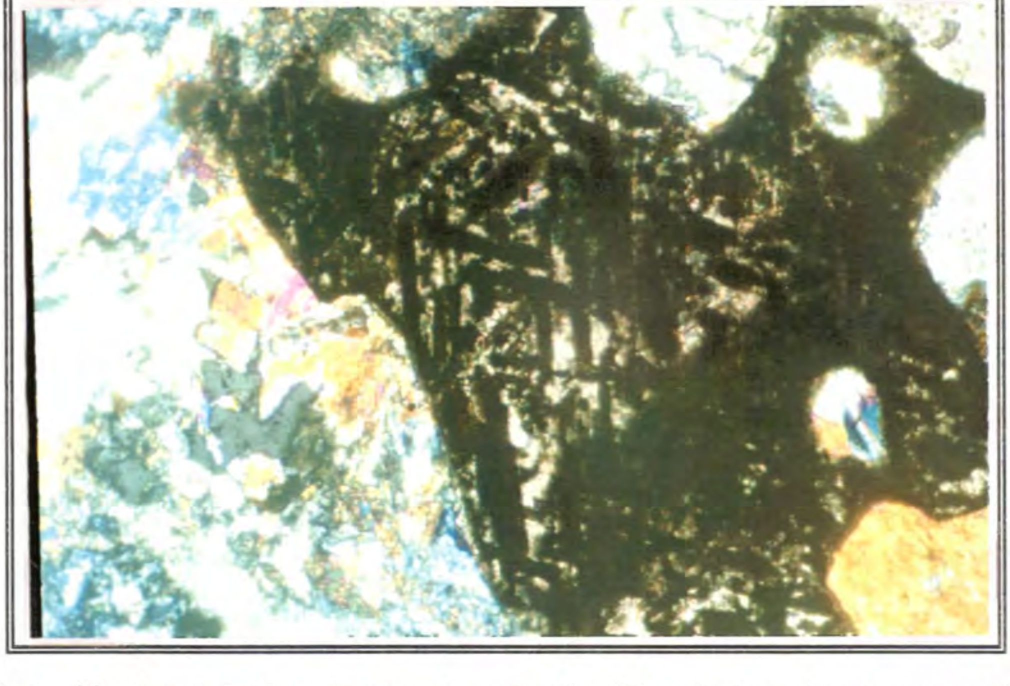

Plate 30. *Basal Gabbro showing skeletal rods of ilmenite in a silicate matrix. The ilmenite rods were exsolved from a now totally replaced grain of magnetite. Section SH10-2 (403.20). Field of view = 1.1 mm*

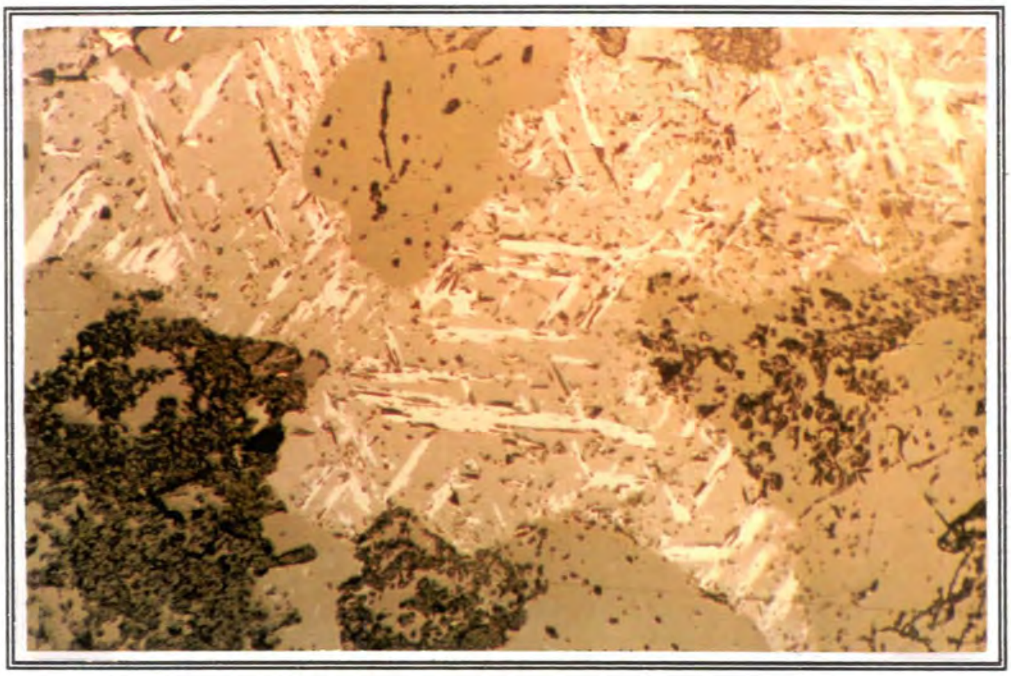

Plate 31. *Basal Gabbro showing skeletal rods of ilmenite in a silicate matrix. The ilmenite rods were exsolved from a now totally replaced grain of magnetite. Note this is a probe section.*
Section SH10-2 (403.20) Field of view = 1.25 mm

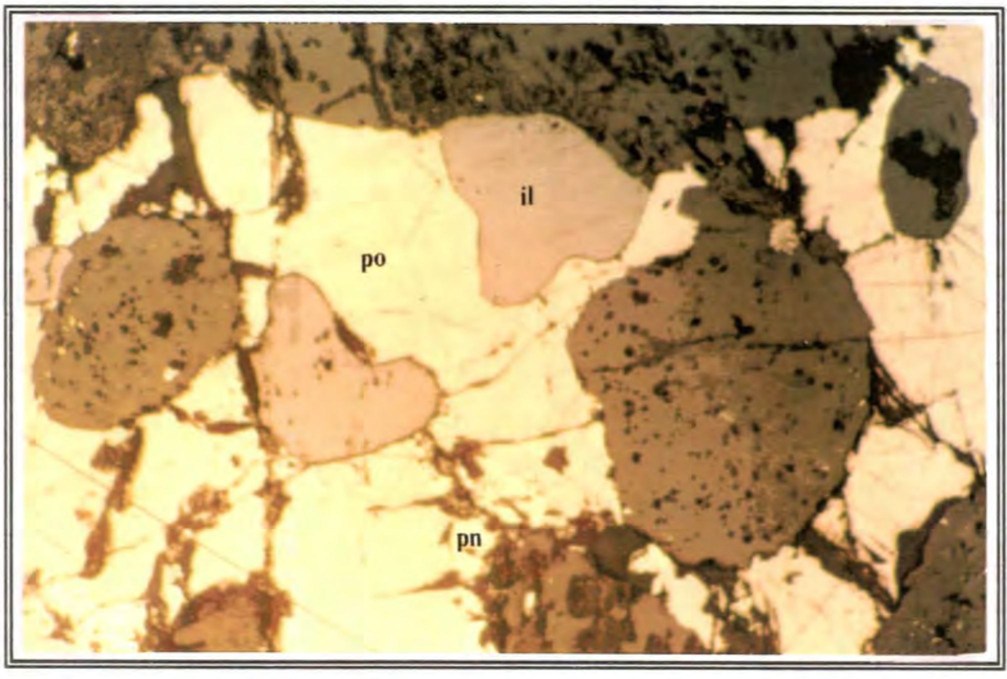

Plate 32. *Basal Gabbro showing ilmenite(il) apparently replacing pyrrhotite(po). The inclusion of ilmenite appears to be replacing the pyrrhotite, but is in a different orientation to the section. Note the pentlandite(pn) aggregating around fractures. This is an electron microprobe section.*
Section SH10.3 (403.43). Field of view = 1.25 mm

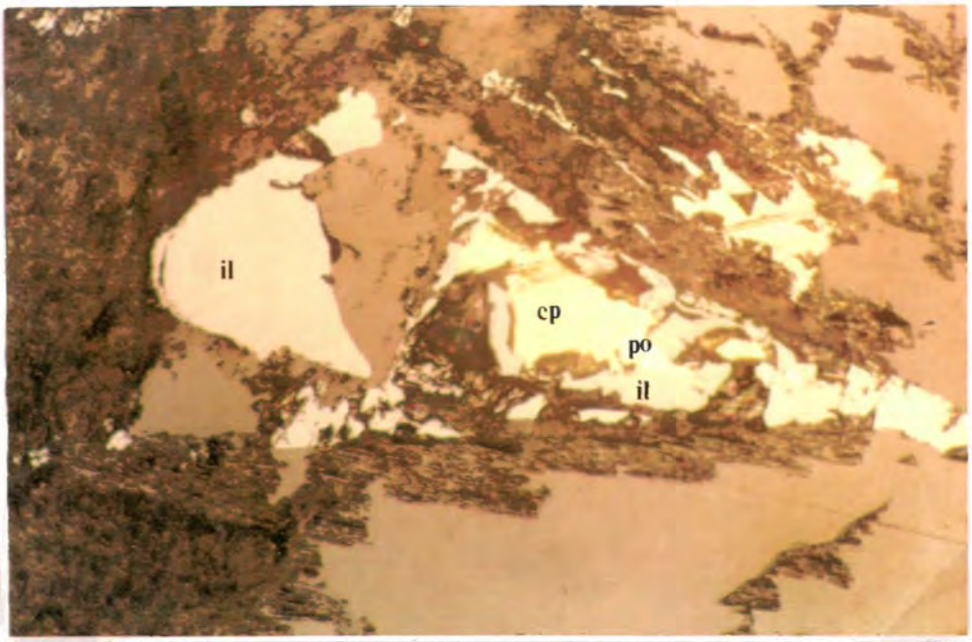

Plate 33. *Basal Gabbro showing ilmenite(il) enclosing and replacing chalcopyrite(cp) and pyrrhotite(po). Note this is an electron microprobe section. Section SH10-4 (404.07) Field of view = 0.625 mm*

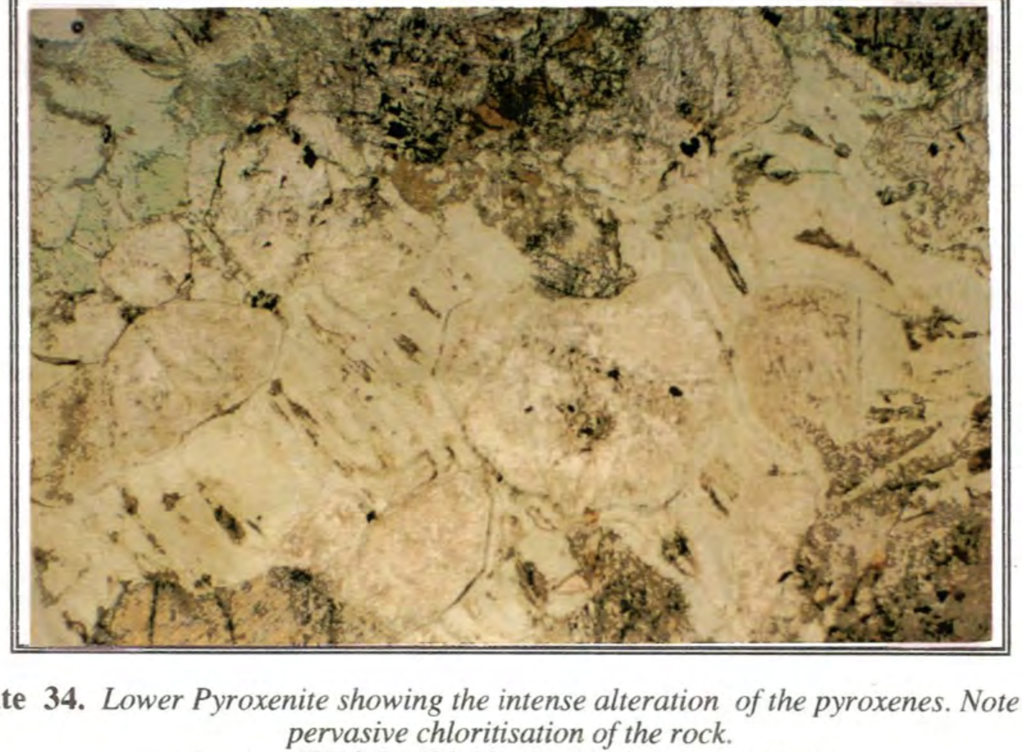

Plate 34. *Lower Pyroxenite showing the intense alteration of the pyroxenes. Note the pervasive chloritisation of the rock. Section SH10.1 (401.10). Field of view = 4.4 mm*

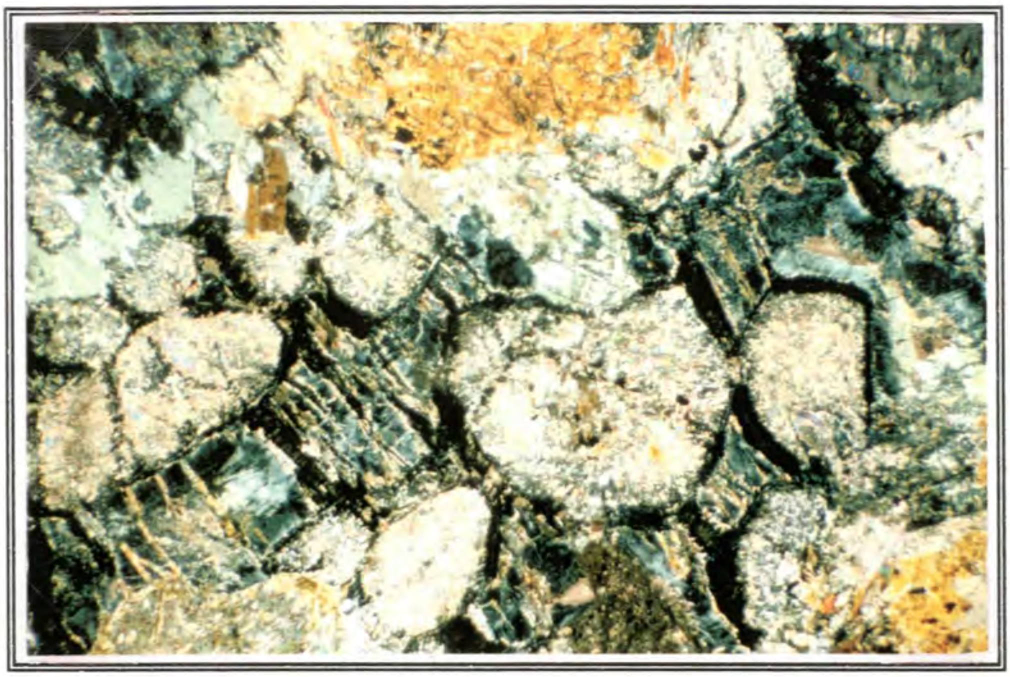

Plate 35. *Lower Pyroxenite showing the pseudomorphing of pyroxene (or olivine?) by talc. The corona textures are produced by a rim of chlorite. The pseudomorphs are separated by serpentine. Crossed nicols photograph of Plate 34. Section SH10-1 (401.10) Field of view = 4.4 mm*

Plate 36. *Diabase sill showing the medium- to fine-grained nature of the rock. The sill has been fairly extensively altered. Section SH10.10 (422.40). Field of view = 4.4 mm*

Appendix B

Borehole Logs

Reproduced with permission of Anglovaal.

GEOLOGICAL LOG

SH3

PROJECT	*SLAAIHOEK*
EXPLORATION COMPANY	*ANGLOVAAL*
FARM	*SLAAIHOEK 540 JT*
DRILLING COMMENCED	*Phase One*
DRILLING COMPLETED	
LOGGED BY	*Relogged 2*
DRILLED BY	

INCLINATION:	*-90*
BEARING:	*0*
X CONSTANT:	*2800000*
X COLLAR COORD.:	*46096.91*
Y COLLAR COORD.:	*40187.13*
ELEVATION (A.M.S.L.) IN METERS:	*1459.3*
FINAL DEPTH (m):	*474.89*
No WEDGES:	*0*

BOREHOLE **SH3** 0.00 to 43.00 m Plotted 06-02-1995 Page 1

Logged by RELOGGED 2 Scale 1: 200

CORE DEPTH (m)	VERT. PROFILE TOT.SULPH %	UNIT C	DESCRIPTION (core depths)	APP DIP deg
0.00		OVB	OVERBURDEN 0.00 -29.13 GRAIN SIZE: Pebble.	
29.13		PRD	PERIDOTITE 29.13 -123.71 Uitkomst Suite GRAIN SIZE: Fine grained. COMMENTS: Pyroxene poikilitically enclosing olivine.	85

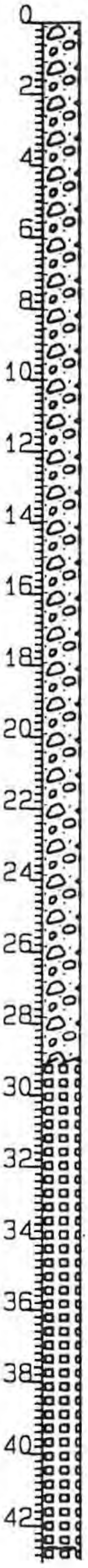

BOREHOLE **SH3** 43.00 to 86.00 m Plotted 06-02-1995 Page 2

Logged by RELOGGED 2 Scale 1: 200

CORE DEPTH (m)	VERT. PROFILE TOT.SULPH %	UNIT C	DESCRIPTION (core depths)		APP DIP deg
			(PERIDOTITE continued)	Uitkomst Suite	85
			SHEAR ZONE 74.71 -74.86 ALTERATION: Talc-alteration quartz carbonate veining. SCRATCH: Medium.	Uitkomst Suite	60
			PERIDOTITE 78.84 -94.44 Cr %: <1. MIN.TEXT: Seam.	Uitkomst Suite	88

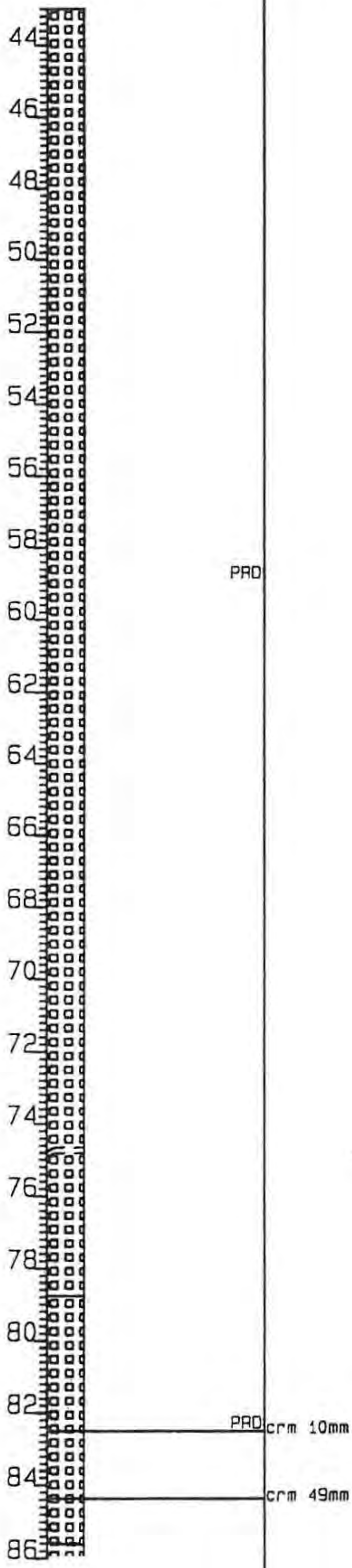

BOREHOLE **SH3** 86.00 to 129.00 m Plotted 06-02-1995 Page 3

Logged by RELOGGED 2 Scale 1: 200

CORE DEPTH (m)	VERT. PROFILE TOT.SULPH %	UNIT C	DESCRIPTION (core depths)	APP DIP deg

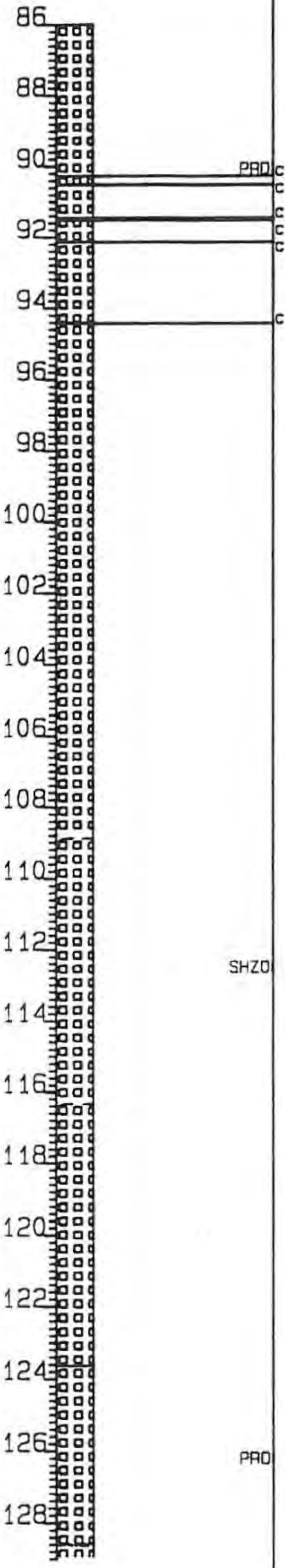

crm 10mm
crm 59mm
crm 29mm
crm 39mm
crm 9mm
crm 10mm

(PERIDOTITE continued)
(PERIDOTITE 78.84 - 94.44 continued) Uitkomst Suite 88

PERIDOTITE 108.92 -116.38 Uitkomst Suite 30
STRUCTURE: Sheared. ALTERATION: Serpentinised.

PERIDOTITE 123.71 -137.76 Uitkomst Suite 85
STRUCTURE: Sheared. ALTERATION: Serpentinised. COMMENTS: Cumulus olivine and pyroxene with interstitial plagioclase. MIN.TEXT: Mt stringer.

BOREHOLE *SH3*   129.00 to   172.00 m   Plotted 06-02-1995   Page 4

Logged by RELOGGED 2   Scale 1: 200

CORE DEPTH (m)	VERT. PROFILE TOT.SULPH %	UNIT C	DESCRIPTION (core depths)	APP DIP deg

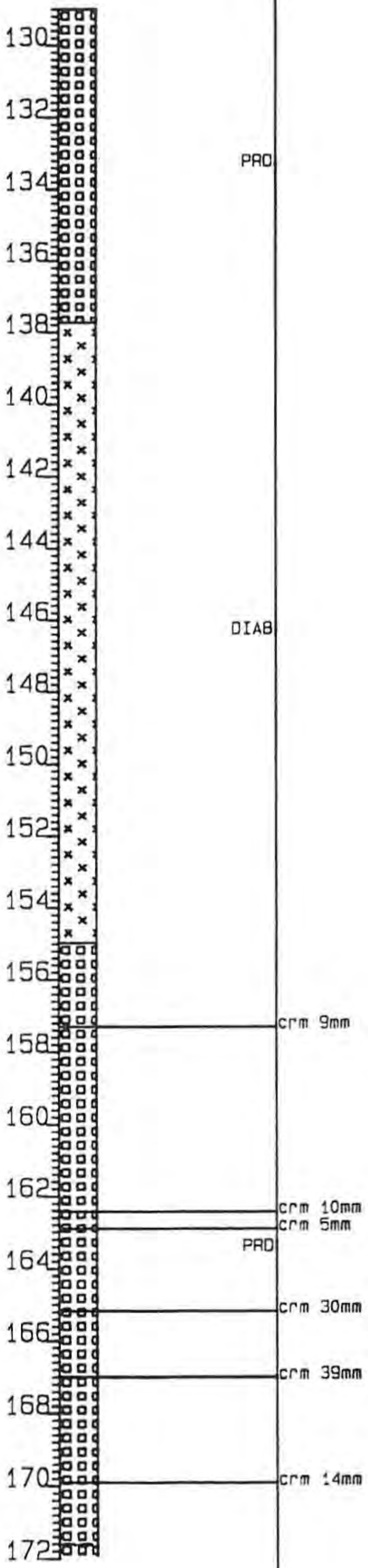

(PERIDOTITE continued)   Uitkomst Suite   85

DIABASE 137.76 -155.03   Uitkomst Suite   90

GRAIN SIZE: Medium grained. COMMENTS: Chilled margins. SILL.

PERIDOTITE 155.03 -178.08   Uitkomst Suite   90

ALTERATION: Talc-alteration serpentinised. COMMENTS: Interstitial plagioclase. Cr %: <1.
MIN.TEXT: Crm seams.

BOREHOLE **SH3** 172.00 to 215.00 m Plotted 06-02-1995 Page 5

Logged by RELOGGED 2 Scale 1: 200

CORE DEPTH (m)	VERT. PROFILE TOT.SULPH %	UNIT C	DESCRIPTION (core depths)	APP DIP deg

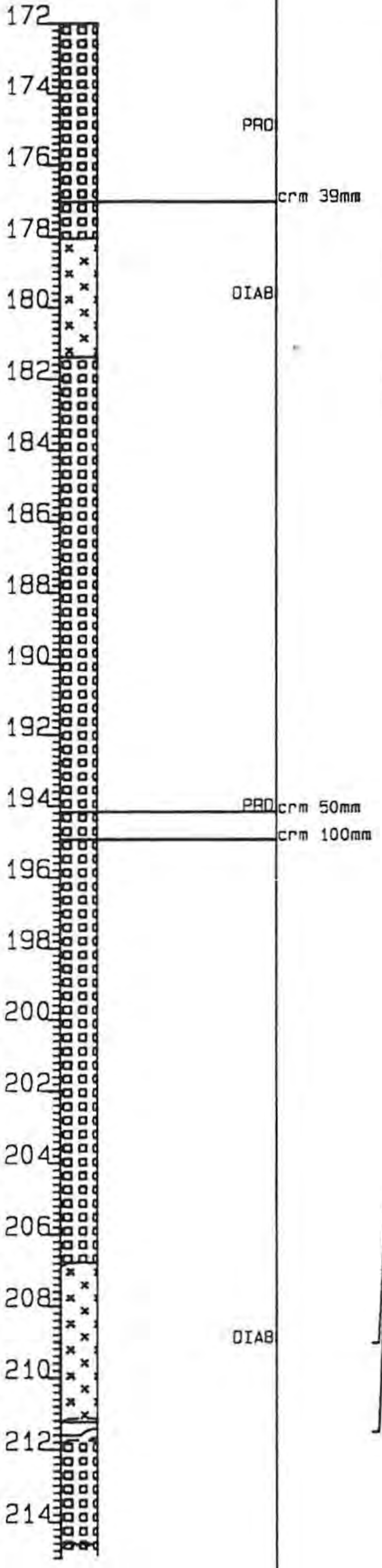

DESCRIPTION (core depths)		APP DIP deg
(PERIDOTITE continued)	Uitkomst Suite	90
DIABASE 178.08 -181.43 GRAIN SIZE: Medium grained. COMMENTS: Chilled margins. SILL.	Uitkomst Suite	90
PERIDOTITE 181.43 -292.44 ALTERATION: Serpentinised. COMMENTS: Pyroxene poikilitically enclosing olivine with inter-cumulus plagioclase. ASBESTOS %: <1. Cr %: <1. MIN.TEXT: Seam.	Uitkomst Suite	82
DIABASE 206.84 -211.20 ALTERATION: Quartz carbonate veining talc-alteration. GRAIN SIZE: Medium grained. COMMENTS: SILL/ DYKE ?.	Uitkomst Suite	45
MASSIVE CHROMITITE 211.20 -211.81 STRUCTURE: Sheared. ALTERATION: Quartz carbonate veining talc-alteration. COLOUR: Black. ASBESTOS %: <1.	Uitkomst Suite	90

BOREHOLE ***SH3*** 215.00 to 258.00 m Plotted 06-02-1995 Page 6

Logged by RELOGGED 2 Scale 1: 200

CORE DEPTH (m) | VERT. PROFILE TOT.SULPH % | UNIT C

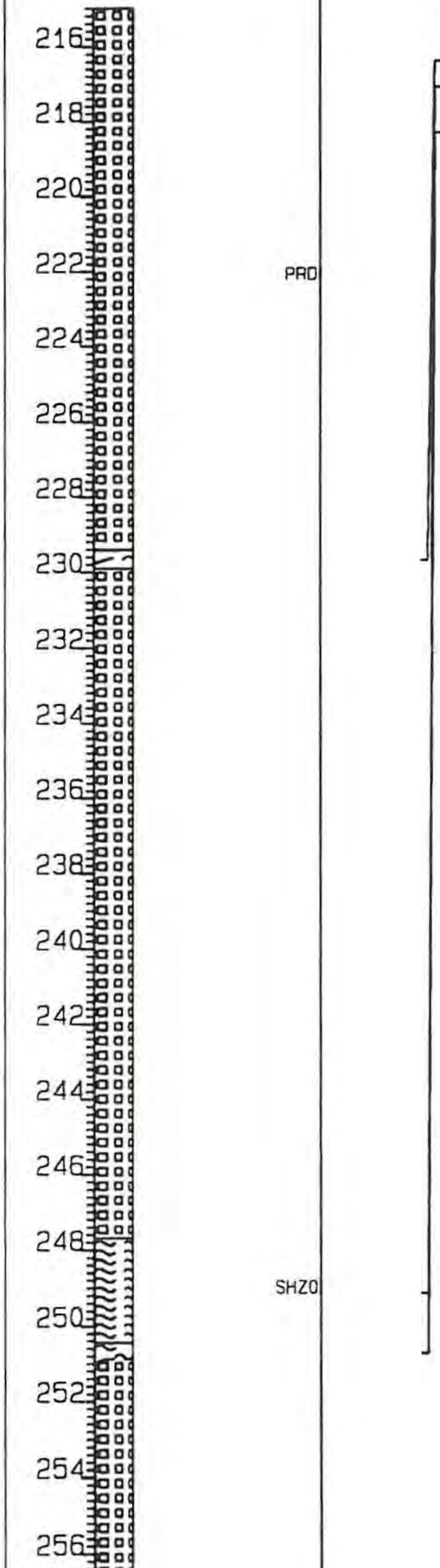

DESCRIPTION (core depths)		APP DIP deg
(PERIDOTITE continued)	Uitkomst Suite	82
SERPENTINITE 229.45 -229.94	Uitkomst Suite	80
SHEAR ZONE 247.76 -250.51 ALTERATION: Quartz carbonate veining serpentinised.	Uitkomst Suite	75
SCHIST 250.51 -250.93 ALTERATION: Talc-alteration quartz carbonate veining.	Uitkomst Suite	70

BOREHOLE **SH3** 258.00 to 301.00 m Plotted 06-02-1995 Page 7

Logged by RELOGGED 2 Scale 1: 200

CORE DEPTH (m)	VERT. PROFILE TOT.SULPH %	UNIT C	DESCRIPTION (core depths)	APP DIP deg

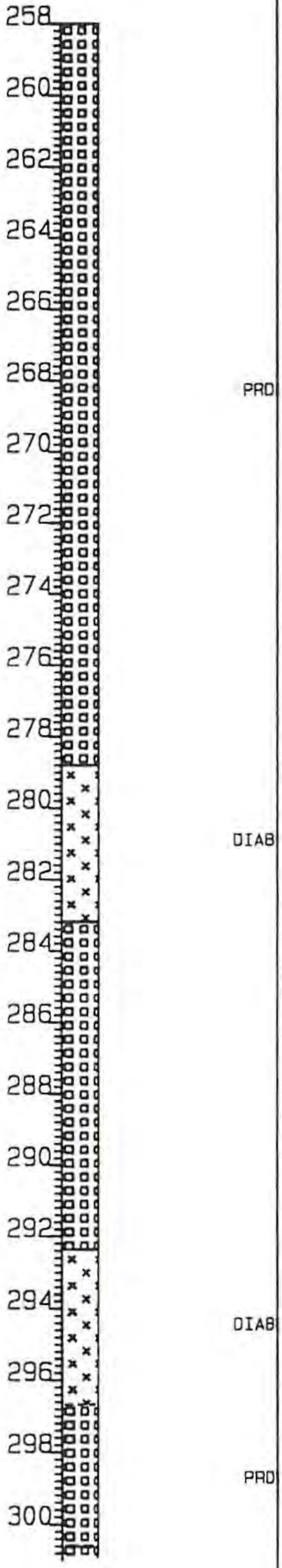

(PERIDOTITE continued) Uitkomst Suite 82

DIABASE 278.86 -283.25 Uitkomst Suite 75
GRAIN SIZE: Medium grained. COMMENTS: Chilled margins. SILL.

DIABASE 292.44 -296.74 Uitkomst Suite 82
ALTERATION: Quartz carbonate veining chloritisation. GRAIN SIZE: Fine grained. COMMENTS: Chilled margins. SILL.

PERIDOTITE 296.74 -304.44 Uitkomst Suite 85
ALTERATION: Quartz carbonate veining. GRAIN SIZE: Fine grained. COMMENTS: Pyroxene poikilitically enclosing olivine.

BOREHOLE **SH3** 301.00 to 344.00 m Plotted 06-02-1995

Logged by RELOGGED 2 Scale 1: 200

UNIT C	DESCRIPTION (core depths)	APP DIP deg
PRD	(PERIDOTITE continued) Uitkomst Suite	85
MCHR	MASSIVE CHROMITITE 304.44 -307.47 Uitkomst Suite STRUCTURE: Sheared. ALTERATION: Quartz carbonate veining. GRAIN SIZE: Fine grained. COLOUR: Black.	80
DIAB	DIABASE 307.47 -335.50 Uitkomst Suite ALTERATION: Quartz carbonate veining. GRAIN SIZE: Medium grained. COMMENTS: Sheared chilled margin. SILL. MIN.TEXT: Crm disseminated. SULPH.MINS.: Sulphides.	79
PCR	CHROMITITIC PYROXENITE 335.50 -351.10 Uitkomst Suite Cr %: 25-50.	83

BOREHOLE *SH3* 344.00 to 387.00 m

Plotted 06-02-1995 Page 9

Logged by RELOGGED 2 Scale 1: 200

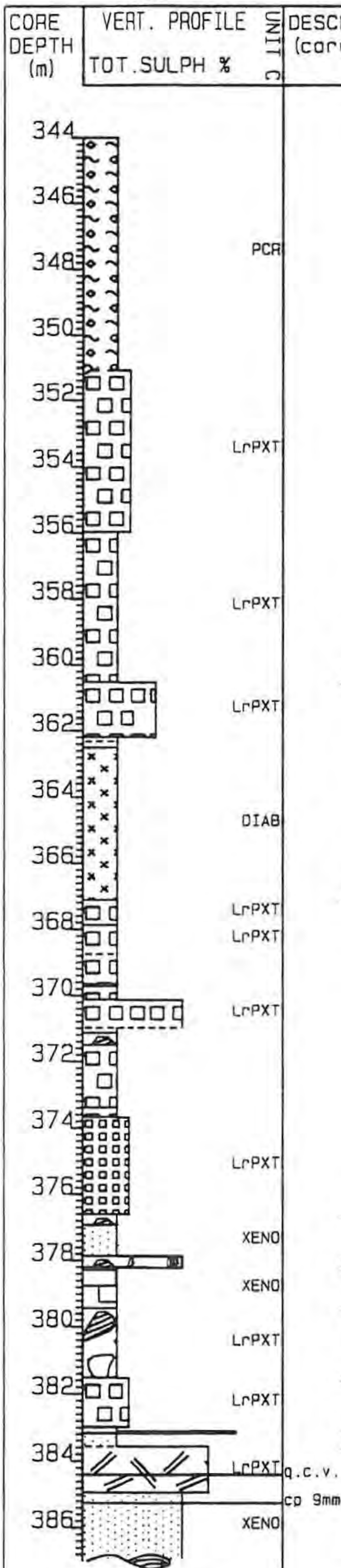

DESCRIPTION (core depths)	APP DIP deg
(CHROMITITIC PYROXENITE continued) Uitkomst Suite	83
PYROXENITE 351.10 -356.02 Uitkomst Suite GRAIN SIZE: Medium grained. TOT.SULPH %: 1-5. MIN.TEXT: Massive po. SULPH.MINS.: Po cp.	82
PYROXENITE 356.02 -360.57 Uitkomst Suite ALTERATION: Serpentinised. GRAIN SIZE: Medium grained. MIN.TEXT: Disseminated. SULPH.MINS.: Po cp.	82
PYROXENITE 360.57 -362.55 Uitkomst Suite ALTERATION: Serpentinised. GRAIN SIZE: Coarse grained. COMMENTS: Plagioclase pyroxene and amphibole. TOT.SULPH %: 5-10. MIN.TEXT: Disseminated. SULPH.MINS.: Po.	82
SERPENTINITE 362.24 -362.35 Uitkomst Suite GRAIN SIZE: Fine grained. COLOUR: Black.	82
AMPHIBOLITE 362.35 -362.55 Uitkomst Suite ALTERATION: Slightly altered. GRAIN SIZE: Coarse grained. COLOUR: Green. COMMENTS: Biotite.	82
DIABASE 362.55 -367.17 Uitkomst Suite GRAIN SIZE: Medium grained. COMMENTS: Chilled margin. SILL.	87
PYROXENITE 367.17 -373.74 Uitkomst Suite ALTERATION: Serpentinised. GRAIN SIZE: Medium grained. COMMENTS: Cumulus pyroxene. MIN.TEXT: Disseminated. SULPH.MINS.: Po cp.	82
PYROXENITE 367.93 -368.79 Uitkomst Suite GRAIN SIZE: Coarse grained. MIN.TEXT: Po disseminated.	82
PEGMATITE 369.72 -369.78 Uitkomst Suite GRAIN SIZE: Pegmatitic. COMMENTS: Comprising plagioclase.	82
PYROXENITE 370.19 -371.03 Uitkomst Suite GRAIN SIZE: Coarse grained. TOT.SULPH %: 10-25. MIN.TEXT: Disseminated. SULPH.MINS.: Po cp.	82
QUARTZITE 371.03 -371.19 Uitkomst Suite STRUCTURE: Xenolith. GRAIN SIZE: Fine sand. COLOUR: Grey white.	82
PEGMATITE 371.19 -371.57 Uitkomst Suite GRAIN SIZE: Pegmatitic. COMMENTS: Comprising plagioclase.	82
PYROXENITE 373.45 -373.73 Uitkomst Suite GRAIN SIZE: Coarse grained. COMMENTS: Amphibole.	82
PERIDOTITE 373.74 -376.68 Uitkomst Suite ALTERATION: Serpentinised. GRAIN SIZE: Medium grained. COMMENTS: Cumulus olivine with inter-cumulus plagioclase. TOT.SULPH %: 1-5. MIN.TEXT: Po disseminated. SULPH.MINS.: Po.	85
PEGMATITE 376.68 -377.00 Uitkomst Suite GRAIN SIZE: Coarse grained. MIN.TEXT: Massive po. SULPH.MINS.: Po cp.	82
QUARTZITE 377.00 -377.93 Uitkomst Suite STRUCTURE: Xenolith. GRAIN SIZE: Fine sand. COLOUR: Grey white. MIN.TEXT: Disseminated. SULPH.MINS.: Po py cp.	82
PEGMATITE 377.93 -378.29 Uitkomst Suite GRAIN SIZE: Coarse grained. TOT.SULPH %: 10-25. MIN.TEXT: Massive to semi-massive cp. SULPH.MINS.: Po cp.	82
DOLOMITE 378.29 -379.50 Uitkomst Suite GRAIN SIZE: Fine grained.	82
PEGMATITE 379.50 -381.59 Uitkomst Suite GRAIN SIZE: Coarse grained.	85
PYROXENITE 381.59 -383.07 Uitkomst Suite ALTERATION: Serpentinised. GRAIN SIZE: Medium grained. COMMENTS: Plagioclase amphibole pyroxene and biotite. TOT.SULPH %: 1-5. MIN.TEXT: Disseminated. SULPH.MINS.: Po cp.	82
QUARTZITE 383.07 -383.63 Uitkomst Suite STRUCTURE: Layered. ALTERATION: Slightly altered. GRAIN SIZE: Fine grained. COLOUR: Grey white. TOT.SULPH %: <1. MIN.TEXT: Disseminated to stringer. SULPH.MINS.: Py.	82
PEGMATITE 383.18 -383.26 Uitkomst Suite GRAIN SIZE: Coarse grained. TOT.SULPH %: >50. MIN.TEXT: Semi-massive. SULPH.MINS.: Po cp.	87
WEHRLITE 383.63 -385.02 Uitkomst Suite GRAIN SIZE: Fine grained. COMMENTS: Inter-cumulus plagioclase and fine grained cumulus olivine. TOT.SULPH %: 25-50. MIN.TEXT: Disseminated. SULPH.MINS.: Po.	82
QUARTZITE 385.02 -388.68 Uitkomst Suite TOT.SULPH %: 10-25. MIN.TEXT: Disseminated. SULPH.MINS.: Po cp.	82

Logged by RELOGGED 2 Scale 1: 200

CORE DEPTH (m) | VERT. PROFILE TOT.SULPH % | UNIT C

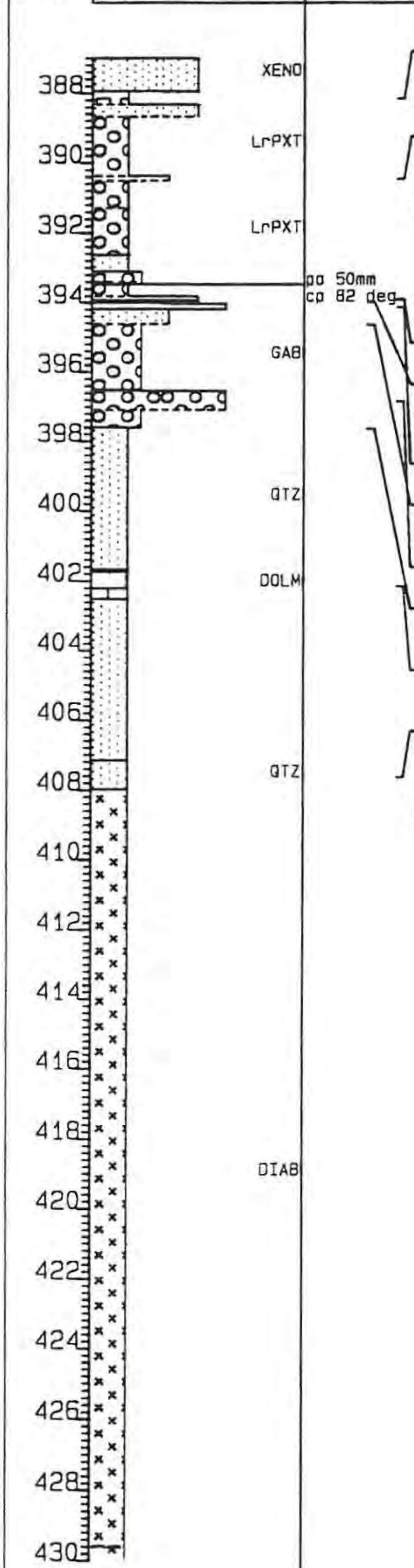

DESCRIPTION (core depths)	APP DIP deg
(QUARTZITE continued) Uitkomst Suite	82
PYROXENITE 387.97 -388.34 Uitkomst Suite GRAIN SIZE: Coarse grained. MIN.TEXT: Disseminated. SULPH.MINS.: Po.	80
GABBRO 388.68 -391.30 Uitkomst Suite GRAIN SIZE: Medium grained. TOT.SULPH %: <1. MIN.TEXT: Disseminated. SULPH.MINS.: Po.	82
GABBRO 390.39 -390.52 Uitkomst Suite GRAIN SIZE: Coarse grained. TOT.SULPH %: 5-10. MIN.TEXT: Massive po. SULPH.MINS.: Po cp.	82
GABBRO 391.30 -393.97 Uitkomst Suite GRAIN SIZE: Medium grained.	82
QUARTZITE 392.67 -393.14 Uitkomst Suite GRAIN SIZE: Fine sand. COLOUR: Grey white.	82
GABBRO 393.14 -393.43 Uitkomst Suite GRAIN SIZE: Medium grained. TOT.SULPH %: 1-5. MIN.TEXT: Po disseminated. SULPH.MINS.: Po.	82
GABBRO 393.83 -393.97 Uitkomst Suite GRAIN SIZE: Medium grained. TOT.SULPH %: 10-25. MIN.TEXT: Disseminated. SULPH.MINS.: Po cp.	82
QUARTZITE 393.97 -394.63 Uitkomst Suite STRUCTURE: Xenolith. ALTERATION: Metamorphosed. GRAIN SIZE: Medium sand. TOT.SULPH %: 5-10. MIN.TEXT: Disseminated. SULPH.MINS.: Cp po.	82
QUARTZITE 394.04 -394.22 Uitkomst Suite STRUCTURE: Xenolith. GRAIN SIZE: Fine grained. COLOUR: Grey. TOT.SULPH %: 25-50. MIN.TEXT: Disseminated. SULPH.MINS.: Po cp.	82
GABBRO 394.63 -397.63 Uitkomst Suite GRAIN SIZE: Medium grained. TOT.SULPH %: 1-5. MIN.TEXT: Disseminated. SULPH.MINS.: Po cp.	82
GABBRO 396.55 -397.11 Uitkomst Suite GRAIN SIZE: Medium grained. TOT.SULPH %: 25-50. MIN.TEXT: Disseminated. SULPH.MINS.: Po cp.	82
QUARTZITE 397.63 -408.03 Malmani Subgroup GRAIN SIZE: Fine sand. COLOUR: Grey white.	82
DOLOMITE 401.71 -402.55 Malmani Subgroup STRUCTURE: Sheared. ALTERATION: Quartz carbonate veining. GRAIN SIZE: Silt. COLOUR: Grey white.	82
QUARTZITE 407.20 -408.03 Malmani Subgroup GRAIN SIZE: Fine sand. COLOUR: Grey white. Py %: <1. MIN.TEXT: Disseminated. SULPH.MINS.: Py.	82
DIABASE 408.03 -430.83 Uitkomst Suite GRAIN SIZE: Medium grained. COMMENTS: Chilled margins. sill.	82

BOREHOLE ***SH3*** 430.00 to 473.00 m Plotted 06-02-1995 Page 11

Logged by RELOGGED 2 Scale 1: 200

CORE DEPTH (m) | VERT. PROFILE TOT.SULPH % | UNIT C

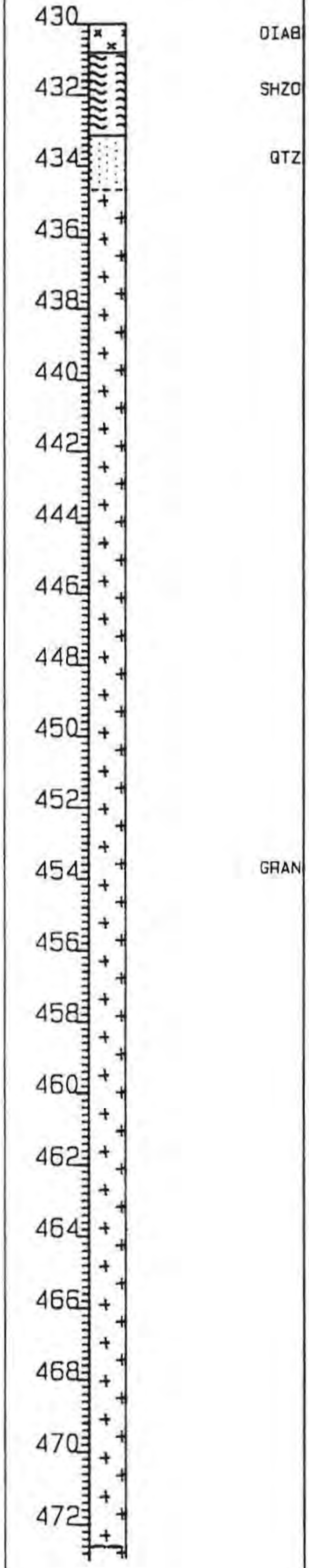

DESCRIPTION (core depths)		APP DIP deg
(DIABASE continued)	Uitkomst Suite	82
SHEAR ZONE 430.83 -433.17 ALTERATION: Quartz carbonate veining. GRAIN SIZE: Silt.	Malmani Subgroup	75
QUARTZITE 433.17 -434.69 GRAIN SIZE: Fine sand. COLOUR: Grey white.	Black Reef Quartzite	82
GRANITE 434.69 -474.89 GRAIN SIZE: Coarse grained.	Nelshoogte Granite	82

BOREHOLE **SH3** 473.00 to 474.89 m Plotted 06-02-1995 Page 12

Logged by RELOGGED 2 Scale 1: 200

CORE DEPTH (m)	VERT. PROFILE TOT.SULPH %	UNIT C	DESCRIPTION (core depths)		APP DIP deg
474	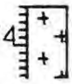	GRAN	(GRANITE continued)	Nelshoogte Granite	82

GEOLOGICAL LOG

sh8

PROJECT	*SLAAIHOEK*
EXPLORATION COMPANY	*ANGLOVAAL*
FARM	*SLAAIHOEK 540 JT*
DRILLING COMMENCED	*Phase One*
DRILLING COMPLETED	
LOGGED BY	*Relogged*

INCLINATION:	*-90*
BEARING:	*0*
X CONSTANT:	*2800000*
X COLLAR COORD.:	*45782.67*
Y COLLAR COORD.:	*40587.95*
ELEVATION (A.M.S.L.) IN METERS:	*1443.7*
FINAL DEPTH (m):	*485.06*
No WEDGES:	*0*

BOREHOLE **SH8**   0.00 to   43.00 m   Plotted 15-12-1994   Page 1

Logged by RELOGGED   Scale 1: 200

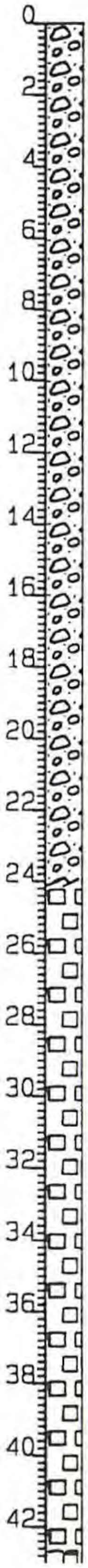

CORE DEPTH (m) / VERT. PROFILE TOT.SULPH %	UNIT C	DESCRIPTION (core depths)	APP DIP deg
	OVB	OVERBURDEN 0.00 -24.04 GRAIN SIZE: Pebble.	80
	UPXT	PYROXENITE 24.04 -45.60 Uitkomst Suite ALTERATION: Serpentinised. GRAIN SIZE: Coarse grained.	85

BOREHOLE **SH8** 43.00 to 86.00 m Plotted 15-12-1994 Page 2

Logged by RELOGGED Scale 1: 200

CORE DEPTH (m) | VERT. PROFILE TOT.SULPH % | UNIT C

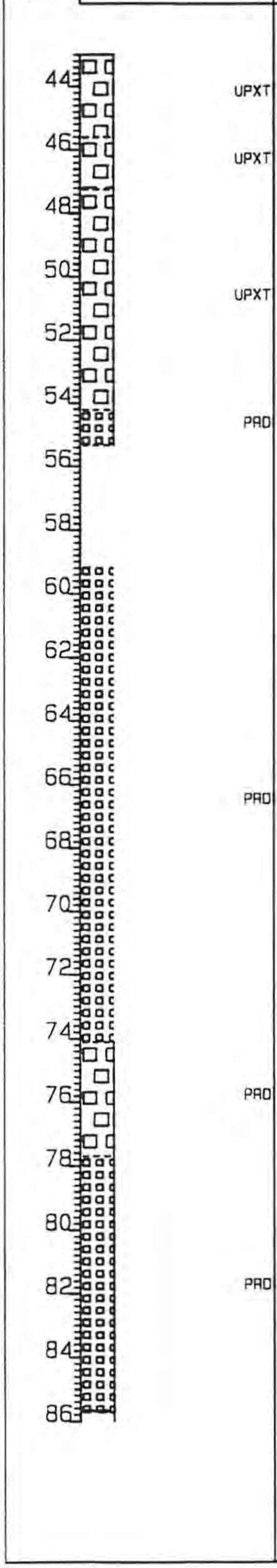

DESCRIPTION (core depths)	APP DIP deg
(PYROXENITE continued) Uitkomst Suite	85
PYROXENITE 45.60 -54.23 Uitkomst Suite GRAIN SIZE: Medium grained. COMMENTS: Comprising pyroxene and olivine.	85
PYROXENITE 45.61 -47.25 Uitkomst Suite GRAIN SIZE: Fine grained.	85
PYROXENITE 47.25 -54.23 Uitkomst Suite ALTERATION: Serpentinised. GRAIN SIZE: Coarse grained. COLOUR: Greyish green. COMMENTS: Interstitial plagioclase minor.	85
PERIDOTITE 54.23 -55.34 Uitkomst Suite GRAIN SIZE: Coarse grained.	85
PERIDOTITE 59.10 -74.10 Uitkomst Suite ALTERATION: Serpentinised. GRAIN SIZE: Coarse grained. COMMENTS: Coarse grained pyroxene poikilitically enclosing olivine.	85
PYROXENITE 74.10 -77.70 Uitkomst Suite ALTERATION: Serpentinised. GRAIN SIZE: Medium grained. COLOUR: Greyish green; COMMENTS: Pyroxene enclosing olivine.	85
PERIDOTITE 77.70 -142.40 Uitkomst Suite ALTERATION: Serpentinised. GRAIN SIZE: Medium grained. COLOUR: Greyish green. COMMENTS: Plagioclase towards the bottom. SULPH.MINS.: Mt.	85

BOREHOLE **SH8**   86.00 to 129.00 m   Plotted 15-12-1994   Page 3

Logged by RELOGGED   Scale 1: 200

CORE DEPTH (m)	VERT. PROFILE TOT.SULPH %	UNIT C	DESCRIPTION (core depths)	APP DIP deg
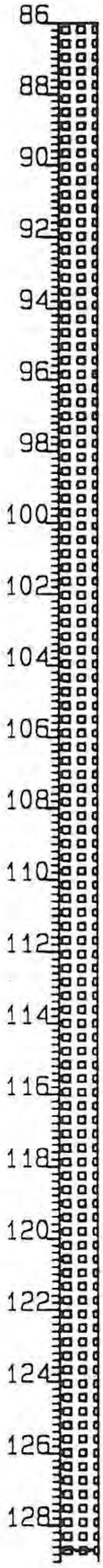		PRD	(PERIDOTITE continued) Uitkomst Suite	85

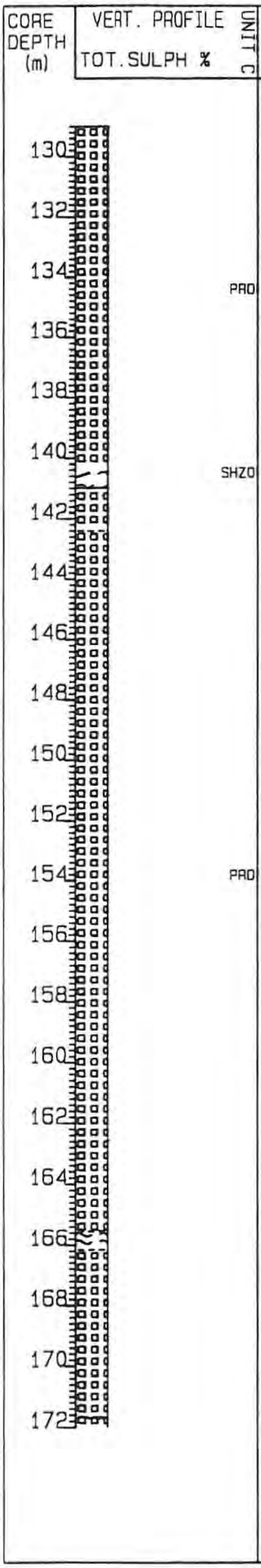

UNIT C	DESCRIPTION (core depths)		APP DIP deg
	(PERIDOTITE continued)	Uitkomst Suite	85
PRD			
	MASSIVE CHROMITITE 140.12 -140.29	Uitkomst Suite	79
SHZO	SERPENTINITE 140.29 -141.00	Uitkomst Suite	5
	MASSIVE CHROMITITE 141.00 -141.06	Uitkomst Suite	79
	PERIDOTITE 142.40 -180.20 ALTERATION: Serpentinised. GRAIN SIZE: Medium grained. COLOUR: Greyish green. COMMENTS: Pyroxene poikilitically enclosing olivine with minor interstitial plagioclase. Cr %: <1. MIN.TEXT: Crm disseminated.	Uitkomst Suite	85
PRD			
	SHEAR ZONE 165.54 -166.16 ALTERATION: Serpentinised talc-alteration.	Uitkomst Suite	85

Logged by RELOGGED

Scale 1: 200

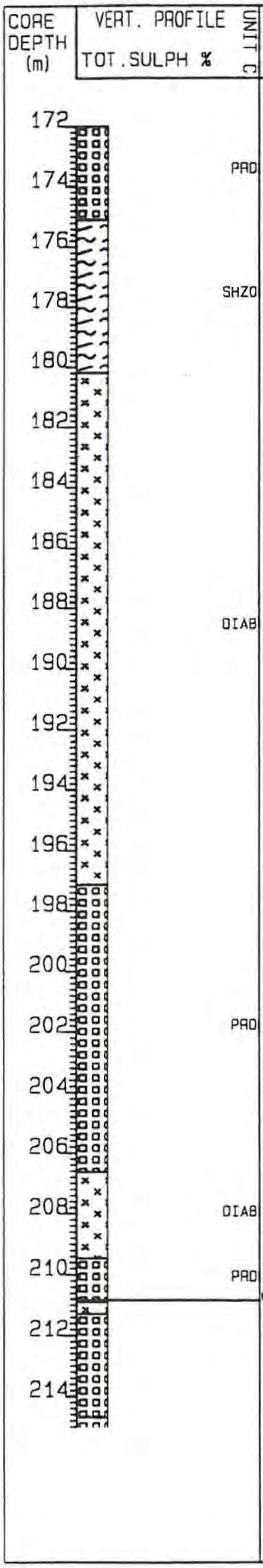

DESCRIPTION (core depths)	APP DIP deg
(PERIDOTITE continued) Uitkomst Suite	85
SERPENTINITE 175.11 -180.20 Uitkomst Suite	85
DIABASE 180.20 -197.15 Uitkomst Suite ALTERATION: Quartz carbonate veining with chloritisation. GRAIN SIZE: Medium grained. COLOUR: Greyish green to light green. COMMENTS: Chilled margins.	85
PERIDOTITE 197.15 -206.65 Uitkomst Suite ALTERATION: Serpentinised. GRAIN SIZE: Medium grained. COLOUR: Greyish green. COMMENTS: Pyroxene poikilitically enclosing olivine.	85
DIABASE 206.65 -209.48 Uitkomst Suite ALTERATION: Chloritisation. GRAIN SIZE: Medium grained. COMMENTS: Chilled margins.	85
PERIDOTITE 209.48 -221.71 Uitkomst Suite GRAIN SIZE: Medium grained. COLOUR: Greyish green. COMMENTS: Pyroxene poikilitically enclosing olivine with minor plagioclase.	85
DIABASE 210.90 -211.30 Uitkomst Suite GRAIN SIZE: Medium grained.	60

BOREHOLE **SH8** 215.00 to 258.00 m Plotted 15-12-1994 Page 6

Logged by RELOGGED Scale 1: 200

CORE DEPTH (m)	VERT. PROFILE TOT.SULPH %	UNIT C	DESCRIPTION (core depths)	APP DIP deg

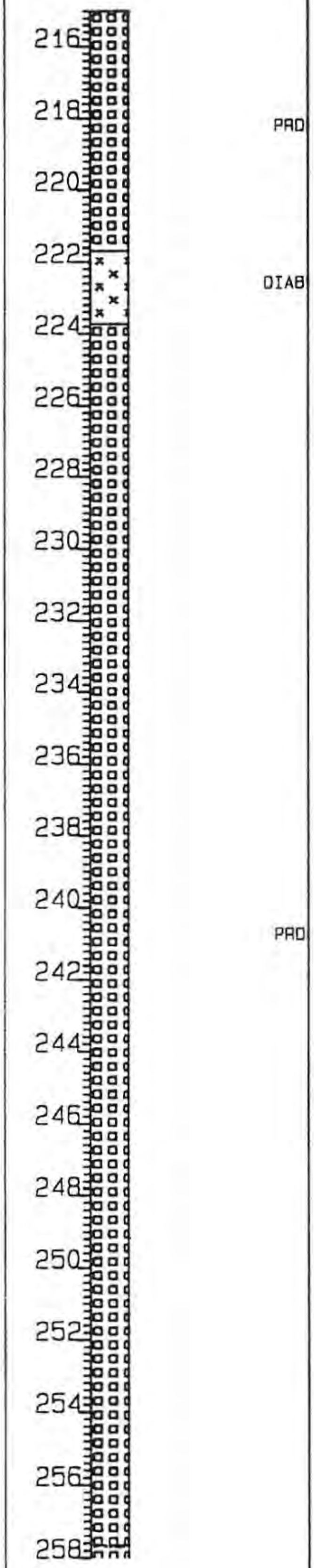

(PERIDOTITE continued) Uitkomst Suite 85

DIABASE 221.71 -223.75 Uitkomst Suite 80
ALTERATION: Quartz carbonate veining with chloritisation. GRAIN SIZE: Medium grained.
COMMENTS: Chilled margins.

PERIDOTITE 223.75 -270.66 Uitkomst Suite 85
ALTERATION: Talc-alteration. GRAIN SIZE: Medium grained. COLOUR: Greyish green. Cr %: Crm <1. TOT.SULPH %: <1. MIN.TEXT: Disseminated towards the bottom. SULPH.MINS.: Po cp.

BOREHOLE **SH8** 258.00 to 301.00 m Plotted 15-12-1994 Page 7

Logged by RELOGGED Scale 1: 200

CORE DEPTH (m) | VERT. PROFILE TOT.SULPH % | UNIT C

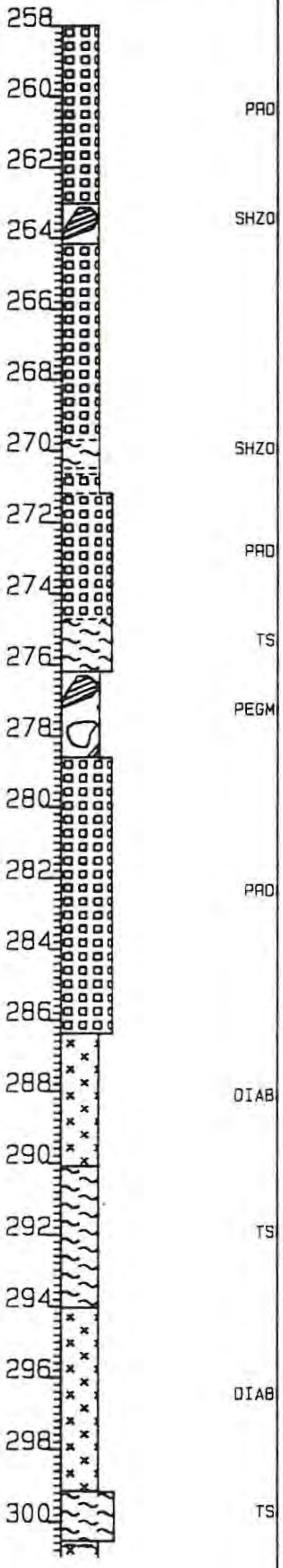

DESCRIPTION (core depths)	APP DIP deg
(PERIDOTITE continued) Uitkomst Suite	85
PEGMATITE 263.04 -264.18 Uitkomst Suite GRAIN SIZE: Pegmatitic.	85
SCHIST 269.70 -270.49 Uitkomst Suite ALTERATION: Serpentinised talc-alteration.	85
PERIDOTITE 270.66 -271.20 Uitkomst Suite GRAIN SIZE: Medium grained. COMMENTS: Pyroxene with olivine and minor plagioclase.	85
PERIDOTITE 271.20 -274.72 Uitkomst Suite ALTERATION: Talc-alteration. GRAIN SIZE: Medium grained. TOT.SULPH %: 1-5. MIN.TEXT: Disseminated. SULPH.MINS.: Po cp.	85
SCHIST 274.72 -276.20 Uitkomst Suite GRAIN SIZE: Coarse grained. TOT.SULPH %: 1-5. MIN.TEXT: Disseminated. SULPH.MINS.: Po cp.	60
PEGMATITE 276.20 -278.61 Uitkomst Suite ALTERATION: Quartz carbonate veining talc-alteration. GRAIN SIZE: Coarse grained.	40
PERIDOTITE 278.61 -286.40 Uitkomst Suite GRAIN SIZE: Coarse grained. COLOUR: Dark green. TOT.SULPH %: 1-5. MIN.TEXT: Disseminated. SULPH.MINS.: Sulphides.	85
DIABASE 286.40 -290.10 Uitkomst Suite ALTERATION: Chloritisation. GRAIN SIZE: Medium grained. COMMENTS: Chilled margins.	80
SCHIST 290.10 -294.04 Uitkomst Suite ALTERATION: Talc-alteration. GRAIN SIZE: Medium grained.	85
DIABASE 294.04 -299.15 Uitkomst Suite GRAIN SIZE: Medium grained. COMMENTS: Chilled margins.	80
SCHIST 299.15 -310.00 Uitkomst Suite ALTERATION: Talc-alteration.	85
SCHIST 299.16 -300.55 Uitkomst Suite TOT.SULPH %: 1-5. MIN.TEXT: Disseminated.	85
DIABASE 300.55 -302.75 Uitkomst Suite ALTERATION: Chloritisation. GRAIN SIZE: Medium grained. COMMENTS: Chilled margins.	75

BOREHOLE ***SH8*** 301.00 to 344.00 m Plotted 15-12-1994 Page 8

Logged by RELOGGED Scale 1: 200

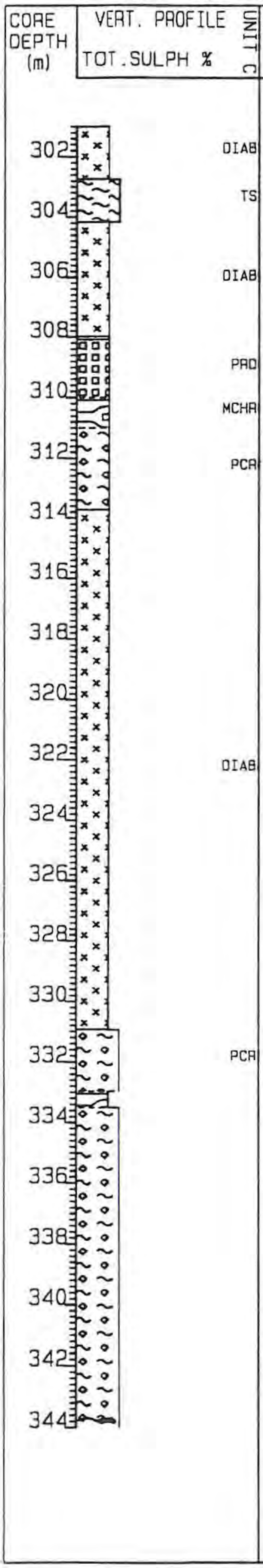

DESCRIPTION (core depths)	APP DIP deg
(SCHIST continued)	
(DIABASE 300.55 - 302.75 continued) Uitkomst Suite	75
SCHIST 302.75 -304.19 Uitkomst Suite GRAIN SIZE: Medium grained. TOT.SULPH %: 1-5. MIN.TEXT: Disseminated. SULPH.MINS.: Sulphides.	85
DIABASE 304.19 -308.00 Uitkomst Suite GRAIN SIZE: Medium grained. COMMENTS: Chilled margins.	85
PERIDOTITE 308.10 -310.00 Uitkomst Suite ALTERATION: Talc-alteration. GRAIN SIZE: Coarse grained. TOT.SULPH %: <1. MIN.TEXT: Disseminated. SULPH.MINS.: Sulphides.	85
MASSIVE CHROMITITE 310.00 -311.00 Uitkomst Suite GRAIN SIZE: Fine grained. COLOUR: Black.	85
CHROMITITIC PYROXENITE 311.00 -313.74 Uitkomst Suite ALTERATION: Talc-alteration. TOT.SULPH %: <1. MIN.TEXT: Disseminated. SULPH.MINS.: Sulphides.	85
DIABASE 313.74 -330.94 Uitkomst Suite ALTERATION: Quartz carbonate veining with chloritisation SILL. GRAIN SIZE: Medium grained. COMMENTS: Chilled margins.	80
CHROMITITIC PYROXENITE 330.94 -373.35 Uitkomst Suite GRAIN SIZE: Medium grained. Cr %: 25-50. TOT.SULPH %: 1-5. MIN.TEXT: Disseminated. SULPH.MINS.: Sulphides.	85
MASSIVE CHROMITITE 332.96 -333.50 Uitkomst Suite GRAIN SIZE: Fine grained. COLOUR: Black. Cr %: >50. MIN.TEXT: Massive.	85

BOREHOLE ***SH8*** 344.00 to 387.00 m Plotted 15-12-1994 Page 9

Logged by RELOGGED Scale 1: 200

CORE DEPTH (m) | VERT. PROFILE TOT.SULPH % | UNIT C

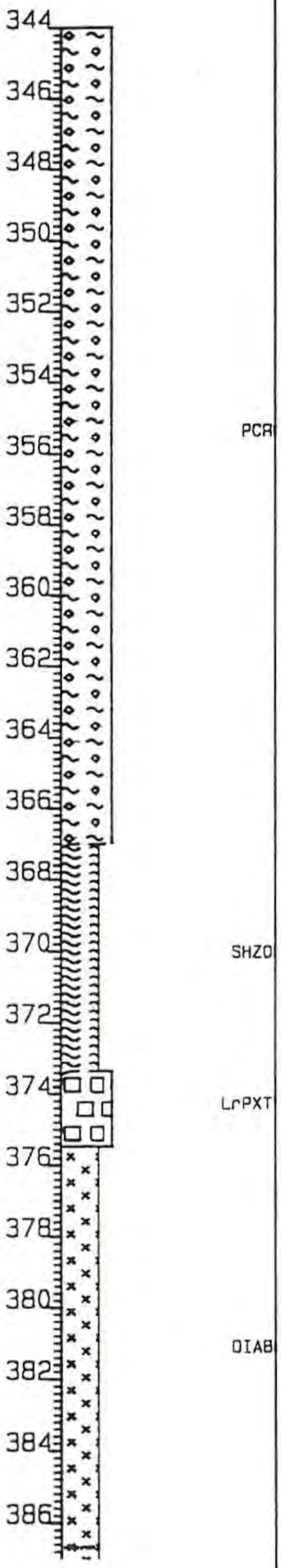

DESCRIPTION (core depths)	APP DIP deg
(CHROMITITIC PYROXENITE continued) Uitkomst Suite	85
SHEAR ZONE 367.00 -373.35 Uitkomst Suite STRUCTURE: Sheared.	85
PYROXENITE 373.35 -375.50 Uitkomst Suite ALTERATION: Silicified. GRAIN SIZE: Coarse grained. COLOUR: Greyish green to dark green. TOT.SULPH %: 1-5. MIN.TEXT: Disseminated. SULPH.MINS.: Po cp.	85
DIABASE 375.50 -404.83 Uitkomst Suite GRAIN SIZE: Medium grained.	85

BOREHOLE **SH8** 387.00 to 430.00 m Plotted 15-12-1994 Page 10

Logged by RELOGGED Scale 1: 200

CORE DEPTH (m) | VERT. PROFILE TOT.SULPH % | UNIT C

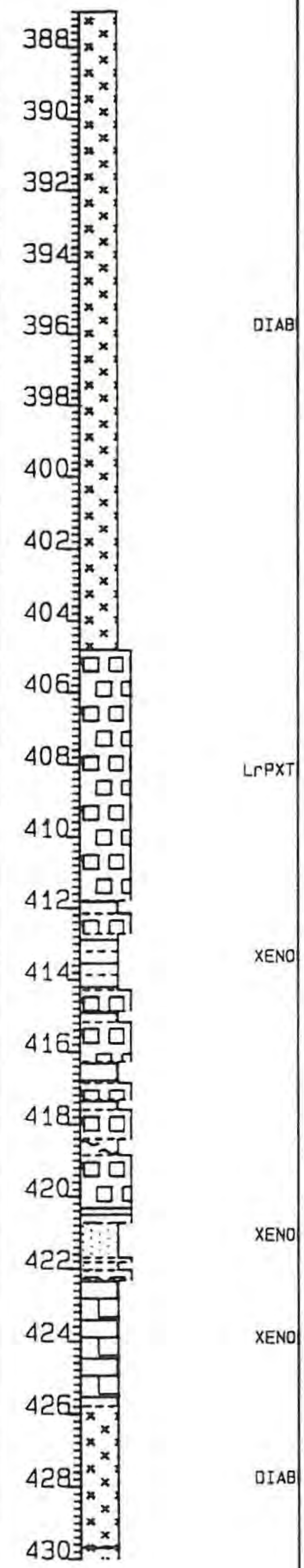

DESCRIPTION (core depths)		APP DIP deg
(DIABASE continued)	Uitkomst Suite	85
PYROXENITE 404.83 -425.79 ALTERATION: Talc-alteration. GRAIN SIZE: Medium grained. COLOUR: Grey green to dark green. COMMENTS: With xenoliths. Py %: <1. TOT.SULPH %: 1-5. MIN.TEXT: Disseminated. SULPH.MINS.: Po py.	Uitkomst Suite	85
DOLOMITE 411.78 -412.15 STRUCTURE: Layered.	Uitkomst Suite	85
CHERT 412.71 -414.28	Uitkomst Suite	85
DOLOMITE 414.87 -415.17 STRUCTURE: Xenolith.	Uitkomst Suite	85
DOLOMITE 416.27 -416.86 STRUCTURE: Xenolith.	Uitkomst Suite	85
DOLOMITE 417.32 -417.60 COLOUR: Green.	Uitkomst Suite	85
SCHIST 418.40 -418.85 ALTERATION: Serpentinised talc-alteration.	Uitkomst Suite	85
PYROXENITE 420.34 -420.52 TOT.SULPH %: 1-5. MIN.TEXT: Disseminated. SULPH.MINS.: Po py cp.	Uitkomst Suite	85
QUARTZITE 420.73 -421.69 STRUCTURE: Layered. ALTERATION: Silicified.	Uitkomst Suite	85
QUARTZITE 421.82 -422.04 STRUCTURE: Laminated layered xenolith.	Uitkomst Suite	85
DOLOMITE 422.31 -425.79 STRUCTURE: Laminated layered xenolith. ALTERATION: Silicified. GRAIN SIZE: Pegmatitic.	Uitkomst Suite	85
DIABASE 425.79 -450.57 GRAIN SIZE: Medium grained. COLOUR: Greenish grey to light green. COMMENTS: Chilled margins.SILL.	Uitkomst Suite	65

Logged by RELOGGED

Scale 1: 200

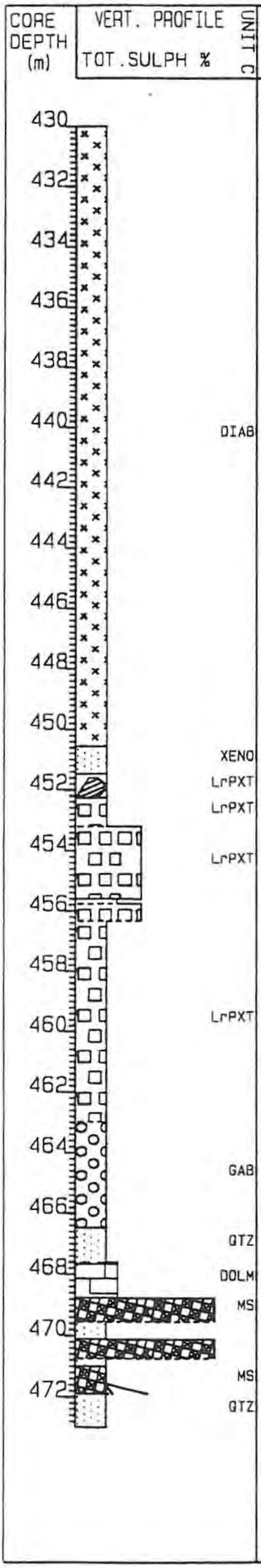

DESCRIPTION (core depths)		APP DIP deg
(DIABASE continued)	Uitkomst Suite	65
QUARTZITE 450.57 -451.49 ALTERATION: Silicified.	Uitkomst Suite	85
PEGMATITE 451.49 -452.28 GRAIN SIZE: Pegmatitic.	Uitkomst Suite	85
PYROXENITE 452.28 -453.20 ALTERATION: Talc-alteration with carbonatisation. GRAIN SIZE: Coarse grained. COLOUR: Greyish green to dark green.	Uitkomst Suite	85
PYROXENITE 453.20 -462.98 GRAIN SIZE: Coarse grained. COLOUR: Greyish green to greenish black. TOT.SULPH %: 5-10. MIN.TEXT: Disseminated. SULPH.MINS.: Po cp.	Uitkomst Suite	85
PYROXENITE 455.62 -455.76 TOT.SULPH %: 1-5. MIN.TEXT: Disseminated. SULPH.MINS.: Sulphides.	Uitkomst Suite	85
PYROXENITE 456.33 -462.98 COMMENTS: Cumulus.	Uitkomst Suite	85
GABBRO 462.98 -466.48 GRAIN SIZE: Medium grained. COLOUR: Greenish grey. COMMENTS: Chilled margin.	Uitkomst Suite	85
QUARTZITE 466.48 -467.61	Malmani Subgroup	85
DOLOMITE 467.61 -468.77 STRUCTURE: Sheared. TOT.SULPH %: 1-5. MIN.TEXT: Disseminated. SULPH.MINS.: Sulphides.	Malmani Subgroup	85
MASSIVE SULPHIDE 468.77 -469.54 COMMENTS: Massive po. TOT.SULPH %: >50. MIN.TEXT: Massive po. SULPH.MINS.: Po.	Uitkomst Suite	85
QUARTZITE 469.54 -470.12	Uitkomst Suite	85
MASSIVE SULPHIDE 470.12 -470.74 COMMENTS: Massive po. TOT.SULPH %: >50. MIN.TEXT: Massive po. SULPH.MINS.: Po.	Uitkomst Suite	85
QUARTZITE 470.74 -471.01	Uitkomst Suite	85
MASSIVE SULPHIDE 471.01 -471.91 COMMENTS: Massive po. MIN.TEXT: Massive po. SULPH.MINS.: Po.	Uitkomst Suite	85
QUARTZITE 471.91 -473.00 GRAIN SIZE: Medium sand.	Black Reef Quartzite	85

BOREHOLE **SH8** 473.00 to 485.06 m Plotted 15-12-1994 Page 12

Logged by RELOGGED Scale 1: 200

CORE DEPTH (m)	VERT. PROFILE TOT.SULPH %	UNIT C	DESCRIPTION (core depths)		APP DIP deg
			(QUARTZITE continued)	Black Reef Quartzite	85
		GRAN	GRANITE 473.00 -478.23 ALTERATION: Silicified. GRAIN SIZE: Coarse grained.	Nelshoogte Granite	85
		GRAN	GRANITE 478.23 -485.06	Nelshoogte Granite	85

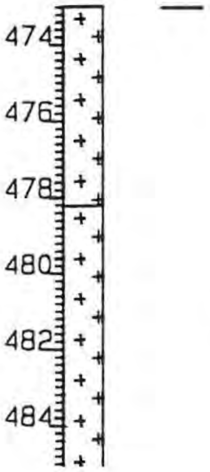

GEOLOGICAL LOG

sh10

PROJECT	*SLAAIHOEK*
EXPLORATION COMPANY	*ANGLOVAAL*
FARM	*SLAAIHOEK 540 JT*
DRILLING COMMENCED	*Phase One*
DRILLING COMPLETED	
LOGGED BY	*Relogged*
DRILLED BY	

INCLINATION:	*-90*
BEARING:	*0*
X CONSTANT:	*2800000*
X COLLAR COORD.:	*46008.09*
Y COLLAR COORD.:	*40141.37*
ELEVATION (A.M.S.L.) IN METERS:	*1470.72*
FINAL DEPTH (m):	*443.32*
No WEDGES:	*0*

BOREHOLE **SH10** 0.00 to 43.00 m Plotted 06-02-1995 Page 1

Logged by Relogged 2 Scale 1: 200

CORE DEPTH (m)	VERT. PROFILE TOT.SULPH %	UNIT C	DESCRIPTION (core depths)	APP DIP deg
		OVB	OVERBURDEN 0.00 -30.66 Uitkomst Suite COMMENTS: No core recovered.	
		PRD	PERIDOTITE 30.66 -136.56 Uitkomst Suite STRUCTURE: Homogeneous. ALTERATION: Slightly weathered and serpentinised. GRAIN SIZE: Medium grained. COLOUR: Grey. COMMENTS: Cumulate texture poikilitic. Cr %: <1. SCRATCH: Hard.	80

BOREHOLE **SH10** 43.00 to 86.00 m Plotted 06-02-1995 Page 2

Logged by Relogged 2 Scale 1: 200

CORE DEPTH (m)	VERT. PROFILE TOT.SULPH %	UNIT C	DESCRIPTION (core depths)	APP DIP deg
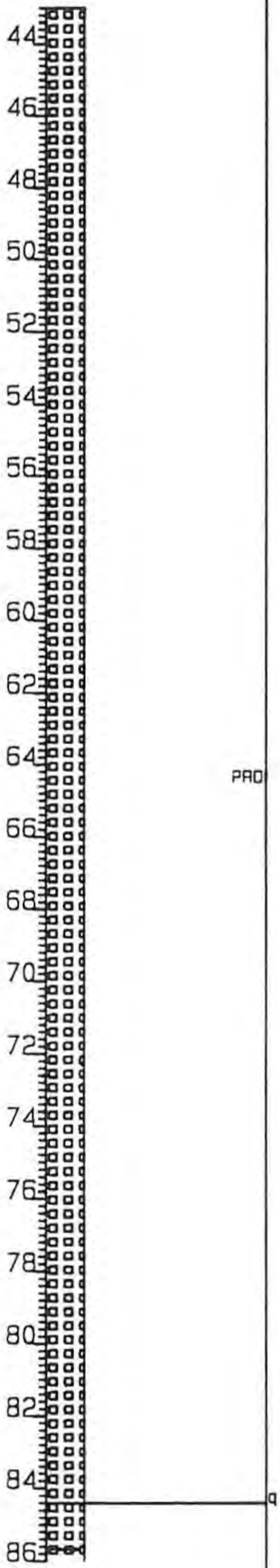		PRD	(PERIDOTITE continued) Uitkomst Suite q.v. 29mm	80

BOREHOLE ***SH10*** 86.00 to 129.00 m Plotted 23-02-1995 Page 3

Logged by Relogged 2

Scale 1: 200

CORE DEPTH (m) | VERT. PROFILE TOT.SULPH % | UNIT C

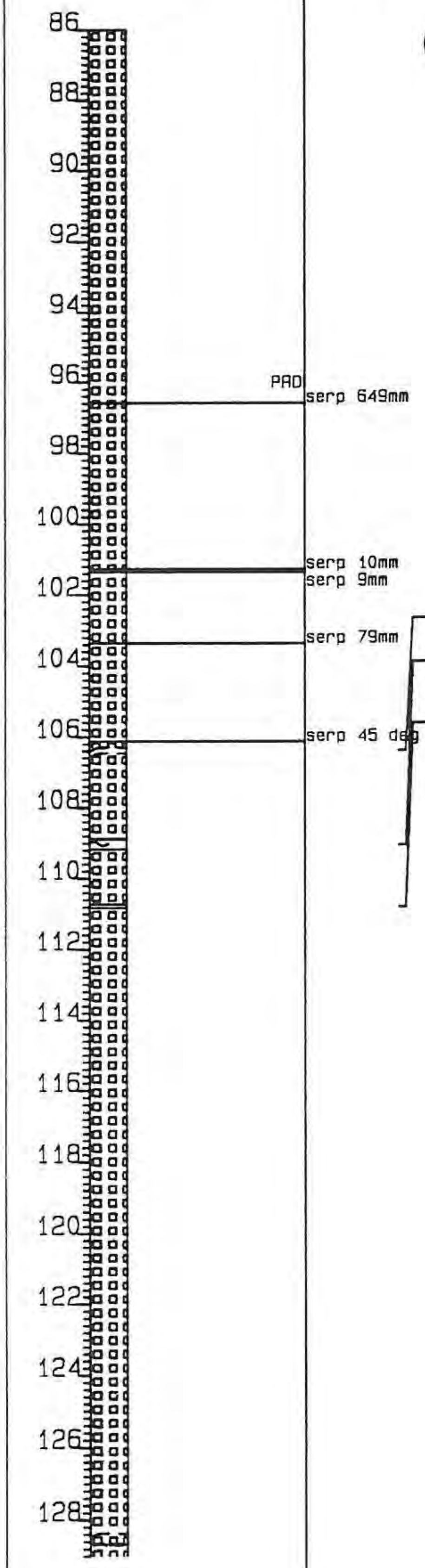

DESCRIPTION (core depths)		APP DIP deg
(PERIDOTITE continued)	Uitkomst Suite	80
QUARTZ CARBONATE VEIN 106.30 -106.46 GRAIN SIZE: Coarse grained. COLOUR: White. SCRATCH: Hard.	Uitkomst Suite	52
SCHIST 108.89 -109.18 ALTERATION: Quartz carbonate veining talc-alteration. GRAIN SIZE: Fine grained. Cr %: <1.	Uitkomst Suite	80
DOLERITE 110.74 -110.84 GRAIN SIZE: Fine grained. COLOUR: Dark grey green. COMMENTS: Sill. SCRATCH: Hard.	Uitkomst Suite	80
PERIDOTITE 128.37 -136.55 STRUCTURE: Sheared veined. GRAIN SIZE: Medium grained. COLOUR: Dark grey. SCRATCH: Hard.	Uitkomst Suite	80

Logged by Relogged 2

Scale 1: 200

CORE DEPTH (m)	VERT. PROFILE TOT.SULPH %	UNIT C	DESCRIPTION (core depths)	APP DIP deg

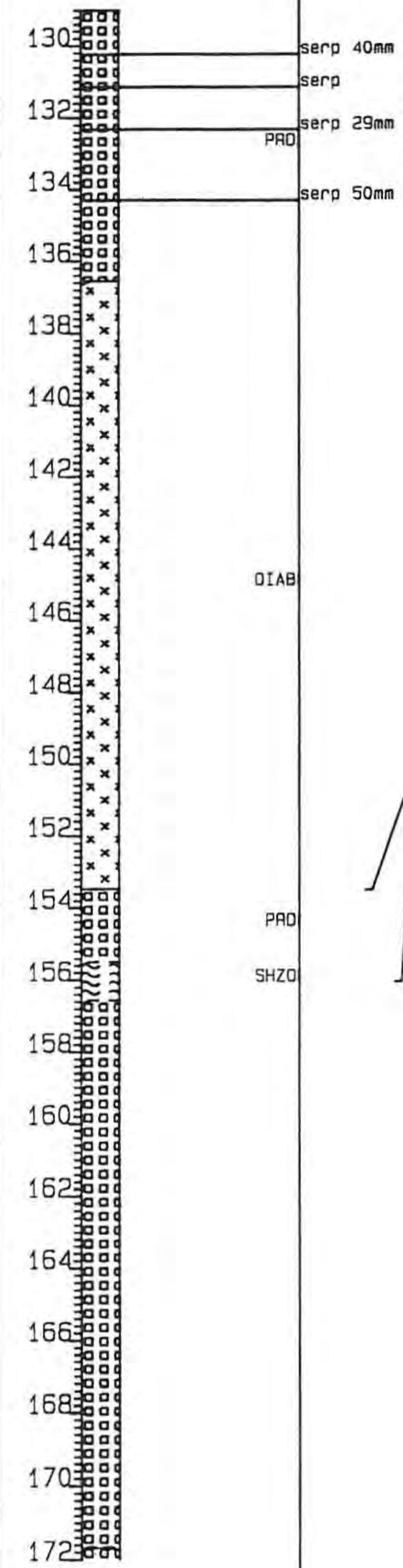

(PERIDOTITE continued)
(PERIDOTITE 128.37 - 136.55 continued) Uitkomst Suite 80

DIABASE 136.56 -153.48 Uitkomst Suite 79
ALTERATION: Quartz carbonate veining. GRAIN SIZE: Medium grained. COLOUR: Grey white.
COMMENTS: Chilled margins (sill). SCRATCH: Hard.

PERIDOTITE 153.48 -179.64 Uitkomst Suite 80
ALTERATION: Serpentinised. COMMENTS: Cumulus pyroxene with inter-cumulus plagioclase.
Cr %: <1. SCRATCH: Hard.

SHEAR ZONE 155.49 -156.56 Uitkomst Suite 55
STRUCTURE: Sheared. GRAIN SIZE: Medium grained. COLOUR: Dark grey.
SCRATCH: Medium.

CORE DEPTH (m) | VERT. PROFILE TOT.SULPH % | UNIT C | DESCRIPTION (core depths) | APP DIP deg

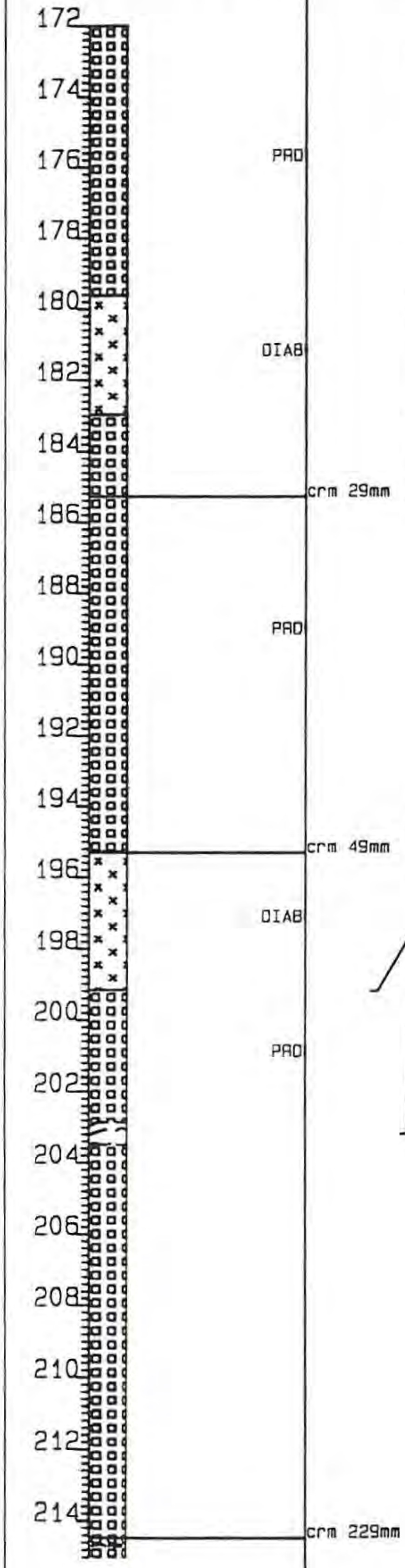

DESCRIPTION (core depths)	APP DIP deg
(PERIDOTITE continued) Uitkomst Suite	80
DIABASE 179.64 -182.98 Uitkomst Suite GRAIN SIZE: Fine grained. COLOUR: Grey. COMMENTS: Chilled margins (sill). SCRATCH: Hard.	75
PERIDOTITE 182.98 -195.29 Uitkomst Suite STRUCTURE: Homogeneous. GRAIN SIZE: Coarse grained. COLOUR: Dark grey. MAGNETISM: Susceptable. COMMENTS: Cumulus olivine with pyroxene and inter-cumulus plagioclase (poikilitic). Cr %: <1. TOT.SULPH %: <1. MIN.TEXT: Disseminated. SCRATCH: Hard. SULPH.MINS.: Po.	80
DIABASE 195.29 -199.18 Uitkomst Suite STRUCTURE: Homogeneous. GRAIN SIZE: Fine grained. COLOUR: Dark grey. COMMENTS: Chilled margins (sill). SCRATCH: Hard.	85
PERIDOTITE 199.18 -225.77 Uitkomst Suite ALTERATION: Serpentinised. GRAIN SIZE: Coarse grained. COLOUR: Dark grey. MAGNETISM: Susceptable. Cr %: 1-5. MIN.TEXT: Seam. SCRATCH: Hard.	80
SERPENTINITE 202.86 -203.49 Uitkomst Suite ALTERATION: Serpentinised. GRAIN SIZE: Fine grained. COLOUR: Dark green. MAGNETISM: Susceptable. SCRATCH: Medium.	5

CORE DEPTH (m) | VERT. PROFILE TOT.SULPH % | UNIT C

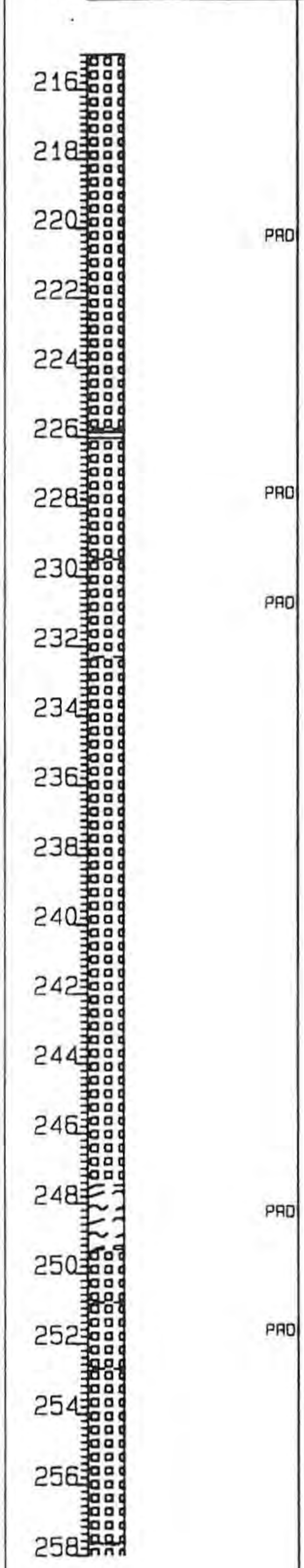

DESCRIPTION (core depths)	APP DIP deg
(PERIDOTITE continued) Uitkomst Suite	80
MASSIVE CHROMITITE 225.77 -226.06 Uitkomst Suite STRUCTURE: Sheared veined. ALTERATION: Quartz carbonate veining. GRAIN SIZE: Fine grained. COLOUR: Black white. SCRATCH: Medium.	81
PERIDOTITE 226.06 -280.34 Uitkomst Suite ALTERATION: Serpentinised. GRAIN SIZE: Coarse grained. COLOUR: Dark grey green. MAGNETISM: Susceptable. COMMENTS: Pyroxene poikilitically enclosing olivine with inter-cumulus plagioclase. Cr %: <1. MIN.TEXT: Crm stringer to blebby. SCRATCH: Hard.	80
PERIDOTITE 229.51 -232.31 Uitkomst Suite STRUCTURE: Sheared veined. ALTERATION: Serpentinised. GRAIN SIZE: Coarse grained. COLOUR: Dark grey green. MAGNETISM: Susceptable. SCRATCH: Hard.	60
SERPENTINITE 247.47 -249.31 Uitkomst Suite ALTERATION: Serpentinised talc-alteration. GRAIN SIZE: Fine grained. COLOUR: Dark grey. MAGNETISM: Susceptable. SCRATCH: Hard.	30
PERIDOTITE 250.82 -252.71 Uitkomst Suite STRUCTURE: Fractured veined. ALTERATION: Talc alteration serpentinised. GRAIN SIZE: Coarse grained. COLOUR: Dark grey. MAGNETISM: Susceptable. SCRATCH: Medium.	80

Logged by Relogged 2

Scale 1: 200

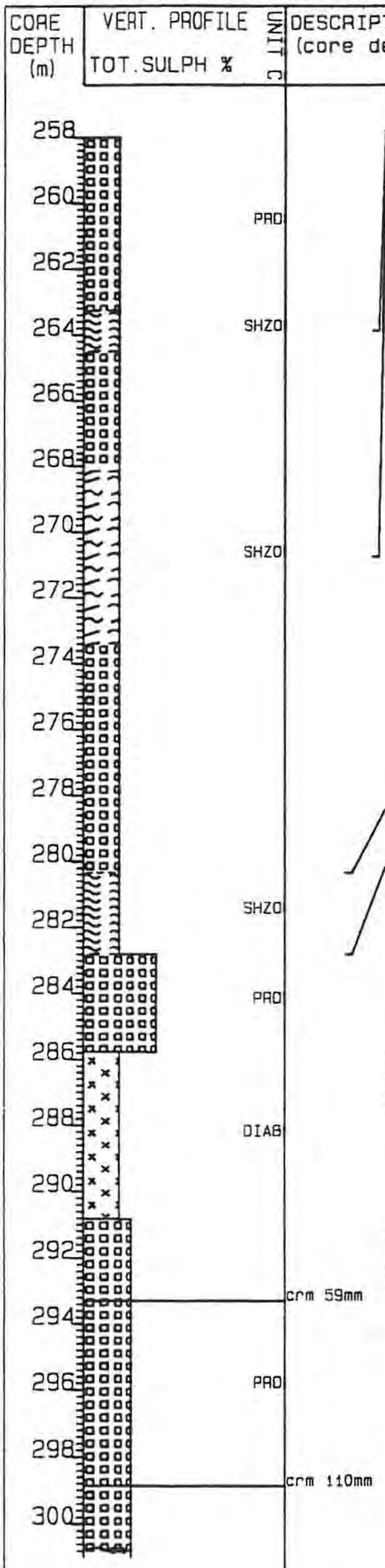

DESCRIPTION (core depths)	APP DIP deg
(PERIDOTITE continued) Uitkomst Suite	80
SHEAR ZONE 263.26 -264.50 Uitkomst Suite STRUCTURE: Sheared. GRAIN SIZE: Fine grained. COLOUR: Dark green. SCRATCH: Medium.	10
SERPENTINITE 268.15 -273.38 Uitkomst Suite STRUCTURE: Sheared fractured. GRAIN SIZE: Medium grained. COLOUR: Dark grey dark green. MAGNETISM: Susceptable. TOT.SULPH %: <1. MIN.TEXT: Disseminated. SCRATCH: Medium. SULPH.MINS.: Po.	78
SHEAR ZONE 280.34 -282.80 Uitkomst Suite STRUCTURE: Sheared. GRAIN SIZE: Coarse grained. COLOUR: Dark grey. MAGNETISM: Susceptable. SCRATCH: Hard.	43
PERIDOTITE 282.80 -285.79 Uitkomst Suite GRAIN SIZE: Coarse grained. COLOUR: Dark grey. MAGNETISM: Susceptable. Cr %: <1. TOT.SULPH %: 5-10. MIN.TEXT: Disseminated clusters. SCRATCH: Hard. SULPH.MINS.: Po.	80
DIABASE 285.79 -290.84 Uitkomst Suite ALTERATION: Quartz carbonate veining chloritisation. GRAIN SIZE: Medium grained. COMMENTS: Chilled margins (sill). SCRATCH: Hard.	68
PERIDOTITE 290.84 -303.39 Uitkomst Suite STRUCTURE: Homogeneous. GRAIN SIZE: Coarse grained. COLOUR: Dark grey. MAGNETISM: Susceptable. COMMENTS: Olivine towards the bottom. Cr %: 1-5. TOT.SULPH %: 1-5. MIN.TEXT: Crm seams and po disseminated. SCRATCH: Hard. SULPH.MINS.: Po.	80

Logged by Relogged 2

Scale 1: 200

CORE DEPTH (m) | VERT. PROFILE TOT.SULPH % | UNIT C | DESCRIPTION (core depths) | APP DIP deg

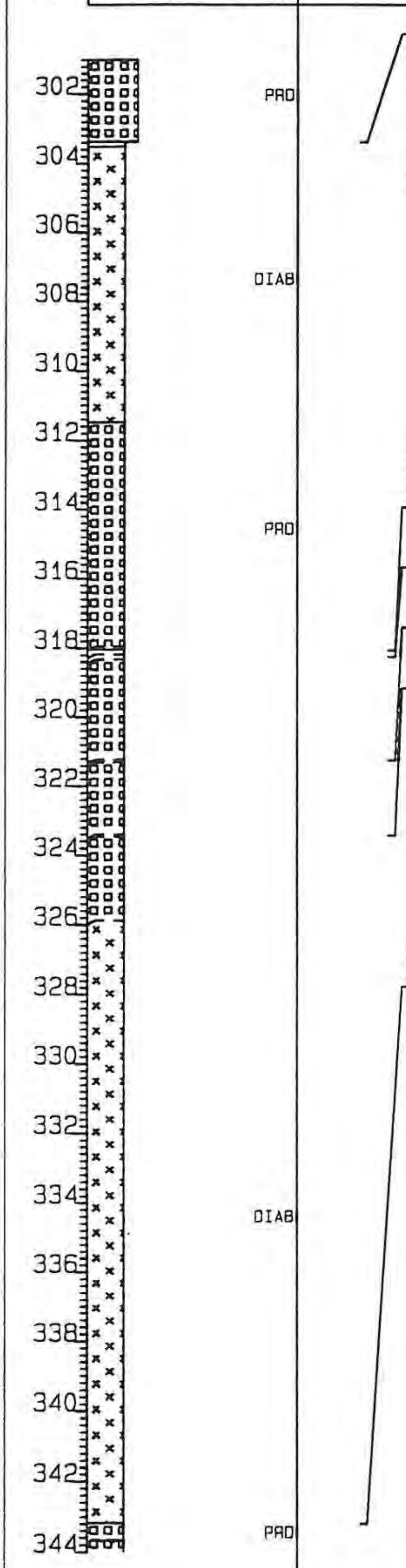

(PERIDOTITE continued) Uitkomst Suite 80

SHEAR ZONE 303.39 -303.53 Uitkomst Suite 80
STRUCTURE: Veined. GRAIN SIZE: Fine grained. COLOUR: Dark grey white. MAGNETISM: Non-susceptable. SCRATCH: Medium.

DIABASE 303.53 -311.50 Uitkomst Suite 80
GRAIN SIZE: Medium grained. COLOUR: Grey white. MAGNETISM: Non-susceptable. COMMENTS: Sill. SCRATCH: Hard.

PERIDOTITE 311.50 -325.88 Uitkomst Suite 80
STRUCTURE: Veined. GRAIN SIZE: Coarse grained. COLOUR: Dark grey. Cr %: 1-5. TOT.SULPH %: <1. MIN.TEXT: Disseminated. SCRATCH: Hard. SULPH.MINS.: Po.

MASSIVE CHROMITITE 317.95 -318.18 Uitkomst Suite 80
STRUCTURE: Veined. ALTERATION: Serpentinised. GRAIN SIZE: Fine grained. COLOUR: Black dark green. Cr %: >50. SCRATCH: Hard.

SHEAR ZONE 318.18 -318.33 Uitkomst Suite 48
STRUCTURE: Sheared veined. GRAIN SIZE: Medium grained. COLOUR: Dark grey white. MAGNETISM: Non-susceptable. SCRATCH: Medium.

SHEAR ZONE 321.22 -321.30 Uitkomst Suite 89
STRUCTURE: Veined. GRAIN SIZE: Medium grained. COLOUR: White dark grey. SCRATCH: Hard.

SHEAR ZONE 323.40 -323.46 Uitkomst Suite 54
STRUCTURE: Sheared. ALTERATION: Serpentinised. GRAIN SIZE: Fine grained. COLOUR: Dark grey dark green. SCRATCH: Medium.

DIABASE 325.88 -343.19 Uitkomst Suite 64
STRUCTURE: Fractured. ALTERATION: Quartz carbonate veining chloritisation. GRAIN SIZE: Medium grained. COLOUR: Dark grey white. SCRATCH: Hard.

PERIDOTITE 343.19 -345.97 Uitkomst Suite 90
ALTERATION: Talc alteration. GRAIN SIZE: Medium grained. COLOUR: Dark grey. MAGNETISM: Susceptable. COMMENTS: Pyroxene poikilitically enclosing olivine with interstitial plagioclase. SCRATCH: Hard.

BOREHOLE ***SH10*** 344.00 to 387.00 m Plotted 06-02-1995

Logged by Relogged 2 Scale 1: 200

CORE DEPTH (m) | VERT. PROFILE TOT.SULPH % | UNIT C | DESCRIPTION (core depths) | APP DIP deg

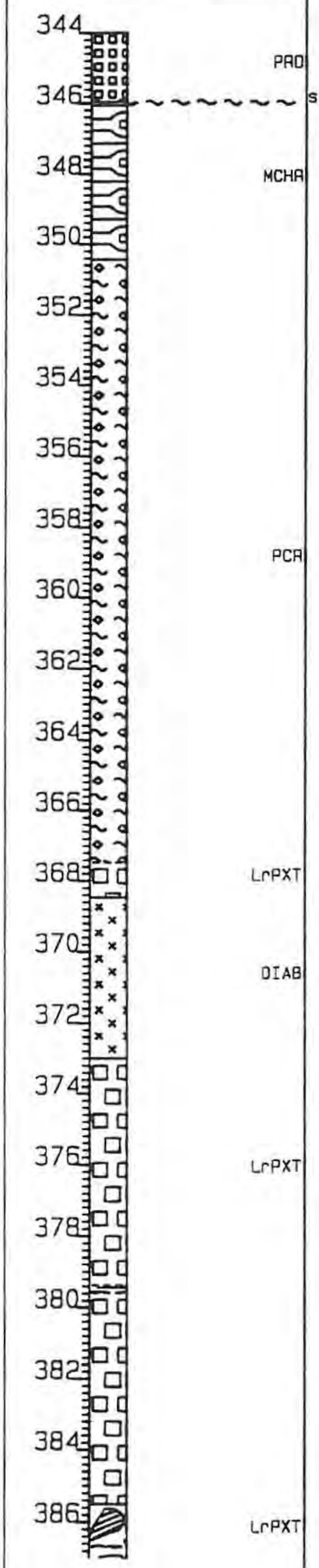

(PERIDOTITE continued) Uitkomst Suite 90

MASSIVE CHROMITITE 345.97 -350.45 Uitkomst Suite 90
STRUCTURE: Veined. ALTERATION: Talc alteration. GRAIN SIZE: Fine grained. COLOUR: Black grey. Cr %: >50. TOT.SULPH %: <1. MIN.TEXT: Clusters blebby. SCRATCH: Medium. SULPH.MINS.: Po.

shear 100mm

CHROMITITIC PYROXENITE 350.45 -367.47 Uitkomst Suite 85
STRUCTURE: Fractured. ALTERATION: Talc alteration. GRAIN SIZE: Fine grained. COLOUR: Black grey. Cr %: 10-25. TOT.SULPH %: <1. MIN.TEXT: Disseminated. SCRATCH: Medium. SULPH.MINS.: Po cp.

PYROXENITE 367.47 -368.48 Uitkomst Suite 80
ALTERATION: Serpentinised. GRAIN SIZE: Coarse grained. COLOUR: Grey. Cr %: <1. TOT.SULPH %: <1. MIN.TEXT: Disseminated clusters. SCRATCH: Medium. SULPH.MINS.: Po.

DIABASE 368.48 -373.01 Uitkomst Suite 85
STRUCTURE: Homogeneous. GRAIN SIZE: Fine grained. COLOUR: Dark grey white. COMMENTS: Sill with chilled contacts. SCRATCH: Hard.

PYROXENITE 373.01 -395.49 Uitkomst Suite 80
ALTERATION: Serpentinised. GRAIN SIZE: Medium grained. COLOUR: Light grey. Cr %: <1. TOT.SULPH %: <1. MIN.TEXT: Blebby. SCRATCH: Hard. SULPH.MINS.: Po cp.

SKARN 379.37 -379.58 Uitkomst Suite 85
GRAIN SIZE: Fine grained. COLOUR: Yellowish grey. MAGNETISM: Non-susceptable. SCRATCH: Hard.

PEGMATITE 385.52 -388.94 Uitkomst Suite 87
STRUCTURE: Homogeneous. GRAIN SIZE: Coarse grained. COLOUR: Light yellowish grey. SCRATCH: Hard.

CORE DEPTH (m) | VERT. PROFILE TOT.SULPH % | UNIT C

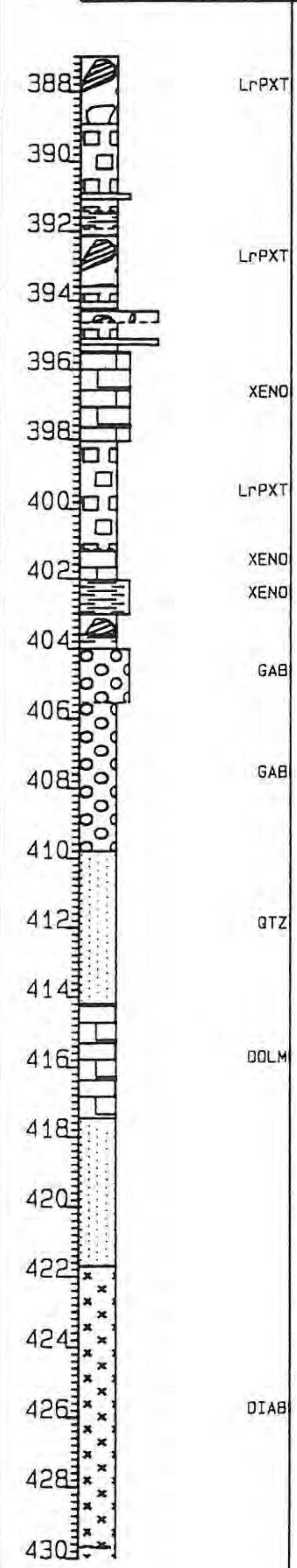

DESCRIPTION (core depths)	APP DIP deg
(PYROXENITE continued)	
(PEGMATITE 385.52 - 388.94 continued) Uitkomst Suite	87
PEGMATITE 390.93 -391.10 Uitkomst Suite STRUCTURE: Homogeneous. GRAIN SIZE: Pegmatitic. COLOUR: Grey white. TOT.SULPH %: 1-5. MIN.TEXT: Blebby disseminated. SCRATCH: Hard. SULPH.MINS.: Po.	85
SKARN 391.42 -391.92 Uitkomst Suite STRUCTURE: Layered. GRAIN SIZE: Fine grained. COLOUR: Light yellowish grey. SCRATCH: Hard.	80
PEGMATITE 392.15 -393.61 Uitkomst Suite GRAIN SIZE: Pegmatitic. COLOUR: Grey white. MAGNETISM: Non-susceptable. TOT.SULPH %: <1. MIN.TEXT: Disseminated. SCRATCH: Hard. SULPH.MINS.: Po.	80
SKARN 394.04 -394.24 Uitkomst Suite GRAIN SIZE: Fine grained. COLOUR: Grey. TOT.SULPH %: <1. MIN.TEXT: Disseminated. SCRATCH: Hard. SULPH.MINS.: Po.	80
PEGMATITE 394.32 -394.64 Uitkomst Suite STRUCTURE: Homogeneous. GRAIN SIZE: Coarse grained. COLOUR: Grey white. TOT.SULPH %: 5-10. MIN.TEXT: Clusters blebby. SCRATCH: Hard. SULPH.MINS.: Po cp.	80
PEGMATITE 395.12 -395.30 Uitkomst Suite STRUCTURE: Homogeneous. GRAIN SIZE: Coarse grained. COLOUR: Grey white. TOT.SULPH %: 5-10. MIN.TEXT: Clusters blebby. SCRATCH: Hard. SULPH.MINS.: Po cp.	80
DOLOMITE 395.49 -398.07 Uitkomst Suite STRUCTURE: Layered. GRAIN SIZE: Fine grained. COLOUR: Light grey. COMMENTS: With numerous pegmatoidal phases. TOT.SULPH %: 1-5. MIN.TEXT: Disseminated clusters blebby. SCRATCH: Hard. SULPH.MINS.: Po cp.	80
PYROXENITE 398.07 -401.16 Uitkomst Suite STRUCTURE: Homogeneous. GRAIN SIZE: Coarse grained. COLOUR: Light green grey. MAGNETISM: Non-susceptable. COMMENTS: Phlogopitic unit. TOT.SULPH %: <1. MIN.TEXT: Disseminated. SCRATCH: Hard. SULPH.MINS.: Po cp.	80
DOLOMITE 401.16 -402.05 Uitkomst Suite STRUCTURE: Layered. GRAIN SIZE: Fine grained. COLOUR: Light grey. SCRATCH: Hard.	85
SKARN 402.05 -403.05 Uitkomst Suite ALTERATION: Serpentinised. GRAIN SIZE: Pegmatitic. COLOUR: Yellowish grey. MAGNETISM: Non-susceptable. TOT.SULPH %: 1-5. MIN.TEXT: Disseminated. SCRATCH: Hard. SULPH.MINS.: Py.	85
PEGMATITE 403.05 -403.62 Uitkomst Suite GRAIN SIZE: Medium grained. COLOUR: Grey white. MAGNETISM: Non-susceptable. SCRATCH: Hard.	80
SKARN 403.62 -404.02 Uitkomst Suite ALTERATION: Serpentinised. GRAIN SIZE: Fine grained. COLOUR: Yellowish grey. MAGNETISM: Non-susceptable. SCRATCH: Hard.	80
GABBRO 404.02 -405.54 Uitkomst Suite STRUCTURE: Homogeneous. GRAIN SIZE: Medium grained. COLOUR: Grey white. TOT.SULPH %: 1-5. MIN.TEXT: Disseminated. SCRATCH: Hard. SULPH.MINS.: Po cp.	90
GABBRO 405.54 -409.82 Uitkomst Suite STRUCTURE: Homogeneous. GRAIN SIZE: Medium grained. COLOUR: Green white. COMMENTS: Unmineralized gabbro with basal chill. SCRATCH: Hard.	90
QUARTZITE 409.82 -421.72 Malmani Subgroup STRUCTURE: Fractured. GRAIN SIZE: Fine sand. COLOUR: White. SCRATCH: Hard.	85
DOLOMITE 414.20 -417.48 Uitkomst Suite ALTERATION: Serpentinised. GRAIN SIZE: Fine grained. COLOUR: Light grey white. SCRATCH: Hard.	90
DIABASE 421.72 -443.32 Uitkomst Suite STRUCTURE: Fractured. GRAIN SIZE: Medium grained. COLOUR: Dark grey white. COMMENTS: Sill. SCRATCH: Hard.	78

BOREHOLE **SH10** 430.00 to 443.32 m Plotted 06-02-1995 Page 11

Logged by Relogged 2 Scale 1: 200

CORE DEPTH (m)	VERT. PROFILE TOT.SULPH %	UNIT C	DESCRIPTION (core depths)	APP DIP deg
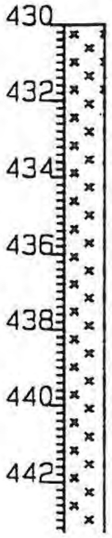		DIAB	(DIABASE continued) Uitkomst Suite	78

GEOLOGICAL LOG

SH18

PROJECT	*SLAAIHOEK*
EXPLORATION COMPANY	*ANGLOVAAL*
FARM	*SLAAIHOEK 540 JT*
DRILLING COMMENCED	*Phase One*
DRILLING COMPLETED	
LOGGED BY	*Relogged* 2
DRILLED BY	

INCLINATION:	*-90*
BEARING:	*0*
X CONSTANT:	*2800000*
X COLLAR COORD.:	*45054.61*
Y COLLAR COORD.:	*41344.62*
ELEVATION (A.M.S.L.) IN METERS:	*1468.78*
FINAL DEPTH (m):	*612.67*
No WEDGES:	*0*

Logged by RELOGGED 2

Scale 1: 200

CORE DEPTH (m)	VERT. PROFILE TOT.SULPH %	UNIT C	DESCRIPTION (core depths)	APP DIP deg
0–30		OVB	OVERBURDEN 0.00 -30.00 GRAIN SIZE: Gritty.	
30–43		NRT	NORITE 30.00 -60.66 Uitkomst Suite GRAIN SIZE: Medium grained. COLOUR: Black grey.	82

Logged by RELOGGED 2

Scale 1: 200

CORE DEPTH (m)	VERT. PROFILE TOT.SULPH %	UNIT C	DESCRIPTION (core depths)	APP DIP deg
44		NRT	(NORITE continued) Uitkomst Suite	82
60.66		UPXT	PYROXENITE 60.66 -80.35 Uitkomst Suite GRAIN SIZE: Medium grained. COLOUR: Grey green. COMMENTS: Biotite.	82
80.35		PEGM	PEGMATITE 80.35 -105.73 Uitkomst Suite ALTERATION: Chloritisation. GRAIN SIZE: Pegmatitic.	39

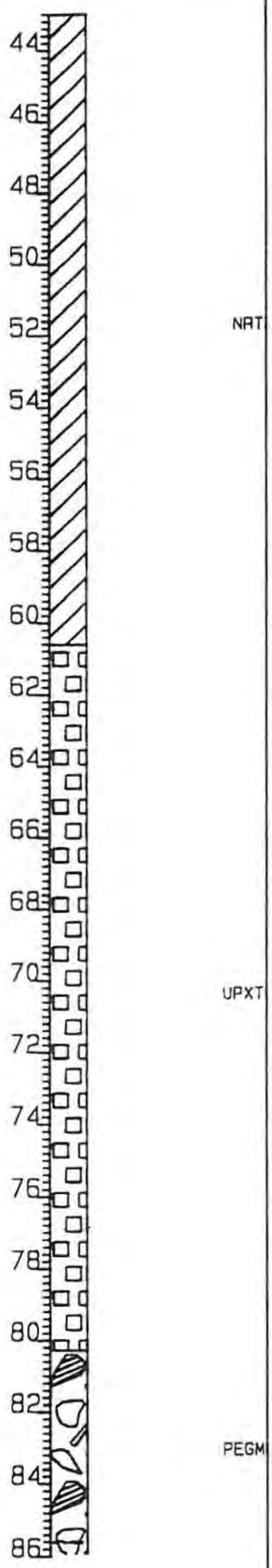

Logged by RELOGGED 2

Scale 1: 200

CORE DEPTH (m) | VERT. PROFILE TOT.SULPH %

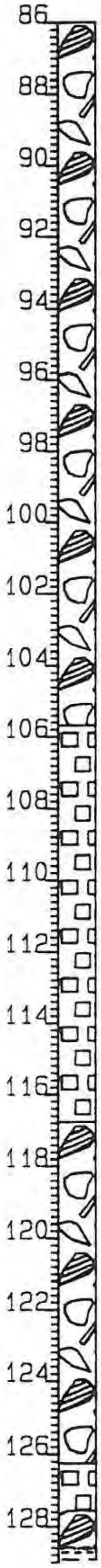

UNIT C	DESCRIPTION (core depths)		APP DIP deg
PEGM	(PEGMATITE continued)	Uitkomst Suite	39
UPXT	PYROXENITE 105.73 -116.83 GRAIN SIZE: Medium grained.	Uitkomst Suite	82
PEGM	PEGMATITE 116.83 -126.34 GRAIN SIZE: Pegmatitic.	Uitkomst Suite	64
UPXT	PYROXENITE 126.34 -129.65 GRAIN SIZE: Medium grained.	Uitkomst Suite	82
PEGM	PEGMATITE 127.64 -128.79 GRAIN SIZE: Pegmatitic.	Uitkomst Suite	32

Logged by RELOGGED 2

Scale 1: 200

CORE DEPTH (m)	VERT. PROFILE TOT.SULPH %	UNIT C	DESCRIPTION (core depths)	APP DIP deg

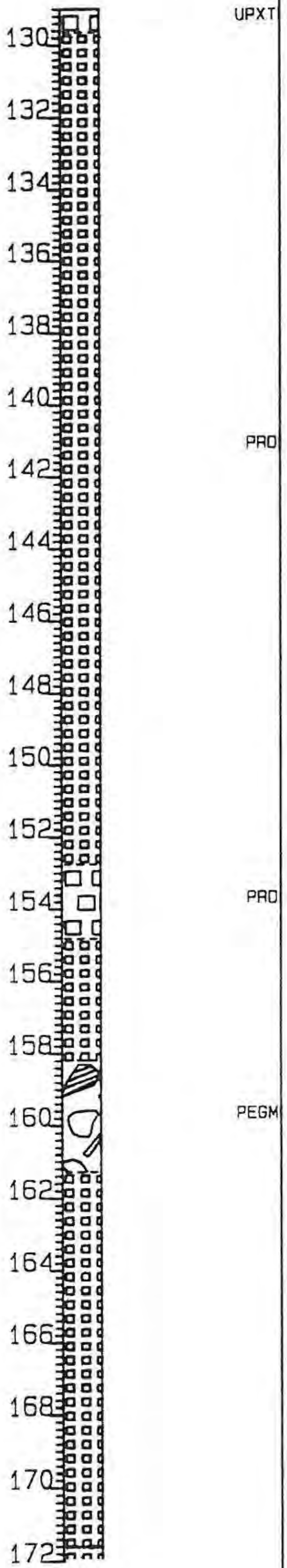

(PYROXENITE continued) Uitkomst Suite 82

PERIDOTITE 129.65 -173.24 Uitkomst Suite 82
ALTERATION: Serpentinised. GRAIN SIZE: Coarse grained.

PYROXENITE 152.79 -154.86 Uitkomst Suite 82
GRAIN SIZE: Medium grained.

PEGMATITE 158.24 -161.34 Uitkomst Suite 30
GRAIN SIZE: Pegmatitic.

BOREHOLE **SH18** 172.00 to 215.00 m Plotted 01-03-1995 Page 5

Logged by RELOGGED 2 Scale 1: 200

CORE DEPTH (m)	VERT. PROFILE TOT.SULPH %	UNIT C	DESCRIPTION (core depths)	APP DIP deg

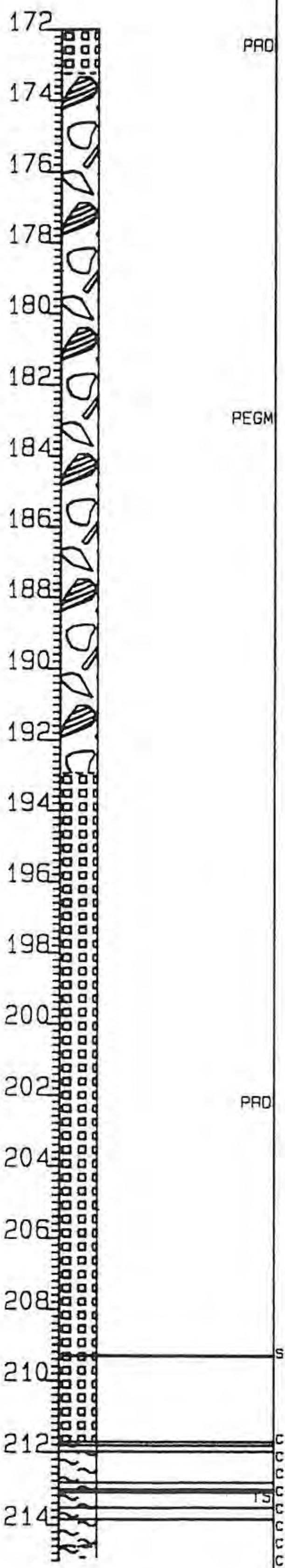

(PERIDOTITE continued) Uitkomst Suite 82

PEGMATITE 173.24 -192.98 Uitkomst Suite 30
GRAIN SIZE: Pegmatitic.

PERIDOTITE 192.98 -228.12 Uitkomst Suite 82
ALTERATION: Serpentinised quartz carbonate veining. GRAIN SIZE: Medium grained. Cr %: <1. TOT.SULPH %: <1. MIN.TEXT: Disseminated. SULPH.MINS.: Po.

serp 29mm

crm 99mm
crm 19mm
crm 29mm
crm 20mm
crm 9mm
crm 29mm
crm 300mm
crm 20mm

SCHIST 211.74 -216.47 Uitkomst Suite 60
ALTERATION: Talc alteration. GRAIN SIZE: Fine grained.

Logged by RELOGGED 2

Scale 1: 200

CORE DEPTH (m)	VERT. PROFILE TOT.SULPH %	UNIT C	DESCRIPTION (core depths)		APP DIP deg

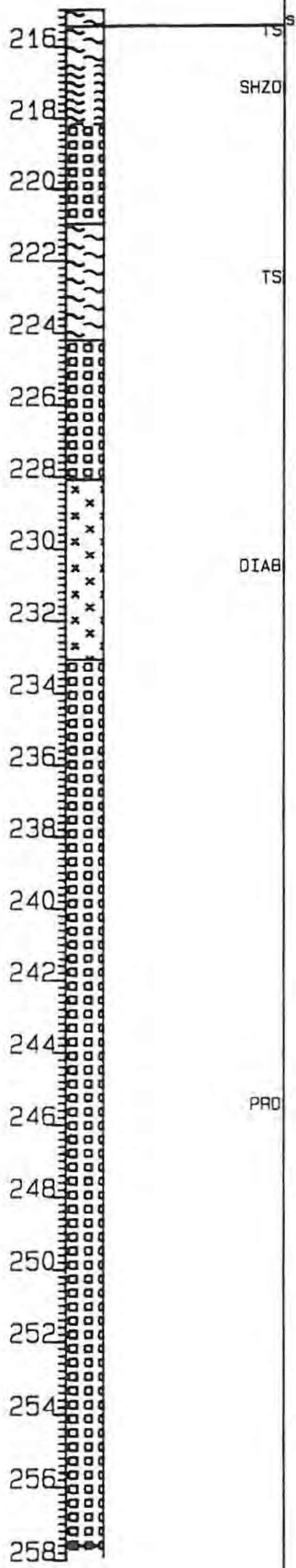

(PERIDOTITE continued)

(SCHIST 211.74 - 216.47 continued) Uitkomst Suite 60

serp 600mm SHEAR ZONE 216.47 -218.18 Uitkomst Suite 65

GRAIN SIZE: Fine grained.

SCHIST 221.00 -224.24 Uitkomst Suite 40

STRUCTURE: Sheared. GRAIN SIZE: Fine grained.

DIABASE 228.12 -233.13 Uitkomst Suite 80

GRAIN SIZE: Medium grained. COMMENTS: Chilled margin. SILL.

PERIDOTITE 233.13 -266.63 Uitkomst Suite 90

GRAIN SIZE: Medium grained. COMMENTS: Pyroxene poikilitically enclosing olivine.

Logged by RELOGGED 2

Scale 1: 200

CORE DEPTH (m)	VERT. PROFILE TOT.SULPH %	UNIT C	DESCRIPTION (core depths)	APP DIP deg

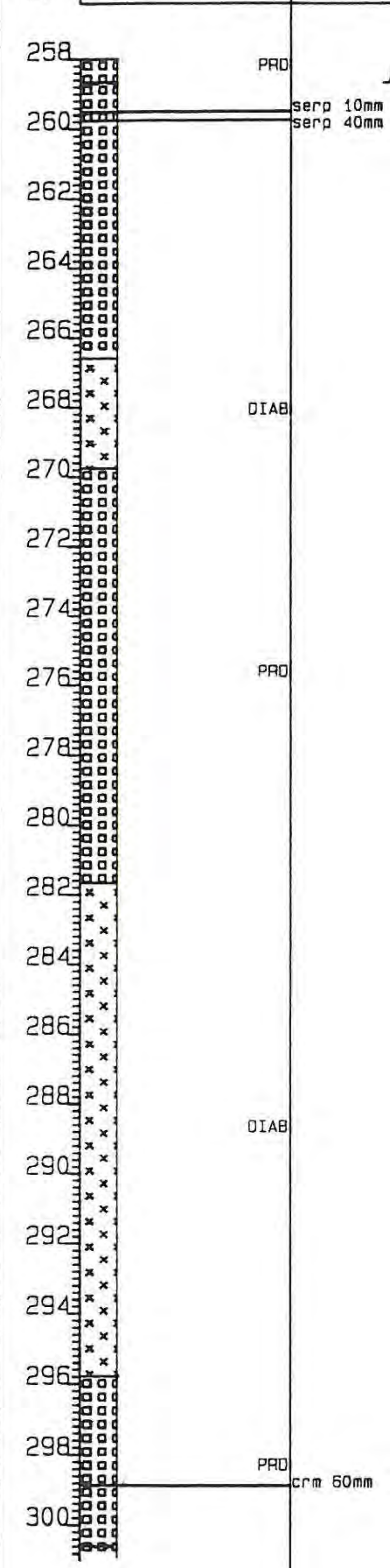

(PERIDOTITE continued) Uitkomst Suite 90

SHEAR ZONE 258.68 -258.71 Uitkomst Suite 50
GRAIN SIZE: Fine grained.

DIABASE 266.63 -269.80 Uitkomst Suite 90
ALTERATION: Quartz carbonate veining. GRAIN SIZE: Medium grained. COMMENTS: Chilled margin. SILL.

PERIDOTITE 269.80 -281.72 Uitkomst Suite 90
GRAIN SIZE: Medium grained. COMMENTS: Pyroxene poikilitically enclosing olivine.

DIABASE 281.72 -295.86 90
GRAIN SIZE: Medium grained. COMMENTS: Chilled margin. SILL.

PERIDOTITE 295.86 -344.94 Uitkomst Suite 90
GRAIN SIZE: Medium grained. COMMENTS: Pyroxene poikilitically enclosing olivine. Cr %: 1-5. MIN.TEXT: Crm seam.

Logged by RELOGGED 2

Scale 1: 200

CORE DEPTH (m)	VERT. PROFILE TOT.SULPH %	UNIT C	DESCRIPTION (core depths)	APP DIP deg

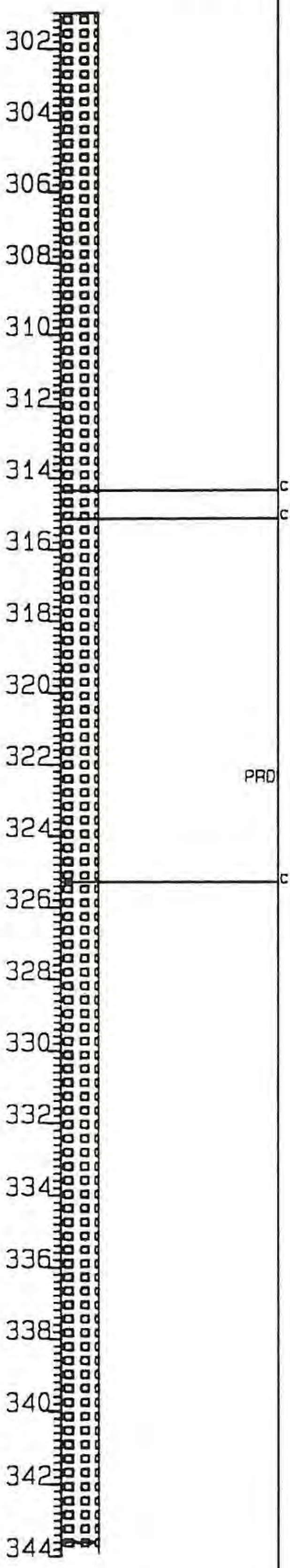

(PERIDOTITE continued) Uitkomst Suite 90

crm 49mm

crm 29mm

crm 29mm

Logged by RELOGGED 2

Scale 1: 200

CORE DEPTH (m) | VERT. PROFILE TOT.SULPH % | UNIT C | DESCRIPTION (core depths) | APP DIP deg

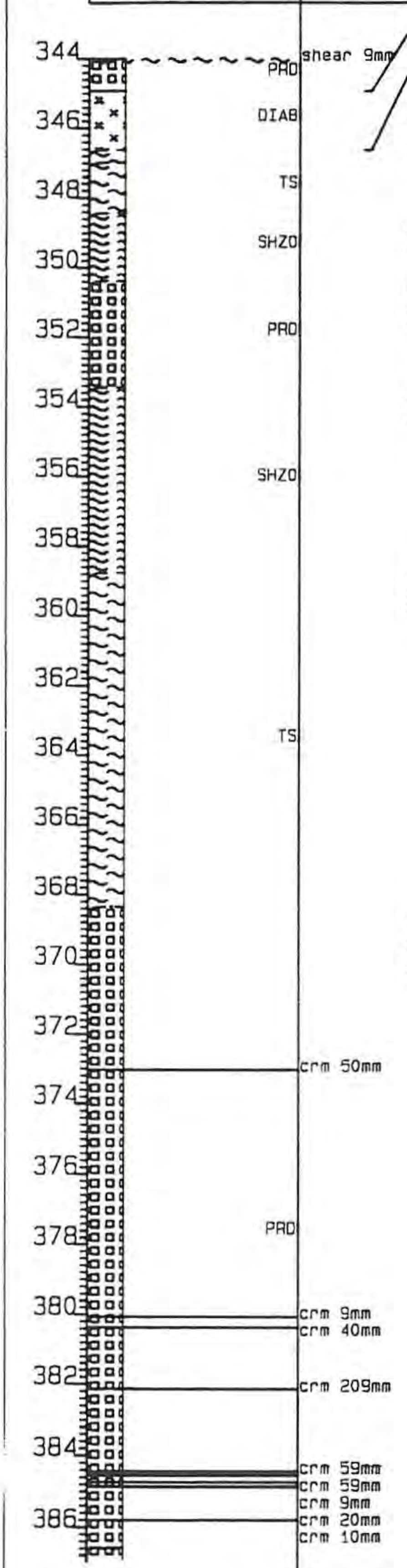

(PERIDOTITE continued) Uitkomst Suite 90

DIABASE 344.94 -346.64 Uitkomst Suite 82
GRAIN SIZE: Medium grained. COMMENTS: Biotite towards the top.

SCHIST 346.64 -347.00 Uitkomst Suite 82
ALTERATION: Talc-alteration. GRAIN SIZE: Fine grained. Cr %: 1-5. MIN.TEXT: Crm blebby.

SCHIST 347.00 -348.45 Uitkomst Suite 82
ALTERATION: Talc-alteration. GRAIN SIZE: Fine grained. COLOUR: Grey.

SHEAR ZONE 348.45 -350.41 Uitkomst Suite 82
GRAIN SIZE: Fine grained.

PERIDOTITE 350.41 -353.47 Uitkomst Suite 82
GRAIN SIZE: Medium grained.

SHEAR ZONE 353.47 -358.80 82
GRAIN SIZE: Fine grained. COLOUR: Grey.

SCHIST 358.80 -368.40 Uitkomst Suite 45
STRUCTURE: Sheared. ALTERATION: Talc-alteration. GRAIN SIZE: Fine grained.

PERIDOTITE 368.40 -397.36 Uitkomst Suite 82
GRAIN SIZE: Medium grained. COMMENTS: Pyroxene poikilitically enclosing olivine. Cr %: 1-5. MIN.TEXT: Seam of crm.

Logged by RELOGGED 2

Scale 1: 200

CORE DEPTH (m)	VERT. PROFILE TOT.SULPH %	UNIT C	DESCRIPTION (core depths)	APP DIP deg

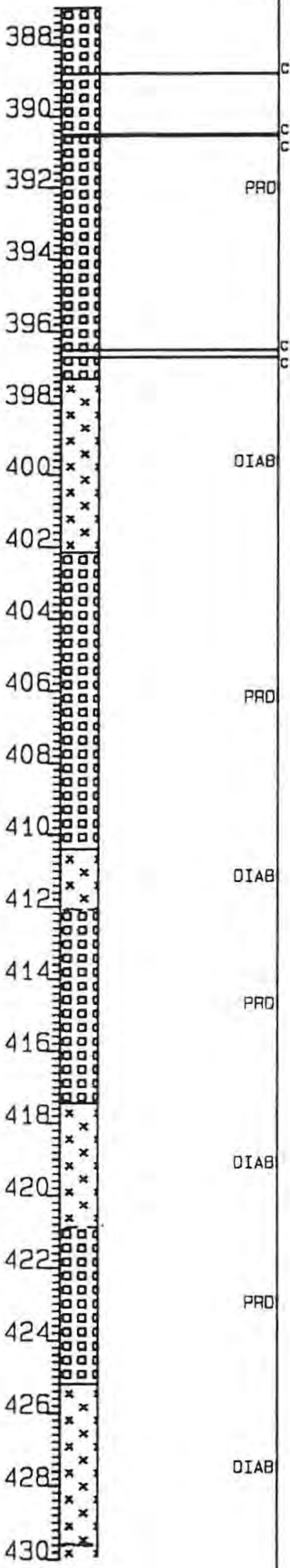

crm 10mm

crm 20mm
crm 9mm

crm 40mm
crm 29mm

(PERIDOTITE continued) Uitkomst Suite 82

DIABASE 397.36 -402.20 Uitkomst Suite 54
GRAIN SIZE: Medium grained. COMMENTS: Chilled margin. SILL.

PERIDOTITE 402.20 -410.46 Uitkomst Suite 82
GRAIN SIZE: Medium grained. COMMENTS: Pyroxene poikilitically enclosing olivine. TOT.SULPH %: <1. MIN.TEXT: Disseminated. SULPH.MINS.: Po.

DIABASE 410.46 -412.12 Uitkomst Suite 57
GRAIN SIZE: Medium grained. COMMENTS: Chilled margin towards the top. SILL/DYKE ?.

PERIDOTITE 412.12 -417.52 Uitkomst Suite 82
GRAIN SIZE: Medium grained. COMMENTS: Pyroxene poikilitically enclosing olivine.

DIABASE 417.52 -420.94 Uitkomst Suite 85
GRAIN SIZE: Medium grained. COMMENTS: Slight chilled margins. SILL.

PERIDOTITE 420.94 -425.28 Uitkomst Suite 90
GRAIN SIZE: Coarse grained. COMMENTS: Coarse grained pyroxene poikilitically enclosing olivine. TOT.SULPH %: <1. MIN.TEXT: Disseminated. SULPH.MINS.: Po.

DIABASE 425.28 -430.26 Uitkomst Suite 90
GRAIN SIZE: Medium grained. COMMENTS: SILL.

BOREHOLE SM10 430.00 to 473.00 m Plotted 01-03-1995

Logged by RELOGGED 2 Scale 1: 200

CORE DEPTH (m)	VERT. PROFILE TOT.SULPH %	UNIT C	DESCRIPTION (core depths)	APP DIP deg
			(DIABASE continued) Uitkomst Suite	90
		PRD	PERIDOTITE 430.26 -437.31 Uitkomst Suite GRAIN SIZE: Medium grained. COMMENTS: Pyroxene oikocrysts poikilitically enclosing olivine.	90
			DOLERITE 430.95 -431.20 Uitkomst Suite GRAIN SIZE: Aphanitic. COLOUR: Grey.	90
		DIAB	DIABASE 437.31 -457.04 Uitkomst Suite GRAIN SIZE: Medium grained. COMMENTS: Chilled margin. SILL.	90
		PRD	PERIDOTITE 457.04 -472.73 Uitkomst Suite GRAIN SIZE: Medium grained. COMMENTS: Pyroxene oikocrysts poikilitically enclosing olivine. TOT.SULPH %: 1-5. MIN.TEXT: Net to disseminated. SULPH.MINS.: Po.	90
			SHEAR ZONE 471.18 -472.73 Uitkomst Suite GRAIN SIZE: Fine grained.	90
		SHZO	DIABASE 472.73 -477.42 Uitkomst Suite GRAIN SIZE: Medium grained. COMMENTS: Chilled margin. SILL.	90

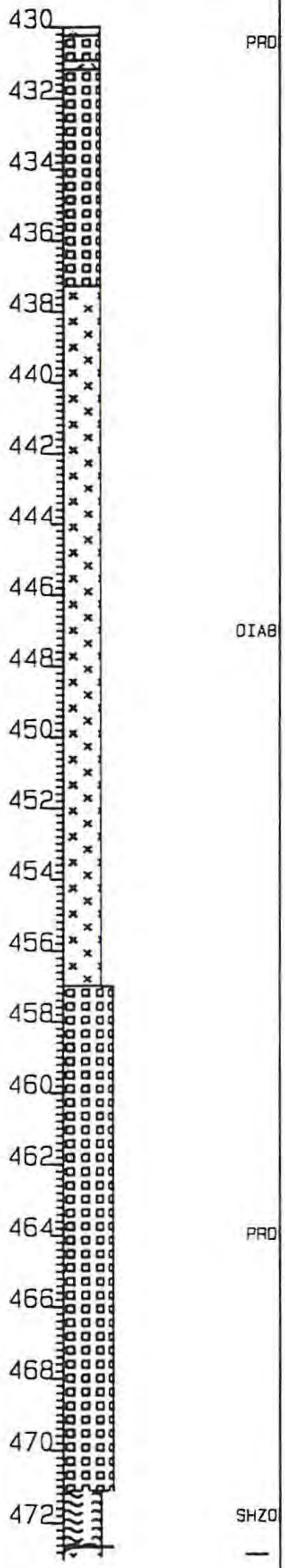

Logged by RELOGGED 2

Scale 1: 200

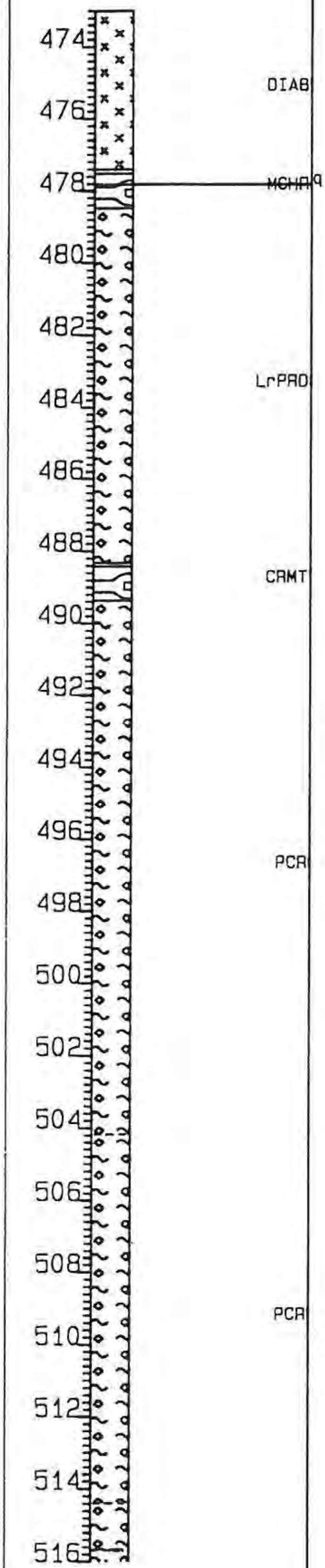

q.c.v. 379mm

DESCRIPTION (core depths)	APP DIP deg
DIABASE 472.73 -477.42 Uitkomst Suite GRAIN SIZE: Medium grained. COMMENTS: Chilled margin. SILL.	90
MASSIVE CHROMITITE 477.42 -478.50 Uitkomst Suite GRAIN SIZE: Fine grained. COLOUR: Black.	82
CHROMITITIC PYROXENITE 478.50 -488.33 Uitkomst Suite STRUCTURE: Sheared. ALTERATION: Talc-alteration. GRAIN SIZE: Fine grained. COLOUR: Grey. Cr %: 10-15. MIN.TEXT: Crm seams.	82
MASSIVE CHROMITITE 488.33 -489.38 Uitkomst Suite GRAIN SIZE: Fine grained. COLOUR: Black. Cr %: >50. MIN.TEXT: Semi-massive to massive crm.	82
CHROMITITIC PYROXENITE 489.38 -518.64 Uitkomst Suite STRUCTURE: Sheared. ALTERATION: Talc-alteration. GRAIN SIZE: Fine grained. COLOUR: Grey. Cr %: 10-25. MIN.TEXT: Crm seams.	82
CHROMITITIC PYROXENITE 504.18 -514.38 Uitkomst Suite STRUCTURE: Sheared. GRAIN SIZE: Fine grained.	48

BOREHOLE SM10 516.00 to 559.00 m Plotted 01-03-1995 Page 13

Logged by RELOGGED 2 Scale 1: 200

CORE DEPTH (m)	VERT. PROFILE TOT.SULPH %	UNIT C	DESCRIPTION (core depths)	APP DIP deg

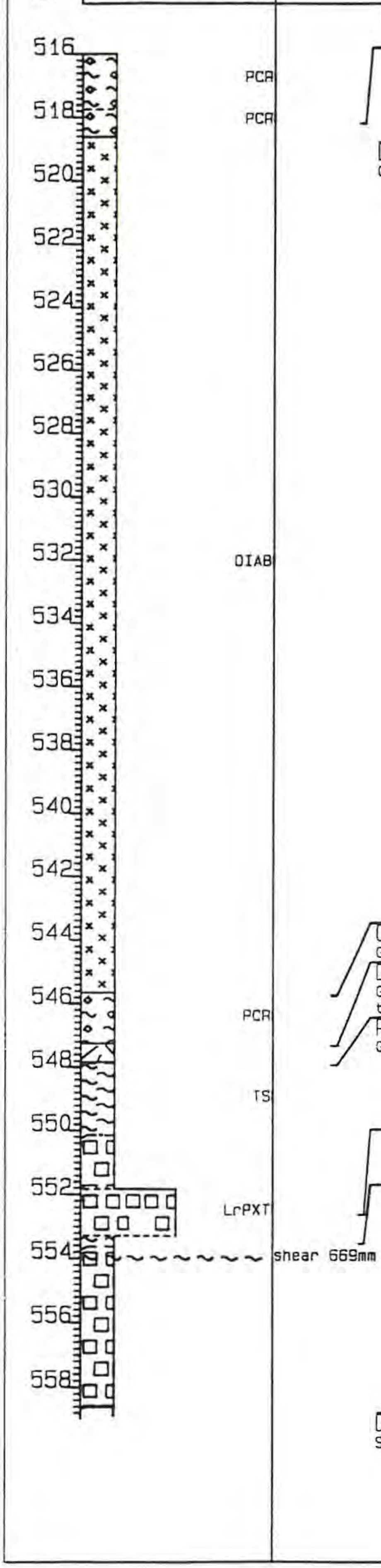

(CHROMITITIC PYROXENITE continued) Uitkomst Suite 82

CHROMITITIC PYROXENITE 517.76 -518.64 Uitkomst Suite 39
STRUCTURE: Sheared. GRAIN SIZE: Fine grained. COLOUR: Grey.

DIABASE 518.64 -545.73 Uitkomst Suite 70
GRAIN SIZE: Medium grained. COLOUR: Grey. COMMENTS: Chilled margin. SILL.

CHROMITITIC PYROXENITE 545.73 -547.32 Uitkomst Suite 54
GRAIN SIZE: Medium grained. COLOUR: Grey. Cr %: 10-25. MIN.TEXT: Crm seams.

DOLERITE 547.32 -547.92 Uitkomst Suite 63
GRAIN SIZE: Aphanitic. COLOUR: Grey. COMMENTS: Chilled margin towards the middle towards the bottom towards the top. SILL.

PYROXENITE 547.92 -558.65 Uitkomst Suite 82
GRAIN SIZE: Medium grained. COLOUR: Grey green.

SCHIST 547.93 -550.20 Uitkomst Suite 60
STRUCTURE: Sheared. ALTERATION: Talc-alteration. GRAIN SIZE: Fine grained. COLOUR: Grey.

PYROXENITE 551.89 -553.36 Uitkomst Suite 82
GRAIN SIZE: Medium grained. COLOUR: Grey green. TOT.SULPH %: 10-25. MIN.TEXT: Net to clusters. SULPH.MINS.: Po cp.

SHEAR ZONE 553.36 -553.69 Uitkomst Suite 90
GRAIN SIZE: Fine grained.

DOLOMITE 558.65 -572.34 Malmani Subgroup 78
STRUCTURE: Xenolith. GRAIN SIZE: Fine sand. COLOUR: Grey.

Logged by RELOGGED 2

Scale 1: 200

CORE DEPTH (m) | VERT. PROFILE TOT.SULPH % | UNIT C

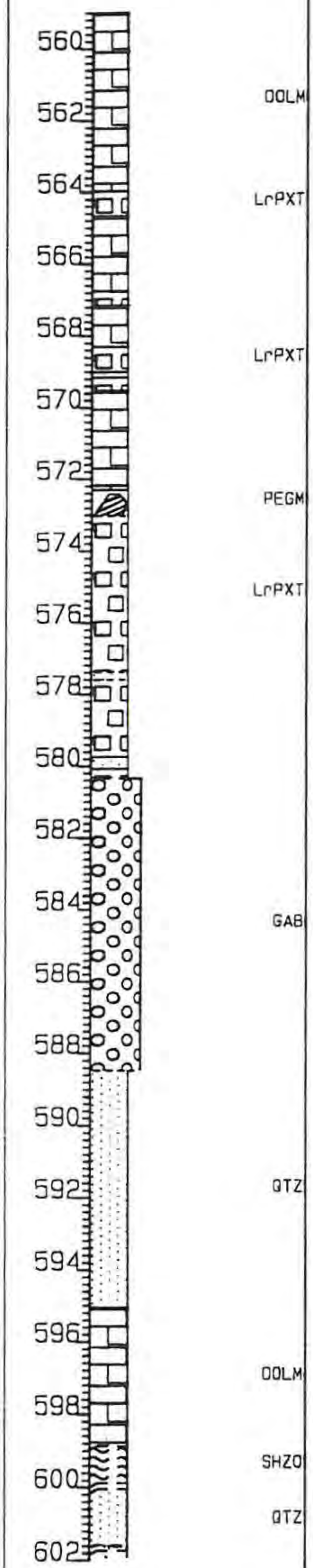

DESCRIPTION (core depths)		APP DIP deg
(DOLOMITE continued)	Malmani Subgroup	78
PYROXENITE 564.00 -564.70 GRAIN SIZE: Fine grained.	Uitkomst Suite	82
PYROXENITE 566.79 -567.19 GRAIN SIZE: Fine grained.	Uitkomst Suite	82
PYROXENITE 568.34 -569.04 GRAIN SIZE: Fine grained.	Uitkomst Suite	90
PYROXENITE 569.20 -569.56 GRAIN SIZE: Fine grained.	Uitkomst Suite	90
PEGMATITE 572.34 -573.06 GRAIN SIZE: Pegmatitic.	Uitkomst Suite	90
PYROXENITE 573.06 -580.38 GRAIN SIZE: Fine grained.	Uitkomst Suite	82
QUARTZITE 577.42 -577.63 STRUCTURE: Xenolith. ALTERATION: Metamorphosed. GRAIN SIZE: Fine sand. COLOUR: Grey.	Uitkomst Suite	82
QUARTZITE 579.80 -580.13 GRAIN SIZE: Fine sand. COLOUR: Grey.	Uitkomst Suite	64
GABBRO 580.38 -588.52 GRAIN SIZE: Medium grained. TOT.SULPH %: 1-5. MIN.TEXT: Disseminated. SULPH.MINS.: Po cp.	Uitkomst Suite	82
QUARTZITE 588.52 -595.12 GRAIN SIZE: Fine sand. COLOUR: Grey.	Malmani Subgroup	67
DOLOMITE 595.12 -600.12 GRAIN SIZE: Silt. COLOUR: Grey. SCRATCH: Hard.	Malmani Subgroup	66
SHEAR ZONE 598.93 -599.95 GRAIN SIZE: Fine grained.	Uitkomst Suite	80
QUARTZITE 600.12 -601.80 GRAIN SIZE: Fine sand. COLOUR: Grey.	Black Reef Quartsite	82
GRANITE 601.80 -612.67 GRAIN SIZE: Coarse grained.	Nelshoogte Granite	82

Logged by RELOGGED 2 Scale 1: 200

CORE DEPTH (m)	VERT. PROFILE TOT.SULPH %	UNIT C	DESCRIPTION (core depths)		APP DIP deg
602 604 606 608 610 612	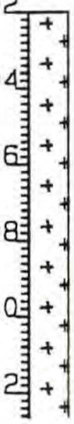	GRAN	(GRANITE continued)	Nelshoogte Granite	82

GEOLOGICAL LOG

SH19

PROJECT	*SLAAIHOEK*
EXPLORATION COMPANY	*ANGLOVAAL*
FARM	*SLAAIHOEK 540 JT*
DRILLING COMMENCED	*Phase One*
DRILLING COMPLETED	
LOGGED BY	*Relogged* 2
DRILLED BY	

INCLINATION:	*-90*
BEARING:	*0*
X CONSTANT:	*2800000*
X COLLAR COORD.:	*45236.93*
Y COLLAR COORD.:	*40985.14*
ELEVATION (A.M.S.L.) IN METERS:	*1460.23*
FINAL DEPTH (m):	*611.86*
No WEDGES:	*0*

BOREHOLE ***SH19*** 0.00 to 43.00 m

Plotted 11-02-1995 Page 1

Logged by RELOGGED 2

Scale 1: 200

CORE DEPTH (m)	VERT. PROFILE TOT.SULPH %	UNIT C	DESCRIPTION (core depths)	APP DIP deg
		OVB	OVERBURDEN 0.00 -44.90 GRAIN SIZE: Pebble.	

Logged by RELOGGED 2

Scale 1: 200

CORE DEPTH (m)	VERT. PROFILE TOT.SULPH %	UNIT C	DESCRIPTION (core depths)	APP DIP deg

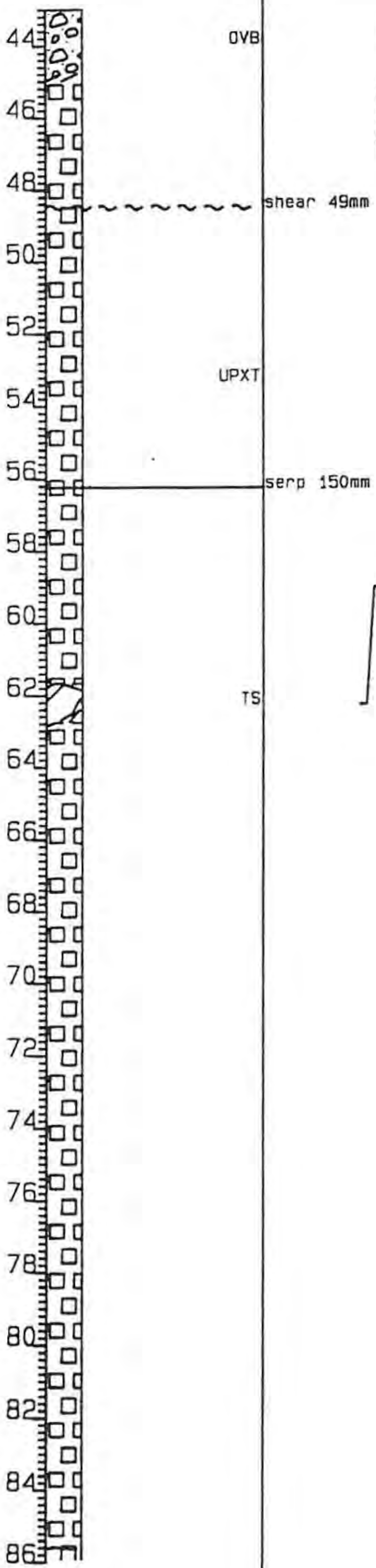

(OVERBURDEN continued)

PYROXENITE 44.90 -102.80 Uitkomst Suite 83
ALTERATION: Serpentinised. GRAIN SIZE: Medium grained. COLOUR: Greyisn green to dark green.

FRACTURED ZONE 61.70 -62.80 Uitkomst Suite 50
ALTERATION: Talc-alteration. GRAIN SIZE: Fine grained.

BOREHOLE ***SH19*** 86.00 to 129.00 m

Plotted 11-02-1995 Page 3

Logged by RELOGGED 2

Scale 1: 200

CORE DEPTH (m) | VERT. PROFILE TOT.SULPH % | UNIT C

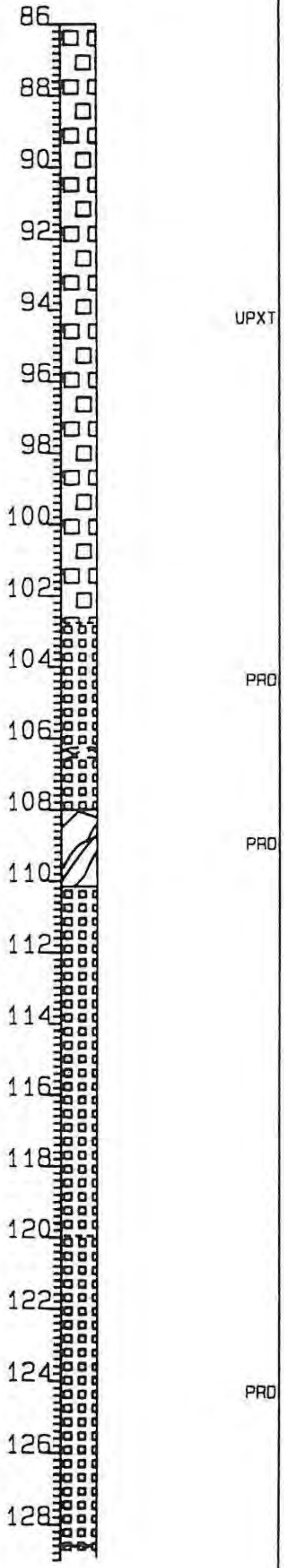

DESCRIPTION (core depths)	APP DIP deg
(PYROXENITE continued) Uitkomst Suite	83
PERIDOTITE 102.80 -141.00 Uitkomst Suite GRAIN SIZE: Medium grained.	85
SHEAR ZONE 106.30 -106.57 Uitkomst Suite STRUCTURE: Sheared. GRAIN SIZE: Medium grained.	62
FRACTURED ZONE 108.06 -110.22 Uitkomst Suite ALTERATION: Veined serpentinised. GRAIN SIZE: Medium grained. MIN.TEXT: Mt stringer.	70
PERIDOTITE 120.00 -130.57 Uitkomst Suite ALTERATION: Veined serpentinised. GRAIN SIZE: Medium grained. MIN.TEXT: Mt stringer.	80

BOREHOLE **SH19**   129.00 to 172.00 m   Plotted 11-02-1995   Page 4

Logged by RELOGGED 2   Scale 1: 200

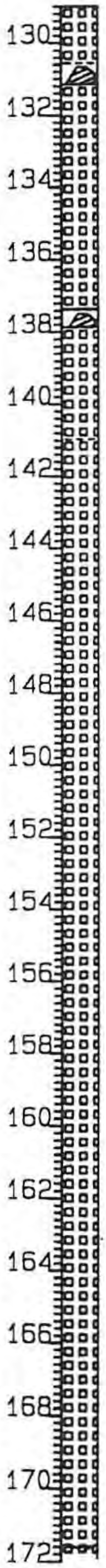

CORE DEPTH (m)	VERT. PROFILE TOT. SULPH %	UNIT C	DESCRIPTION (core depths)		APP DIP deg
			(PERIDOTITE continued)		
			(PERIDOTITE 120 - 130.57 continued)	Uitkomst Suite	80
		PRD	PEGMATITE 130.57 -131.17 GRAIN SIZE: Pegmatitic.	Uitkomst Suite	40
			PEGMATITE 137.40 -137.90 GRAIN SIZE: Pegmatitic.	Uitkomst Suite	70
			PERIDOTITE 141.00 -188.00 ALTERATION: Serpentinised metamorphosed. GRAIN SIZE: Coarse grained. COMMENTS: Pyroxene oikocrysts poikilitically enclosing olivine with interstitial plagioclase.	Uitkomst Suite	80
		PRD			

BOREHOLE **SH19** 172.00 to 215.00 m Plotted 11-02-1995 Page 5

Logged by RELOGGED 2

Scale 1: 200

CORE DEPTH (m)	VERT. PROFILE TOT. SULPH %	UNIT C	DESCRIPTION (core depths)	APP DIP deg

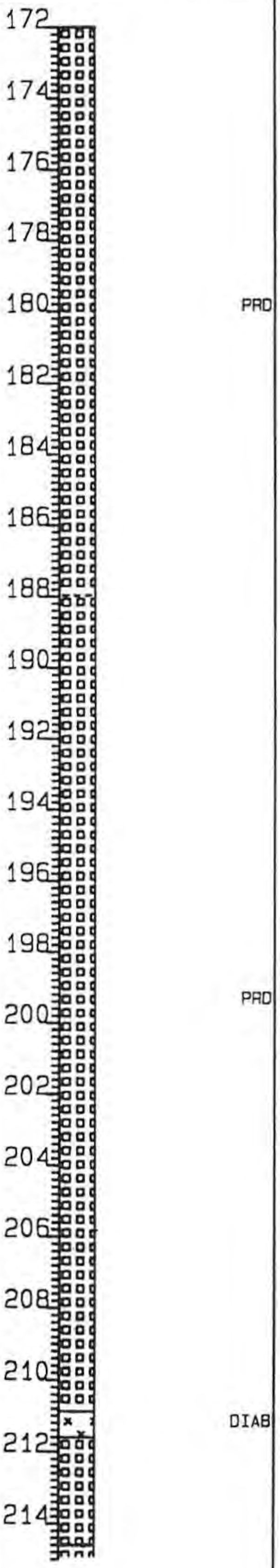

(PERIDOTITE continued) Uitkomst Suite 80

PERIDOTITE 188.00 -235.00 Uitkomst Suite 85
GRAIN SIZE: Coarse grained. ASBESTOS %: <1. Cr %: <1.

DIABASE 210.96 -211.68 Uitkomst Suite 76
ALTERATION: Chloritisation quartz carbonate veining. GRAIN SIZE: Medium grained. COLOUR: Grey green. COMMENTS: Chilled margin. sill.

BOREHOLE **SH19** 215.00 to 258.00 m Plotted 11-02-1995 Page 6

Logged by RELOGGED 2 Scale 1: 200

CORE DEPTH (m)	VERT. PROFILE TOT.SULPH %	UNIT C	DESCRIPTION (core depths)	APP DIP deg

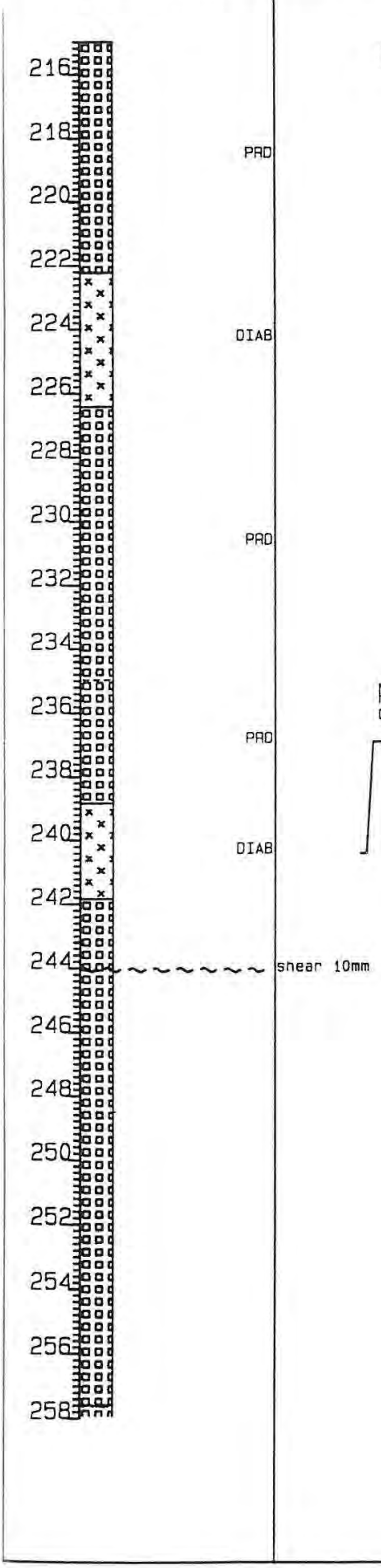

DESCRIPTION (core depths)	APP DIP deg
(PERIDOTITE continued) Uitkomst Suite	85
DIABASE 222.25 -226.46 Uitkomst Suite GRAIN SIZE: Medium grained. COLOUR: Greyish green to light green. COMMENTS: SILL.	71
PERIDOTITE 226.46 -235.00 Uitkomst Suite COLOUR: Green.	80
PERIDOTITE 235.00 -285.60 Uitkomst Suite GRAIN SIZE: Medium grained. Cr %: <1.	80
DIABASE 238.90 -241.90 Uitkomst Suite ALTERATION: Chloritisation and quartz carbonate veining. GRAIN SIZE: Medium grained. COMMENTS: Chilled margin. SILL.	72

Logged by RELOGGED 2

Scale 1: 200

CORE DEPTH (m)	VERT. PROFILE TOT.SULPH %	UNIT C	DESCRIPTION (core depths)	APP DIP deg

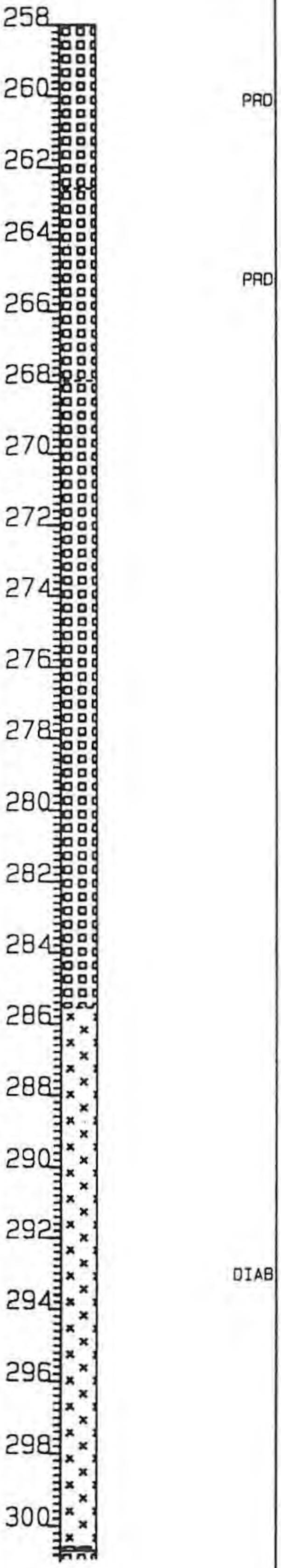

(PERIDOTITE continued) Uitkomst Suite 80

PERIDOTITE 262.60 -268.00 Uitkomst Suite 80
ALTERATION: Slightly altered. GRAIN SIZE: Medium grained. COLOUR: Greyish green.

DIABASE 285.60 -300.78 Uitkomst Suite 65
ALTERATION: Talc-alteration. GRAIN SIZE: Medium grained. COLOUR: Greyish green to green. COMMENTS: SILL.

PERIDOTITE 300.78 -359.83 Uitkomst Suite 80
GRAIN SIZE: Medium grained.

BOREHOLE ***SH19*** 301.00 to 344.00 m

Plotted 11-02-1995 Page 8

Logged by RELOGGED 2

Scale 1: 200

CORE DEPTH (m) | VERT. PROFILE TOT. SULPH % | UNIT C

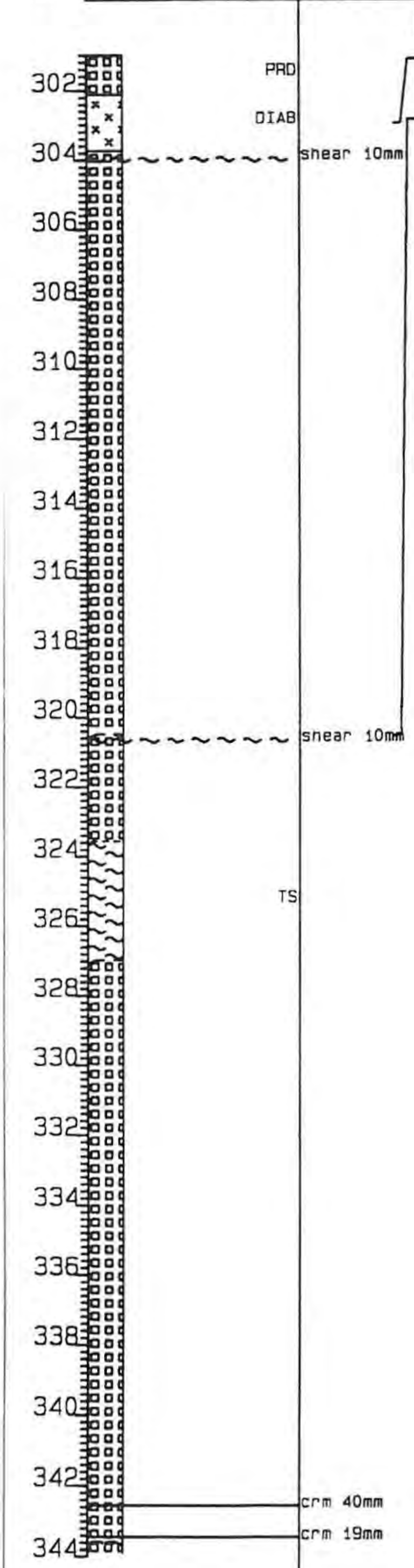

DESCRIPTION (core depths)	APP DIP deg
(PERIDOTITE continued) Uitkomst Suite	80
DIABASE 302.15 -303.77 Uitkomst Suite GRAIN SIZE: Medium grained. COLOUR: Greyish green. COMMENTS: Chilled margin. SILL.	70
SHEAR ZONE 320.52 -320.54 Uitkomst Suite STRUCTURE: Sheared. GRAIN SIZE: Medium grained.	58
SCHIST 323.62 -327.02 Uitkomst Suite ALTERATION: Talc-alteration. GRAIN SIZE: Fine grained.	60

BOREHOLE **SH19** 344.00 to 387.00 m

Plotted 11-02-1995 Page 9

Logged by RELOGGED 2

Scale 1: 200

CORE DEPTH (m) | VERT. PROFILE TOT. SULPH % | UNIT C | DESCRIPTION (core depths) | APP DIP deg

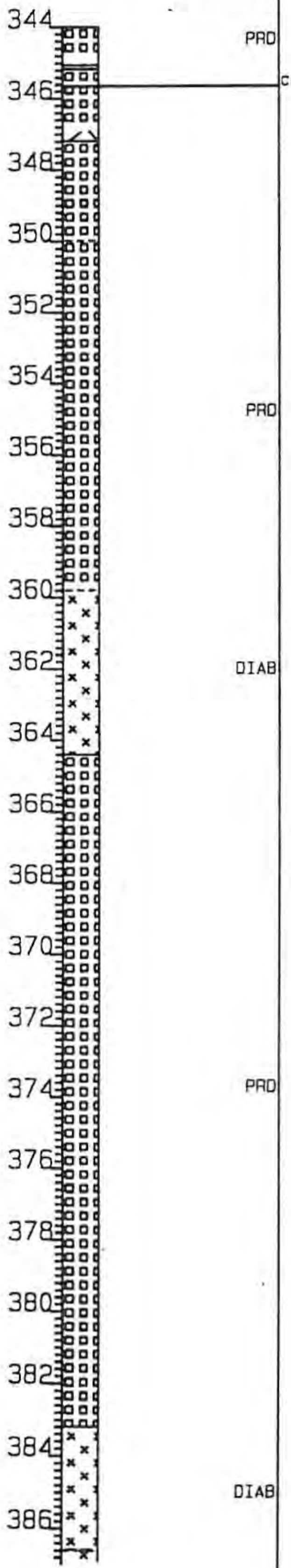

(PERIDOTITE continued) Uitkomst Suite 80

MASSIVE CHROMITITE 344.97 -345.19 Uitkomst Suite 72
GRAIN SIZE: Medium grained. Cr %: >50.

crm 160mm

DOLERITE 346.86 -347.22 Uitkomst Suite 67
GRAIN SIZE: Fine grained. COLOUR: Grey. COMMENTS: Chilled margin. SILL.

PERIDOTITE 350.00 -359.83 Uitkomst Suite 85
GRAIN SIZE: Coarse grained. COLOUR: Dark green. COMMENTS: Pyroxene poikilitically enclosing olivine.

DIABASE 359.83 -364.45 Uitkomst Suite 86
GRAIN SIZE: Medium grained. COLOUR: Greyish green. COMMENTS: Chilled margin. SILL.

PERIDOTITE 364.45 -383.27 Uitkomst Suite 80
ALTERATION: Serpentinised. GRAIN SIZE: Medium grained. COLOUR: Greyish green to dark green. COMMENTS: Pyroxene poikilitically enclosing olivine with interstitial plagioclase. Cr %: <1. MIN.TEXT: Mt stringer.

DIABASE 383.27 -389.13 Uitkomst Suite 80
ALTERATION: Quartz carbonate veining with chloritisation. GRAIN SIZE: Medium grained. COLOUR: Greyish green. COMMENTS: Chilled margin. sill.

BOREHOLE **SH19** 387.00 to 430.00 m Plotted 11-02-1995 Page 10

Logged by RELOGGED 2 Scale 1: 200

CORE DEPTH (m)	VERT. PROFILE TOT.SULPH %	UNIT C	DESCRIPTION (core depths)	APP DIP deg

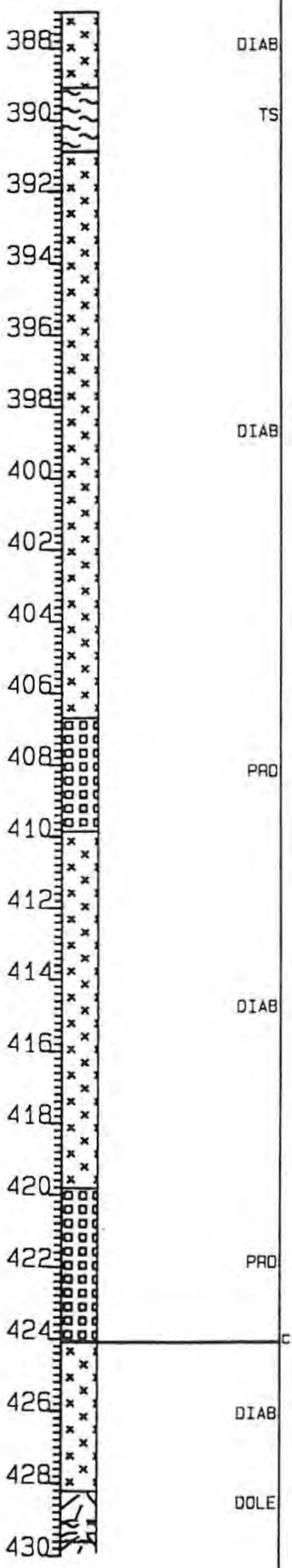

(DIABASE continued) Uitkomst Suite 80

SCHIST 389.13 -390.92 Uitkomst Suite 78
ALTERATION: Serpentinised. GRAIN SIZE: Medium grained.

DIABASE 390.92 -406.75 Uitkomst Suite 80
GRAIN SIZE: Medium grained. COLOUR: Greyish green. COMMENTS: Chilled margin. SILL.

PERIDOTITE 406.75 -409.92 Uitkomst Suite 80
ALTERATION: Quartz carbonate veining. GRAIN SIZE: Medium grained. COLOUR: Dark green.

DIABASE 409.92 -419.89 Uitkomst Suite 86
GRAIN SIZE: Medium grained. COLOUR: Greyish green to dark green. COMMENTS: SILL.

PERIDOTITE 419.89 -424.14 Uitkomst Suite 85
GRAIN SIZE: Medium grained. COLOUR: Dark green. Cr %: 1-5. MIN.TEXT: Crm stringers and seams.

DIABASE 424.14 -428.30 Uitkomst Suite 84
GRAIN SIZE: Medium grained. COLOUR: Greyish green. COMMENTS: Chilled margin. SILL.

DOLERITE 428.30 -498.25 Uitkomst Suite 25
GRAIN SIZE: Fine grained. COLOUR: Greyish green. COMMENTS: DYKE.

SHEAR ZONE 429.09 -429.44 Uitkomst Suite 59

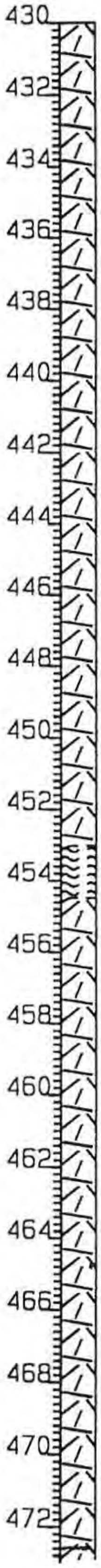

CORE DEPTH (m)	VERT. PROFILE TOT.SULPH %	UNIT C	DESCRIPTION (core depths)		APP DIP deg
			(DOLERITE continued)	Uitkomst Suite	25
		DOLE			
		SHZO	SHEAR ZONE 453.07 -454.54	Uitkomst Suite	12

BOREHOLE **SH19** 473.00 to 516.00 m Plotted 11-02-1995 Page 12

Logged by RELOGGED 2 Scale 1: 200

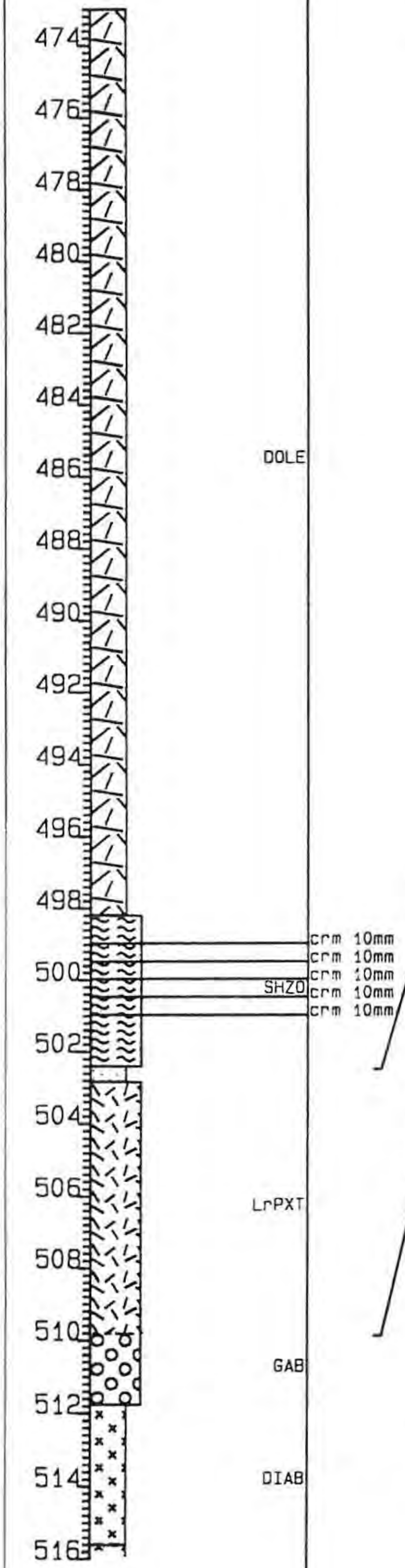

DESCRIPTION (core depths)	APP DIP deg
(DOLERITE continued) Uitkomst Suite	25
SHEAR ZONE 498.25 -502.48 Uitkomst Suite ALTERATION: Talc-alteration. GRAIN SIZE: Fine grained. TOT.SULPH %: 1-5. MIN.TEXT: Disemminated. SCRATCH: Medium. SULPH.MINS.: Po.	35
QUARTZITE 502.48 -502.90 Uitkomst Suite GRAIN SIZE: Fine sand. COLOUR: Grey. TOT.SULPH %: <1. MIN.TEXT: Blebby. SCRATCH: Medium. SULPH.MINS.: Py.	70
AMPHIBOLITE 502.90 -509.87 Uitkomst Suite GRAIN SIZE: Medium grained. Py %: 1-5. TOT.SULPH %: 1-5. MIN.TEXT: Net. SULPH.MINS.: Po py cp.	85
GABBRO 509.87 -511.84 Uitkomst Suite GRAIN SIZE: Medium grained. COLOUR: Greyish black. COMMENTS: VISUALLY INDISTINGUISHABLE FROM DIABASE. TOT.SULPH %: 1-5. MIN.TEXT: Disseminated. SULPH.MINS.: Po cp.	80
DIABASE 511.84 -558.54 Uitkomst Suite ALTERATION: Quartz carbonate veining with chloritisation. GRAIN SIZE: Fine grained. COLOUR: Greyish green. COMMENTS: Chilled margin. SILL.	82

Logged by RELOGGED 2

Scale 1: 200

CORE DEPTH (m)	VERT. PROFILE TOT.SULPH %	UNIT C	DESCRIPTION (core depths)	APP DIP deg

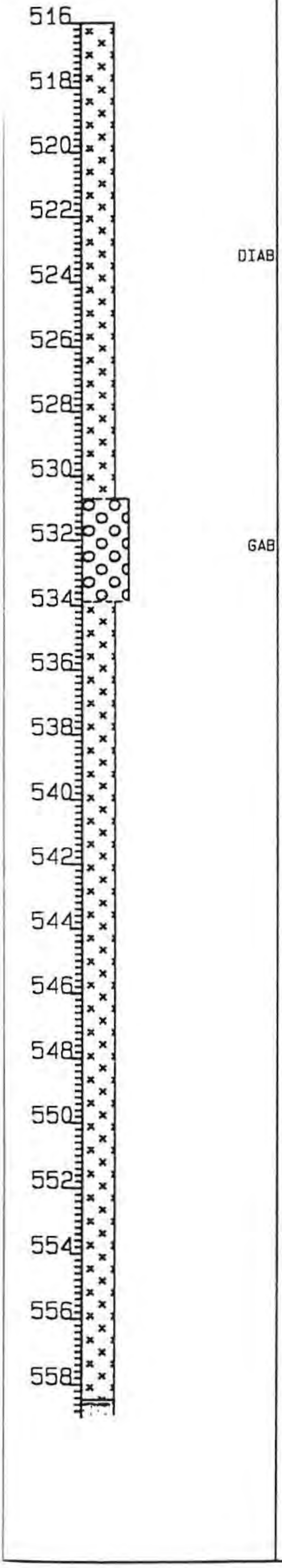

(DIABASE continued) Uitkomst Suite 82

GABBRO 530.75 -533.91 Uitkomst Suite 80
GRAIN SIZE: Medium grained. COLOUR: Greyish black. COMMENTS: Without chilled margins. TOT.SULPH %: 1-5. MIN.TEXT: Disseminated. SULPH.MINS.: Po.

QUARTZITE 558.54 -560.30 Malmani Subgroup 85
GRAIN SIZE: Fine sand. COLOUR: Grey.

BOREHOLE *SH19* 559.00 to 602.00 m Plotted 11-02-1995 Page 14

Logged by RELOGGED 2 Scale 1: 200

CORE DEPTH (m) | VERT. PROFILE TOT. SULPH % | UNIT C

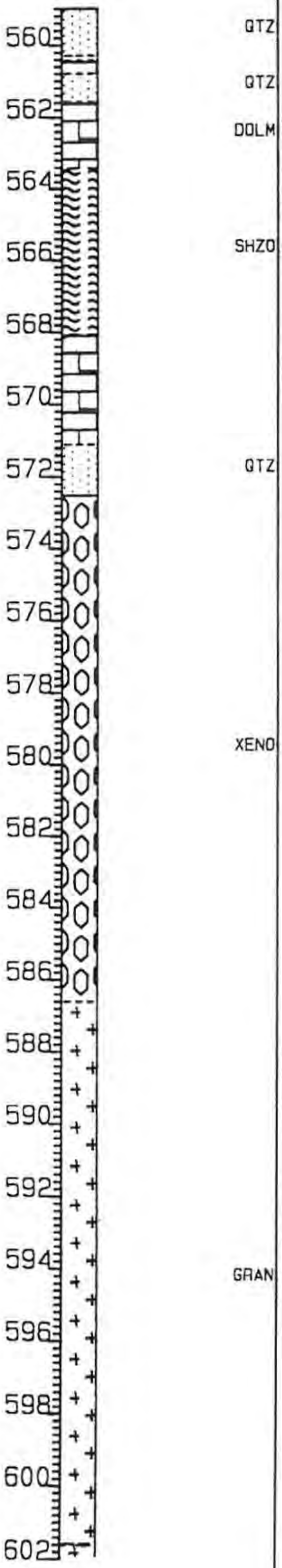

DESCRIPTION (core depths)		APP DIP deg
(QUARTZITE continued)	Malmani Subgroup	85
DOLERITE 560.30 -560.81 GRAIN SIZE: Fine grained. COLOUR: Grey. COMMENTS: Dyke?.	Uitkomst Suite	40
DOLOMITE 560.44 -560.81 GRAIN SIZE: Fine grained.	Malmani Subgroup	85
QUARTZITE 560.81 -561.60 GRAIN SIZE: Fine sand.	Malmani Subgroup	85
DOLOMITE 561.60 -571.14 GRAIN SIZE: Silt.	Malmani Subgroup	85
SHEAR ZONE 563.44 -568.08	Uitkomst Suite	75
QUARTZITE 571.14 -572.57 GRAIN SIZE: Medium sand.	Black Reef Quartsite	80
HORNFELS 572.57 -586.65 GRAIN SIZE: Medium grained. COLOUR: Grey.	Nelshoogte Granite	70
GRANITE 586.65 -611.86 GRAIN SIZE: Coarse grained.	Nelshoogte Granite	85

Logged by RELOGGED 2 Scale 1: 200

CORE DEPTH (m)	VERT. PROFILE TOT.SULPH %	UNIT C	DESCRIPTION (core depths)		APP DIP deg
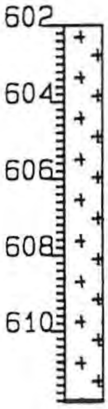		GRAN	(GRANITE continued)	Nelshoogte Granite	85

GEOLOGICAL LOG

sh25

PROJECT	*SLAAIHOEK*
EXPLORATION COMPANY	*ANGLOVAAL*
FARM	*SLAAIHOEK 540 JT*
DRILLING COMMENCED	*Phase One*
DRILLING COMPLETED	
LOGGED BY	*Relogged 2*
DRILLED BY	*Rosond*
	(W R D Marchini)
	Wedges : Phase 2 deflection drilling
INCLINATION:	*-90*
BEARING:	*0*
X CONSTANT:	*2800000*
X COLLAR COORD.:	*44910.3*
Y COLLAR COORD.:	*41373.22*
ELEVATION (A.M.S.L.) IN METERS:	*1507.92*
FINAL DEPTH (m):	*667.26*
No WEDGES:	*0*

BOREHOLE **SH25** 0.00 to 43.00 m Plotted 06-03-1995 Page 1

Logged by W R D Marchini Scale 1: 200

CORE DEPTH (m)	VERT. PROFILE TOT.SULPH %	UNIT C	DESCRIPTION (core depths)	APP DIP deg
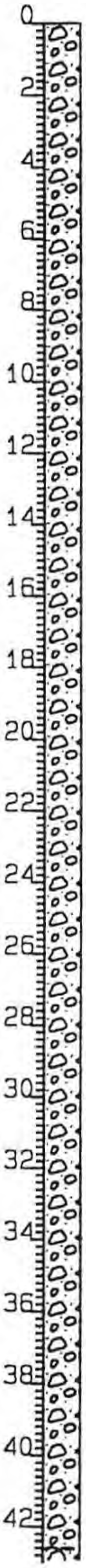		OVB	OVERBURDEN 0.00 -71.70 GRAIN SIZE: Pebble.	78

BOREHOLE **SH25** 43.00 to 86.00 m Plotted 06-03-1995 Page 2

Logged by W R D Marchini Scale 1: 200

CORE DEPTH (m)	VERT. PROFILE TOT.SULPH %	UNIT C	DESCRIPTION (core depths)	APP DIP deg
			(OVERBURDEN continued)	78
			NORITE 71.70 -94.91 Uitkomst Suite GRAIN SIZE: Medium grained. COMMENTS: Grading downwards to pyroxenite. SCRATCH: Medium.	78

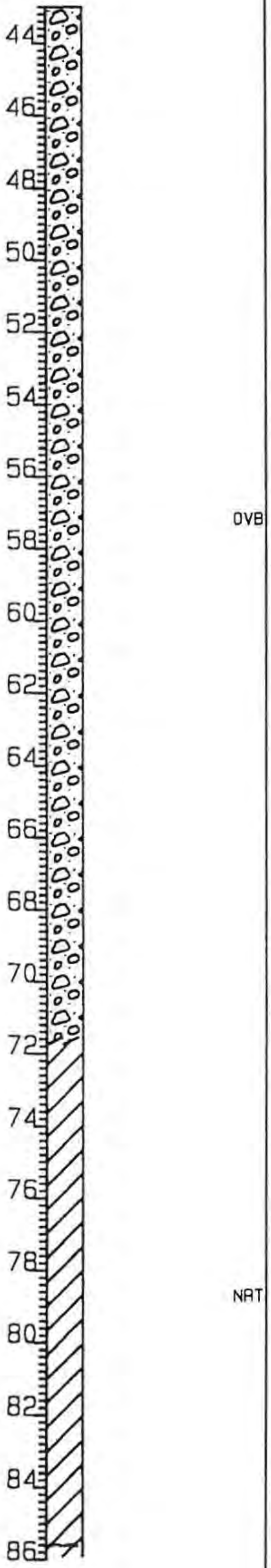

BOREHOLE **SH25** 86.00 to 129.00 m Plotted 06-03-1995

Logged by W R D Marchini Scale 1: 200

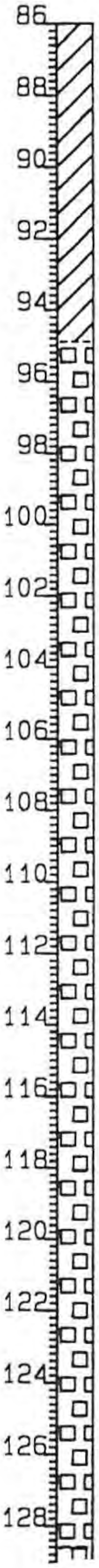

CORE DEPTH (m)	VERT. PROFILE TOT.SULPH %	UNIT C	DESCRIPTION (core depths)		APP DIP deg
		NRT	(NORITE continued)	Uitkomst Suite	78
		UPXT	PYROXENITE 94.91 -162.97 STRUCTURE: Sheared. GRAIN SIZE: Medium grained. SCRATCH: Medium.	Uitkomst Suite	78

Logged by W R D Marchini

Scale 1: 200

CORE DEPTH (m)	VERT. PROFILE TOT. SULPH %	UNIT	DESCRIPTION (core depths)	APP DIP deg

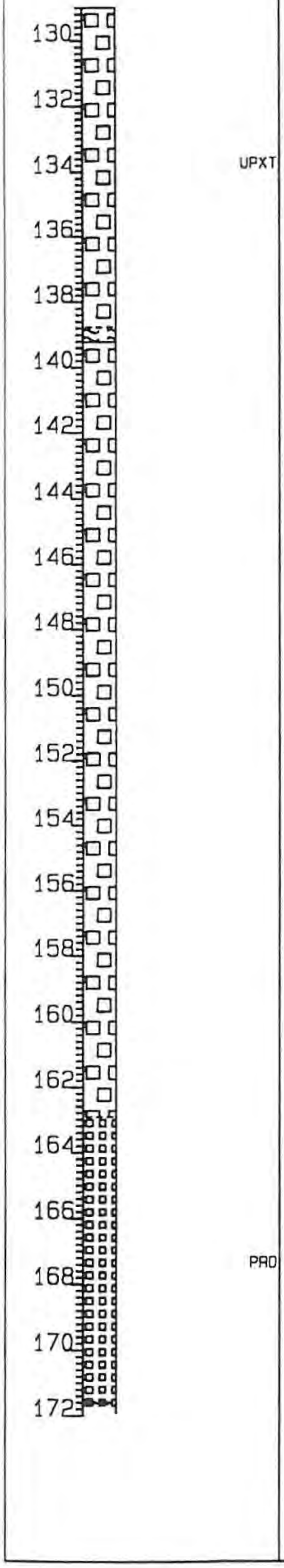

(PYROXENITE continued) Uitkomst Suite 78

SHEAR ZONE 138.80 -139.27 Uitkomst Suite 41
ALTERATION: Talc-alteration. GRAIN SIZE: Fine grained. SCRATCH: Medium.

PERIDOTITE 162.97 -182.78 Uitkomst Suite 90
GRAIN SIZE: Coarse grained. COMMENTS: Fine grained cumulus olivine . Pyroxene poikilitically enclosing olivine. SCRATCH: Medium.

Logged by W R D Marchini

Scale 1: 200

CORE DEPTH (m)	VERT. PROFILE TOT.SULPH %	UNIT C	DESCRIPTION (core depths)	APP DIP deg

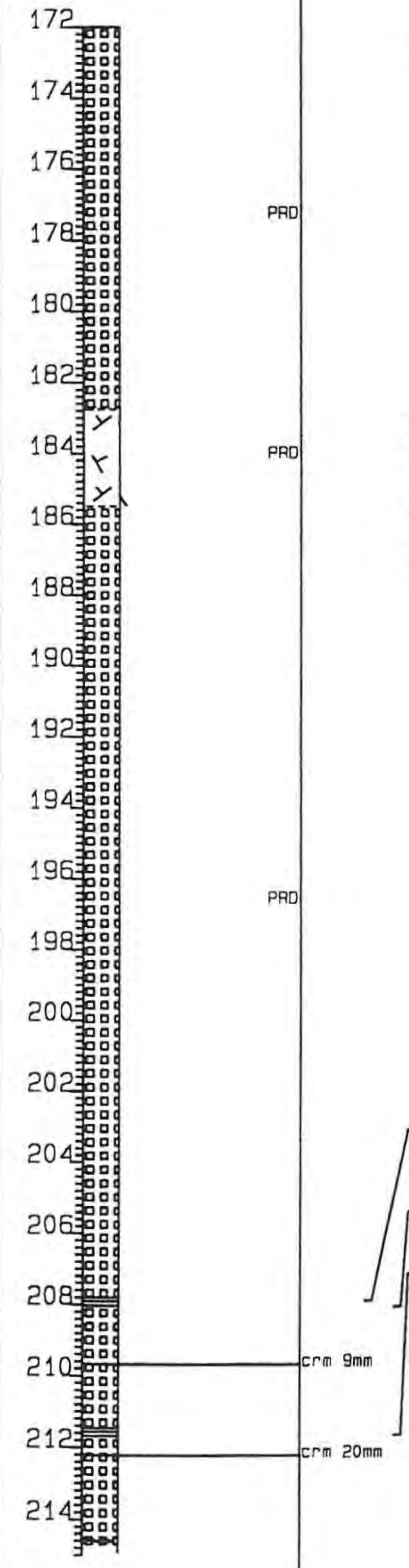

(PERIDOTITE continued) Uitkomst Suite 90

DUNITE 182.78 -185.53 Uitkomst Suite 78
GRAIN SIZE: Medium grained. SCRATCH: Medium.

PERIDOTITE 185.53 -207.88 Uitkomst Suite 79
GRAIN SIZE: Medium grained. COMMENTS: Grading towards pyroxenite locally.
SCRATCH: Medium.

PERIDOTITE 207.88 -223.08 Uitkomst Suite 78
GRAIN SIZE: Medium grained. Cr %: <1. TOT.SULPH %: <1. MIN.TEXT: Po disseminated.
SCRATCH: Medium. SULPH.MINS.: Po.

MASSIVE CHROMITITE 207.98 -208.10 Uitkomst Suite 88
GRAIN SIZE: Fine grained. COLOUR: Black. MAGNETISM: Non-susceptable. Cr
%: >50. SCRATCH: Medium.

MASSIVE CHROMITITE 211.54 -211.77 Uitkomst Suite 85
GRAIN SIZE: Fine grained. COLOUR: Black. MAGNETISM: Non-susceptable. Cr
%: >50. SCRATCH: Medium.

Logged by W R D Marchini

Scale 1: 200

CORE DEPTH (m)	VERT. PROFILE TOT.SULPH %	UNIT	DESCRIPTION (core depths)	APP DIP deg

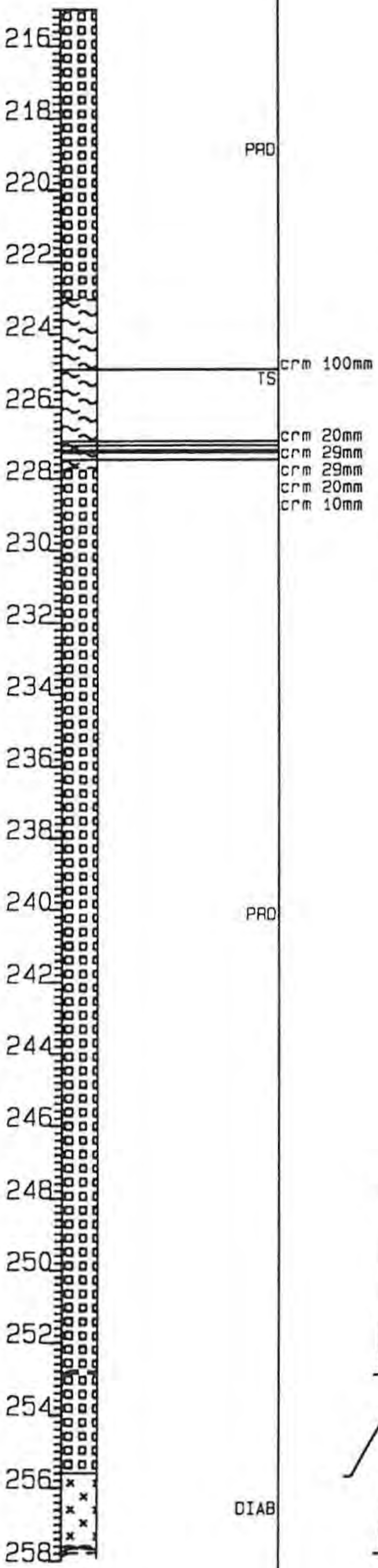

(PERIDOTITE continued) Uitkomst Suite 78

SCHIST 223.08 -227.72 Uitkomst Suite 51

ALTERATION: Talc-alteration. GRAIN SIZE: Fine grained. COLOUR: Grey. MAGNETISM: Non-susceptable. Cr %: <1. SCRATCH: Medium.

PERIDOTITE 227.72 -255.67 Uitkomst Suite 78

STRUCTURE: Veined. ALTERATION: Serpentinised. GRAIN SIZE: Medium grained. COMMENTS: Pyroxene poikilitically enclosing olivine with plagioclase interstitial to olivine. SCRATCH: Medium.

SHEAR ZONE 252.84 -252.91 Uitkomst Suite 42

STRUCTURE: Sheared. GRAIN SIZE: Fine grained. COLOUR: Grey. MAGNETISM: Non-susceptable. SCRATCH: Medium.

DIABASE 255.67 -261.93 Uitkomst Suite 61

GRAIN SIZE: Medium grained. COMMENTS: Sill, with chilled margin. SCRATCH: Medium.

SHEAR ZONE 257.74 -257.85 Uitkomst Suite 12

STRUCTURE: Sheared. GRAIN SIZE: Fine grained. COLOUR: Grey. MAGNETISM: Non-susceptable. SCRATCH: Medium.

Logged by W R D Marchini

Scale 1: 200

CORE DEPTH (m) | VERT. PROFILE TOT.SULPH % | UNIT C

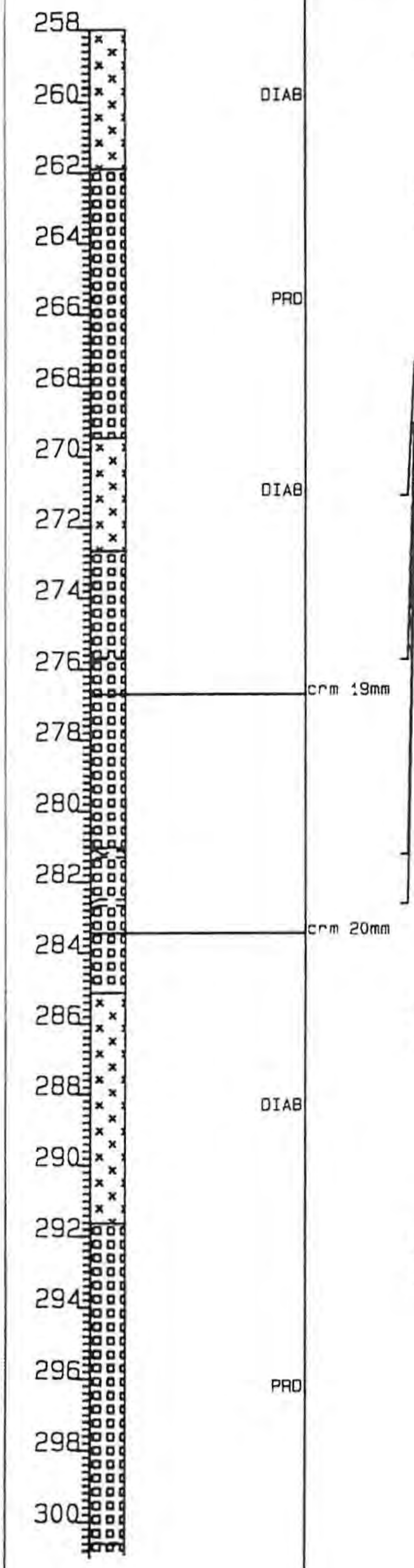

DESCRIPTION (core depths)	APP DIP deg
(DIABASE continued) Uitkomst Suite	61
PERIDOTITE 261.93 -285.20 Uitkomst Suite STRUCTURE: Sheared. ALTERATION: Serpentinised. GRAIN SIZE: Medium grained. Cr %: <1. MIN.TEXT: Crm disseminated and with seam. SCRATCH: Medium.	78
DIABASE 269.52 -272.72 Uitkomst Suite GRAIN SIZE: Medium grained. COLOUR: Grey. MAGNETISM: Non-susceptable. COMMENTS: Sill. SCRATCH: Medium.	78
SHEAR ZONE 275.71 -275.75 Uitkomst Suite STRUCTURE: Sheared. GRAIN SIZE: Fine grained. COLOUR: Grey. MAGNETISM: Non-susceptable. SCRATCH: Medium.	68
SHEAR ZONE 281.08 -281.34 Uitkomst Suite STRUCTURE: Sheared. GRAIN SIZE: Fine grained. COLOUR: Grey. MAGNETISM: Non-susceptable. SCRATCH: Medium.	45
SHEAR ZONE 282.53 -282.70 Uitkomst Suite STRUCTURE: Sheared. GRAIN SIZE: Fine grained. COLOUR: Grey. MAGNETISM: Non-susceptable. SCRATCH: Medium.	45
DIABASE 285.20 -291.70 Uitkomst Suite ALTERATION: Quartz carbonate veining. GRAIN SIZE: Medium grained. COMMENTS: Sill, with chilled margin. SCRATCH: Medium.	78
PERIDOTITE 291.70 -326.78 Uitkomst Suite STRUCTURE: Sheared towards the bottom. ALTERATION: Serpentinised. GRAIN SIZE: Medium grained. Cr %: <1. MIN.TEXT: Crm wisps. SCRATCH: Medium.	78

Logged by W R D Marchini

Scale 1: 200

CORE DEPTH (m)	VERT. PROFILE TOT.SULPH %	UNIT C	DESCRIPTION (core depths)	APP DIP deg

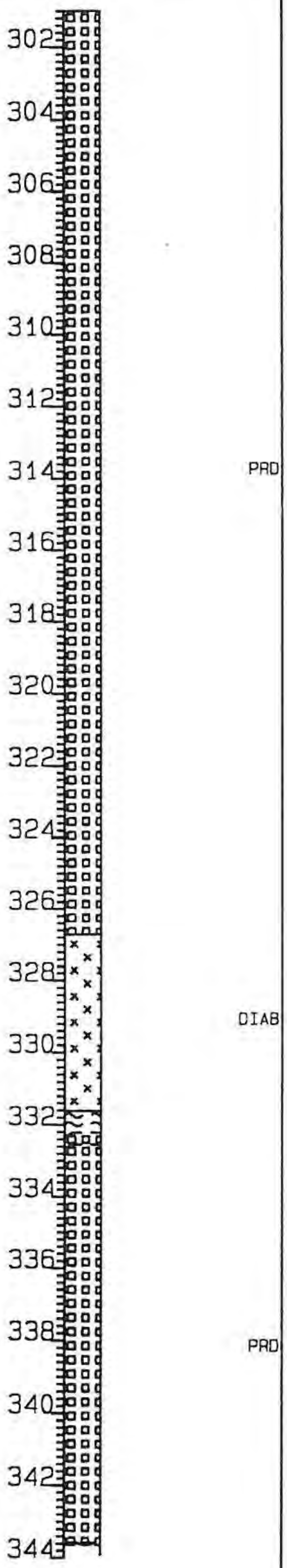

(PERIDOTITE continued) Uitkomst Suite 78

DIABASE 326.78 -331.68 Uitkomst Suite 78
GRAIN SIZE: Medium grained. COMMENTS: Sill, chilled margin absent at the top.
SCRATCH: Medium.

SHEAR ZONE 331.68 -332.28 Uitkomst Suite 50
STRUCTURE: Sheared. GRAIN SIZE: Fine grained. COLOUR: Grey. MAGNETISM: Non-susceptable.
SCRATCH: Medium.

PERIDOTITE 332.28 -332.61 Uitkomst Suite 75
ALTERATION: Serpentinised. GRAIN SIZE: Medium grained. COLOUR: Grey green.
SCRATCH: Medium.

PERIDOTITE 332.61 -366.11 Uitkomst Suite 78
ALTERATION: Serpentinised talc-alteration. GRAIN SIZE: Medium grained. Cr %: <1.
MIN.TEXT: Crm stringer. SCRATCH: Medium.

BOREHOLE *SH25* 344.00 to 387.00 m Plotted 22-03-1995

Logged by W R D Marchini

Scale 1: 200

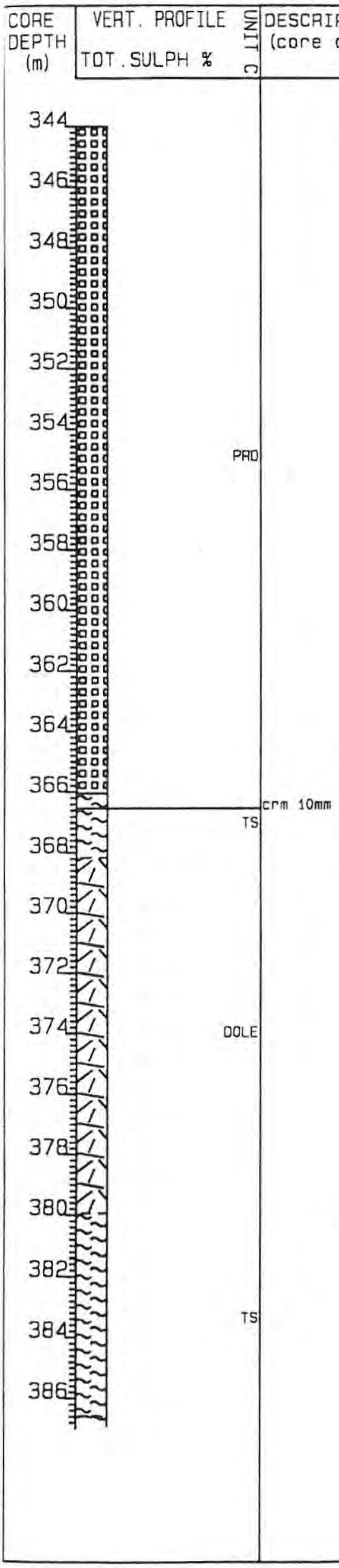

DESCRIPTION (core depths)	APP DIP deg
PERIDOTITE 332.61 -366.11 Uitkomst Suite ALTERATION: Serpentinised talc-alteration. GRAIN SIZE: Medium grained. Cr %: <1. MIN.TEXT: Crm stringer. SCRATCH: Medium.	78
SCHIST 366.11 -368.21 Uitkomst Suite ALTERATION: Talc-alteration. GRAIN SIZE: Fine grained. SCRATCH: Medium.	40
DOLERITE 368.21 -380.00 Uitkomst Suite ALTERATION: Quartz carbonate veining. GRAIN SIZE: Medium grained. COLOUR: Grey. MAGNETISM: Non-susceptable. COMMENTS: Highly altered dyke ?. SCRATCH: Medium.	78
SCHIST 380.00 -410.98 Uitkomst Suite ALTERATION: Talc-alteration. GRAIN SIZE: Fine grained. Cr %: <1. TOT.SULPH %: <1. MIN.TEXT: Disseminated stringer. SCRATCH: Medium. SULPH.MINS.: Po py cp.	40

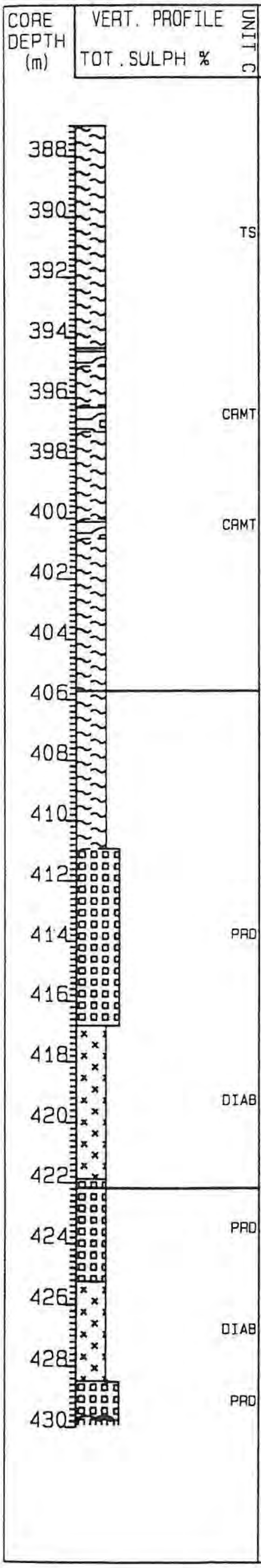

q.c.v. 370mm

crm 89mm

DESCRIPTION (core depths)	APP DIP deg
(SCHIST continued) Uitkomst Suite	40
MASSIVE CHROMITITE 394.39 -394.98 Uitkomst Suite ALTERATION: Talc-alteration. GRAIN SIZE: Fine grained. COLOUR: Black. MAGNETISM: Non-susceptable. Cr %: >50. SCRATCH: Medium.	50
MASSIVE CHROMITITE 396.25 -397.15 Uitkomst Suite GRAIN SIZE: Fine grained. COLOUR: Black. Cr %: >50. MIN.TEXT: Disseminated. SCRATCH: Medium.	55
MASSIVE CHROMITITE 400.05 -400.70 Uitkomst Suite STRUCTURE: Sheared. ALTERATION: Quartz carbonate veining. GRAIN SIZE: Fine grained. COLOUR: Black. Cr %: >50. MIN.TEXT: Disseminated. SCRATCH: Medium.	45
PERIDOTITE 410.98 -416.88 Uitkomst Suite GRAIN SIZE: Medium grained. Cr %: 1-5. TOT.SULPH %: 1-5. MIN.TEXT: Po disseminated crm blebby. SCRATCH: Medium. SULPH.MINS.: Po.	78
DIABASE 416.88 -421.94 Uitkomst Suite GRAIN SIZE: Medium grained. COMMENTS: Sill, chilled margin. SCRATCH: Medium.	78
PERIDOTITE 421.94 -425.32 Uitkomst Suite STRUCTURE: Sheared. ALTERATION: Serpentinised talc-alteration. GRAIN SIZE: Medium grained. Cr %: <1. TOT.SULPH %: <1. MIN.TEXT: Po disseminated. SCRATCH: Medium. SULPH.MINS.: Po.	78
DIABASE 425.32 -428.57 Uitkomst Suite ALTERATION: Chloritisation slightly altered. GRAIN SIZE: Medium grained. COMMENTS: Sill, chilled margin. SCRATCH: Medium.	78
PERIDOTITE 428.57 -432.90 Uitkomst Suite GRAIN SIZE: Medium grained. COLOUR: Dark green grey. TOT.SULPH %: 1-5. MIN.TEXT: Disseminated. SCRATCH: Medium. SULPH.MINS.: Po.	78

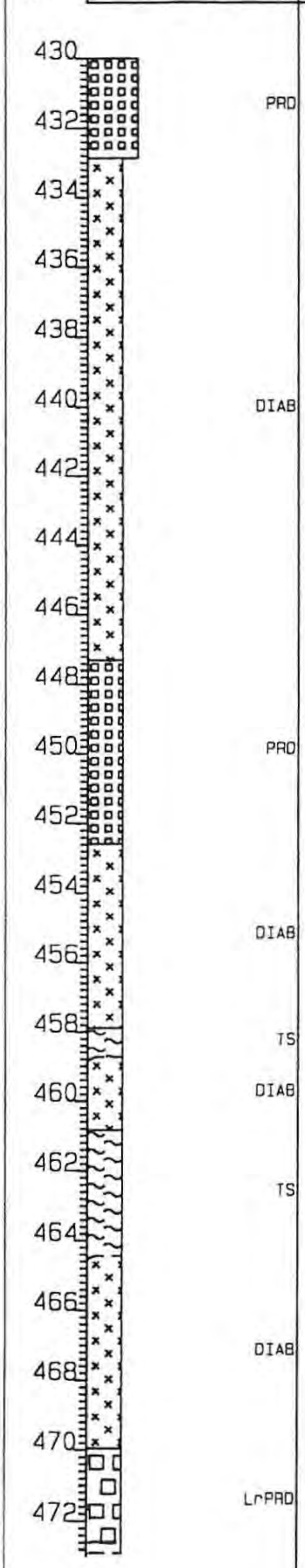

DESCRIPTION (core depths)	APP DIP deg
(PERIDOTITE continued) Uitkomst Suite	78
DIABASE 432.90 -447.36 Uitkomst Suite ALTERATION: Quartz carbonate veining. GRAIN SIZE: Medium grained. COMMENTS: Sill, chilled margin. SCRATCH: Medium.	78
PERIDOTITE 447.36 -452.64 Uitkomst Suite ALTERATION: Talc-alteration towards the bottom. GRAIN SIZE: Medium grained. TOT.SULPH %: <1. MIN.TEXT: Disseminated. SCRATCH: Medium. SULPH.MINS.: Po.	78
DIABASE 452.64 -457.96 Uitkomst Suite ALTERATION: Chloritisation. GRAIN SIZE: Medium grained. COMMENTS: Sill, chilled margin. SCRATCH: Medium.	78
SCHIST 457.96 -458.78 Uitkomst Suite STRUCTURE: Sheared. ALTERATION: Talc-alteration. GRAIN SIZE: Fine grained. TOT.SULPH %: <1. SCRATCH: Medium. SULPH.MINS.: Po py cp.	45
DIABASE 458.78 -460.90 Uitkomst Suite ALTERATION: Quartz carbonate veining. GRAIN SIZE: Fine grained. COMMENTS: Sill, chilled margin. SCRATCH: Medium.	35
SCHIST 460.90 -464.49 Uitkomst Suite STRUCTURE: Sheared. ALTERATION: Talc-alteration quartz carbonate veining. GRAIN SIZE: Fine grained. COLOUR: Grey. TOT.SULPH %: <1. MIN.TEXT: Disseminated. SCRATCH: Medium.	40
DIABASE 464.49 -470.03 Uitkomst Suite GRAIN SIZE: Medium grained. COMMENTS: Sill, chilled margin. SCRATCH: Medium.	78
PYROXENITE 470.03 -475.42 Uitkomst Suite GRAIN SIZE: Medium grained. TOT.SULPH %: <1. MIN.TEXT: Disseminated. SCRATCH: Medium. SULPH.MINS.: Po.	78

BOREHOLE SH25 473.00 to 516.00 m Plotted 06-03-1995 Page 12

Logged by W R D Marchini Scale 1: 200

CORE DEPTH (m) | VERT. PROFILE TOT.SULPH % | UNIT C

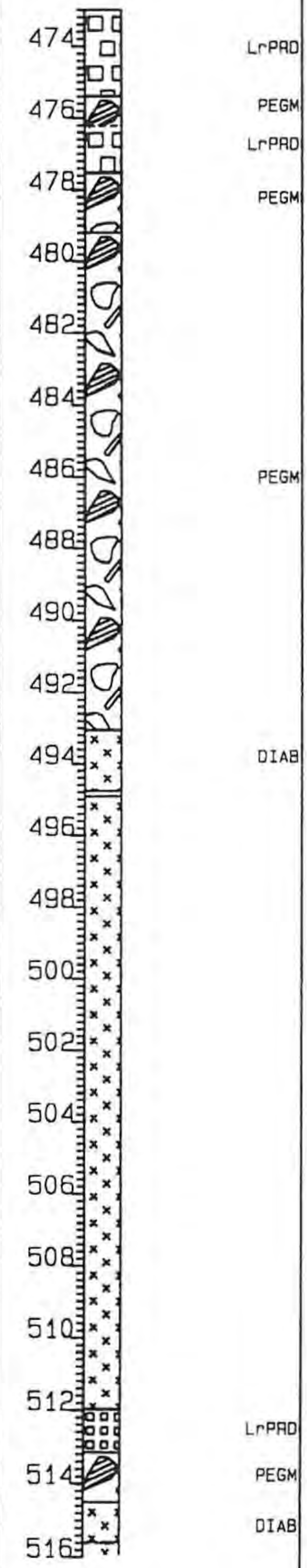

DESCRIPTION (core depths)	APP DIP deg
(PYROXENITE continued) Uitkomst Suite	78
PEGMATITE 475.42 -476.24 Uitkomst Suite ALTERATION: Metamorphosed. GRAIN SIZE: Fine sand. COLOUR: Grey. SCRATCH: Medium.	78
PYROXENITE 476.24 -477.56 Uitkomst Suite GRAIN SIZE: Fine grained. SCRATCH: Medium.	78
PEGMATITE 477.56 -479.23 Uitkomst Suite ALTERATION: Carbonatisation. GRAIN SIZE: Pegmatitic. SCRATCH: Medium.	10
PEGMATITE 479.23 -493.11 Uitkomst Suite STRUCTURE: Xenolith. ALTERATION: Carbonatisation quartz carbonate veining silicified. GRAIN SIZE: Fine sand. COLOUR: Grey. MAGNETISM: Non-susceptable. COMMENTS: Dyke like pegmatite body. Contacts difficult to discern.SCRATCH: Medium.	12
DIABASE 493.11 -512.05 Uitkomst Suite ALTERATION: Quartz carbonate veining. GRAIN SIZE: Medium grained. COMMENTS: Sill, chilled margin. SCRATCH: Medium.	78
DOLERITE 494.82 -494.98 Uitkomst Suite GRAIN SIZE: Fine grained. COLOUR: Grey. MAGNETISM: Non-susceptable. COMMENTS: Dyke. SCRATCH: Medium.	40
PERIDOTITE 512.05 -513.24 Uitkomst Suite ALTERATION: Talc-alteration. GRAIN SIZE: Fine grained. SCRATCH: Medium.	78
PEGMATITE 513.24 -514.59 Uitkomst Suite ALTERATION: Metamorphosed carbonatisation silicified. GRAIN SIZE: Pegmatitic. SCRATCH: Medium.	78
DIABASE 514.59 -517.51 Uitkomst Suite ALTERATION: Quartz carbonate veining chloritisation. GRAIN SIZE: Medium grained. COLOUR: Grey. MAGNETISM: Non-susceptable. COMMENTS: Highly altered sill.SCRATCH: Medium.	78

Logged by W R D Marchini

Scale 1: 200

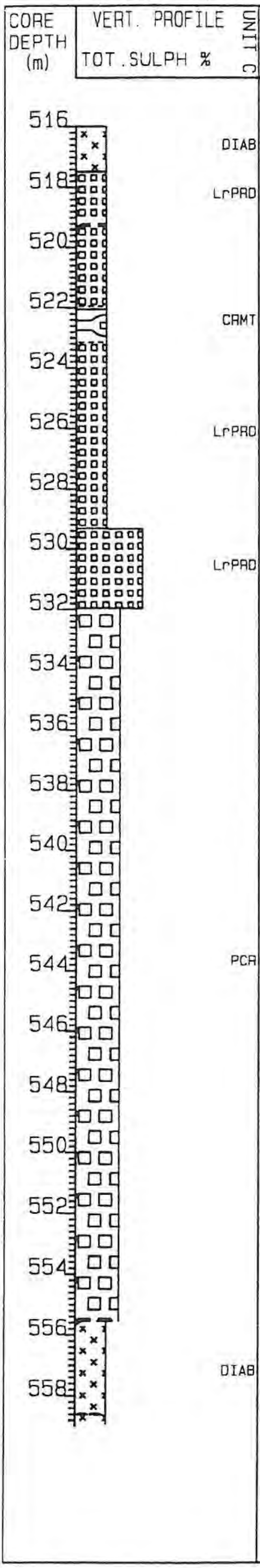

DESCRIPTION (core depths)	APP DIP deg
(DIABASE continued) Uitkomst Suite	78
PERIDOTITE 517.51 -521.97 Uitkomst Suite ALTERATION: Quartz carbonate veining. GRAIN SIZE: Fine grained. COMMENTS: Pyroxene poikilitically enclosing olivine. SCRATCH: Medium.	78
SHEAR ZONE 519.23 -519.30 Uitkomst Suite STRUCTURE: Sheared. GRAIN SIZE: Fine grained. COLOUR: Grey. MAGNETISM: Non-susceptable. SCRATCH: Medium.	85
MASSIVE CHROMITITE 521.97 -523.16 Uitkomst Suite GRAIN SIZE: Fine grained. COLOUR: Black. Cr %: >50. MIN.TEXT: Crm disseminated to massive. SCRATCH: Medium.	78
PERIDOTITE 523.16 -529.37 Uitkomst Suite ALTERATION: Talc-alteration. GRAIN SIZE: Fine grained. COLOUR: Grey. Cr %: >50. MIN.TEXT: Crm semi-massive to massive. SCRATCH: Medium.	78
PERIDOTITE 529.37 -532.02 Uitkomst Suite ALTERATION: Talc-alteration. GRAIN SIZE: Fine grained. COLOUR: Grey. TOT.SULPH %: 5-10. MIN.TEXT: Disseminated. SCRATCH: Medium. SULPH.MINS.: Po.	78
PYROXENITE 532.02 -555.62 Uitkomst Suite STRUCTURE: Sheared towards the bottom. ALTERATION: Talc-alteration. GRAIN SIZE: Medium grained. COLOUR: Green grey. Cr %: 10-25. TOT.SULPH %: 1-5. MIN.TEXT: Massive to semi-massive crm. SCRATCH: Medium. SULPH.MINS.: Po. SHEARED TOWARDS BASE .	78
DIABASE 555.62 -579.80 Uitkomst Suite ALTERATION: Quartz carbonate veining chloritisation. GRAIN SIZE: Medium grained. COLOUR: Grey. MAGNETISM: Non-susceptable. COMMENTS: Sill. SCRATCH: Medium.	78

BOREHOLE ***SH25*** 559.00 to 602.00 m Plotted 06-03-1995 Page 14

Logged by W R D Marchini Scale 1: 200

CORE DEPTH (m) | VERT. PROFILE TOT.SULPH % | UNIT C

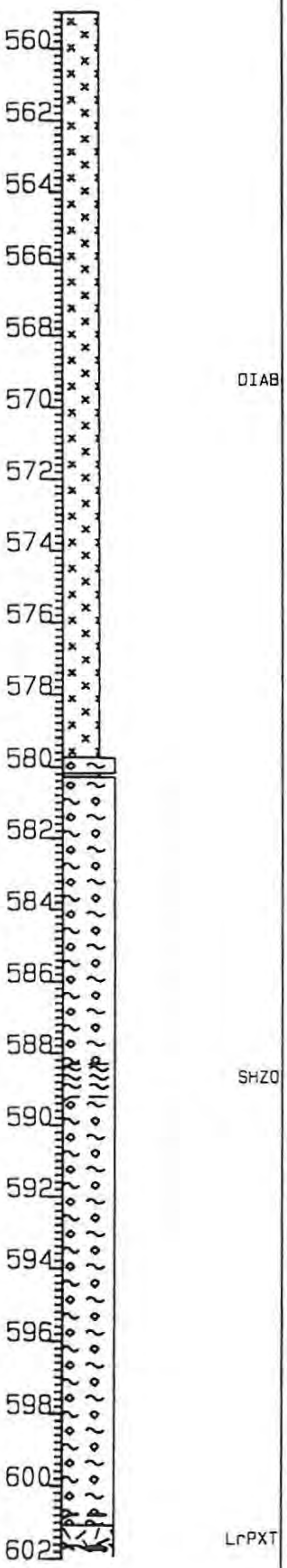

DESCRIPTION (core depths)	APP DIP deg
(DIABASE continued) Uitkomst Suite	78
CHROMITITIC PYROXENITE 579.80 -601.16 Uitkomst Suite STRUCTURE: Sheared. ALTERATION: Talc-alteration. GRAIN SIZE: Medium grained. Cr %: 1-5. TOT.SULPH %: 1-5. SCRATCH: Medium. SULPH.MINS.: Po.	78
DIABASE 580.23 -580.34 Uitkomst Suite GRAIN SIZE: Fine grained. COLOUR: Grey. MAGNETISM: Non-susceptable. COMMENTS: Sill. SCRATCH: Medium.	81
SHEAR ZONE 588.36 -589.27 Uitkomst Suite STRUCTURE: Sheared. ALTERATION: Talc-alteration quartz carbonate veining. GRAIN SIZE: Fine grained. COLOUR: Grey. TOT.SULPH %: 1-5. MIN.TEXT: Disseminated. SCRATCH: Medium. SULPH.MINS.: Po.	75
SHEAR ZONE 600.84 -600.87 Uitkomst Suite STRUCTURE: Sheared. ALTERATION: Talc-alteration quartz carbonate veining. GRAIN SIZE: Fine grained. COLOUR: Grey. TOT.SULPH %: 1-5. MIN.TEXT: Disseminated. SCRATCH: Medium. SULPH.MINS.: Po.	81
AMPHIBOLITE 601.16 -603.77 Uitkomst Suite ALTERATION: Metamorphosed. GRAIN SIZE: Fine grained. COLOUR: Green. TOT.SULPH %: 1-5. MIN.TEXT: Disseminated. SCRATCH: Medium.	78

BOREHOLE *SH25* 602.00 to 645.00 m

Plotted 06-03-1995 Page 15

Logged by W R D Marchini

Scale 1: 200

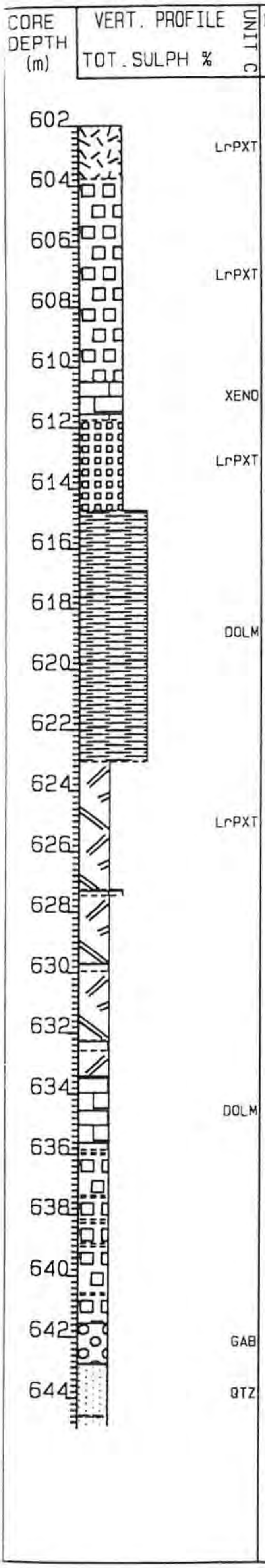

DESCRIPTION (core depths)	APP DIP deg
(AMPHIBOLITE continued) Uitkomst Suite	78
PYROXENITE 603.77 -610.47 Uitkomst Suite ALTERATION: Metamorphosed. GRAIN SIZE: Fine grained. COLOUR: Green grey. TOT.SULPH %: 1-5. MIN.TEXT: Disseminated. SCRATCH: Medium.	78
DOLOMITE 610.47 -611.77 Uitkomst Suite ALTERATION: Metamorphosed. GRAIN SIZE: Fine grained. COLOUR: Grey. TOT.SULPH %: 1-5. MIN.TEXT: Disseminated. SCRATCH: Medium.	78
PERIDOTITE 611.77 -614.77 Uitkomst Suite GRAIN SIZE: Fine grained. COLOUR: Green black. TOT.SULPH %: 1-5. MIN.TEXT: Disseminated. SCRATCH: Medium. SULPH.MINS.: Po.	78
SKARN 614.77 -623.10 Malmani Subgroup STRUCTURE: Xenolith. ALTERATION: Metamorphosed. GRAIN SIZE: Medium sand. COLOUR: Grey. TOT.SULPH %: 5-10. MIN.TEXT: Disseminated. SULPH.MINS.: Po.	81
WEHRLITE 623.10 -633.50 Uitkomst Suite GRAIN SIZE: Medium grained. MIN.TEXT: Disseminated. SCRATCH: Medium. SULPH.MINS.: Po cp.	78
DOLOMITE 627.31 -627.51 Uitkomst Suite STRUCTURE: Xenolith. GRAIN SIZE: Fine sand. COLOUR: Grey. TOT.SULPH %: 1-5. MIN.TEXT: Po blebby. SCRATCH: Medium. SULPH.MINS.: Po.	78
DOLOMITE 629.73 -630.01 Uitkomst Suite GRAIN SIZE: Silt. COLOUR: Grey. SCRATCH: Medium.	76
DOLOMITE 632.29 -632.64 Uitkomst Suite GRAIN SIZE: Fine sand. COLOUR: Grey. SCRATCH: Medium.	87
DOLOMITE 633.50 -635.90 Malmani Subgroup GRAIN SIZE: Fine sand. COLOUR: Grey green.	66
PYROXENITE 635.90 -641.63 Uitkomst Suite ALTERATION: Slightly altered. GRAIN SIZE: Medium grained. COLOUR: Grey green. SCRATCH: Medium.	90
QUARTZITE 636.00 -636.05 Uitkomst Suite STRUCTURE: Xenolith. ALTERATION: Metamorphosed. GRAIN SIZE: Fine sand. COLOUR: Grey. SCRATCH: Medium.	82
QUARTZITE 637.42 -637.48 Uitkomst Suite STRUCTURE: Xenolith. ALTERATION: Metamorphosed. GRAIN SIZE: Fine sand. COLOUR: Grey. SCRATCH: Medium.	71
QUARTZITE 638.21 -638.32 Uitkomst Suite GRAIN SIZE: Fine sand. COLOUR: Grey. SCRATCH: Medium.	78
QUARTZITE 638.99 -639.09 Uitkomst Suite STRUCTURE: Xenolith. ALTERATION: Metamorphosed. GRAIN SIZE: Fine sand. COLOUR: Grey. SCRATCH: Medium.	70
QUARTZITE 640.62 -640.68 Uitkomst Suite GRAIN SIZE: Fine sand. COLOUR: Grey. SCRATCH: Medium.	63
GABBRO 641.63 -642.97 Uitkomst Suite GRAIN SIZE: Medium grained. COLOUR: Grey black. TOT.SULPH %: <1. MIN.TEXT: Disseminated. SCRATCH: Medium.	90
QUARTZITE 642.97 -646.41 Malmani Subgroup GRAIN SIZE: Fine sand. COLOUR: White.	90

BOREHOLE **SH25** 645.00 to 667.26 m Plotted 06-03-1995 Page 16

Logged by W R D Marchini Scale 1: 200

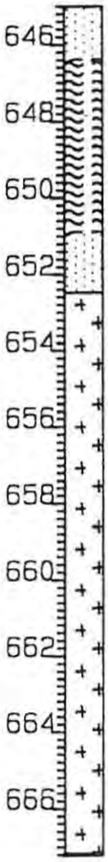

CORE DEPTH (m)	VERT. PROFILE TOT. SULPH %	UNIT C	DESCRIPTION (core depths)		APP DIP deg
		QTZ	(QUARTZITE continued)	Malmani Subgroup	90
		SHZO	SHEAR ZONE 646.41 -650.90 GRAIN SIZE: Fine sand. COLOUR: Grey. MAGNETISM: Non-susceptable. COMMENTS: Basal shear.	Malmani Subgroup	42
		QTZ	QUARTZITE 650.90 -652.52 GRAIN SIZE: Medium sand. COLOUR: Grey.	Black Reef Quartsite	90
		GRAN	GRANITE 652.52 -667.26 GRAIN SIZE: Coarse grained.	Nelshoogte Granite	78

GEOLOGICAL LOG

sh26

PROJECT	*SLAAIHOEK*
EXPLORATION COMPANY	*ANGLOVAAL*
FARM	*SLAAIHOEK 540 JT*
DRILLING COMMENCED	*Phase One*
DRILLING COMPLETED	
LOGGED BY	*Relogged*
DRILLED BY	

INCLINATION:	*-90*
BEARING:	*0*
X CONSTANT:	*2800000*
X COLLAR COORD.:	*45403.95*
Y COLLAR COORD.:	*40409.78*
ELEVATION (A.M.S.L.) IN METERS:	*1489.55*
FINAL DEPTH (m):	*520.54*
No WEDGES:	*0*

BOREHOLE **SH26** 0.00 to 43.00 m Plotted 15-12-1994 Page 1

Logged by RELOGGED

Scale 1: 200

CORE DEPTH (m)	VERT. PROFILE TOT.SULPH %	UNIT C	DESCRIPTION (core depths)	APP DIP deg
		OVB	OVERBURDEN 0.00 -46.17 GRAIN SIZE: Pebble.	

BOREHOLE **SH26** 43.00 to 86.00 m Plotted 15-12-1994 Page 2

Logged by RELOGGED

Scale 1: 200

CORE DEPTH (m)	VERT. PROFILE TOT.SULPH %	UNIT C	DESCRIPTION (core depths)	APP DIP deg

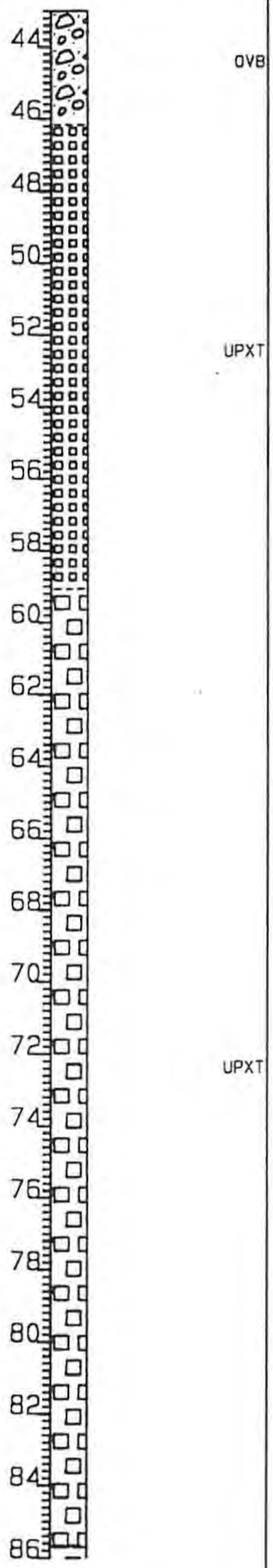

(OVERBURDEN continued)

PERIDOTITE 46.17 -59.06 Uitkomst Suite 83

ALTERATION: Serpentinised. COMMENTS: Cumulus olivine with interstitial plagioclase and minor pyroxene and biotite.

PYROXENITE 59.06 -95.83 Uitkomst Suite 83

GRAIN SIZE: Medium grained. COMMENTS: Olivine and plagioclase.

BOREHOLE **SH26** 86.00 to 129.00 m Plotted 15-12-1994 Page 3

Logged by RELOGGED Scale 1: 200

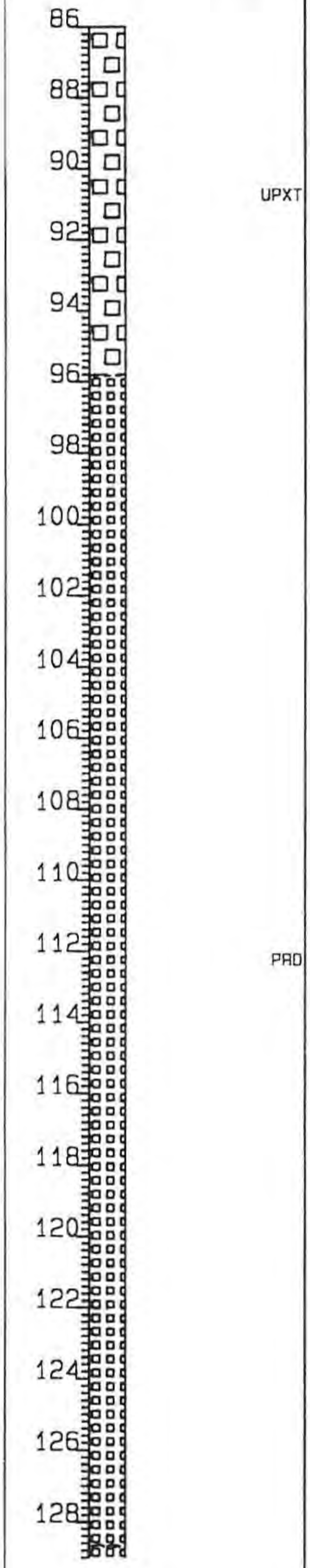

DESCRIPTION (core depths)	APP DIP deg
(PYROXENITE continued) Uitkomst Suite	83
PERIDOTITE 95.83 -201.88 Uitkomst Suite GRAIN SIZE: Fine grained. COMMENTS: Pyroxene poikilitically enclosing olivine.	83

BOREHOLE **SH26** 129.00 to 172.00 m Plotted 15-12-1994 Page 4

Logged by RELOGGED Scale 1: 200

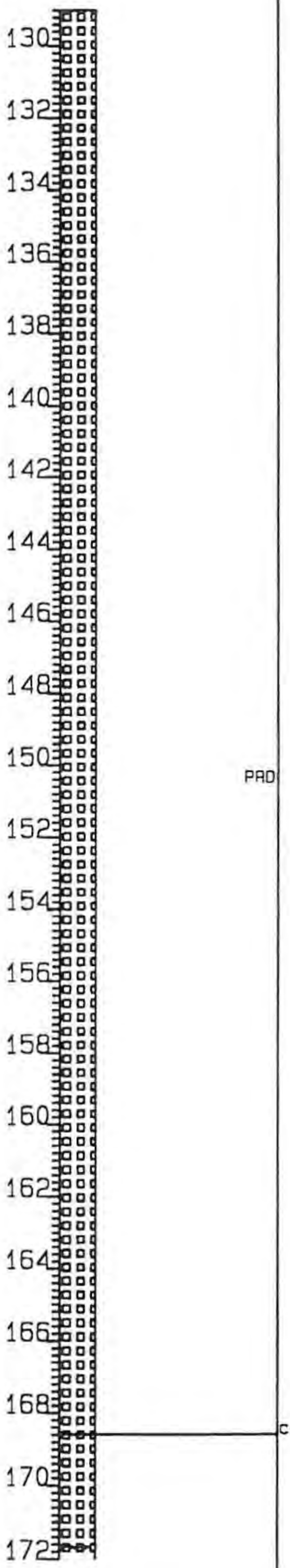

CORE DEPTH (m)	VERT. PROFILE TOT.SULPH %	UNIT C	DESCRIPTION (core depths)	APP DIP deg
			(PERIDOTITE continued) Uitkomst Suite	83
		PRD		
			crm 450mm	

BOREHOLE SN20 172.00 to 215.00 m Plotted 15-12-1994 Page 5

Logged by RELOGGED Scale 1: 200

CORE DEPTH (m) | VERT. PROFILE TOT.SULPH % | UNIT C

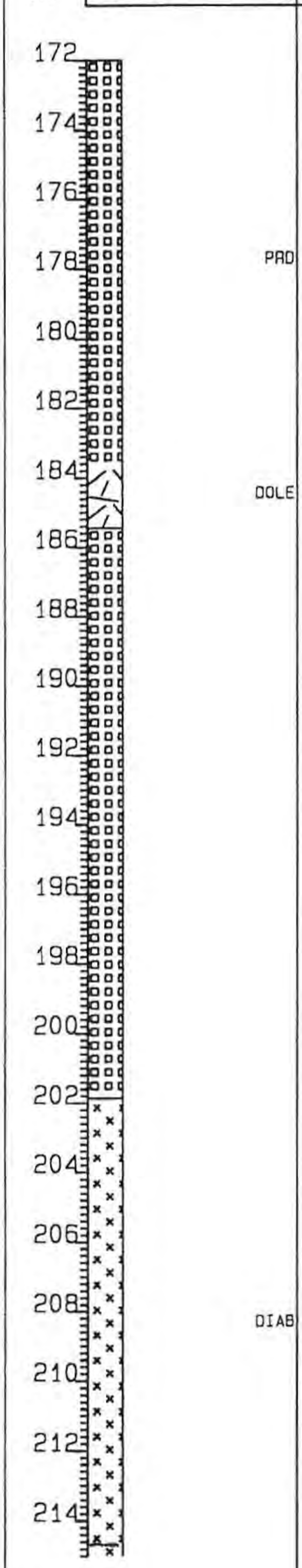

DESCRIPTION (core depths)	APP DIP deg
(PERIDOTITE continued) Uitkomst Suite	83
DOLERITE 183.71 -185.47 Uitkomst Suite STRUCTURE: Veined. ALTERATION: QUARTZ CARBONATE VEIN. GRAIN SIZE: Medium grained. COMMENTS: SILL/DYKE ? chilled margin towards the bottom.	45
DIABASE 201.88 -217.59 Uitkomst Suite GRAIN SIZE: Medium grained. COMMENTS: Chilled margin SILL.	60

BOREHOLE **SH26**   215.00 to 258.00 m   Plotted 15-12-1994   Page 6

Logged by RELOGGED   Scale 1: 200

CORE DEPTH (m)	VERT. PROFILE TOT.SULPH %	UNIT C	DESCRIPTION (core depths)	APP DIP deg

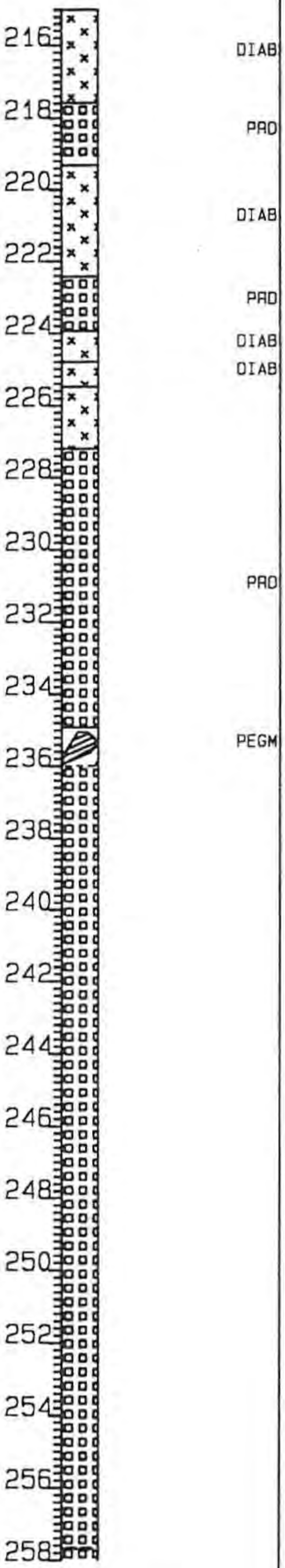

(DIABASE continued)   Uitkomst Suite   60

PERIDOTITE 217.59 -219.33   Uitkomst Suite   83
ALTERATION: Serpentinised. GRAIN SIZE: Medium grained.

DIABASE 219.33 -222.43   Uitkomst Suite   60
STRUCTURE: Veined. ALTERATION: QUARTZ CARBONATE VEIN. GRAIN SIZE: Medium grained.
COMMENTS: Chilled margin towards the bottom SILL.

PERIDOTITE 222.43 -223.95   Uitkomst Suite   83
ALTERATION: Serpentinised. GRAIN SIZE: Medium grained.

DIABASE 223.95 -227.22   Uitkomst Suite   70
GRAIN SIZE: Medium grained. COMMENTS: Chilled margin SILL.

DIABASE 224.81 -225.50   Uitkomst Suite   62
GRAIN SIZE: Fine grained.

PERIDOTITE 227.22 -325.96   Uitkomst Suite   83
GRAIN SIZE: Medium grained. COMMENTS: Pyroxene oikocrysts poikilitically enclosing olivine.

PEGMATITE 234.94 -236.00   Uitkomst Suite   83
GRAIN SIZE: Pegmatitic. COMMENTS: Comprising plagioclase and pyroxene.

BOREHOLE ***SH26*** 258.00 to 301.00 m Plotted 15-12-1994 Page 7

Logged by RELOGGED Scale 1: 200

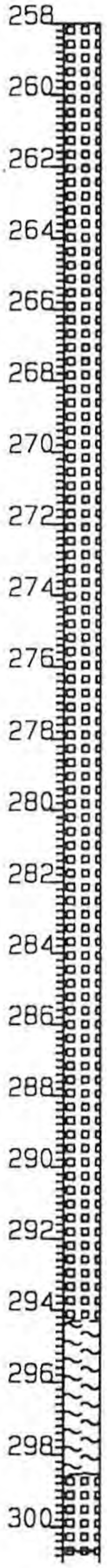

CORE DEPTH (m)	VERT. PROFILE TOT.SULPH %	UNIT C	DESCRIPTION (core depths)	APP DIP deg
		PRD	(PERIDOTITE continued) Uitkomst Suite	83
		TS	SCHIST 294.30 -298.55 Uitkomst Suite STRUCTURE: Sheared. ALTERATION: Talc-alteration. GRAIN SIZE: Fine grained.	21

Logged by RELOGGED

Scale 1: 200

CORE DEPTH (m) | VERT. PROFILE TOT.SULPH % | UNIT C

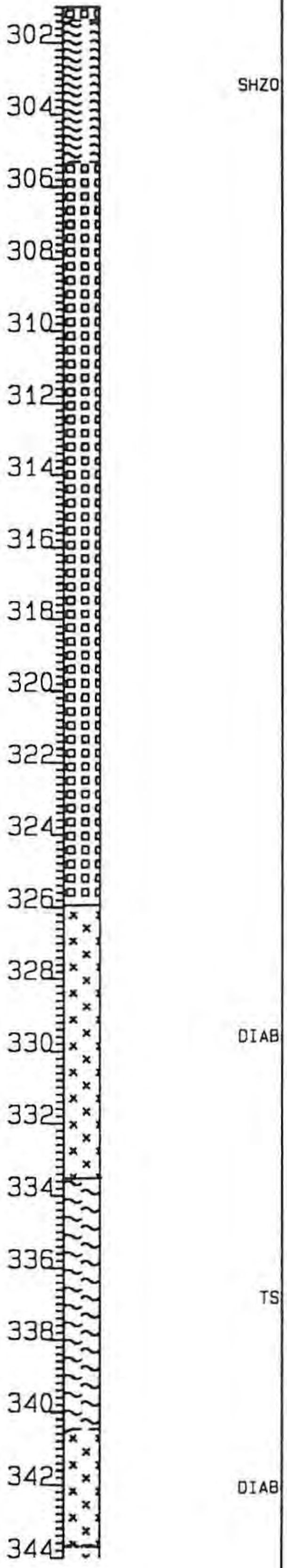

DESCRIPTION (core depths)	APP DIP deg
(PERIDOTITE continued) Uitkomst Suite	83
SHEAR ZONE 301.38 -305.31 Uitkomst Suite STRUCTURE: Sheared. ALTERATION: Talc-alteration. GRAIN SIZE: Fine grained.	75
DIABASE 325.96 -333.54 Uitkomst Suite GRAIN SIZE: Medium grained. COMMENTS: Chilled margin.	83
SCHIST 333.54 -340.46 Uitkomst Suite STRUCTURE: Sheared. ALTERATION: Talc-alteration. GRAIN SIZE: Fine grained.	40
DIABASE 340.46 -355.48 Uitkomst Suite ALTERATION: Chloritisation. GRAIN SIZE: Medium grained. COMMENTS: QUARTZ CARBONATE VEIN SILL.	63

BOREHOLE ***SH26*** 344.00 to 387.00 m Plotted 15-12-1994

Logged by RELOGGED Scale 1: 200

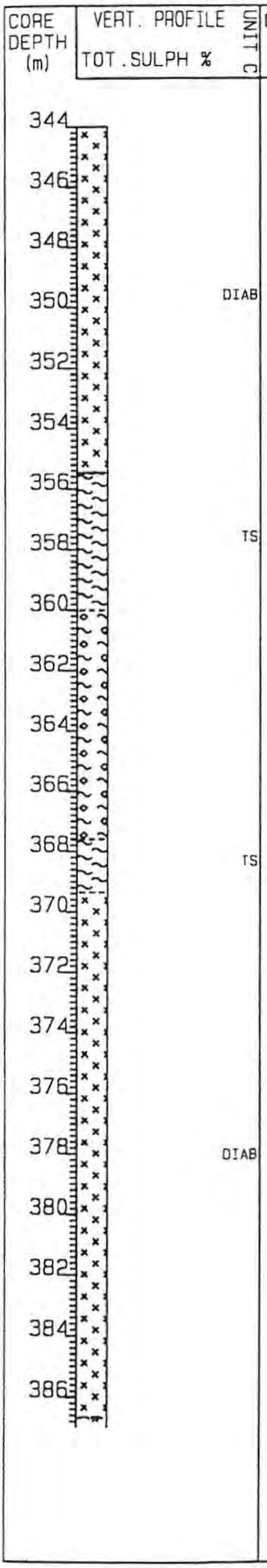

DESCRIPTION (core depths)	APP DIP deg
(DIABASE continued) Uitkomst Suite	63
CHROMITITIC PYROXENITE 355.48 -369.36 Uitkomst Suite STRUCTURE: Sheared layered. ALTERATION: Talc-alteration. GRAIN SIZE: Fine grained. Cr %: 10-25. MIN.TEXT: Crm massive to disseminated.	83
SCHIST 355.49 -360.00 Uitkomst Suite STRUCTURE: Sheared. ALTERATION: Talc-alteration. GRAIN SIZE: Fine grained.	33
SCHIST 367.60 -369.36 Uitkomst Suite STRUCTURE: Sheared. ALTERATION: Talc-alteration. GRAIN SIZE: Fine grained.	47
DIABASE 369.36 -389.64 Uitkomst Suite GRAIN SIZE: Medium grained. COMMENTS: Chilled margin SILL.	83

BOREHOLE SH26 387.00 to 430.00 m Plotted 15-12-1994

Logged by RELOGGED

Scale 1: 200

CORE DEPTH (m)	VERT. PROFILE TOT.SULPH %	UNIT C	DESCRIPTION (core depths)	APP DIP deg

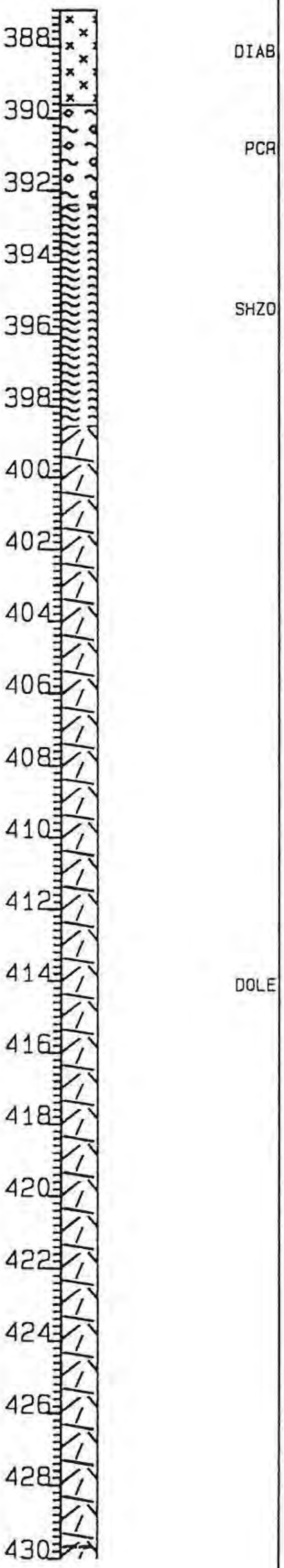

(DIABASE continued) Uitkomst Suite 83

CHROMITITIC PYROXENITE 389.64 -398.57 Uitkomst Suite 83

STRUCTURE: Sheared. ALTERATION: Talc-alteration. GRAIN SIZE: Fine grained. Cr %: 10-25.
MIN.TEXT: Crm semi-massive towards the bottom.

SHEAR ZONE 392.40 -398.57 Uitkomst Suite 11

STRUCTURE: Sheared. ALTERATION: Talc-alteration. GRAIN SIZE: Fine grained.

DOLERITE 398.57 -433.00 Uitkomst Suite 68

GRAIN SIZE: Medium grained. COMMENTS: DYKE?

Logged by RELOGGED

Scale 1: 200

CORE DEPTH (m)	VERT. PROFILE TOT. SULPH %	UNIT C	DESCRIPTION (core depths)	APP DIP deg

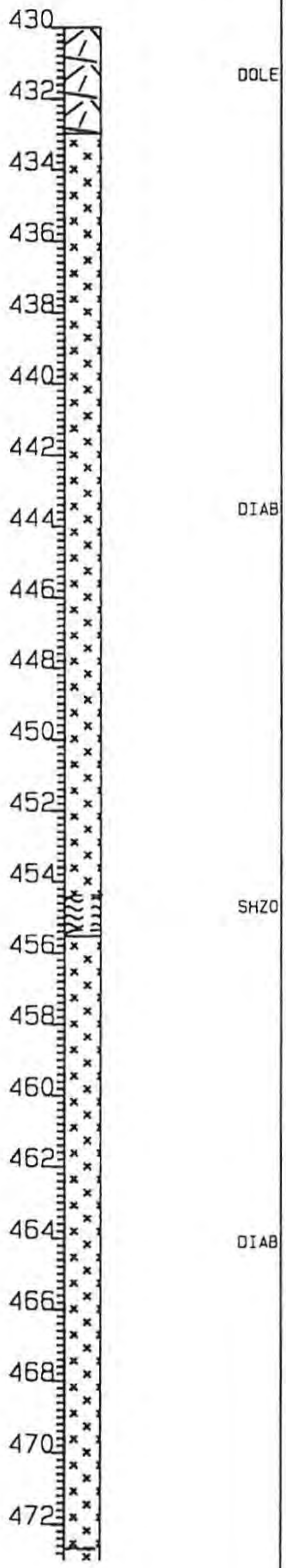

(DOLERITE continued) Uitkomst Suite 68

DIABASE 433.00 -455.55 Uitkomst Suite 68
STRUCTURE: Q.c.v. Veined. GRAIN SIZE: Medium grained. COMMENTS: Chilled margin.

SHEAR ZONE 454.39 -455.36 Uitkomst Suite 56
STRUCTURE: Sheared. ALTERATION: Talc-alteration. GRAIN SIZE: Fine grained.

DIABASE 455.55 -475.19 Uitkomst Suite 68
STRUCTURE: Q.c.v. Veined. GRAIN SIZE: Medium grained. COMMENTS: Chilled margin SILL.

BOREHOLE SH26 473.00 to 516.00 m Plotted 15-12-1994

Logged by RELOGGED Scale 1: 200

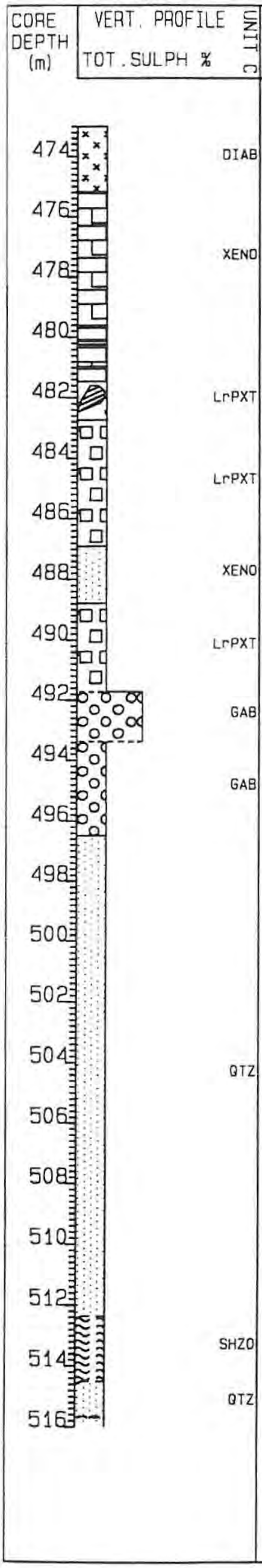

DESCRIPTION (core depths)		APP DIP deg
(DIABASE continued)	Uitkomst Suite	68
DOLOMITE 475.19 -481.48 GRAIN SIZE: Fine sand. COLOUR: Yellowish grey to grey.	Uitkomst Suite	90
PEGMATITE 479.62 -479.65 GRAIN SIZE: Pegmatitic.	Uitkomst Suite	83
PEGMATITE 480.10 -480.15 GRAIN SIZE: Pegmatitic.	Uitkomst Suite	50
PEGMATITE 480.25 -480.29 GRAIN SIZE: Pegmatitic.	Uitkomst Suite	83
PEGMATITE 480.97 -481.00 GRAIN SIZE: Pegmatitic.	Uitkomst Suite	83
PEGMATITE 481.48 -482.76 GRAIN SIZE: Pegmatitic. COMMENTS: Comprising feldspar amphibole.	Uitkomst Suite	83
PYROXENITE 482.76 -486.92 ALTERATION: Slightly altered. GRAIN SIZE: Medium grained. Py %: <1. MIN.TEXT: Py blebby. SULPH.MINS.: Py.	Uitkomst Suite	68
QUARTZITE 486.92 -488.80 GRAIN SIZE: Medium sand. COMMENTS: With PEGMATITE bands.	Uitkomst Suite	90
PYROXENITE 488.80 -491.73 GRAIN SIZE: Medium grained. COMMENTS: Biotite.	Uitkomst Suite	90
GABBRO 491.73 -493.38 GRAIN SIZE: Medium grained. COMMENTS: Comprising feldspar and amphibole. TOT.SULPH %: 5-10. MIN.TEXT: Po disseminated. SULPH.MINS.: Po.	Uitkomst Suite	90
GABBRO 493.38 -496.51 GRAIN SIZE: Coarse grained.	Uitkomst Suite	90
QUARTZITE 496.51 -512.36 ALTERATION: Slightly altered. GRAIN SIZE: Fine sand. COLOUR: Greenish grey.	Malmani Subgroup	76
SHEAR ZONE 512.36 -514.50 STRUCTURE: Sheared. ALTERATION: Talc-alteration. GRAIN SIZE: Fine grained. MIN.TEXT: Mt disseminated towards the top. BASAL SHZO.	Malmani Subgroup	66
QUARTZITE 514.50 -516.22 GRAIN SIZE: Medium sand. COMMENTS: With amphibole.	Black Reef Quartzite	67

BOREHOLE ***SH26*** 516.00 to 520.54 m Plotted 15-12-1994 Page 13

Logged by RELOGGED Scale 1: 200

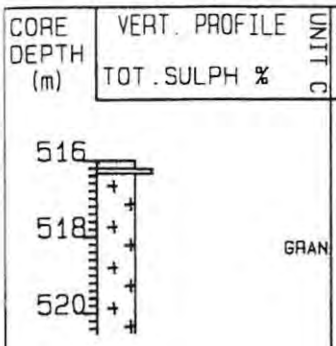

DESCRIPTION (core depths)		APP DIP deg
(QUARTZITE continued)	Black Reef Quartzite	67
PYROXENITE 516.22 -516.36 GRAIN SIZE: Medium grained. TOT.SULPH %: 1-5. MIN.TEXT: Po disseminated. SULPH.MINS.: Po.	Black Reef Quartzite	68
GRANITE 516.36 -520.54 GRAIN SIZE: Coarse grained.	Nelshoogte Granite	83

GEOLOGICAL LOG

SH27

PROJECT	*SLAAIHOEK*
EXPLORATION COMPANY	*ANGLOVAAL*
FARM	*SLAAIHOEK 540 JT*
DRILLING COMMENCED	*Phase One*
DRILLING COMPLETED	
LOGGED BY	*Relogged 2*
DRILLED BY	

INCLINATION:	*-90*
BEARING:	*0*
X CONSTANT:	*2800000*
X COLLAR COORD.:	*45058.82*
Y COLLAR COORD.:	*40899.43*
ELEVATION (A.M.S.L.) IN METERS:	*1481.04*
FINAL DEPTH (m):	*602.55*
No WEDGES:	*0*

BOREHOLE **SH27** 0.00 to 43.00 m Plotted 15-02-1995 Page 1

Logged by Relogged 2

Scale 1: 200

CORE DEPTH (m)	VERT. PROFILE TOT.SULPH %	UNIT C	DESCRIPTION (core depths)	APP DIP deg
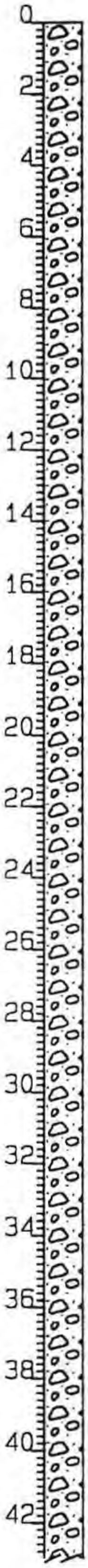		OVB	OVERBURDEN 0.00 -43.00 Uitkomst Suite GRAIN SIZE: Pebble.	

Logged by Relogged 2

Scale 1: 200

CORE DEPTH (m) | VERT. PROFILE TOT.SULPH %

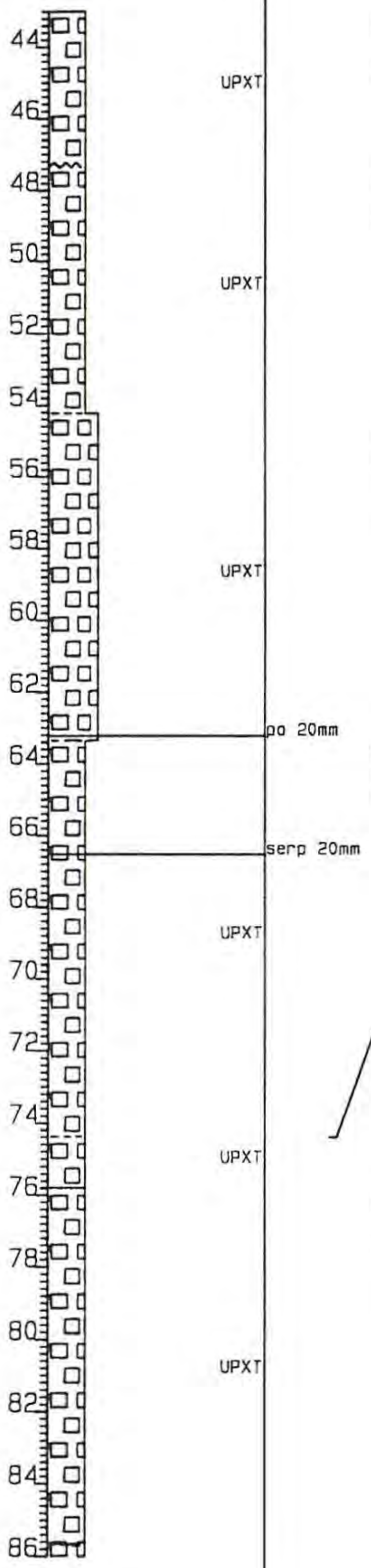

UNIT C	DESCRIPTION (core depths)	APP DIP deg
UPXT	PYROXENITE 43.00 -47.30 Uitkomst Suite ALTERATION: Highly weathered. GRAIN SIZE: Coarse grained. COLOUR: Greyish green to brown.	
UPXT	PYROXENITE 47.30 -54.23 Uitkomst Suite GRAIN SIZE: Medium grained. COLOUR: Brownish grey. MAGNETISM: Non-susceptable. SCRATCH: Hard.	75
UPXT	PYROXENITE 54.23 -63.35 Uitkomst Suite GRAIN SIZE: Medium grained. COLOUR: Greyish green. MAGNETISM: Non-susceptable. TOT.SULPH %: 1-5. MIN.TEXT: Disseminated. SCRATCH: Hard. SULPH.MINS.: Po.	75
	po 20mm	
	serp 20mm	
UPXT	PYROXENITE 63.35 -74.38 Uitkomst Suite GRAIN SIZE: Medium grained. COLOUR: Greyish green. MAGNETISM: Non-susceptable. SCRATCH: Hard.	75
UPXT	PYROXENITE 74.38 -75.81 Uitkomst Suite ALTERATION: Serpentinised. GRAIN SIZE: Medium grained. COLOUR: Greyish green. MAGNETISM: Non-susceptable. COMMENTS: Feldspar. SCRATCH: Hard.	75
UPXT	PYROXENITE 75.81 -96.98 Uitkomst Suite GRAIN SIZE: Medium grained. COLOUR: Greyish green. MAGNETISM: Non-susceptable. TOT.SULPH %: <1. MIN.TEXT: Disseminated. SCRATCH: Hard. SULPH.MINS.: Po cp.	75

BOREHOLE **SH27** 86.00 to 129.00 m Plotted 15-02-1995 Page 3

Logged by Relogged 2 Scale 1: 200

CORE DEPTH (m)	VERT. PROFILE TOT.SULPH %	UNIT C	DESCRIPTION (core depths)	APP DIP deg

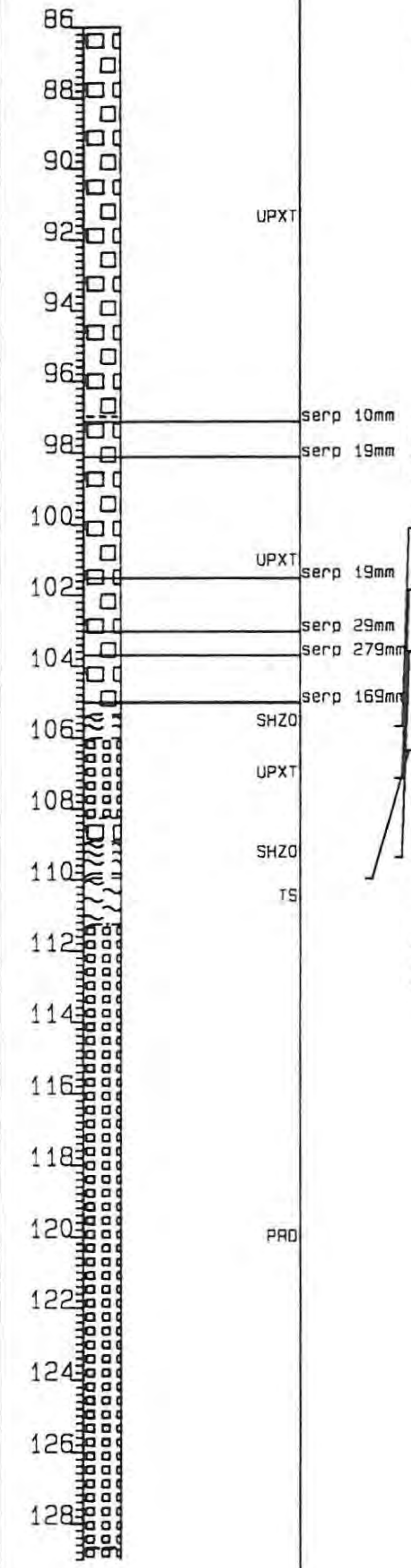

(PYROXENITE continued) Uitkomst Suite 75

PYROXENITE 96.98 -109.95 Uitkomst Suite 75
ALTERATION: Serpentinised. GRAIN SIZE: Medium grained. COLOUR: Greyish green to dark green. MAGNETISM: Non-susceptable. SCRATCH: Hard.

SHEAR ZONE 105.34 -106.00 Uitkomst Suite 60
STRUCTURE: Veined q.c.v. ALTERATION: Talc-alteration. GRAIN SIZE: Fine grained. COLOUR: Light grey. MAGNETISM: Non-susceptable. SCRATCH: Medium.

PERIDOTITE 106.00 -108.26 Uitkomst Suite 75
ALTERATION: Talc-alteration. GRAIN SIZE: Fine grained. COLOUR: Greyish green to light green. MAGNETISM: Non-susceptable. SCRATCH: Medium.

SHEAR ZONE 108.90 -109.82 Uitkomst Suite 55
ALTERATION: Talc-alteration. GRAIN SIZE: Fine grained. COLOUR: Light grey. MAGNETISM: Non-susceptable. SCRATCH: Medium.

SCHIST 109.95 -111.24 Uitkomst Suite 60
STRUCTURE: Sheared. ALTERATION: Serpentinised talc-alteration. GRAIN SIZE: Fine grained. COLOUR: Grey. MAGNETISM: Non-susceptable. SCRATCH: Soft.

PERIDOTITE 111.24 -288.20 Uitkomst Suite 75
ALTERATION: Serpentinised. GRAIN SIZE: Medium grained. COLOUR: Greyish green to dark green. MAGNETISM: Susceptable. Cr %: <1. MIN.TEXT: Stringers. SCRATCH: Hard.

BOREHOLE ***SH27*** 129.00 to 172.00 m Plotted 15-02-1995 Page 4

Logged by Relogged 2

Scale 1: 200

CORE DEPTH (m)	VERT. PROFILE TOT.SULPH %	UNIT C	DESCRIPTION (core depths)	APP DIP deg
			(PERIDOTITE continued) Uitkomst Suite	75
			crm 50mm	
		PRD		

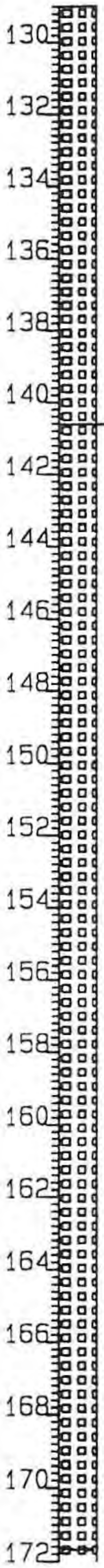

BOREHOLE **SH27** 172.00 to 215.00 m Plotted 15-02-1995

Logged by Relogged 2 Scale 1: 200

CORE DEPTH (m)	VERT. PROFILE TOT.SULPH %	UNIT C	DESCRIPTION (core depths)	APP DIP deg

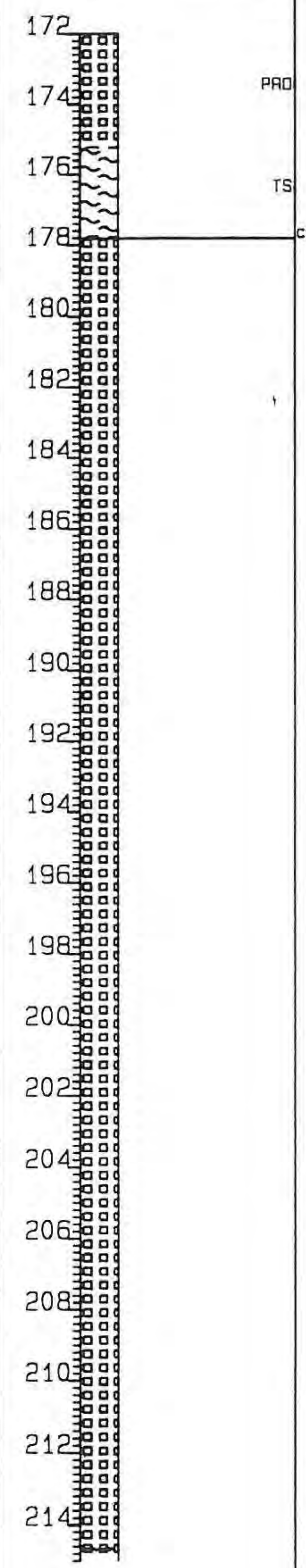

(PERIDOTITE continued) Uitkomst Suite 75

SCHIST 175.23 -177.76 Uitkomst Suite 55

ALTERATION: Talc-alteration. GRAIN SIZE: Fine grained. COLOUR: Grey.
MAGNETISM: Non-susceptable. SCRATCH: Medium.

BOREHOLE SMZ1 215.00 to 258.00 m Plotted 15-02-1995 Page 6

Logged by Relogged 2 Scale 1: 200

CORE DEPTH (m) | VERT. PROFILE TOT.SULPH % | UNIT C | DESCRIPTION (core depths) | APP DIP deg

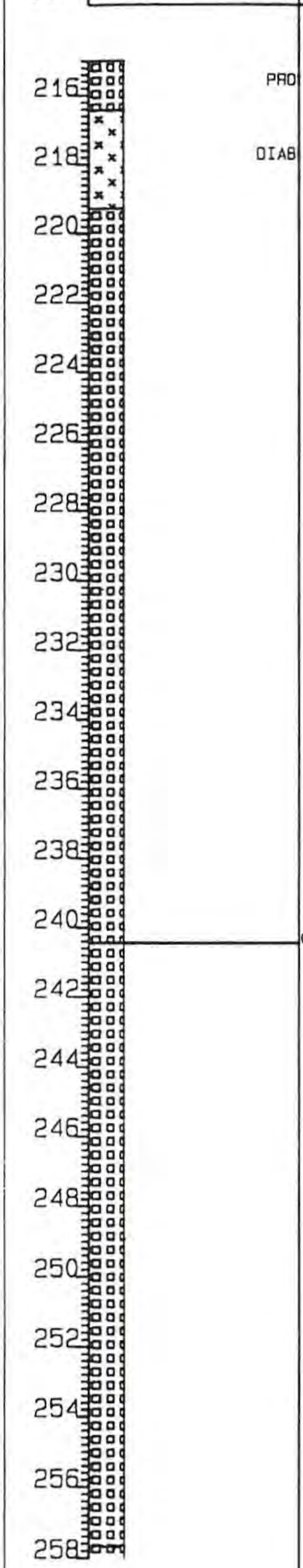

(PERIDOTITE continued) Uitkomst Suite 75

DIABASE 216.45 -219.30 75

STRUCTURE: Veined q.c.v. ALTERATION: Chloritisation. GRAIN SIZE: Medium grained. COLOUR: Greyish green. MAGNETISM: Non-susceptable. COMMENTS: Chilled margin, sill. SCRATCH: Hard.

crm 50mm

BOREHOLE SH21 258.00 to 301.00 m Plotted 15-02-1995

Logged by Relogged 2

Scale 1: 200

CORE DEPTH (m)	VERT. PROFILE TOT.SULPH %	UNIT C	DESCRIPTION (core depths)	APP DIP deg

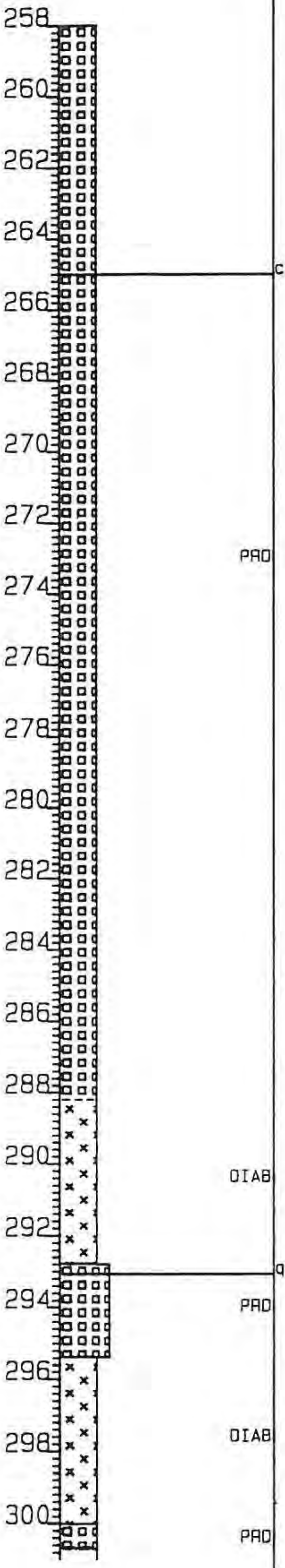

(PERIDOTITE continued) Uitkomst Suite 75

crm 50mm

DIABASE 288.20 -292.80 75
GRAIN SIZE: Medium grained. COLOUR: Greyish green. MAGNETISM: Non-susceptable.
COMMENTS: Chilled margin, sill. SCRATCH: Hard.

PERIDOTITE 292.80 -295.40 Uitkomst Suite 75
GRAIN SIZE: Medium grained. COLOUR: Greyish green to dark green. MAGNETISM: Susceptable.
COMMENTS: Poikilitic texture. TOT.SULPH %: 1-5. MIN.TEXT: Disseminated. SCRATCH: Hard.
SULPH.MINS.: Po.

q.c.v. 250mm

DIABASE 295.40 -300.03 75
GRAIN SIZE: Medium grained. COLOUR: Greyish green. MAGNETISM: Non-susceptable.
COMMENTS: Chilled margins, sill. SCRATCH: Hard.

PERIDOTITE 300.03 -312.53 Uitkomst Suite 75
GRAIN SIZE: Medium grained. COLOUR: Greenish grey. MAGNETISM: Non-susceptable.
COMMENTS: Poikilitic texture. SCRATCH: Hard.

Logged by Relogged 2

Scale 1: 200

CORE DEPTH (m) | VERT. PROFILE TOT.SULPH % | UNIT C | DESCRIPTION (core depths) | APP DIP deg

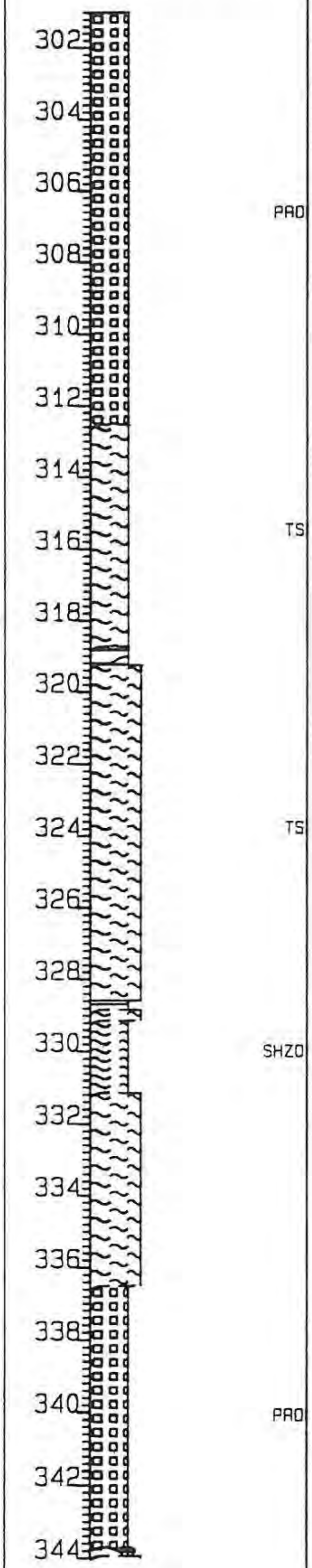

(PERIDOTITE continued) Uitkomst Suite 75

SCHIST 312.53 -318.73 Uitkomst Suite 70
ALTERATION: Talc-alteration. GRAIN SIZE: Medium grained. COLOUR: Grey.
MAGNETISM: Non-susceptable. Cr %: <1. Py %: <1. TOT.SULPH %: <1. MIN.TEXT: Disseminated.
SCRATCH: Medium. SULPH.MINS.: Po py.

MASSIVE CHROMITITE 318.73 -319.25 Uitkomst Suite 70
STRUCTURE: Veined. GRAIN SIZE: Fine grained. COLOUR: Black. MAGNETISM: Non-susceptable.
Cr %: >50. MIN.TEXT: Massive. SCRATCH: Medium.

SCHIST 319.25 -336.50 Uitkomst Suite 70
ALTERATION: Talc-alteration. GRAIN SIZE: Medium grained. COLOUR: Grey.
MAGNETISM: Non-susceptable. Cr %: 1-5. TOT.SULPH %: 1-5. MIN.TEXT: Disseminated.
SCRATCH: Soft. SULPH.MINS.: Po.

MASSIVE CHROMITITE 328.60 -328.84 Uitkomst Suite 70
ALTERATION: Talc-alteration. GRAIN SIZE: Fine grained. COLOUR: Black.
MAGNETISM: Non-susceptable. Cr %: >50. MIN.TEXT: Massive. SCRATCH: Medium.

SHEAR ZONE 329.14 -331.14 Uitkomst Suite 50
STRUCTURE: Veined. ALTERATION: Talc-alteration. GRAIN SIZE: Fine grained.
COLOUR: Grey and white. MAGNETISM: Non-susceptable. SCRATCH: Soft.

PERIDOTITE 336.50 -343.93 Uitkomst Suite 75
GRAIN SIZE: Fine grained. COLOUR: Dark green. MAGNETISM: Susceptable. SCRATCH: Hard.

SCHIST 343.93 -352.18 Uitkomst Suite 75
ALTERATION: Talc-alteration. GRAIN SIZE: Medium grained. COLOUR: Grey.
MAGNETISM: Non-susceptable. TOT.SULPH %: 1-5. MIN.TEXT: Disseminated. SCRATCH: Soft.
SULPH.MINS.: Cp.

Logged by Relogged 2 Scale 1: 200

CORE DEPTH (m) | VERT. PROFILE TOT.SULPH % | UNIT C

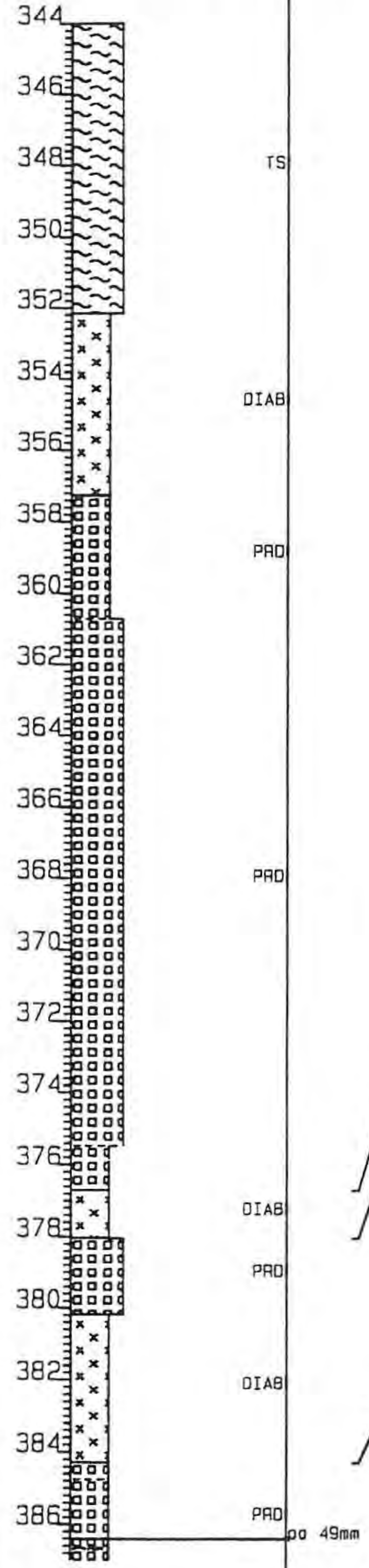

DESCRIPTION (core depths)	APP DIP deg
(SCHIST continued) Uitkomst Suite	75
DIABASE 352.18 -357.27 GRAIN SIZE: Medium grained. COLOUR: Greyish green. MAGNETISM: Non-susceptable. COMMENTS: Chilled margin, multiple intrusion, sill. SCRATCH: Hard.	75
PERIDOTITE 357.27 -376.72 Uitkomst Suite ALTERATION: Talc alteration. GRAIN SIZE: Medium grained. COLOUR: Greyish green. MAGNETISM: Non-susceptable. SCRATCH: Medium.	75
PERIDOTITE 360.72 -375.47 Uitkomst Suite ALTERATION: Serpentinised. GRAIN SIZE: Medium grained. COLOUR: Dark green. MAGNETISM: Susceptable. TOT.SULPH %: 1-5. MIN.TEXT: Disseminated. SCRATCH: Hard. SULPH.MINS.: Po.	75
DIABASE 376.72 -378.05 Uitkomst Suite STRUCTURE: Veined q.c.v.ALTERATION: Chloritisation. GRAIN SIZE: Medium grained. COLOUR: Grey. MAGNETISM: Non-susceptable. COMMENTS: Dyke (?). SCRATCH: Hard.	50
PERIDOTITE 378.05 -380.20 Uitkomst Suite ALTERATION: Serpentinised. GRAIN SIZE: Medium grained. COLOUR: Dark green. MAGNETISM: Susceptable. TOT.SULPH %: 1-5. MIN.TEXT: Disseminated. SCRATCH: Hard. SULPH.MINS.: Po.	75
DIABASE 380.20 -384.30 Uitkomst Suite GRAIN SIZE: Medium grained. COLOUR: Greyish green. MAGNETISM: Non-susceptable. COMMENTS: Chilled margins, sill. SCRATCH: Hard.	78
PERIDOTITE 384.30 -384.76 Uitkomst Suite GRAIN SIZE: Medium grained. COLOUR: Dark grey. MAGNETISM: Susceptable. TOT.SULPH %: <1. MIN.TEXT: Disseminated to blebby. SCRATCH: Hard. SULPH.MINS.: Po.	75
PERIDOTITE 384.76 -391.00 Uitkomst Suite ALTERATION: Talc-alteration. GRAIN SIZE: Medium grained. COLOUR: Dark grey. MAGNETISM: Susceptable. SCRATCH: Hard.	75

BOREHOLE SK27 387.00 to 430.00 m Plotted 15-02-1995

Logged by Relogged 2 Scale 1: 200

CORE DEPTH (m)	VERT. PROFILE TOT.SULPH %	UNIT C	DESCRIPTION (core depths)	APP DIP deg

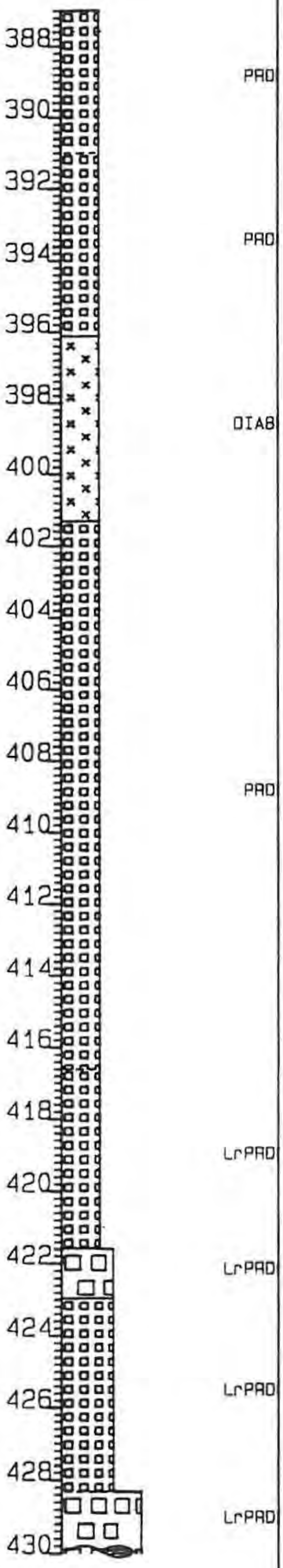

(PERIDOTITE continued) Uitkomst Suite 75

PERIDOTITE 391.00 -396.14 Uitkomst Suite 80
GRAIN SIZE: Medium grained. COLOUR: Dark grey. MAGNETISM: Susceptable. Cr %: 5-10. MIN.TEXT: Stringers. SCRATCH: Hard.

DIABASE 396.14 -401.33 45
STRUCTURE: Veined q.c.v. ALTERATION: Chloritisation. GRAIN SIZE: Medium grained. COLOUR: Grey and white. MAGNETISM: Non-susceptable. COMMENTS: Chilled margins, sill (?). SCRATCH: Hard.

PERIDOTITE 401.33 -416.61 Uitkomst Suite 75
ALTERATION: Serpentinised. GRAIN SIZE: Medium grained. COLOUR: Greyish green to dark green. MAGNETISM: Susceptable. Cr %: <1. TOT.SULPH %: <1. MIN.TEXT: Disseminated. SCRATCH: Hard. SULPH.MINS.: Po.

PERIDOTITE 416.61 -421.59 Uitkomst Suite 75
ALTERATION: Serpentinised. GRAIN SIZE: Coarse grained. COLOUR: Dark grey. MAGNETISM: Susceptable. Cr %: 1-5. TOT.SULPH %: <1. MIN.TEXT: Disseminated. SCRATCH: Hard. SULPH.MINS.: Po.

PYROXENITE 421.59 -422.98 Uitkomst Suite 75
GRAIN SIZE: Coarse grained. COLOUR: Greenish grey. MAGNETISM: Non-susceptable. Py %: <1. TOT.SULPH %: 1-5. MIN.TEXT: Clusters. SCRATCH: Hard. SULPH.MINS.: Po cp.

PERIDOTITE 422.98 -428.31 Uitkomst Suite 75
ALTERATION: Serpentinised. GRAIN SIZE: Medium grained. COLOUR: Dark green. MAGNETISM: Susceptable. Cr %: 1-5. TOT.SULPH %: 1-5. SCRATCH: Hard. SULPH.MINS.: Po cp.

PYROXENITE 428.31 -430.37 Uitkomst Suite 75
GRAIN SIZE: Medium grained. COLOUR: Grey. MAGNETISM: Non-susceptable. Cr %: 5-10. TOT.SULPH %: 5-10. MIN.TEXT: Stringer and clusters. SCRATCH: Hard. SULPH.MINS.: Po.

BOREHOLE SMZ1 430.00 to 473.00 m Plotted 15-02-1995 Page 11

Logged by Relogged 2 Scale 1: 200

CORE DEPTH (m)	VERT. PROFILE TOT.SULPH %	UNIT C	DESCRIPTION (core depths)	APP DIP deg

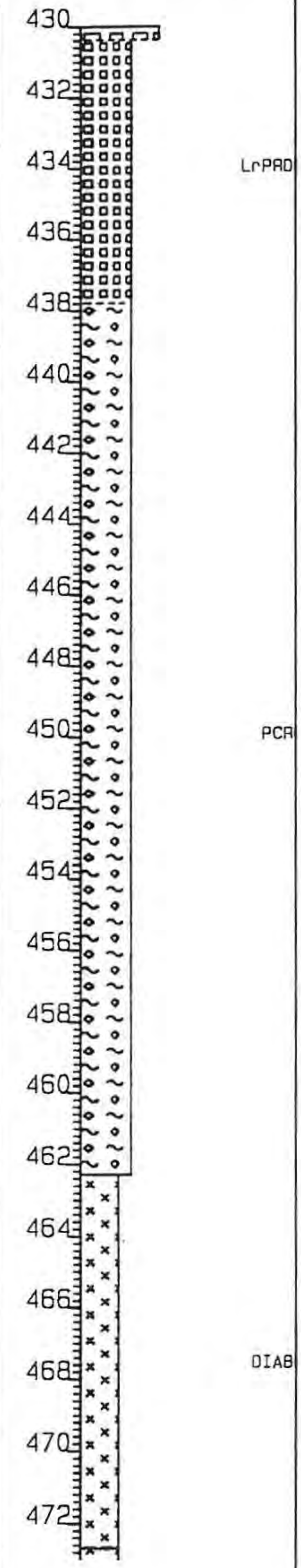

(PYROXENITE continued) Uitkomst Suite 75

PERIDOTITE 430.37 -437.78 Uitkomst Suite 75

ALTERATION: Talc-alteration. GRAIN SIZE: Medium grained. COLOUR: Greyish green to dark green. MAGNETISM: Non-susceptable. Cr %: 1-5. TOT.SULPH %: 1-5. MIN.TEXT: Stringers and clusters. SCRATCH: Hard. SULPH.MINS.: Po.

CHROMITITIC PYROXENITE 437.78 -492.44 Uitkomst Suite 75

GRAIN SIZE: Medium grained. COLOUR: Grey and black. MAGNETISM: Non-susceptable. Cr %: 1-5. TOT.SULPH %: 1-5. MIN.TEXT: Stringers and clusters. SCRATCH: Medium. SULPH.MINS.: Po cp.

DIABASE 462.30 -482.58 Uitkomst Suite 65

GRAIN SIZE: Medium grained. COLOUR: Greyish green. MAGNETISM: Non-susceptable. COMMENTS: Chilled margins, sill. SCRATCH: Hard.

BOREHOLE **SH27**   473.00 to 516.00 m   Plotted 15-02-1995   Page 12

Logged by Relogged 2   Scale 1: 200

CORE DEPTH (m)	VERT. PROFILE TOT.SULPH %	UNIT C	DESCRIPTION (core depths)	APP DIP deg

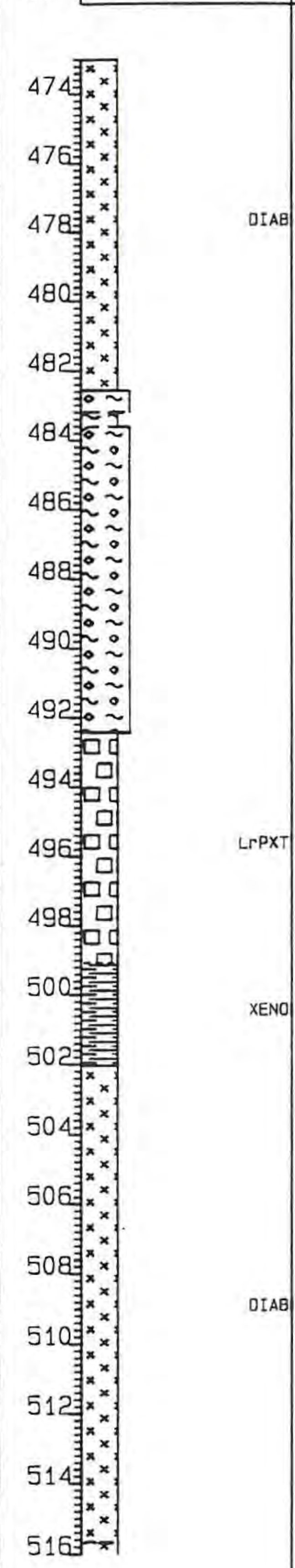

(CHROMITITIC PYROXENITE continued)

(DIABASE 462.3 - 482.58 continued)   Uitkomst Suite   65

SHEAR ZONE 483.19 -483.61   Uitkomst Suite   80

STRUCTURE: Veined. ALTERATION: Talc alteration. GRAIN SIZE: Fine grained. COLOUR: Black and white. MAGNETISM: Non-susceptable. Cr %: 10-25. MIN.TEXT: Semi-massive. SCRATCH: Medium.

PYROXENITE 492.44 -499.07   Uitkomst Suite   78

GRAIN SIZE: Medium grained. COLOUR: Light green. MAGNETISM: Non-susceptable. SCRATCH: Hard.

SKARN 499.07 -502.05   Uitkomst Suite   78

STRUCTURE: Xenolith. GRAIN SIZE: Coarse grained. COLOUR: Grey. MAGNETISM: Non-susceptable. SCRATCH: Hard.

DIABASE 502.05 -526.63   Uitkomst Suite   80

STRUCTURE: Veined q.c.v.ALTERATION: Chloritisation. GRAIN SIZE: Medium grained. COLOUR: Greyish green. MAGNETISM: Non-susceptable. COMMENTS: Chilled margins, sill. SCRATCH: Hard.

Logged by Relogged 2

Scale 1: 200

CORE DEPTH (m) | VERT. PROFILE TOT.SULPH % | UNIT C

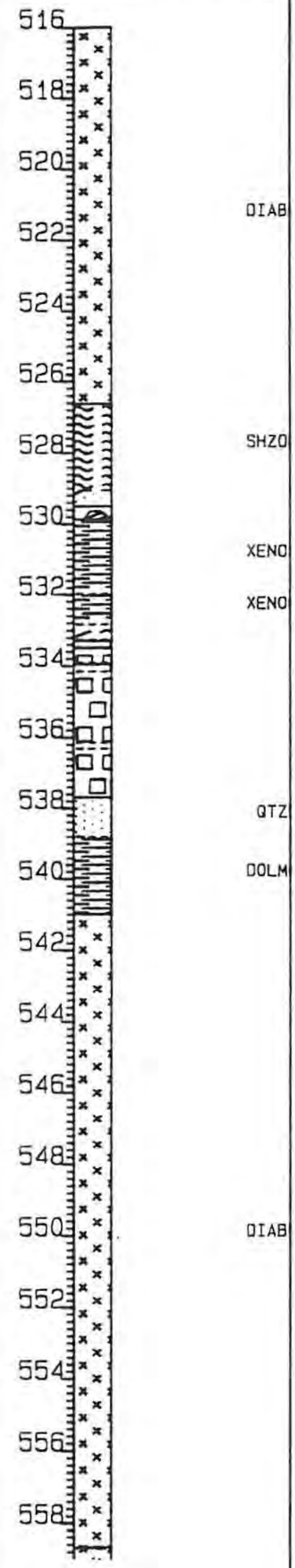

DESCRIPTION (core depths)	APP DIP deg
(DIABASE continued) Uitkomst Suite	80
SHEAR ZONE 526.63 -529.05 Uitkomst Suite STRUCTURE: Sheared. ALTERATION: Talc-alteration. GRAIN SIZE: Fine grained. COLOUR: Grey. MAGNETISM: Non-susceptable. SCRATCH: Medium.	60
QUARTZITE 529.05 -529.52 Uitkomst Suite STRUCTURE: Xenolith. GRAIN SIZE: Fine sand. COLOUR: Light grey. MAGNETISM: Non-susceptable. SCRATCH: Hard.	85
PEGMATITE 529.52 -529.88 Uitkomst Suite GRAIN SIZE: Medium grained. COLOUR: Grey. MAGNETISM: Non-susceptable. TOT.SULPH %: <1. MIN.TEXT: Disseminated. SCRATCH: Hard. SULPH.MINS.: Po.	80
SKARN 529.88 -531.97 Uitkomst Suite GRAIN SIZE: Fine grained. COLOUR: Grey. MAGNETISM: Non-susceptable. SCRATCH: Hard.	80
SKARN 531.97 -532.83 Uitkomst Suite STRUCTURE: Sheared xenolith. GRAIN SIZE: Medium grained. COLOUR: Grey. MAGNETISM: Non-susceptable. SCRATCH: Hard.	80
SERPENTINITE 532.83 -533.25 Uitkomst Suite GRAIN SIZE: Fine grained. COLOUR: Dark grey. MAGNETISM: Susceptable. SCRATCH: Medium.	80
DOLOMITE 533.25 -533.50 Uitkomst Suite GRAIN SIZE: Fine sand. COLOUR: Light grey. MAGNETISM: Non-susceptable. SCRATCH: Hard.	80
PYROXENITE 533.50 -537.70 Uitkomst Suite GRAIN SIZE: Medium grained. COLOUR: Greenish grey. MAGNETISM: Non-susceptable. SCRATCH: Hard.	80
DOLOMITE 533.90 -534.15 Uitkomst Suite GRAIN SIZE: Fine grained. COLOUR: Light grey. MAGNETISM: Non-susceptable. SCRATCH: Hard.	80
DOLOMITE 536.14 -536.30 Uitkomst Suite GRAIN SIZE: Fine grained. COLOUR: Light grey. MAGNETISM: Non-susceptable. SCRATCH: Hard.	80
QUARTZITE 537.70 -538.80 Malmani Subgroup GRAIN SIZE: Fine sand. COLOUR: Light grey. MAGNETISM: Non-susceptable. SCRATCH: Hard.	80
SKARN 538.80 -541.00 Malmani Subgroup GRAIN SIZE: Fine grained. COLOUR: Grey. MAGNETISM: Non-susceptable. ASBESTOS %: 1-5. SCRATCH: Hard.	80
DIABASE 541.00 -567.12 GRAIN SIZE: Medium grained. COLOUR: Grey and white. MAGNETISM: Non-susceptable. COMMENTS: Chilled margins, sill. SCRATCH: Hard.	80

Logged by Relogged 2 . Scale 1: 200

CORE DEPTH (m) | VERT. PROFILE TOT.SULPH % | UNIT | DESCRIPTION (core depths) | APP DIP deg

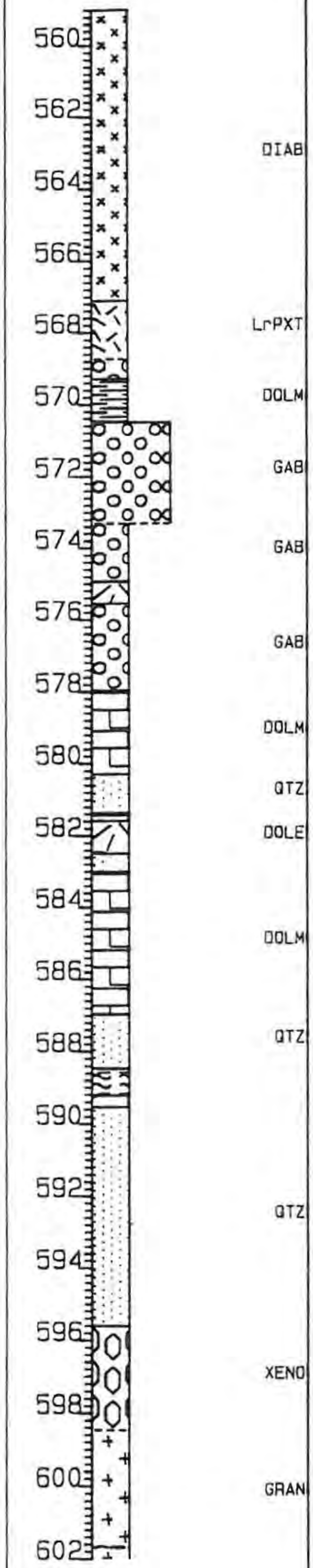

(DIABASE continued) 80

AMPHIBOLITE 567.12 -568.73 Uitkomst Suite 80
GRAIN SIZE: Medium grained. COLOUR: Dark green to greyish green. MAGNETISM: Non-susceptable. COMMENTS: Phlogopitic unit. TOT.SULPH %: <1. MIN.TEXT: Disseminated. SCRATCH: Hard. SULPH.MINS.: Po.

GABBRO 568.73 -569.30 Uitkomst Suite 80
GRAIN SIZE: Medium grained. COLOUR: Greenish grey. MAGNETISM: Non-susceptable. SCRATCH: Hard.

SKARN 569.30 -570.50 Malmani Subgroup 80
GRAIN SIZE: Medium grained. COLOUR: Yellowish grey. MAGNETISM: Non-susceptable. SCRATCH: Hard.

GABBRO 570.50 -573.30 Uitkomst Suite 80
GRAIN SIZE: Medium grained. COLOUR: Grey and white. MAGNETISM: Non-susceptable. TOT.SULPH %: 5-10. MIN.TEXT: Disseminated. SCRATCH: Hard. SULPH.MINS.: Po.

GABBRO 573.30 -574.95 Uitkomst Suite 80
GRAIN SIZE: Medium grained. COLOUR: Grey and white. MAGNETISM: Non-susceptable. SCRATCH: Hard.

DOLERITE 574.95 -575.57 75
GRAIN SIZE: Medium grained. COLOUR: Dark grey. MAGNETISM: Non-susceptable. COMMENTS: Sill. SCRATCH: Hard.

GABBRO 575.57 -577.98 Uitkomst Suite 78
GRAIN SIZE: Medium grained. COLOUR: Grey and white. MAGNETISM: Non-susceptable. COMMENTS: Chilled margin towards the bottom. SCRATCH: Hard.

DOLOMITE 577.98 -580.30 Malmani Subgroup 78
ALTERATION: Metamorphosed. GRAIN SIZE: Medium grained. COLOUR: Greyish green. MAGNETISM: Non-susceptable. SCRATCH: Hard.

QUARTZITE 580.30 -581.38 Malmani Subgroup 78
GRAIN SIZE: Medium sand. COLOUR: Light grey. MAGNETISM: Non-susceptable. SCRATCH: Hard.

DOLOMITE 581.38 -581.60 Malmani Subgroup 78
GRAIN SIZE: Aphanitic. COLOUR: Grey. MAGNETISM: Non-susceptable. SCRATCH: Hard.

DOLERITE 581.60 -582.51 75
ALTERATION: Metamorphosed. GRAIN-SIZE: Medium grained. COLOUR: Grey. MAGNETISM: Non-susceptable. COMMENTS: Sill. SCRATCH: Hard.

QUARTZITE 582.51 -583.01 Malmani Subgroup 75
GRAIN SIZE: Fine sand. COLOUR: Yellowish grey. MAGNETISM: Non-susceptable. SCRATCH: Hard.

DOLOMITE 583.01 -586.98 Malmani Subgroup 75
STRUCTURE: Laminated. ALTERATION: Silicified. GRAIN SIZE: Aphanitic. COLOUR: Light grey. MAGNETISM: Non-susceptable. SCRATCH: Hard.

QUARTZITE 586.98 -588.48 Malmani Subgroup 75
STRUCTURE: Brecciated. GRAIN SIZE: Fine sand. COLOUR: White. MAGNETISM: Non-susceptable. SCRATCH: Hard.

DOLOMITE 588.48 -589.55 Malmani Subgroup 70
ALTERATION: Talc-alteration. GRAIN SIZE: Aphanitic. COLOUR: White. MAGNETISM: Non-susceptable. SCRATCH: Hard.

SHEAR ZONE 588.58 -589.17 Malmani Subgroup 55
STRUCTURE: Veined. ALTERATION: Talc-alteration. GRAIN SIZE: Medium grained. COLOUR: Dark grey and white. MAGNETISM: Non-susceptable. COMMENTS: Basal shear. SCRATCH: Medium.

QUARTZITE 589.55 -595.62 Black Reef Quartzite 75
GRAIN SIZE: Medium sand. COLOUR: Light green. MAGNETISM: Non-susceptable.. SCRATCH: Hard.

HORNFELS 595.62 -598.46 Nelshoogte Granite
GRAIN SIZE: Coarse grained. COLOUR: Greyish brown. MAGNETISM: Non-susceptable. SCRATCH: Hard.

GRANITE 598.46 -602.55 Nelshoogte Granite
GRAIN SIZE: Coarse grained. COLOUR: Black and white. MAGNETISM: Non-susceptable. SCRATCH: Hard.

BOREHOLE SHZ1 602.00 to 602.55 m Plotted 15-02-1995 Page 15

Logged by Relogged 2 Scale 1: 200

CORE DEPTH (m)	VERT. PROFILE TOT.SULPH %	UNIT C	DESCRIPTION (core depths)		APP DIP deg
602	+		(GRANITE continued)	Nelshoogte Granite	

Appendix C

Electron Microprobe Analyses

Analysis #	153	154	155	156	158	159	160	161	162	163	164	165	166	167
Section	10-9	10-9	10-9	10-9	10-9	10-9	10-9	10-9	10-9	10-9	10-9	10-9	10-9	10-9
Depth	409.40	409.40	409.40	409.40	409.40	409.40	409.40	409.40	409.40	409.40	409.40	409.40	409.40	409.40
Label	*OPX 1C*	*OPX 1R*	*OPX 2C*	*OPX 2R*	*OPX 3C*	*OPX 4C*	*OPX 4R*	*OPX 5C*	*OPX 5R*	*OPX 6C*	*OPX 7C*	*OPX 7R*	*OPX 8C*	*OPX 8R*
SiO_2	51.09	50.12	49.96	49.87	53.90	50.21	50.21	49.94	49.91	52.41	53.31	53.12	49.74	49.38
TiO_2	0.39	0.35	0.27	0.27	0.14	0.31	0.30	0.21	0.25	0.15	0.28	0.25	0.23	0.32
Al_2O_3	2.31	1.26	0.85	0.72	0.55	1.70	1.28	0.65	0.57	0.61	1.88	1.86	0.63	0.75
FeO	25.79	29.01	30.21	30.15	16.39	28.74	28.73	29.61	29.73	21.35	18.34	18.98	30.29	31.49
Cr_2O_3	0.12	0.02	0.02	0.02	0.00	0.04	0.00	0.00	0.02	0.00	0.07	0.09	0.01	0.00
MnO	0.37	0.58	0.53	0.55	0.30	0.48	0.54	0.51	0.55	0.37	0.28	0.32	0.52	0.61
NiO	0.04	0.04	0.02	0.00	0.00	0.03	0.03	0.04	0.02	0.02	0.05	0.08	0.02	0.03
MgO	17.35	15.62	15.60	15.66	26.31	16.85	16.86	16.11	16.02	23.10	23.66	23.12	16.54	15.52
CaO	2.11	2.25	1.56	1.53	1.23	2.30	2.11	1.74	1.87	1.50	2.21	2.18	1.86	1.73
Na_2O	0.05	0.05	0.00	0.03	0.03	0.07	0.12	0.00	0.00	0.03	0.08	0.11	0.01	0.00
K_2O	0.01	0.00	0.01	0.01	0.02	0.00	0.03	0.00	0.00	0.01	0.01	0.00	0.00	0.00
Total	99.64	99.31	99.02	98.81	98.86	100.73	100.20	98.81	98.94	99.56	100.16	100.10	99.84	99.83
Cations based on 6 oxygens														
Si	1.9513	1.9585	1.9656	1.9667	1.9778	1.9304	1.9416	1.9657	1.9643	1.9606	1.9531	1.9539	1.9457	1.9438
Ti	0.0113	0.0102	0.0081	0.0081	0.0037	0.0091	0.0087	0.0061	0.0074	0.0041	0.0077	0.0070	0.0067	0.0094
Al	0.1038	0.0581	0.0393	0.0334	0.0236	0.0770	0.0582	0.0301	0.0265	0.0271	0.0813	0.0805	0.0291	0.0348
Fe^{2+}	0.8237	0.9478	0.9940	0.9941	0.5028	0.9239	0.9289	0.9746	0.9783	0.6679	0.5618	0.5836	0.9907	1.0365
Cr	0.0036	0.0008	0.0005	0.0008	0.0001	0.0012	0.0000	0.0000	0.0006	0.0000	0.0020	0.0027	0.0002	0.0000
Mn	0.0121	0.0193	0.0175	0.0185	0.0094	0.0158	0.0178	0.0171	0.0185	0.0117	0.0085	0.0098	0.0173	0.0204
Ni	0.0014	0.0011	0.0005	0.0000	0.0001	0.0010	0.0009	0.0012	0.0005	0.0007	0.0015	0.0022	0.0005	0.0008
Mg	0.9879	0.9099	0.9150	0.9207	1.4393	0.9659	0.9720	0.9453	0.9400	1.2882	1.2919	1.2676	0.9645	0.9107
Ca	0.0863	0.0942	0.0656	0.0645	0.0483	0.0946	0.0874	0.0732	0.0788	0.0601	0.0866	0.0860	0.0778	0.0729
Na	0.0040	0.0040	0.0000	0.0020	0.0020	0.0054	0.0089	0.0000	0.0000	0.0023	0.0059	0.0081	0.0011	0.0000
K	0.0007	0.0000	0.0006	0.0007	0.0009	0.0001	0.0015	0.0000	0.0000	0.0005	0.0005	0.0000	0.0000	0.0001
Mg#	0.55	0.49	0.48	0.48	0.74	0.51	0.51	0.49	0.49	0.66	0.70	0.68	0.49	0.47
En content	51.72	46.16	45.93	46.09	71.97	48.29	48.45	47.02	46.63	63.52	66.29	65.10	47.04	44.63
Fs content	43.76	49.06	50.78	50.68	25.61	46.98	47.19	49.33	49.45	33.51	29.26	30.48	49.16	51.79
Wo content	4.52	4.78	3.29	3.23	2.42	4.73	4.35	3.64	3.91	2.96	4.44	4.42	3.79	3.57

Table C-1 *Electron microprobe analyses of orthopyroxenes from borehole SH10.*

Analysis #	88	89	90	91	92	93	94	95	96	97	98	99	1	2
Section	**10-8**	**10-8**	**10-8**	**10-8**	**10-8**	**10-8**	**10-8**	**10-8**	**10-8**	**10-8**	**10-8**	**10-8**	**10-7**	**10-7**
Depth	408.60	408.60	408.60	408.60	408.60	408.60	408.60	408.60	408.60	408.60	408.60	408.60	407.20	407.20
Label	*OPX 1C*	*OPX 1R*	*OPX 2C*	*OPX 2R*	*OPX 3C*	*OPX 3R*	*OPX 4C*	*OPX 4R*	*OPX 5C*	*OPX 5R*	*OPX 6C*	*OPX 6R*	*OPX 1C*	*OPX 1R*
SiO_2	49.57	49.78	50.04	49.38	49.90	49.76	50.05	49.92	50.11	49.79	50.37	50.05	51.52	52.14
TiO_2	0.28	0.29	0.34	0.24	0.26	0.27	0.20	0.27	0.32	0.26	0.26	0.35	0.26	0.30
Al_2O_3	0.85	0.73	0.77	0.68	0.85	0.70	0.63	0.75	1.41	0.63	1.03	0.84	1.56	1.58
FeO	30.86	30.14	29.29	31.50	29.77	30.24	29.25	29.68	29.05	30.13	28.19	29.26	24.33	22.28
Cr_2O_3	0.00	0.01	0.04	0.06	0.03	0.00	0.00	0.00	0.00	0.00	0.06	0.00	0.07	0.09
MnO	0.55	0.58	0.55	0.69	0.50	0.61	0.55	0.55	0.45	0.59	0.54	0.51	0.35	0.30
NiO	0.00	0.06	0.01	0.01	0.03	0.02	0.03	0.01	0.00	0.02	0.00	0.00	0.05	0.03
MgO	16.05	16.66	16.38	15.52	15.98	16.58	16.42	16.05	15.59	15.68	17.32	15.51	19.58	20.32
CaO	1.33	1.67	1.69	1.60	1.90	1.75	1.24	1.40	2.12	1.89	1.97	1.85	1.57	2.55
Na_2O	0.00	0.08	0.09	0.04	0.04	0.00	0.03	0.00	0.16	0.00	0.14	0.01	0.06	0.00
K_2O	0.01	0.01	0.00	0.03	0.01	0.01	0.00	0.01	0.00	0.02	0.00	0.01	0.00	0.01
Total	99.50	100.00	99.19	99.75	99.26	99.94	98.40	98.65	99.21	99.01	99.87	98.39	99.36	99.60
Cations based on 6 oxygens														
Si	1.9478	1.9429	1.9588	1.9463	1.9572	1.9439	1.9718	1.9666	1.9583	1.9626	1.9484	1.9741	1.9578	1.9603
Ti	0.0082	0.0084	0.0099	0.0070	0.0078	0.0079	0.0060	0.0080	0.0094	0.0076	0.0075	0.0103	0.0074	0.0085
Al	0.0394	0.0334	0.0357	0.0315	0.0394	0.0324	0.0290	0.0350	0.0649	0.0295	0.0469	0.0388	0.0701	0.0702
Fe^{2+}	1.0141	0.9837	0.9588	1.0381	0.9763	0.9880	0.9637	0.9778	0.9492	0.9931	0.9118	0.9649	0.7732	0.7004
Cr	0.0000	0.0002	0.0011	0.0019	0.0009	0.0000	0.0000	0.0000	0.0000	0.0000	0.0018	0.0000	0.0021	0.0028
Mn	0.0184	0.0192	0.0181	0.0229	0.0166	0.0203	0.0182	0.0184	0.0148	0.0196	0.0176	0.0172	0.0113	0.0097
Ni	0.0000	0.0018	0.0003	0.0004	0.0009	0.0005	0.0010	0.0003	0.0000	0.0008	0.0000	0.0000	0.0015	0.0008
Mg	0.9402	0.9693	0.9559	0.9119	0.9345	0.9657	0.9644	0.9426	0.9083	0.9214	0.9988	0.9120	1.1092	1.1392
Ca	0.0562	0.0699	0.0708	0.0678	0.0798	0.0732	0.0523	0.0590	0.0887	0.0799	0.0817	0.0780	0.0640	0.1027
Na	0.0000	0.0058	0.0068	0.0031	0.0028	0.0000	0.0020	0.0000	0.0124	0.0000	0.0105	0.0011	0.0044	0.0000
K	0.0003	0.0003	0.0000	0.0015	0.0005	0.0005	0.0000	0.0003	0.0000	0.0009	0.0000	0.0007	0.0000	0.0003
Mg#	0.48	0.50	0.50	0.47	0.49	0.49	0.50	0.49	0.49	0.48	0.52	0.49	0.59	0.62
En content	46.34	47.47	47.71	44.69	46.56	47.17	48.25	47.18	46.32	45.75	49.70	46.25	56.66	58.36
Fs content	50.89	49.11	48.76	51.99	49.47	49.25	49.13	49.87	49.16	50.28	46.24	49.80	40.07	36.38
Wo content	2.77	3.42	3.53	3.32	3.98	3.58	2.61	2.95	4.52	3.97	4.07	3.95	3.27	5.26

Table C-1 (cont) *Electron microprobe analyses of orthopyroxenes from borehole SH10.*

Analysis #	3	5	6	7	8	9	10	11	12	13	14	15	16	18	20
Section	10-7	10-7	10-7	10-7	10-7	10-7	10-7	10-7	10-7	10-7	10-7	10-6	10-6	10-6	10-6
Depth	407.20	407.20	407.20	407.20	407.20	407.20	407.20	407.20	407.20	407.20	407.20	405.50	405.50	405.50	405.50
Label	*OPX 2C*	*OPX 4C*	*OPX 4R*	*OPX 5C*	*OPX 5R*	*OPX 6C*	*OPX 6R*	*OPX 7C*	*OPX 7R*	*OPX 8C*	*OPX 8R*	*OPX 1C*	*OPX 1R*	*OPX 3C*	*OPX 3R*
SiO_2	51.57	50.21	50.36	51.16	50.34	50.70	50.01	50.76	50.60	50.82	50.55	50.82	50.55	50.10	49.65
TiO_2	0.32	0.28	0.35	0.35	0.31	0.32	0.28	0.22	0.33	0.33	0.35	0.29	0.38	0.28	0.22
Al_2O_3	1.60	1.09	0.97	1.83	1.49	1.57	0.96	1.50	1.24	2.07	1.59	1.25	1.04	0.77	0.54
FeO	24.16	28.72	28.23	25.55	28.28	27.07	29.39	26.89	27.42	26.67	27.58	26.68	27.58	29.10	30.61
Cr_2O_3	0.07	0.02	0.00	0.04	0.05	0.10	0.01	0.05	0.04	0.13	0.09	0.04	0.08	0.00	0.00
MnO	0.42	0.48	0.50	0.51	0.53	0.46	0.50	0.44	0.47	0.45	0.47	0.60	0.54	0.62	0.53
NiO	0.03	0.05	0.04	0.04	0.05	0.06	0.02	0.00	0.02	0.02	0.03	0.04	0.02	0.04	0.07
MgO	18.73	16.87	16.29	17.55	16.24	17.26	16.30	17.42	16.97	16.61	16.83	16.60	16.83	16.54	15.27
CaO	2.70	1.78	1.97	2.49	1.75	2.01	1.73	1.70	2.16	2.97	2.33	1.59	1.79	1.76	1.46
Na_2O	0.03	0.00	0.00	0.07	0.03	0.05	0.02	0.10	0.00	0.03	0.11	0.01	0.11	0.13	0.10
K_2O	0.02	0.00	0.02	0.02	0.01	0.01	0.00	0.01	0.00	0.01	0.04	0.01	0.02	0.00	0.01
Total	99.65	99.49	98.73	99.60	99.08	99.62	99.23	99.08	99.23	100.09	99.97	97.93	98.94	99.35	98.45
Cations based on 6 oxygens															
Si	1.9588	1.9525	1.9694	1.9569	1.9601	1.9526	1.9567	1.9610	1.9603	1.9471	1.9475	1.9846	1.9661	1.9576	1.9713
Ti	0.0092	0.0080	0.0102	0.0099	0.0092	0.0093	0.0082	0.0064	0.0095	0.0095	0.0101	0.0086	0.0110	0.0082	0.0064
Al	0.0717	0.0500	0.0446	0.0825	0.0681	0.0712	0.0444	0.0683	0.0568	0.0932	0.0721	0.0574	0.0477	0.0356	0.0254
Fe^{2+}	0.7672	0.9337	0.9231	0.8172	0.9209	0.8719	0.9617	0.8687	0.8882	0.8543	0.8884	0.8712	0.8970	0.9510	1.0163
Cr	0.0021	0.0007	0.0000	0.0011	0.0015	0.0032	0.0004	0.0016	0.0011	0.0040	0.0026	0.0013	0.0025	0.0000	0.0000
Mn	0.0135	0.0156	0.0165	0.0166	0.0174	0.0150	0.0165	0.0142	0.0154	0.0145	0.0152	0.0198	0.0177	0.0206	0.0178
Ni	0.0008	0.0015	0.0014	0.0013	0.0016	0.0017	0.0007	0.0000	0.0005	0.0006	0.0010	0.0014	0.0008	0.0012	0.0021
Mg	1.0606	0.9779	0.9497	1.0010	0.9427	0.9910	0.9508	1.0033	0.9801	0.9484	0.9666	0.9662	0.9759	0.9636	0.9039
Ca	0.1098	0.0743	0.0827	0.1019	0.0730	0.0829	0.0725	0.0702	0.0894	0.1217	0.0961	0.0665	0.0745	0.0736	0.0620
Na	0.0021	0.0000	0.0000	0.0050	0.0026	0.0039	0.0015	0.0074	0.0000	0.0022	0.0086	0.0005	0.0081	0.0101	0.0081
K	0.0010	0.0000	0.0011	0.0008	0.0003	0.0003	0.0001	0.0005	0.0000	0.0006	0.0021	0.0006	0.0012	0.0002	0.0004
Mg #	0.58	0.51	0.51	0.55	0.51	0.53	0.50	0.54	0.52	0.53	0.52	0.53	0.52	0.50	0.47
En content	54.36	48.86	48.16	51.69	48.25	50.54	47.50	51.28	49.67	48.92	49.16	50.23	49.66	47.97	45.20
Fs content	40.01	47.43	47.64	43.05	48.02	45.23	48.87	45.13	45.79	44.81	45.95	46.32	46.55	48.37	51.70
Wo content	5.63	3.71	4.19	5.26	3.74	4.23	3.62	3.59	4.53	6.28	4.89	3.46	3.79	3.66	3.10

Table C-1 (cont) *Electron microprobe analyses of orthopyroxenes from borehole SH10.*

Analysis #	21	22	23	25	26	27	29	30	31	32	33	34	35	36	37
Section	10-6	10-6	10-6	10-6	10-6	10-6	10-6	10-6	10-6	10-5	10-5	10-5	10-5	10-5	10-5
Depth	405.50	405.50	405.50	405.50	405.50	405.50	405.50	405.50	405.50	404.80	404.80	404.80	404.80	404.80	404.80
Label	*OPX 4C*	*OPX 4R*	*OPX 4CR*	*OPX 6C*	*OPX 6R*	*OPX 7C*	*OPX 7R*	*OPX 8C*	*OPX 8R*	*OPX 1C*	*OPX 1R*	*OPX 2C*	*OPX 2R*	*OPX 3C*	*OPX 3R*
SiO_2	51.00	50.32	50.87	50.43	50.20	49.98	49.83	49.94	49.79	50.98	49.49	49.59	49.17	50.15	49.54
TiO_2	0.32	0.35	0.33	0.33	0.24	0.36	0.24	0.23	0.13	0.39	0.23	0.34	0.60	0.39	0.12
Al_2O_3	0.90	0.97	0.96	1.04	0.70	0.98	0.84	0.69	0.68	1.06	0.64	0.85	0.82	0.18	1.07
FeO	26.07	28.35	26.51	27.98	28.77	29.49	29.98	29.64	30.14	26.15	31.14	30.80	32.20	28.94	30.97
Cr_2O_3	0.04	0.05	0.00	0.00	0.02	0.01	0.00	0.04	0.00	0.00	0.02	0.00	0.00	0.00	0.01
MnO	0.51	0.47	0.52	0.54	0.45	0.61	0.77	0.54	0.55	0.50	0.66	0.64	0.66	0.57	0.65
NiO	0.05	0.03	0.04	0.05	0.03	0.09	0.02	0.06	0.05	0.06	0.04	0.04	0.06	0.30	0.14
MgO	17.11	16.18	17.74	17.49	17.83	17.22	17.80	17.09	16.67	18.04	16.82	16.11	14.95	16.68	16.96
CaO	2.00	1.89	1.98	1.90	1.72	1.60	1.30	1.60	1.39	2.01	1.61	1.23	1.54	2.01	1.19
Na_2O	0.01	0.07	0.02	0.15	0.07	0.11	0.00	0.00	0.06	0.07	0.00	0.07	0.00	0.00	0.01
K_2O	0.00	0.01	0.00	0.00	0.00	0.00	0.00	0.00	0.01	0.00	0.01	0.02	0.00	0.00	0.01
Total	98.01	98.68	98.95	99.91	100.02	100.46	100.78	99.81	99.47	99.25	100.65	99.68	99.99	99.20	100.66
Cations based on 6 oxygens															
Si	1.9865	1.9698	1.9674	1.9478	1.9435	1.9348	1.9268	1.9462	1.9512	1.9624	1.9292	1.9455	1.9391	1.9648	1.9264
Ti	0.0093	0.0103	0.0095	0.0095	0.0070	0.0104	0.0070	0.0066	0.0038	0.0112	0.0068	0.0101	0.0177	0.0115	0.0035
Al	0.0415	0.0448	0.0436	0.0471	0.0319	0.0447	0.0382	0.0315	0.0316	0.0481	0.0293	0.0392	0.0379	0.0083	0.0491
Fe^{2+}	0.8489	0.9280	0.8573	0.9038	0.9315	0.9546	0.9693	0.9659	0.9876	0.8418	1.0151	1.0104	1.0617	0.9481	1.0070
Cr	0.0011	0.0015	0.0000	0.0000	0.0008	0.0004	0.0000	0.0013	0.0000	0.0000	0.0005	0.0000	0.0000	0.0000	0.0003
Mn	0.0167	0.0155	0.0169	0.0178	0.0147	0.0199	0.0252	0.0179	0.0183	0.0162	0.0218	0.0212	0.0221	0.0188	0.0215
Ni	0.0017	0.0009	0.0012	0.0016	0.0009	0.0029	0.0006	0.0018	0.0016	0.0018	0.0013	0.0014	0.0018	0.0094	0.0043
Mg	0.9937	0.9442	1.0228	1.0071	1.0292	0.9938	1.0261	0.9930	0.9740	1.0353	0.9776	0.9423	0.8789	0.9743	0.9832
Ca	0.0833	0.0791	0.0821	0.0788	0.0712	0.0666	0.0538	0.0667	0.0585	0.0830	0.0673	0.0516	0.0649	0.0843	0.0494
Na	0.0005	0.0052	0.0013	0.0109	0.0049	0.0084	0.0000	0.0000	0.0046	0.0051	0.0000	0.0052	0.0000	0.0000	0.0009
K	0.0000	0.0003	0.0000	0.0000	0.0000	0.0001	0.0000	0.0001	0.0007	0.0000	0.0003	0.0008	0.0000	0.0000	0.0004
Mg #	0.54	0.50	0.54	0.53	0.52	0.51	0.51	0.51	0.50	0.55	0.49	0.48	0.45	0.51	0.49
En content	51.15	48.01	51.68	50.17	50.29	48.84	49.46	48.59	47.78	52.39	46.96	46.52	43.35	48.10	47.70
Fs content	44.56	47.97	44.17	45.91	46.23	47.89	47.95	48.14	49.35	43.41	49.81	50.93	53.45	47.74	49.90
Wo content	4.29	4.02	4.15	3.92	3.48	3.27	2.59	3.26	2.87	4.20	3.23	2.55	3.20	4.16	2.40

Table C-1 (cont) *Electron microprobe analyses of orthopyroxenes from borehole SH10.*

Analysis #	38	39	40	41	42	43	48	49	50	51	54	55	56	57
Section	10-5	10-5	10-5	10-5	10-5	10-5	10-5	10-5	10-4	10-4	10-4	10-4	10-4	10-4
Depth	404.80	404.80	404.80	404.80	404.80	404.80	404.80	404.80	404.07	404.07	404.07	404.07	404.07	404.07
Label	*OPX 4C*	*OPX 4R*	*OPX 5C*	*OPX 5R*	*OPX 6C*	*OPX 6R*	*OPX 7C*	*OPX 7R*	*OPX 1C*	*OPX 1R*	*OPX 3C*	*OPX 3R*	*OPX 4C*	*OPX 4R*
SiO_2	51.15	50.62	50.85	50.47	51.02	50.58	51.45	50.37	53.61	53.36	53.21	53.19	53.82	53.67
TiO_2	0.39	0.38	0.36	0.37	0.38	0.35	0.30	0.34	0.43	0.46	0.36	0.42	0.58	0.49
Al_2O_3	1.00	1.05	1.18	0.88	1.21	1.09	1.82	0.88	1.63	1.43	1.23	1.39	1.78	1.30
FeO	25.58	27.34	26.58	27.84	26.02	27.48	24.57	28.17	17.35	18.19	18.69	18.74	16.65	17.14
Cr_2O_3	0.05	0.06	0.00	0.00	0.02	0.00	0.07	0.00	0.05	0.04	0.00	0.02	0.01	0.06
MnO	0.48	0.44	0.56	0.54	0.52	0.50	0.43	0.50	0.25	0.27	0.25	0.28	0.16	0.27
NiO	0.05	0.06	0.07	0.08	0.05	0.06	0.05	0.07	0.10	0.06	0.08	0.09	0.07	0.06
MgO	18.52	17.04	17.86	17.62	18.15	17.92	18.38	17.33	24.49	23.78	23.36	23.31	25.08	24.67
CaO	2.06	2.04	1.91	1.80	1.97	2.00	4.26	1.93	2.12	1.83	2.14	1.72	2.05	1.92
Na_2O	0.04	0.10	0.04	0.06	0.08	0.10	0.16	0.12	0.07	0.02	0.02	0.08	0.08	0.02
K_2O	0.02	0.02	0.00	0.00	0.00	0.01	0.01	0.00	0.00	0.02	0.00	0.00	0.01	0.00
Total	99.34	99.17	99.42	99.65	99.42	100.08	101.52	99.72	100.10	99.46	99.34	99.25	100.30	99.60
Cations based on 6 oxygens														
Si	1.9620	1.9628	1.9583	1.9526	1.9591	1.9452	1.9325	1.9514	1.9559	1.9651	1.9685	1.9682	1.9516	1.9647
Ti	0.0112	0.0112	0.0105	0.0107	0.0110	0.0100	0.0085	0.0100	0.0119	0.0128	0.0101	0.0117	0.0159	0.0134
Al	0.0454	0.0482	0.0536	0.0401	0.0546	0.0496	0.0806	0.0403	0.0699	0.0621	0.0537	0.0606	0.0760	0.0561
Fe^{2+}	0.8206	0.8862	0.8560	0.9004	0.8355	0.8838	0.7718	0.9126	0.5293	0.5600	0.5783	0.5799	0.5050	0.5247
Cr	0.0014	0.0019	0.0000	0.0000	0.0008	0.0000	0.0022	0.0000	0.0014	0.0012	0.0000	0.0006	0.0004	0.0018
Mn	0.0154	0.0145	0.0184	0.0176	0.0169	0.0162	0.0137	0.0163	0.0076	0.0084	0.0077	0.0088	0.0050	0.0084
Ni	0.0015	0.0019	0.0021	0.0023	0.0017	0.0017	0.0016	0.0023	0.0030	0.0018	0.0025	0.0028	0.0022	0.0018
Mg	1.0591	0.9850	1.0254	1.0162	1.0390	1.0274	1.0291	1.0009	1.3322	1.3059	1.2882	1.2860	1.3559	1.3462
Ca	0.0848	0.0848	0.0787	0.0744	0.0808	0.0823	0.1715	0.0803	0.0830	0.0720	0.0848	0.0681	0.0795	0.0754
Na	0.0032	0.0078	0.0028	0.0045	0.0058	0.0073	0.0116	0.0087	0.0047	0.0017	0.0015	0.0057	0.0056	0.0013
K	0.0008	0.0011	0.0002	0.0000	0.0001	0.0003	0.0007	0.0001	0.0000	0.0008	0.0000	0.0000	0.0006	0.0000
Mg#	0.56	0.53	0.55	0.53	0.55	0.54	0.57	0.52	0.72	0.70	0.69	0.69	0.73	0.72
En content	53.49	49.99	51.83	50.59	52.68	51.12	51.81	49.79	68.25	67.09	65.76	66.19	69.70	68.87
Fs content	42.23	45.71	44.20	45.70	43.22	44.78	39.55	46.21	27.50	29.21	29.91	30.30	26.22	27.27
Wo content	4.29	4.30	3.98	3.71	4.10	4.10	8.63	3.99	4.25	3.70	4.33	3.51	4.08	3.86

Table C-1 (cont) *Electron microprobe analyses of orthopyroxenes from borehole SH10.*

Analysis #	58	59	60	62	63	64	65	66	67	71	72	73	74	75
Section	**10-4**	**10-4**	**10-4**	**10-4**	**10-4**	**10-4**	**10-4**	**10-4**	**10-4**	**10-4**	**10-3**	**10-3**	**10-3**	**10-3**
Depth	404.07	404.07	404.07	404.07	404.07	404.07	404.07	404.07	404.07	404.07	403.43	403.43	403.43	403.43
Label	*OPX 5C*	*OPX 5R*	*OPX C*	*OPX 6C*	*OPX 6R*	*OPX 7C*	*OPX 7R*	*OPX 8C*	*OPX 8R*	*OPX 9C*	*OPX 1C*	*OPX 1R*	*OPX 2C*	*OPX 2R*
SiO_2	53.80	53.27	53.16	53.41	53.20	53.52	53.21	53.65	53.40	53.42	51.01	50.60	50.55	50.32
TiO_2	0.50	0.48	0.34	0.50	0.48	0.42	0.40	0.53	0.39	0.45	0.35	0.30	0.27	0.21
Al_2O_3	1.98	1.28	1.97	1.85	1.43	1.13	1.21	1.81	1.66	1.20	1.17	1.04	0.79	0.63
FeO	16.71	18.47	18.87	18.01	18.70	17.63	18.70	17.21	18.04	17.97	26.03	27.42	27.58	28.35
Cr_2O_3	0.05	0.03	0.24	0.09	0.06	0.01	0.04	0.02	0.11	0.05	0.15	0.07	0.00	0.00
MnO	0.28	0.21	0.30	0.30	0.30	0.25	0.33	0.27	0.29	0.33	0.48	0.41	0.52	0.60
NiO	0.06	0.09	0.05	0.09	0.10	0.08	0.07	0.08	0.08	0.10	0.06	0.06	0.02	0.02
MgO	25.03	23.54	23.21	23.93	23.35	24.25	23.35	24.61	23.91	23.96	18.14	17.97	17.83	17.18
CaO	2.22	1.77	1.28	1.58	1.95	1.99	1.85	1.86	1.51	1.87	2.09	1.77	1.76	1.62
Na_2O	0.05	0.13	0.00	0.02	0.00	0.09	0.01	0.03	0.00	0.05	0.01	0.00	0.09	0.06
K_2O	0.01	0.03	0.00	0.00	0.01	0.00	0.00	0.03	0.01	0.01	0.00	0.01	0.01	0.03
Total	100.69	99.29	99.40	99.80	99.58	99.39	99.16	100.10	99.39	99.42	99.49	99.65	99.42	99.01
Cations based on 6 oxygens														
Si	1.9456	1.9685	1.9612	1.9571	1.9633	1.9690	1.9710	1.9541	1.9644	1.9681	1.9582	1.9513	1.9571	1.9642
Ti	0.0135	0.0134	0.0093	0.0139	0.0134	0.0116	0.0112	0.0145	0.0108	0.0124	0.0100	0.0088	0.0077	0.0061
Al	0.0843	0.0555	0.0857	0.0799	0.0620	0.0491	0.0527	0.0777	0.0719	0.0519	0.0531	0.0474	0.0359	0.0290
Fe^{2+}	0.5053	0.5707	0.5821	0.5518	0.5771	0.5424	0.5791	0.5242	0.5547	0.5537	0.8355	0.8841	0.8929	0.9253
Cr	0.0013	0.0008	0.0069	0.0027	0.0016	0.0004	0.0010	0.0006	0.0031	0.0015	0.0046	0.0020	0.0001	0.0000
Mn	0.0085	0.0065	0.0094	0.0093	0.0094	0.0078	0.0103	0.0083	0.0092	0.0103	0.0155	0.0135	0.0171	0.0198
Ni	0.0018	0.0026	0.0015	0.0027	0.0029	0.0023	0.0022	0.0023	0.0022	0.0029	0.0017	0.0018	0.0007	0.0006
Mg	1.3497	1.2969	1.2766	1.3074	1.2844	1.3300	1.2897	1.3362	1.3113	1.3162	1.0381	1.0331	1.0291	0.9997
Ca	0.0861	0.0699	0.0506	0.0620	0.0771	0.0786	0.0732	0.0727	0.0593	0.0739	0.0858	0.0732	0.0729	0.0675
Na	0.0035	0.0090	0.0000	0.0017	0.0002	0.0065	0.0010	0.0019	0.0000	0.0033	0.0009	0.0000	0.0069	0.0043
K	0.0007	0.0014	0.0000	0.0000	0.0003	0.0001	0.0000	0.0012	0.0006	0.0006	0.0000	0.0003	0.0005	0.0015
Mg#	0.73	0.69	0.69	0.70	0.69	0.71	0.69	0.72	0.70	0.70	0.55	0.54	0.54	0.52
En content	69.23	66.72	66.54	67.72	65.93	67.90	66.06	68.83	67.78	67.36	52.56	51.55	51.15	49.68
Fs content	26.35	29.69	30.83	29.06	30.11	28.09	30.19	27.43	29.15	28.86	43.09	44.79	45.23	46.97
Wo content	4.42	3.59	2.64	3.21	3.96	4.01	3.75	3.74	3.07	3.78	4.34	3.65	3.62	3.36

Table C-1 (cont) *Electron microprobe analyses of orthopyroxenes from borehole SH10.*

Analysis #	76	77	80	81	82	83	84	85	86	87
Section	10-3	10-3	10-3	10-3	10-3	10-3	10-3	10-3	10-3	10-3
Depth	403.43	403.43	403.43	403.43	403.43	403.43	403.43	403.43	403.43	403.43
Label	*OPX 3C*	*OPX 3R*	*OPX 5C*	*OPX 5R*	*OPX 6C*	*OPX 6R*	*OPX 7C*	*OPX 7R*	*OPX 8C*	*OPX 8R*
SiO_2	50.21	50.08	50.47	50.00	50.74	50.50	51.03	50.52	50.95	50.41
TiO_2	0.36	0.18	0.33	0.28	0.32	0.39	0.41	0.39	0.40	0.21
Al_2O_3	1.13	0.50	1.22	0.90	1.35	0.96	1.41	1.03	1.01	0.55
FeO	28.73	29.15	27.86	29.42	26.95	27.74	25.97	27.70	26.25	28.07
Cr_2O_3	0.06	0.12	0.13	0.06	0.23	0.05	0.12	0.02	0.02	0.06
MnO	0.52	0.61	0.48	0.50	0.38	0.53	0.49	0.51	0.53	0.54
NiO	0.03	0.07	0.03	0.03	0.06	0.07	0.08	0.04	0.06	0.03
MgO	16.86	16.51	17.60	16.27	18.37	17.70	18.20	17.73	17.96	17.42
CaO	1.93	1.31	1.84	1.49	1.53	1.69	2.03	1.90	2.15	1.60
Na_2O	0.10	0.00	0.05	0.20	0.00	0.03	0.07	0.05	0.03	0.00
K_2O	0.00	0.01	0.01	0.05	0.01	0.02	0.01	0.01	0.00	0.02
Total	99.92	98.55	100.01	99.21	99.94	99.69	99.83	99.89	99.35	98.90
Cations based on 6 oxygens										
Si	1.9459	1.9713	1.9445	1.9580	1.9446	1.9512	1.9515	1.9477	1.9614	1.9661
Ti	0.0105	0.0053	0.0096	0.0082	0.0092	0.0113	0.0118	0.0114	0.0116	0.0061
Al	0.0516	0.0233	0.0553	0.0416	0.0609	0.0439	0.0636	0.0469	0.0456	0.0254
Fe^{2+}	0.9312	0.9593	0.8975	0.9634	0.8637	0.8963	0.8304	0.8930	0.8450	0.9154
Cr	0.0017	0.0039	0.0041	0.0019	0.0070	0.0016	0.0037	0.0007	0.0008	0.0019
Mn	0.0169	0.0204	0.0155	0.0167	0.0122	0.0174	0.0158	0.0165	0.0171	0.0178
Ni	0.0010	0.0021	0.0010	0.0010	0.0019	0.0022	0.0024	0.0013	0.0017	0.0009
Mg	0.9742	0.9688	1.0109	0.9499	1.0496	1.0195	1.0376	1.0191	1.0308	1.0130
Ca	0.0800	0.0552	0.0758	0.0624	0.0627	0.0700	0.0833	0.0785	0.0887	0.0668
Na	0.0074	0.0000	0.0041	0.0152	0.0000	0.0020	0.0053	0.0041	0.0024	0.0000
K	0.0001	0.0006	0.0003	0.0026	0.0007	0.0008	0.0005	0.0003	0.0000	0.0011
Mg#	0.51	0.50	0.53	0.50	0.55	0.53	0.56	0.53	0.55	0.53
En content	48.65	48.35	50.55	47.68	52.79	50.89	52.75	50.78	52.02	50.32
Fs content	47.35	48.90	45.66	49.19	44.06	45.61	43.02	45.31	43.51	46.36
Wo content	4.00	2.75	3.79	3.13	3.15	3.50	4.24	3.91	4.48	3.32

Table C-1 (cont) *Electron microprobe analyses of orthopyroxenes from borehole SH10.*

Analysis #	100	101	103	104	105	107	108	111	112	113	114	115	116	117
Section	3-13	3-13	3-13	3-13	3-13	3-13	3-13	3-11	3-11	3-11	3-11	3-11	3-11	3-11
Depth	397.35	397.35	397.35	397.35	397.35	397.35	397.35	396.08	396.08	396.08	396.08	396.08	396.08	396.08
Label	*OPX 1C*	*OPX 1R*	*OPX 3C*	*OPX 3R*	*OPX 4C*	*OPX 5C*	*OPX 5R*	*OPX 1C*	*OPX 1R*	*OPX 2C*	*OPX 2R*	*OPX 3C*	*OPX 3R*	*OPX 4C*
SiO_2	51.22	50.97	50.50	50.57	50.78	50.61	50.28	51.40	51.45	51.06	50.64	51.08	51.10	50.82
TiO_2	0.34	0.30	0.27	0.31	0.38	0.28	0.28	0.07	0.34	0.34	0.32	0.30	0.36	0.33
Al_2O_3	1.79	1.03	0.74	0.78	0.88	1.20	0.80	0.46	1.19	1.16	0.81	1.07	1.06	1.16
FeO	25.35	26.18	27.74	27.51	26.81	27.38	28.48	24.74	24.56	25.88	27.28	25.82	25.76	26.67
Cr_2O_3	0.05	0.00	0.00	0.05	0.00	0.04	0.00	0.06	0.00	0.00	0.04	0.01	0.00	0.00
MnO	0.37	0.43	0.53	0.45	0.50	0.54	0.48	0.42	0.47	0.43	0.54	0.42	0.48	0.43
NiO	0.02	0.00	0.02	0.00	0.01	0.01	0.00	0.03	0.03	0.01	0.00	0.00	0.01	0.03
MgO	17.72	18.02	17.70	17.89	18.49	17.00	17.07	21.24	20.39	19.27	17.09	19.32	19.38	18.61
CaO	2.37	1.82	1.83	1.90	1.78	1.93	1.83	0.65	2.04	2.09	1.47	1.94	1.85	2.21
Na_2O	0.01	0.08	0.09	0.10	0.11	0.01	0.03	0.02	0.10	0.08	0.15	0.10	0.02	0.10
K_2O	0.00	0.01	0.00	0.02	0.02	0.00	0.01	0.00	0.00	0.01	0.00	0.02	0.04	0.00
Total	99.25	98.84	99.43	99.57	99.76	99.00	99.27	99.07	100.58	100.33	98.34	100.07	100.06	100.35
Cations based on 6 oxygens														
Si	1.9614	1.9684	1.9572	1.9546	1.9515	1.9644	1.9582	1.9616	1.9397	1.9422	1.9767	1.9466	1.9467	1.9414
Ti	0.0098	0.0087	0.0079	0.0089	0.0111	0.0082	0.0081	0.0019	0.0096	0.0097	0.0093	0.0085	0.0104	0.0094
Al	0.0810	0.0468	0.0336	0.0357	0.0397	0.0547	0.0369	0.0205	0.0527	0.0519	0.0375	0.0479	0.0475	0.0521
Fe^{2+}	0.8117	0.8454	0.8990	0.8890	0.8614	0.8885	0.9274	0.7896	0.7741	0.8231	0.8903	0.8228	0.8206	0.8517
Cr	0.0016	0.0001	0.0000	0.0015	0.0000	0.0013	0.0000	0.0017	0.0000	0.0000	0.0012	0.0003	0.0000	0.0001
Mn	0.0119	0.0139	0.0173	0.0146	0.0163	0.0177	0.0159	0.0134	0.0151	0.0139	0.0180	0.0136	0.0155	0.0138
Ni	0.0005	0.0000	0.0008	0.0000	0.0002	0.0004	0.0001	0.0010	0.0009	0.0003	0.0000	0.0000	0.0004	0.0008
Mg	1.0118	1.0375	1.0226	1.0308	1.0593	0.9837	0.9910	1.2085	1.1459	1.0927	0.9945	1.0977	1.1008	1.0598
Ca	0.0974	0.0754	0.0762	0.0787	0.0734	0.0802	0.0762	0.0266	0.0825	0.0850	0.0616	0.0793	0.0755	0.0906
Na	0.0007	0.0060	0.0068	0.0073	0.0085	0.0005	0.0026	0.0011	0.0074	0.0060	0.0113	0.0071	0.0017	0.0071
K	0.0000	0.0004	0.0000	0.0009	0.0010	0.0001	0.0004	0.0000	0.0000	0.0007	0.0000	0.0011	0.0018	0.0000
Mg#	0.55	0.55	0.53	0.54	0.55	0.53	0.52	0.60	0.60	0.57	0.53	0.57	0.57	0.55
En content	52.35	52.60	50.75	51.20	52.69	49.93	49.29	59.30	56.79	54.24	50.63	54.52	54.70	52.57
Fs content	42.61	43.57	45.47	44.89	43.66	46.00	46.92	39.40	39.12	41.54	46.24	41.54	41.55	42.94
Wo content	5.04	3.82	3.78	3.91	3.65	4.07	3.79	1.30	4.09	4.22	3.14	3.94	3.75	4.49

Table C-2*Electron microprobe analyses of orthopyroxenes from borehole SH3.*

Analysis #	118	119	120	121	122	123	124	125	126	127	128	129	131
Section	3-6	3-6	3-6	3-6	3-6	3-6	3-6	3-6	3-5	3-5	3-5	3-5	3-5
Depth	390.98	390.98	390.98	390.98	390.98	390.98	390.98	390.98	389.82	389.82	389.82	389.82	389.82
Label	*OPX 1C*	*OPX 2C*	*OPX 3C*	*OPX 3R*	*OPX 4C*	*OPX 5C*	*OPX 5R*	*OPX 6C*	*OPX 1C*	*OPX 1R*	*OPX 2C*	*OPX 2R*	*OPX 3C*
SiO_2	52.27	52.03	52.51	52.89	52.72	52.31	51.96	52.42	52.19	52.01	51.15	51.20	51.72
TiO_2	0.38	0.41	0.42	0.29	0.27	0.35	0.32	0.35	0.37	0.40	0.34	0.29	0.39
Al_2O_3	1.18	1.02	1.22	0.84	1.47	1.56	0.73	1.06	1.69	1.13	1.07	0.80	1.18
FeO	21.84	22.64	21.03	19.75	20.32	21.70	22.85	21.32	22.10	22.69	25.57	25.41	23.68
Cr_2O_3	0.03	0.10	0.08	0.00	0.37	0.31	0.01	0.04	0.34	0.04	0.09	0.00	0.01
MnO	0.35	0.36	0.40	0.26	0.32	0.38	0.40	0.32	0.39	0.43	0.39	0.37	0.39
NiO	0.14	0.15	0.11	0.13	0.12	0.13	0.18	0.12	0.03	0.05	0.06	0.03	0.07
MgO	21.70	21.01	22.38	23.46	21.98	20.81	20.83	22.13	20.47	20.97	18.53	19.67	20.13
CaO	1.78	1.68	1.80	1.15	1.86	2.82	1.60	1.82	1.73	1.99	1.98	1.89	2.09
Na_2O	0.04	0.13	0.02	0.19	0.09	0.07	0.15	0.10	0.12	0.08	0.05	0.04	0.11
K_2O	0.03	0.00	0.01	0.22	0.00	0.02	0.01	0.00	0.01	0.01	0.02	0.03	0.00
Total	99.73	99.52	99.98	99.18	99.52	100.46	99.05	99.67	99.43	99.81	99.26	99.73	99.76
Cations based on 6 oxygens													
Si	1.9575	1.9610	1.9539	1.9702	1.9637	1.9498	1.9705	1.9596	1.9615	1.9562	1.9625	1.9536	1.9558
Ti	0.0106	0.0115	0.0119	0.0081	0.0077	0.0097	0.0092	0.0097	0.0103	0.0113	0.0098	0.0083	0.0110
Al	0.0522	0.0452	0.0536	0.0370	0.0644	0.0687	0.0325	0.0465	0.0749	0.0502	0.0484	0.0360	0.0524
Fe^{2+}	0.6838	0.7136	0.6544	0.6153	0.6328	0.6763	0.7247	0.6665	0.6945	0.7135	0.8205	0.8106	0.7489
Cr	0.0010	0.0030	0.0024	0.0000	0.0108	0.0092	0.0003	0.0011	0.0100	0.0012	0.0026	0.0000	0.0004
Mn	0.0111	0.0116	0.0125	0.0081	0.0101	0.0121	0.0129	0.0100	0.0123	0.0136	0.0128	0.0121	0.0124
Ni	0.0043	0.0044	0.0032	0.0038	0.0037	0.0039	0.0054	0.0035	0.0008	0.0014	0.0018	0.0010	0.0020
Mg	1.2116	1.1806	1.2416	1.3028	1.2205	1.1564	1.1776	1.2333	1.1471	1.1757	1.0599	1.1189	1.1350
Ca	0.0713	0.0679	0.0717	0.0459	0.0740	0.1127	0.0649	0.0730	0.0698	0.0804	0.0815	0.0771	0.0849
Na	0.0026	0.0092	0.0015	0.0136	0.0068	0.0049	0.0109	0.0074	0.0085	0.0060	0.0037	0.0033	0.0082
K	0.0012	0.0001	0.0006	0.0104	0.0000	0.0008	0.0007	0.0000	0.0005	0.0006	0.0009	0.0014	0.0000
Mg#	0.64	0.62	0.65	0.68	0.66	0.63	0.62	0.65	0.62	0.62	0.56	0.58	0.60
En content	61.26	59.82	62.70	66.06	63.00	59.08	59.47	62.20	59.63	59.29	53.68	55.43	57.29
Fs content	35.14	36.74	33.68	31.61	33.18	35.17	37.25	34.12	36.74	36.66	42.20	40.75	38.43
Wo content	3.61	3.44	3.62	2.33	3.82	5.76	3.28	3.68	3.63	4.05	4.13	3.82	4.28

Table C-2 (cont) *Electron microprobe analyses of orthopyroxenes from borehole SH3.*

Analysis #	132	133	134	135	136	137	138	139	140	141	142	144	145
Section	3-5	3-5	3-5	3-4	3-4	3-4	3-4	3-4	3-4	3-4	3-4	3-3	3-3
Depth	389.82	389.82	389.82	389.26	389.26	389.26	389.26	389.26	389.26	389.26	389.26	388.93	388.93
Label	*OPX 5C*	*OPX 5R*	*OPX 6C*	*OPX 1C*	*OPX 1R*	*OPX 2C*	*OPX 2R*	*OPX 3C*	*OPX 3R*	*OPX 4C*	*OPX 5C*	*OPX 1C*	*OPX 1R*
SiO_2	52.79	52.81	52.37	52.19	52.00	52.54	52.02	51.85	52.08	51.85	53.06	52.20	51.99
TiO_2	0.21	0.29	0.24	0.31	0.48	0.25	0.45	0.32	0.16	0.38	0.22	0.39	0.35
Al_2O_3	1.44	1.63	1.24	1.27	0.89	1.68	1.07	1.12	0.50	0.93	1.47	1.61	0.85
FeO	20.08	20.03	21.51	22.11	22.73	20.93	22.68	23.25	23.12	23.25	19.19	22.07	22.76
Cr_2O_3	0.11	0.27	0.26	0.19	0.10	0.31	0.09	0.12	0.00	0.12	0.13	0.14	0.11
MnO	0.35	0.28	0.39	0.31	0.30	0.21	0.34	0.36	0.42	0.34	0.29	0.32	0.42
NiO	0.04	0.04	0.05	0.05	0.04	0.06	0.05	0.04	0.01	0.02	0.06	0.09	0.04
MgO	22.81	22.23	21.97	21.47	20.94	21.46	20.98	20.50	21.16	20.50	22.94	20.50	20.49
CaO	1.50	2.22	1.76	1.76	1.97	2.75	2.14	1.45	1.45	1.85	2.42	2.01	2.06
Na_2O	0.05	0.07	0.01	0.10	0.11	0.12	0.03	0.06	0.02	0.09	0.01	0.08	0.06
K_2O	0.00	0.02	0.00	0.02	0.00	0.01	0.02	0.01	0.00	0.02	0.01	0.00	0.01
Total	99.40	99.87	99.79	99.76	99.55	100.31	99.85	99.06	98.91	99.35	99.80	99.42	99.15
Cations based on 6 oxygens													
Si	1.9629	1.9577	1.9565	1.9560	1.9608	1.9510	1.9555	1.9659	1.9765	1.9634	1.9608	1.9625	1.9696
Ti	0.0060	0.0080	0.0066	0.0086	0.0135	0.0068	0.0126	0.0090	0.0047	0.0107	0.0062	0.0109	0.0100
Al	0.0631	0.0712	0.0547	0.0561	0.0394	0.0735	0.0472	0.0501	0.0226	0.0415	0.0641	0.0714	0.0378
Fe^{2+}	0.6243	0.6208	0.6719	0.6928	0.7166	0.6499	0.7130	0.7370	0.7337	0.7362	0.5929	0.6938	0.7209
Cr	0.0032	0.0078	0.0077	0.0057	0.0029	0.0090	0.0026	0.0035	0.0000	0.0036	0.0039	0.0042	0.0034
Mn	0.0111	0.0087	0.0122	0.0097	0.0095	0.0065	0.0107	0.0117	0.0134	0.0111	0.0091	0.0102	0.0134
Ni	0.0013	0.0013	0.0015	0.0016	0.0011	0.0019	0.0014	0.0012	0.0002	0.0007	0.0017	0.0028	0.0014
Mg	1.2644	1.2284	1.2237	1.1996	1.1771	1.1882	1.1759	1.1588	1.1972	1.1574	1.2637	1.1489	1.1572
Ca	0.0597	0.0881	0.0704	0.0705	0.0796	0.1092	0.0862	0.0588	0.0588	0.0751	0.0960	0.0811	0.0837
Na	0.0037	0.0047	0.0009	0.0071	0.0083	0.0089	0.0024	0.0043	0.0013	0.0066	0.0006	0.0060	0.0043
K	0.0002	0.0009	0.0001	0.0009	0.0000	0.0007	0.0010	0.0003	0.0000	0.0010	0.0006	0.0000	0.0005
Mg#	0.67	0.66	0.65	0.63	0.62	0.65	0.62	0.61	0.62	0.61	0.68	0.62	0.62
En content	64.53	63.13	61.86	60.81	59.36	60.81	59.22	58.93	59.77	58.46	64.42	59.40	58.58
Fs content	32.43	32.35	34.58	35.61	36.62	33.60	36.44	38.08	37.30	37.75	30.69	36.40	37.18
Wo content	3.04	4.53	3.56	3.57	4.02	5.59	4.34	2.99	2.94	3.79	4.89	4.19	4.24

Table C-2 (cont) *Electron microprobe analyses of orthopyroxenes from borehole SH3.*

Analysis #	157	4	17	24	44	45	46	47	61	68	70
Section	10-9	10-7	10-6	10-6	10-5	10-5	10-5	10-5	10-4	10-4	10-4
Depth	409.40	407.20	405.50	405.50	404.80	404.80	404.80	404.80	404.07	404.07	404.07
Label	*CPX 1C*	*CPX 3C*	*CPX 2C*	*CPX 5C*	*CPX 1C*	*CPX 1R*	*CPX 2C*	*CPX 2R*	*CPX 1R*	*CPX 2C*	*CPX 2R*
SiO_2	51.35	47.03	52.52	53.24	52.33	51.94	51.87	51.89	51.22	52.78	52.83
TiO_2	0.22	1.75	0.40	0.22	0.63	0.23	0.31	0.16	0.92	0.46	0.34
Al_2O_3	0.99	7.73	1.66	0.96	2.02	1.00	1.18	0.82	3.09	1.92	1.85
FeO	14.86	17.42	20.99	13.47	12.62	12.89	13.13	13.06	8.68	7.35	7.51
Cr_2O_3	0.00	0.06	0.11	0.04	0.06	0.01	0.00	0.00	0.21	0.40	0.15
MnO	0.31	0.09	0.36	0.32	0.30	0.32	0.31	0.27	0.17	0.17	0.09
NiO	0.01	0.03	0.04	0.04	0.02	0.01	0.07	0.00	0.00	0.05	0.04
MgO	11.94	13.60	20.99	12.29	11.80	11.84	11.94	11.35	13.10	15.39	15.08
CaO	19.45	11.60	6.59	19.80	20.53	21.64	21.26	22.05	22.13	22.39	22.87
Na_2O	0.31	2.16	0.29	0.42	0.55	0.41	0.44	0.35	0.49	0.42	0.49
K_2O	0.01	1.53	0.00	0.00	0.06	0.02	0.00	0.02	0.00	0.00	0.00
Total	99.44	103.01	103.95	100.80	100.93	100.32	100.51	99.97	100.01	101.34	101.25
Cations based on 6 oxygens											
Si	1.9697	1.7541	1.9072	1.9958	1.9595	1.9684	1.9624	1.9765	1.9130	1.9333	1.9391
Ti	0.0062	0.0491	0.0108	0.0063	0.0177	0.0066	0.0088	0.0046	0.0258	0.0127	0.0095
Al	0.0449	0.3399	0.0712	0.0422	0.0892	0.0448	0.0524	0.0369	0.1361	0.0830	0.0801
Fe^{2+}	0.4767	0.5432	0.6374	0.4221	0.3952	0.4085	0.4154	0.4161	0.2710	0.2253	0.2305
Cr	0.0000	0.0017	0.0032	0.0011	0.0018	0.0004	0.0000	0.0000	0.0061	0.0117	0.0042
Mn	0.0102	0.0030	0.0110	0.0101	0.0095	0.0102	0.0100	0.0087	0.0055	0.0051	0.0026
Ni	0.0003	0.0010	0.0013	0.0011	0.0007	0.0004	0.0022	0.0000	0.0001	0.0013	0.0013
Mg	0.6828	0.7560	1.1363	0.6868	0.6587	0.6689	0.6735	0.6445	0.7294	0.8404	0.8252
Ca	0.7991	0.4634	0.2564	0.7954	0.8237	0.8788	0.8617	0.8996	0.8855	0.8788	0.8992
Na	0.0228	0.1565	0.0203	0.0305	0.0396	0.0298	0.0325	0.0260	0.0354	0.0299	0.0349
K	0.0005	0.0727	0.0000	0.0001	0.0031	0.0011	0.0000	0.0008	0.0000	0.0000	0.0000
Mg#	0.59	0.58	0.64	0.62	0.63	0.62	0.62	0.61	0.73	0.79	0.78
En content	34.68	42.82	55.67	35.88	34.91	34.02	34.35	32.73	38.57	43.11	42.15
Fs content	24.73	30.93	31.77	22.58	21.45	21.29	21.70	21.58	14.62	11.82	11.91
Wo content	40.59	26.25	12.56	41.55	43.65	44.69	43.95	45.69	46.82	45.07	45.93

Table C-3 *Electron microprobe analyses of clinopyroxenes from boreholes SH10 and SH3.*

Analysis #	78	79	102	109	110	130	143	151	152
Section	10-3	10-3	3-13	3-13	3-13	3-5	3-3	3-2	3-2
Depth	403.43	403.43	397.35	397.35	397.35	389.82	388.93	383.96	383.96
Label	*CPX 4C*	*CPX 4R*	*CPX 2C*	*CPX 6C*	*CPX 7C*	*CPX 1*	*CPX 1*	*CPX 4C*	*CPX 5C*
SiO_2	51.62	52.02	50.88	51.76	51.56	51.45	51.97	44.41	51.71
TiO_2	0.60	0.56	0.54	0.44	0.49	0.82	0.62	1.90	0.88
Al_2O_3	3.95	3.84	1.59	1.30	1.69	2.51	3.85	11.46	3.27
FeO	17.94	17.21	15.30	16.78	15.31	10.69	13.63	12.50	10.00
Cr_2O_3	0.06	0.00	0.02	0.05	0.03	0.00	0.09	0.00	0.04
MnO	0.18	0.18	0.23	0.29	0.24	0.21	0.26	0.14	0.22
NiO	0.07	0.06	0.03	0.02	0.02	0.06	0.02	0.07	0.04
MgO	14.12	13.48	12.39	12.80	12.01	14.02	16.04	13.59	13.35
CaO	11.56	11.47	18.54	15.63	18.25	20.04	11.46	10.38	17.65
Na_2O	1.34	1.39	0.30	0.32	0.44	0.53	1.36	3.23	0.47
K_2O	0.51	0.53	0.01	0.02	0.02	0.01	0.49	1.28	0.00
Total	101.95	100.74	99.83	99.42	100.06	100.35	99.79	98.95	97.64
Cations based on 6 oxygens									
Si	1.9183	1.9467	1.9438	1.9782	1.9605	1.9217	1.9338	1.6878	1.9583
Ti	0.0167	0.0156	0.0154	0.0126	0.0140	0.0231	0.0173	0.0542	0.0251
Al	0.1729	0.1695	0.0717	0.0586	0.0755	0.1107	0.1690	0.5133	0.1461
Fe^{2+}	0.5573	0.5385	0.4888	0.5364	0.4868	0.3339	0.4240	0.3972	0.3167
Cr	0.0016	0.0000	0.0005	0.0015	0.0010	0.0000	0.0025	0.0000	0.0013
Mn	0.0057	0.0058	0.0075	0.0094	0.0077	0.0067	0.0083	0.0044	0.0070
Ni	0.0022	0.0019	0.0008	0.0007	0.0007	0.0018	0.0006	0.0021	0.0013
Mg	0.7823	0.7521	0.7057	0.7293	0.6808	0.7807	0.8898	0.7700	0.7537
Ca	0.4604	0.4600	0.7589	0.6400	0.7434	0.8019	0.4569	0.4226	0.7161
Na	0.0965	0.1005	0.0225	0.0239	0.0325	0.0384	0.0981	0.2376	0.0346
K	0.0242	0.0253	0.0007	0.0012	0.0010	0.0006	0.0235	0.0621	0.0000
Mg#	0.58	0.58	0.59	0.58	0.58	0.70	0.68	0.66	0.70
En content	43.32	42.82	35.99	38.08	35.48	40.59	50.02	48.30	42.02
Fs content	31.18	30.99	25.31	28.50	25.77	17.71	24.30	25.19	18.05
Wo content	25.50	26.19	38.70	33.42	38.75	41.70	25.68	26.51	39.93

Table C-3 (cont) *Electron microprobe analyses of clinopyroxenes from boreholes SH10 and SH3.*

Point	17	18	1	2	3	4	5	6	7	8	9	10	11	12
Section	10-8	10-8	10-7	10-7	10-7	10-7	10-6	10-6	10-6	10-5	10-4	10-3	10-3	10-3
Depth	408.60	408.60	407.20	407.20	407.20	407.20	405.50	405.50	405.50	404.80	404.07	403.43	403.43	403.43
Label	*actinolite*	*magnesio-hornblende*	*magnesio-hornblende*	*magnesio-hornblende*	*magnesio-hornblende*	*magnesio-hornblende*	*actinolite*	*magnesio-hornblende*	*magnesio-hornblende*	*actinolitic hornblende*	*actinolitic hornblende*	*magnesio-hornblende*	*magnesio-hornblende*	*magnesio-hornblende*
SiO_2	53.32	44.58	46.03	47.12	48.85	45.81	55.78	45.81	45.43	50.81	52.01	50.32	50.70	51.52
TiO_2	0.09	1.04	0.06	1.41	1.42	0.51	0.02	0.49	0.71	0.43	0.04	0.59	0.88	0.60
Al_2O_3	2.95	8.04	0.94	7.00	6.52	5.16	0.62	5.33	5.20	1.56	0.50	4.63	4.25	4.09
Cr_2O_3	0.07	0.00	0.00	0.04	0.00	0.01	0.00	0.07	0.01	0.05	0.17	0.12	0.05	0.05
FeO	18.33	20.48	30.98	18.73	18.14	20.13	16.28	18.45	19.57	13.29	5.75	18.40	18.46	17.79
MnO	0.14	0.30	0.20	0.18	0.09	0.34	0.27	0.29	0.17	0.36	0.09	0.21	0.24	0.20
MgO	12.28	10.89	11.45	11.71	11.69	12.40	15.32	14.84	13.79	12.18	16.73	13.27	13.35	13.83
CaO	12.63	11.91	11.01	10.96	10.78	11.58	12.43	11.66	11.89	21.54	24.71	10.82	10.52	10.36
Na_2O	0.40	1.52	0.18	1.93	1.91	1.37	0.04	1.19	1.28	0.32	0.06	1.11	1.51	1.42
K_2O	0.05	0.85	0.07	1.25	1.10	0.60	0.01	0.40	0.55	0.00	0.00	0.50	0.50	0.51
Total	100.26	99.61	100.91	100.34	100.50	97.90	100.76	98.52	98.60	100.54	100.05	99.97	100.46	100.37
Cations based on 23 oxygens (after Mogessie et al., 1988)														
Si	7.643	6.554	6.629	6.813	7.038	6.781	7.785	6.591	6.628	7.396	7.405	7.135	7.169	7.231
Ti	0.009	0.115	0.009	0.157	0.156	0.053	0.000	0.052	0.079	0.043	0.008	0.060	0.093	0.068
Al	0.500	1.395	0.156	1.190	1.108	0.899	0.101	0.908	0.894	0.271	0.086	0.776	0.705	0.675
Cr	0.009	0.000	0.000	0.009	0.000	0.000	0.000	0.009	0.000	0.008	0.017	0.017	0.008	0.008
Fe^{3+}	0.182	0.924	3.102	0.712	0.438	1.237	0.571	1.800	1.504	0.000	0.000	1.126	1.074	1.126
Fe^{2+}	2.015	1.593	0.628	1.557	1.743	1.255	1.334	0.423	0.880	1.617	0.684	1.056	1.110	0.968
Mn	0.017	0.035	0.026	0.026	0.009	0.044	0.034	0.035	0.018	0.043	0.008	0.026	0.025	0.025
Mg	2.629	2.385	2.457	2.529	2.510	2.741	3.188	3.183	2.999	2.640	3.549	2.805	2.811	2.894
Ca	1.938	1.872	1.696	1.695	1.662	1.833	1.863	1.799	1.858	3.357	3.770	1.645	1.597	1.561
K	0.009	0.159	0.009	0.235	0.199	0.116	0.000	0.069	0.105	0.000	0.000	0.094	0.093	0.093
Na	0.112	0.433	0.052	0.539	0.537	0.391	0.008	0.329	0.359	0.088	0.017	0.307	0.416	0.388
Total	15.063	15.465	14.764	15.462	15.400	15.350	14.884	15.198	15.325	15.463	15.544	15.047	15.100	15.036
Al^{IV}	0.357	1.395	0.156	1.187	0.962	0.899	0.101	0.908	0.894	0.271	0.086	0.776	0.705	0.675
Al^{VI}	0.143	0.000	0.000	0.003	0.146	0.000	0.000	0.000	0.000	0.000	0.000	0.000	0.000	0.000
(Ca + Na)I	2.000	2.000	1.748	2.000	2.000	2.000	1.871	2.000	2.000	3.357	3.770	1.952	2.000	1.949
NaB	0.062	0.128	0.052	0.305	0.338	0.167	0.008	0.201	0.142	0.000	0.000	0.307	0.403	0.388
(Na + K)A	0.059	0.464	0.090	0.469	0.398	0.340	0.000	0.197	0.322	0.088	0.017	0.094	0.106	0.093

Table C-4 *Electron microprobe analyses of amphiboles from boreholes SH10 and SH3.*

Point	13	14	15	16	19	20	21	22	23	24	25	26	27	28
Section	10-3	10-2	10-2	10-2	3-10	3-10	3-8	3-8	3-8	3-7	3-7	3-7	3-6	3-3
Depth	403.43	403.20	403.20	403.20	394.80	394.80	393.29	393.29	393.29	391.96	391.96	391.96	390.98	388.93
Label	*actinolitic hornblende*	*actinolitic hornblende*	*actinolitic hornblende*	*actinolite*	*magnesio-hornblende*	*actinolitic hornblende*	*actinolite*	*actinolite*	*actinolite*	*actinolite*	*actinolitic hornblende*	*magnesio-hornblende*	*magnesio-hornblende*	*magnesio-hornblende*
SiO_2	51.45	51.16	51.16	54.99	48.34	52.20	53.35	54.10	54.03	52.62	52.63	50.49	50.22	51.54
TiO_2	0.03	0.49	0.45	0.05	1.19	0.03	0.18	0.04	0.04	0.03	0.29	1.07	1.24	0.58
Al_2O_3	1.21	3.77	3.83	0.23	5.18	1.81	1.23	0.85	0.58	0.59	1.67	4.05	5.46	3.91
Cr_2O_3	0.00	0.16	0.21	0.07	0.30	0.14	0.10	0.27	0.02	0.00	0.08	0.07	0.01	0.16
FeO	22.05	16.84	17.15	14.58	10.59	14.49	10.13	17.89	17.58	17.75	9.47	13.41	14.81	15.21
MnO	0.35	0.20	0.23	0.27	0.17	0.28	0.23	0.36	0.36	0.28	0.14	0.22	0.13	0.25
MgO	11.86	13.20	13.46	16.35	17.20	16.78	14.14	14.20	15.09	15.08	19.80	16.52	15.32	15.75
CaO	13.24	12.43	11.31	13.47	12.87	14.45	20.87	12.47	12.52	13.67	13.56	12.58	11.44	11.94
Na_2O	0.10	1.22	1.19	0.13	1.21	0.31	0.61	0.20	0.29	0.28	0.58	1.59	1.77	1.20
K_2O	0.17	0.42	0.40	0.03	0.39	0.13	0.02	0.07	0.03	0.04	0.19	0.47	0.72	0.44
Total	100.46	99.89	99.38	100.16	97.43	100.61	100.86	100.45	100.54	100.33	98.39	100.46	101.12	100.97
Cations based on 23 oxygens (after Mogessie et al., 1988)														
Si	7.496	7.388	7.321	7.742	6.963	7.388	7.580	7.655	7.613	7.527	7.396	7.130	7.027	7.193
Ti	0.000	0.052	0.052	0.008	0.130	0.000	0.017	0.009	0.008	0.000	0.034	0.110	0.134	0.059
Al	0.210	0.642	0.645	0.042	0.883	0.306	0.205	0.145	0.093	0.103	0.279	0.671	0.899	0.645
Cr	0.000	0.017	0.026	0.008	0.035	0.017	0.008	0.034	0.000	0.000	0.008	0.008	0.000	0.017
Fe^{3+}	0.579	0.178	0.712	0.372	0.542	0.406	0.000	0.664	0.812	0.566	0.590	0.498	0.740	0.856
Fe^{2+}	2.110	1.854	1.344	1.346	0.730	1.311	1.204	1.454	1.263	1.556	0.525	1.089	0.991	0.921
Mn	0.044	0.026	0.026	0.034	0.017	0.034	0.026	0.043	0.042	0.034	0.017	0.025	0.017	0.034
Mg	2.574	2.847	2.874	3.435	3.694	3.537	2.996	2.994	3.166	3.213	4.145	3.480	3.194	3.278
Ca	2.067	1.928	1.738	2.031	1.981	2.194	3.176	1.888	1.889	2.096	2.043	1.902	1.714	1.785
K	0.035	0.078	0.069	0.008	0.069	0.026	0.000	0.009	0.008	0.009	0.034	0.085	0.126	0.075
Na	0.026	0.338	0.327	0.034	0.338	0.085	0.170	0.051	0.076	0.077	0.160	0.432	0.479	0.327
Total	15.140	15.348	15.134	15.060	15.381	15.304	15.382	14.945	14.970	15.181	15.230	15.430	15.321	15.190
Al^{IV}	0.210	0.612	0.645	0.042	0.883	0.306	0.205	0.145	0.093	0.103	0.279	0.671	0.899	0.645
Al^{VI}	0.000	0.030	0.000	0.000	0.000	0.000	0.000	0.000	0.000	0.000	0.000	0.000	0.000	0.000
(Ca + Na)I	2.067	2.000	2.000	2.031	2.000	2.194	3.176	1.939	1.965	2.096	2.043	2.000	2.000	2.000
NaB	0.000	0.072	0.262	0.000	0.019	0.000	0.000	0.051	0.076	0.000	0.000	0.098	0.286	0.215
(Na + K)A	0.061	0.344	0.134	0.042	0.388	0.111	0.170	0.009	0.008	0.086	0.194	0.419	0.319	0.187

Table C-4 (cont) *Electron microprobe analyses of amphiboles from boreholes SH10 and SH3.*

Appendix D

X-Ray Fluorescence Spectrometry

Appendix D: X-Ray Fluorescence Spectrometry

Whole-rock analyses were carried out by XRF wavelength dispersive techniques using a Phillips 1410 X-ray spectrometer for all the elements except sulphur. Sulphur analyses were carried out at the University of Cape Town, using a Phillips 1410 wavelength dispersive X-ray spectrometer. The major elements, apart from sodium, were determined using duplicate fusion discs, prepared according to the method of Norrish and Hutton (1969). All iron was determined as Fe_2O_3. Sodium and trace elements were determined on 5g pressed powder pellets.

H_2O- and loss on ignition (LOI) were determined gravimetrically by heating samples for eight hours at 110° C and 950° C respectively. Standard departmental FORTRAN programs were used to process the data. Corrections were made for background and matrix effects, spectral line and tube interferences, instrumental drift and dead time. Working curves were calculated by using a variety of international and in-house rock standards. Details of analytical conditions for major and trace element runs are given in Table D-1.

Element	Tube	Line	kV	mA	Crystal	Time	Counter	Collimator
Si	Sc - Mo	Kα	50	50	PE	40	Gas Flow	coarse
Ti	Sc - Mo	Kα	50	50	LiF(200)	40	Gas Flow	fine
Al	Sc - Mo	Kα	50	50	PE	40	Gas Flow	coarse
Fe	Sc - Mo	Kα	50	50	LiF(200)	20	Gas Flow	fine
Mn	Sc - Mo	Kα	50	50	LiF(200)	20	Gas Flow	fine
Mg	Sc - Mo	Kα	50	50	PX1	60	Gas Flow	fine
Ca	Sc - Mo	Kα	50	50	LiF(200)	10	Gas Flow	fine
Na	Sc - Mo	Kα	50	50	PX1	100	Gas Flow	fine
K	Sc - Mo	Kα	50	50	LiF(200)	10	Gas Flow	fine
P	Sc - Mo	Kα	50	50	Ge	40	Gas Flow	coarse
Zn	Sc - Mo	Kα	55	40	LiF(200)	200	Both	fine
Cu	Sc - Mo	Kα	55	40	LiF(200)	200	Both	fine
Ni	Sc - Mo	Kα	55	40	LiF(200)	200	Both	fine
Nb	W	Kα	70	35	LiF(200)	200	Scintillation	fine
Zr	W	Kα	70	35	LiF(200)	100	Scintillation	fine
Y	W	Kα	70	35	LiF(200)	100	Scintillation	fine
Sr	W	Kα	70	35	LiF(200)	100	Scintillation	fine
Rb	W	Kα	70	35	LiF(200)	200	Scintillation	fine
Co	W	Kα	50	50	LiF(200)	200	Gas Flow	fine
Cr	W	Kα	50	50	LiF(200)	200	Gas Flow	fine
V	W	Kα	50	50	LiF(200)	200	Gas Flow	fine
Ce	W	Lβ	45	60	LiF(200)	200	Gas Flow	fine
Nd	W	Lα	45	60	LiF(200)	200	Gas Flow	fine
La	W	Lα	45	60	LiF(200)	200	Gas Flow	fine
Ba	Cr	Lα	45	60	LiF(200)	200	Gas Flow	fine
Sc	Cr	Kα	45	60	LiF(200)	200	Gas Flow	fine
Th	Sc - Mo	Lα	75	35	LiF(200)	300	Both	fine
Pb	Sc - Mo	Lβ	75	35	LiF(200)	300	Both	fine

Table D-1 Details of analytical conditions

Calculation of iron content (FeO) of silicates:

1. Analyses of Fe_2O_3, Cu, Ni, and S, are converted into elemental ppm, so that:

   Total Fe = $Fe_2O_3 \div 1.43$

2. The atomic weight ratios of the various sulphide phases are calculated according to the stoichiometric formulae, so that:

   Chalcopyrite [$CuFeS_2$] has Cu:S ratio of 1.98
   Pentlandite [$(Ni,Fe)_8S_9$] has Ni:S ratio of 1.83
   and Pyrrhotite [$Fe_{1-x}S$] has Fe:S ratio of 1.74

3. Assuming all Cu is in chalcopyrite, CuS is calculated so that:

   CuS = Cu content (ppm) + [Cu content (ppm) $\div$ 1.98]

4. Assuming all Ni is in pentlandite, NiS is calculated so that:

   NiS = Ni content (ppm) + [Ni content (ppm) $\div$ 1.83]

5. Assuming that the remaining sulphur is associated with Fe in pyrrhotite, FeS is calculated so that:

   FeS = Remaining S (ppm) + [Remaining S (ppm) × 1.74]

6. Assuming that all the Fe is either as FeO or FeS, the FeO content is calculated as:

   FeO = (Total Fe - [Remaining S (ppm) × 1.74]) × 1.286

Estimation of sulphide values for samples with no major element data:

1. Regression line calculated for net peaks (background corrected) and sulphur content (ppm):

$$\text{Sulphur}_{(ppm)} = 1.375 \times \text{net peak}_{(cps)} + 25.593$$

2. Regression line calculated for sulphur content (ppm) and sulphide content (wt%):

$$\text{Sulphide}_{(wt\%)} = 2.8289 \times \text{Sulphur}_{(ppm)} + 162.5151$$

SAMPLE	SH8-12	SH8-13	SH8-14	SH8-1	SH8-2	SH8-3	SH8-4	SH8-5	SH8-6	SH8-7
Depth m	*450.24*	*451.41*	*452.80*	*453.66*	*455.41*	*457.45*	*457.92*	*459.41*	*460.34*	*461.92*
	Diabase	Quartzite	LrPXT	LrPXT	LrPXT	LrPXT	Hybrid	Hybrid	Hybrid	Basal Gabbro
SiO_2	49.05	80.65	48.08	40.99	46.86	44.79	47.38	50.58	47.92	53.41
TiO_2	2.43	0.17	0.22	0.57	0.37	0.82	0.39	0.98	1.24	1.19
Al_2O_3	14.26	2.08	2.54	5.65	5.47	6.95	9.27	6.25	10.15	11.31
FeO	12.83	3.58	6.52	15.54	6.67	12.19	7.66	10.29	9.25	10.01
MnO	0.18	0.08	0.14	0.18	0.23	0.23	0.17	0.22	0.19	0.17
MgO	4.48	3.46	18.36	24.37	16.94	19.89	13.61	14.49	9.41	8.85
CaO	7.41	6.13	17.55	4.55	15.78	8.39	16.52	11.35	8.66	6.92
Na_2O	3.50	1.30	0.11	0.14	0.44	0.13	1.25	1.12	2.05	2.42
K_2O	1.62	0.13	0.13	0.26	0.39	0.40	0.46	0.53	0.90	1.61
P_2O_5	0.50	0.04	0.08	0.04	0.05	0.08	0.06	0.10	0.10	0.11
FeS	0.500	0.073	1.840	0.136	2.811	0.110	0.675	0.880	5.373	0.586
CuS	0.009	0.004	0.028	0.006	0.106	0.011	0.027	0.134	0.674	0.069
NiS	0.010	0.008	0.042	0.207	0.140	0.127	0.062	0.137	0.407	0.059
LOI	1.08	1.64	3.67	6.03	3.70	4.38	3.14	2.07	2.53	1.81
H_2O^-	0.25	0.16	0.18	0.47	0.36	0.50	0.30	0.23	0.31	0.42
TOTAL	98.11	99.49	99.50	99.14	100.31	98.99	100.96	99.36	99.17	98.94
Zn	130.90	24.10	40.10	81.10	53.80	98.50	73.00	71.90	75.40	78.10
Cu	58.90	29.70	185.00	38.80	706.40	72.50	182.10	893.50	4477.80	458.40
Ni	64.70	52.20	273.30	1338.60	906.20	820.00	399.90	886.60	2634.90	378.40
Nb	18.89	1.30	1.78	3.12	0.03	6.09	3.76	5.56	5.33	11.90
Zr	348.53	52.67	37.00	47.19	79.30	85.41	101.26	111.02	128.45	200.98
Y	52.25	7.14	12.65	8.80	10.95	15.60	23.28	25.88	21.46	26.11
Sr	347.29	26.99	70.76	22.12	144.15	30.19	283.15	107.68	368.59	242.07
Rb	51.03	4.67	5.18	11.00	14.53	16.92	9.91	17.80	26.69	62.79
Co	50.60	11.40	41.00	152.80	27.10	111.30	29.40	72.40	137.00	60.70
Cr	30.10	90.30	58.90	189.60	27.70	448.20	177.50	493.80	400.40	191.60
V	277.70	41.30	38.80	75.30	56.20	148.70	54.50	198.00	243.60	169.20
Ce	91.68	9.18	12.66	15.52	18.10	27.46	31.20	33.89	38.95	41.26
Nd	51.48	4.47	7.04	6.78	11.18	14.12	16.29	18.48	20.96	20.28
La	33.22	3.45	4.82	5.19	7.22	8.72	8.15	9.05	12.98	13.63
Ba	446.70	12.70	9.80	30.70	45.70	54.40	83.90	100.30	210.40	283.20
Sc	23.30	7.90	5.30	16.60	6.10	25.20	6.90	34.30	29.00	25.80
Th	3.94	2.48	2.24	2.25	1.27	2.33	2.43	3.11	2.35	4.69
Pb	3.14	3.86	1.49	1.38	6.74	0.57	5.08	5.66	5.61	7.79
S	1887.39	308.16	6953.43	1245.26	11100.88	884.56	2772.88	4145.25	23293.02	2573.98

Table D-2 *Whole-rock XRF analyses of borehole SH8, including $H2O^-$ and LOI.*

SAMPLE	SH8-8	SH8-9	SH8-10	SH8-11	SH8-15	SH8-16	SH8-17
Depth m	*463.34*	*465.07*	*465.97*	*466.40*	*466.73*	*468.26*	*469.86*
	Basal Gabbro	Basal Gabbro	Basal Gabbro	BG - chill	Quartzite	Dolomite	Diabase
SiO_2	48.07		52.09	50.24	96.64	24.38	49.77
TiO_2	1.33		1.87	1.65	0.02	0.24	2.61
Al_2O_3	12.86		14.65	14.21	0.71	6.12	14.44
FeO	7.18		8.24	6.98	1.22	4.44	10.88
MnO	0.15		0.13	0.11	0.02	0.32	0.33
MgO	5.02		5.14	5.62	0.33	16.23	4.88
CaO	7.40		6.16	9.59	0.24	23.62	6.80
Na_2O	2.63		3.71	3.46	0.23	0.01	3.68
K_2O	1.13		1.06	1.64	0.01	0.08	2.04
P_2O_5	0.14		0.21	0.20	0.00	0.06	0.52
FeS	9.273		1.596	0.077	0.059	0.194	0.241
CuS	1.718		0.291	0.017	0.006	0.034	0.093
NiS	0.434		0.104	0.021	0.004	0.023	0.023
LOI	2.53		2.86	4.29	0.27	22.06	1.18
H_2O^-	0.19		0.38	0.34	0.15	0.36	0.38
TOTAL	100.05		98.49	98.45	99.92	98.17	97.84
Zn	80.10	91.00	54.90	50.20	8.80	66.10	113.00
Cu	11417.20	14335.00	1933.10	110.90	37.20	227.50	617.40
Ni	2804.20	2251.20	673.70	136.90	26.50	148.40	147.00
Nb	7.57	9.97	11.57	11.16	-0.45	3.83	20.02
Zr	146.91	142.02	149.34	127.36	51.84	47.99	394.68
Y	24.82	25.10	30.74	36.36	1.16	12.54	51.84
Sr	399.98	443.23	297.48	371.99	11.11	122.80	378.70
Rb	40.72	52.00	31.06	63.90	0.62	4.07	80.37
Co	137.10	114.90	52.30	24.30	2.80	20.30	31.70
Cr	84.30	48.80	40.50	51.40	56.90	142.90	31.90
V	220.30	233.70	230.00	224.20	8.80	41.70	278.20
Ce	57.41	55.14	46.77	48.47	2.28	15.23	90.82
Nd	27.79	26.51	23.26	30.91	1.41	8.39	47.93
La	20.31	17.71	13.70	18.43	1.52	4.97	35.55
Ba	223.00	356.90	261.80	364.00	5.30	-22.40	328.50
Sc	25.30	24.90	23.20	24.50	0.40	-0.90	24.50
Th	4.17	8.92	3.32	0.39	0.90	3.12	4.14
Pb	16.87	20.86	5.52	0.98	6.14	1.93	17.74
S	41108.18	0.00	7162.47	413.18	249.98	904.40	1269.83

Table D-2 (cont) *Whole-rock XRF analyses of borehole SH8, including $H2O^-$ and LOI.*

SAMPLE	SH10-17	SH10-18	SH10-1	SH10-2	SH10-3	SH10-4	SH10-5	SH10-19	SH10-6	SH10-7	SH10-8
Depth m	*371.70*	*386.13*	*390.45*	*393.17*	*396.89*	*398.74*	*400.16*	*400.95*	*401.09*	*403.18*	*403.49*
	Diabase	LrPXT	LrPXT	LrPXT	LrPXT	LrPXT	LrPXT	LrPXT	LrPXT	Basal Gabbro	Basal Gabbro
SiO_2	48.50	55.02	41.21	41.96	48.75	43.57	46.85	49.94	44.29	50.44	52.42
TiO_2	2.37	0.59	0.31	0.30	0.90	0.34	0.96	1.14	0.98	0.85	1.69
Al_2O_3	14.30	13.70	12.42	6.16	9.82	5.36	7.84	7.24	8.59	13.26	10.82
FeO	12.93	4.77	13.69	12.19	6.60	14.95	12.33	11.18	13.43	7.30	8.96
MnO	0.18	0.11	0.20	0.25	0.32	0.20	0.17	0.17	0.17	0.20	0.21
MgO	5.02	8.18	26.17	25.50	10.53	25.11	19.59	15.67	20.27	7.51	7.96
CaO	7.66	7.15	4.12	6.56	16.52	4.67	6.53	6.30	5.17	15.07	9.06
Na_2O	3.12	4.00	0.47	0.70	2.06	0.68	1.32	0.93	0.11	1.20	2.81
K_2O	1.47	0.77	0.58	0.37	0.55	0.22	0.47	1.28	0.98	1.32	1.10
P_2O_5	0.46	0.17	0.07	0.02	0.07	0.02	0.07	0.10	0.07	0.14	0.08
FeS	0.504	0.009	0.222	4.209	1.759	1.371	0.964	1.868	0.666	0.498	1.725
CuS	0.011	0.001	0.049	0.209	0.083	0.231	0.087	0.229	0.084	0.005	0.118
NiS	0.015	0.023	0.270	0.380	0.095	0.313	0.179	0.180	0.178	0.046	0.086
LOI	1.18	3.15	5.24	1.24	1.76	1.61	1.43	2.23	4.71	1.19	1.57
H_2O^-	0.25	0.26	0.43	0.20	0.19	0.18	0.18	0.27	0.23	0.09	0.12
TOTAL	97.98	97.91	105.44	100.24	100.01	98.82	98.97	98.72	99.93	99.12	98.75
Zn	132.00	28.50	92.80	106.30	55.60	119.30	95.00	89.40	101.50	50.70	73.20
Cu	72.90	9.90	322.60	1389.00	550.10	1537.80	575.40	1521.70	557.90	36.00	786.10
Ni	94.90	150.10	1745.20	2454.80	617.20	2025.50	1157.00	1161.20	1153.70	296.60	553.90
Nb	16.29	11.24	2.77	1.31	2.27	1.84	5.65	5.90	5.14	5.97	11.41
Zr	329.40	384.74	43.64	31.61	74.92	36.36	74.56	98.35	59.81	110.65	164.54
Y	46.76	18.90	7.67	6.70	20.85	7.34	13.61	16.26	12.24	16.65	26.10
Sr	412.79	291.22	107.63	131.52	809.45	161.39	224.65	179.25	73.33	285.91	314.65
Rb	47.34	27.60	15.59	11.95	18.02	7.66	16.83	54.12	45.36	21.57	39.49
Co	56.50	19.50	157.50	195.70	56.70	177.50	129.50	112.50	141.20	38.50	73.00
Cr	32.80	16.40	130.60	611.00	368.90	302.10	454.50	758.90	294.80	390.30	447.40
V	275.30	56.10	47.20	73.10	224.30	68.90	136.70	186.90	109.70	127.50	232.10
Ce	74.34	21.86	21.66	16.97	26.30	18.98	23.92	31.53	22.34	35.73	41.95
Nd	44.06	12.28	11.48	6.18	14.09	8.33	12.51	16.95	8.33	18.20	22.29
La	32.66	9.64	7.73	1.97	9.92	4.88	9.37	10.78	5.91	15.45	14.46
Ba	439.70	128.20	126.00	126.70	445.40	102.20	172.30	210.80	94.90	244.60	284.10
Sc	22.60	6.50	12.50	19.70	36.50	16.40	23.10	26.00	15.90	21.90	29.50
Th	2.29	11.40	2.29	3.82	-2.38	2.16	2.33	2.65	2.17	2.62	2.33
Pb	8.89	6.34	4.31	13.98	7.66	11.86	3.96	7.22	2.32	10.67	7.82
S	1925.65	120.68	1924.30	17392.21	7028.93	6882.48	4439.01	8214.64	3341.79	1994.90	6990.33

Table D-3 *Whole-rock XRF analyses of borehole SH10, including $H2O^-$ and LOI.*

SAMPLE	SH10-20	SH10-21	SH10-22	SH10-9	SH10-10	SH10-11	SH10-12	SH10-13	SH10-14	SH10-15	SH10-16
Depth m	*403.59*	*403.70*	*403.99*	*404.07*	*404.90*	*405.40*	*405.66*	*407.22*	*408.58*	*409.46*	*422.40*
	Basal Gabbro	Dolomite	Dolomite	Basal Gabbro	Basal Gabbro	Basal Gabbro	Basal Gabbro	Basal Gabbro	Basal Gabbro	BG - chill	Diabase
SiO_2	49.88	42.43	39.66	46.20	43.31	43.41	50.95	51.09	50.57	50.47	50.15
TiO_2	1.09	0.47	1.01	1.02	1.41	1.48	1.67	1.53	1.75	1.80	2.39
Al_2O_3	8.53	6.03	6.20	8.00	11.76	12.81	14.51	13.58	14.55	14.53	14.21
FeO	8.16	6.95	7.55	13.21	6.58	7.02	11.07	10.61	11.03	11.20	12.17
MnO	0.26	0.17	0.16	0.19	0.15	0.15	0.16	0.17	0.16	0.16	0.16
MgO	8.62	15.90	19.69	18.96	6.12	5.76	6.04	6.36	5.70	5.52	4.10
CaO	14.13	21.75	16.49	5.86	8.30	8.53	9.34	8.57	9.19	9.22	7.28
Na_2O	2.56	0.03	0.14	0.71	1.96	2.12	2.79	2.83	2.90	3.12	3.23
K_2O	0.49	0.02	0.12	0.44	0.52	0.63	0.73	1.08	0.87	0.69	1.59
P_2O_5	0.05	0.07	0.09	0.09	0.08	0.07	0.09	0.11	0.15	0.18	0.51
FeS	2.643	1.332	1.392	0.153	16.243	14.025	0.505	0.731	0.491	0.541	0.460
CuS	0.161	0.154	0.083	0.034	1.483	1.287	0.026	0.029	0.015	0.015	0.008
NiS	0.110	0.117	0.096	0.145	0.754	0.645	0.015	0.029	0.013	0.013	0.008
LOI	2.27	3.49	5.87	3.42	2.03	2.46	0.51	1.56	1.00	0.67	0.99
H_2O^-	0.28	0.30	0.46	0.26	0.02	0.14	0.10	0.18	0.10	0.10	0.10
TOTAL	99.23	99.21	99.02	98.67	100.72	100.54	98.50	98.45	98.47	98.23	97.37
Zn	68.40	22.90	35.50	110.20	56.50	71.40	96.50	78.50	94.00	104.60	112.20
Cu	1073.00	1022.70	550.70	225.30	9858.70	8551.80	174.80	192.40	97.70	99.40	54.00
Ni	710.10	754.90	624.10	939.00	4878.50	4171.60	98.70	186.40	84.30	83.60	54.90
Nb	6.71	2.53	3.43	7.56	5.36	4.02	6.57	9.17	7.35	7.86	18.58
Zr	116.55	95.54	137.66	90.83	87.39	74.28	109.19	121.40	110.68	103.58	349.94
Y	32.17	19.46	27.17	16.30	18.80	19.57	22.11	24.35	24.28	25.61	52.56
Sr	361.27	58.94	68.36	240.95	361.26	442.91	473.11	416.29	481.95	485.77	354.64
Rb	10.17	1.60	4.41	17.66	20.65	22.55	27.98	40.94	31.36	23.42	56.06
Co	81.80	51.10	72.20	116.10	310.10	250.60	58.70	58.10	55.90	55.60	46.90
Cr	703.00	183.30	470.30	276.70	113.60	85.40	61.60	87.90	47.20	43.50	25.70
V	256.20	68.50	92.30	138.40	241.40	317.50	281.10	248.30	276.90	270.10	263.80
Ce	36.13	27.55	30.88	31.81	32.24	34.47	32.55	36.45	37.69	42.05	91.44
Nd	24.99	16.00	18.52	15.80	17.27	14.89	19.46	20.21	20.93	23.31	49.49
La	12.60	9.68	13.36	9.77	9.48	5.45	7.86	9.96	11.36	11.01	33.56
Ba	133.00	-8.20	29.40	165.10	198.50	279.70	251.30	220.80	234.60	250.20	457.20
Sc	30.40	7.10	18.70	19.30	26.70	26.60	26.50	27.30	26.30	25.70	21.50
Th	1.00	3.19	2.36	1.21	3.02	3.19	0.75	1.36	0.78	0.13	4.75
Pb	5.99	3.58	3.94	4.71	12.39	0.74	5.67	5.12	3.62	3.95	5.30
S	10566.08	5786.99	5694.82	1184.18	66873.45	57741.73	1985.42	2864.42	1886.33	2067.14	1734.40

Table D-3 (cont) *Whole-rock XRF analyses of borehole SH10, including $H2O^-$ and LOI.*

SAMPLE	SH25-1	SH25-2	SH25-3	SH25-4	SH25-5
Depth m	*641.38*	*641.74*	*642.09*	*642.39*	*642.78*
	LrPXT	Basal Gabbro	Basal Gabbro	Basal Gabbro	Basal Gabbro
SiO_2	46.61	52.61	52.47	54.12	53.01
TiO_2	0.85	0.94	1.05	1.36	1.48
Al_2O_3	7.65	14.93	14.20	14.43	14.85
FeO	14.41	8.05	8.39	8.66	8.98
MnO	0.18	0.14	0.16	0.16	0.17
MgO	16.84	6.50	6.12	4.86	5.05
CaO	5.92	8.13	7.60	6.58	6.32
Na_2O	0.23	3.01	3.57	3.60	4.37
K_2O	2.02	2.25	1.74	1.91	1.04
P_2O_5	0.10	0.11	0.12	0.17	0.15
FeS	0.137	0.486	0.267	0.279	0.118
CuS	0.012	0.031	0.027	0.034	0.019
NiS	0.144	0.026	0.016	0.012	0.013
LOI	3.31	1.59	2.46	2.18	2.51
H_2O^-	0.31	0.32	0.32	0.26	0.36
TOTAL	98.71	99.12	98.51	98.62	98.43
Zn	99.90	75.80	73.20	60.90	46.90
Cu	79.30	208.30	181.30	224.40	125.40
Ni	928.80	167.60	103.60	74.90	81.40
Nb	4.41	7.01	5.60	10.75	8.72
Zr	68.33	115.66	119.50	182.70	81.93
Y	15.01	21.47	22.92	29.42	20.22
Sr	78.29	467.83	320.16	320.71	237.59
Rb	148.07	82.57	45.20	54.80	24.30
Co	142.00	51.40	42.00	37.10	32.00
Cr	234.20	82.00	71.00	44.10	39.20
V	134.40	164.80	174.30	197.20	227.80
Ce	26.56	36.88	35.40	51.91	29.86
Nd	12.47	19.53	20.63	27.43	17.19
La	6.98	14.19	13.98	19.53	11.03
Ba	88.40	312.90	312.30	340.00	181.70
Sc	18.80	24.30	24.30	22.70	24.00
Th	2.89	0.54	0.82	3.85	0.88
Pb	2.70	3.95	5.37	2.70	2.71
S	1045.10	1967.41	1123.53	1170.34	536.50

Table D-4 *Whole-rock XRF analyses of borehole SH25, including H2O⁻ and LOI.*

SAMPLE	SH26-1	SH26-2	SH26-3	SH26-4	SH26-5	SH26-6	SH26-7	SH26-8	SH26-9	SH26-1C
Depth m	*491.06*	*491.68*	*492.02*	*492.58*	*493.20*	*493.46*	*494.21*	*494.88*	*496.74*	*498.97*
	LrPXT	Basal Gabbro	Basal Gabbro	Basal Gabbro	Basal Gabbro	Basal Gabbro	Basal Gabbro	Basal Gabbro	Basal Gabbro	Basal Gabbro
SiO_2	43.66	43.50	47.56	42.38	48.77	53.36	54.56	53.73	53.81	55.84
TiO_2	1.21	1.11	1.10	1.09	1.46	1.53	1.54	1.50	0.66	1.48
Al_2O_3	7.15	8.94	11.39	9.33	13.13	14.26	14.36	13.89	16.67	14.44
FeO	12.36	14.55	7.73	6.03	6.64	8.67	7.48	9.43	5.17	7.54
MnO	0.19	0.22	0.16	0.17	0.16	0.16	0.12	0.17	0.07	0.14
MgO	19.64	14.96	7.20	6.80	4.46	4.45	5.01	5.08	2.93	4.07
CaO	8.17	8.72	8.03	7.70	8.01	7.07	7.45	6.89	4.56	6.80
Na_2O	0.12	0.54	2.56	1.93	3.86	3.99	3.93	3.93	0.46	5.10
K_2O	0.12	0.29	1.58	1.07	0.91	1.55	2.13	1.46	10.56	1.28
P_2O_5	0.10	0.19	0.29	0.13	0.17	0.19	0.20	0.19	0.11	0.19
FeS	0.356	0.679	7.601	18.670	8.491	1.757	0.045	0.220	0.026	0.385
CuS	0.038	0.010	0.716	0.209	0.817	0.200	0.010	0.020	0.001	0.007
NiS	0.146	0.134	0.401	1.204	0.439	0.077	0.011	0.013	0.007	0.009
LOI	4.88	4.30	2.93	3.57	2.06	1.37	1.52	1.42	3.39	1.28
H_2O^-	0.58	0.40	0.36	0.19	0.17	0.30	0.34	0.40	0.42	0.20
TOTAL	98.71	98.53	99.59	100.47	99.56	98.93	98.70	98.34	98.86	98.75
Zn	84.00	88.60	46.20	59.90	24.90	49.40	36.70	69.70	29.10	45.70
Cu	249.70	65.40	4756.90	1391.50	5430.00	1330.80	68.60	132.90	9.50	43.40
NI	944.10	864.60	2594.10	7790.10	2841.40	495.20	68.60	82.60	47.20	56.10
Nb	7.63	7.03	8.73	8.11	11.03	15.25	14.27	13.49	27.45	12.90
Zr	114.53	100.70	157.97	130.64	179.67	213.08	208.49	202.42	615.08	215.25
Y	14.66	19.25	35.18	23.87	26.79	30.26	33.95	31.99	31.93	30.90
Sr	25.79	46.99	253.83	270.97	397.25	348.92	297.06	308.10	213.85	359.99
Rb	3.56	6.90	52.35	37.67	22.19	45.58	57.99	47.75	268.40	41.46
Co	93.90	76.70	180.50	426.70	164.90	56.30	19.10	37.50	12.00	32.20
Cr	277.70	193.10	192.80	231.50	51.60	45.40	34.90	70.80	6.90	37.70
V	158.80	207.40	245.20	219.20	215.40	214.20	201.30	208.50	36.90	199.90
Ce	24.19	35.11	67.80	43.40	54.05	59.10	56.49	57.12	34.59	58.00
Nd	10.48	18.42	37.68	23.42	29.33	32.45	30.64	30.53	22.60	30.37
La	10.12	11.39	25.66	19.78	22.76	23.84	21.74	24.91	15.12	23.91
Ba	6.80	54.90	372.10	286.90	255.00	398.90	654.20	374.40	3787.50	402.10
Sc	17.20	18.30	27.60	27.40	23.30	23.10	23.70	24.20	7.90	21.80
Th	3.32	4.42	5.05	6.31	5.04	4.46	3.41	4.35	16.21	3.03
Pb	3.16	5.82	5.76	6.84	5.76	5.66	1.53	4.22	1.16	2.39
S	1940.11	2980.84	31536.93	73042.96	35255.42	7350.45	235.29	915.14	124.62	1458.23

Table D-5 *Whole-rock XRF analyses of borehole SH26, including H2O$^-$ and LOI.*

SAMPLE	SH27-13	SH27-14	SH27-1	SH27-2	SH27-3	SH27-15	SH27-4	SH27-5
Depth m	*564.40*	*566.98*	*567.32*	*568.59*	*569.01*	*570.33*	*570.68*	*571.30*
	Diabase	Dia - chill	LrPXT	LrPXT	LrPXT	Dolomite	Basal Gabbro	Basal Gabbro
SiO_2	49.04	48.32	45.00	47.46	46.31	38.05	52.62	50.81
TiO_2	2.35	2.55	0.66	1.04	1.11	0.61	0.91	1.20
Al_2O_3	14.13	14.24	6.61	7.49	8.90	7.78	10.65	10.45
FeO	12.81	13.29	13.11	11.31	13.22	5.45	8.98	8.90
MnO	0.16	0.18	0.20	0.17	0.16	0.25	0.15	0.15
MgO	4.88	4.75	20.34	17.65	17.45	21.38	9.48	8.93
CaO	7.50	7.91	6.60	5.01	6.02	17.16	8.03	8.16
Na_2O	3.28	3.25	0.17	0.73	0.83	0.02	2.30	2.33
K_2O	1.61	1.29	0.78	1.20	1.06	0.01	0.95	0.96
P_2O_5	0.46	0.52	0.09	0.11	0.08	0.06	0.08	0.13
FeS	0.457	0.520	0.390	2.511	0.375	0.517	2.513	4.491
CuS	0.008	0.009	0.020	0.272	0.062	0.027	0.199	0.101
NiS	0.013	0.010	0.182	0.346	0.140	0.043	0.182	0.313
LOI	1.27	0.94	4.23	2.90	3.10	7.21	1.58	1.95
H_2O^-	0.24	0.20	0.42	0.35	0.42	0.36	0.29	0.26
TOTAL	98.20	97.96	98.81	98.55	99.24	98.92	98.92	99.14
Zn	65.20	118.30	87.40	94.30	103.40	24.50	61.70	86.10
Cu	54.70	56.80	134.20	1809.10	408.90	178.40	1321.00	670.30
Ni	86.60	67.80	1179.90	2235.90	905.10	280.60	1177.40	2023.80
Nb	17.42	18.57	5.08	7.85	8.27	3.04	6.62	7.81
Zr	336.36	315.27	78.51	93.03	87.36	111.56	139.34	167.11
Y	48.82	52.49	15.86	15.18	16.79	20.37	21.13	25.98
Sr	370.56	368.69	62.62	157.29	222.60	15.90	271.50	268.74
Rb	57.96	39.64	41.63	57.54	40.67	0.69	37.63	39.85
Co	53.20	54.10	138.40	158.10	118.90	33.00	99.50	131.90
Cr	31.30	30.60	294.00	580.80	382.00	63.10	617.50	742.10
V	281.50	296.80	132.80	147.50	179.60	51.80	180.40	220.30
Ce	78.96	86.36	31.14	34.64	34.46	19.28	37.00	46.29
Nd	45.08	49.30	12.93	15.83	16.31	13.43	19.79	22.99
La	32.64	36.39	10.74	13.08	14.59	7.48	11.06	15.31
Ba	483.10	434.50	95.90	287.30	208.90	5.40	229.60	172.00
Sc	23.10	24.40	21.90	19.70	21.80	8.10	31.00	31.20
Th	2.91	1.93	2.85	3.32	2.97	1.14	3.61	4.13
Pb	2.47	2.09	2.05	4.15	3.97	0.83	7.72	6.69
S	1740.95	1962.66	2135.29	11289.70	2066.63	2129.14	10473.52	17822.10

Table D-6 *Whole-rock XRF analyses of borehole SH27, including $H2O^-$ and LOI.*

SAMPLE	SH27-6	SH27-7	SH27-8	SH27-9	SH27-16	SH27-10	SH27-11	SH27-12
Depth m	*572.04*	*572.82*	*573.75*	*574.58*	*575.07*	*575.72*	*576.58*	*577.56*
	Basal Gabbro	Basal Gabbro	Basal Gabbro	Basal Gabbro	Diabase	Basal Gabbro	Basal Gabbro	Basal Gabbro
SiO_2			54.14	54.34	50.24	54.65	54.62	54.98
TiO_2			1.55	1.52	2.40	1.53	1.47	1.52
Al_2O_3			14.35	14.29	14.25	14.50	14.31	14.46
FeO			9.89	9.14	11.68	9.48	9.36	8.50
MnO			0.15	0.13	0.16	0.14	0.15	0.11
MgO			4.53	4.48	4.40	4.43	4.43	4.29
CaO			7.21	7.45	7.85	7.46	7.39	7.37
Na_2O			3.36	3.27	3.57	3.37	3.14	3.44
K_2O			1.59	1.37	1.44	1.33	1.50	1.23
P_2O_5			0.18	0.18	0.49	0.18	0.17	0.18
FeS			0.361	0.802	0.520	0.426	0.488	0.738
CuS			0.016	0.024	0.014	0.013	0.046	0.029
NIS			0.011	0.011	0.010	0.010	0.014	0.012
LOI			1.76	1.64	0.91	1.31	1.47	1.35
H_2O^-			0.35	0.31	0.19	0.27	0.29	0.24
TOTAL			99.44	98.95	98.12	99.08	98.86	98.42
Zn	11.40	30.70	61.10	54.10	62.50	78.00	82.90	32.20
Cu	14233.10	15491.60	108.20	159.60	94.30	83.20	308.60	193.60
Ni	2217.10	4423.60	70.80	68.40	63.40	64.20	92.30	74.80
Nb	11.51	8.92	12.24	12.60	18.61	13.49	12.07	13.01
Zr	118.85	127.56	188.66	205.74	367.92	186.80	202.43	204.38
Y	25.03	22.79	19.02	30.44	52.64	28.92	30.04	30.36
Sr	278.30	460.04	404.29	401.48	358.13	415.70	390.99	366.92
Rb	31.47	41.17	52.46	51.99	53.52	51.76	56.20	46.62
Co	150.50	253.90	42.20	46.60	46.80	44.20	42.40	41.20
Cr	495.40	53.00	40.00	40.10	29.90	37.60	39.00	34.70
V	237.60	235.10	209.90	217.30	276.60	214.00	208.30	216.70
Ce	50.49	54.85	57.17	58.22	85.12	61.47	54.97	55.69
Nd	27.09	25.69	28.22	29.23	46.73	31.42	29.26	29.65
La	16.68	15.29	21.16	21.60	34.51	21.63	22.20	21.81
Ba	156.50	252.80	347.30	288.70	467.60	352.90	371.30	230.30
Sc	29.10	22.80	23.10	22.90	23.50	22.80	22.30	23.10
Th	3.54	7.01	3.37	3.74	3.30	3.05	3.87	4.34
Pb	4.96	14.94	3.35	4.45	2.30	6.09	4.75	2.75
S	0.00	0.00	1409.72	3043.91	1979.60	1631.02	1985.16	2831.29

Table D-6 (cont) *Whole-rock XRF analyses of borehole SH27, including $H2O^-$ and LOI.*

SAMPLE	SH8-12	SH8-13	SH8-14	SH8-1	SH8-2	SH8-3	SH8-4	SH8-5	SH8-6	SH8-7
Depth m	*450.24*	*451.41*	*452.80*	*453.66*	*455.41*	*457.45*	*457.92*	*459.41*	*460.34*	*461.92*
	Diabase	Quartzite	LrPXT	LrPXT	LrPXT	LrPXT	Hybrid	Hybrid	Hybrid	Basal Gabbro
SiO_2	50.68	82.56	50.27	44.25	48.68	47.59	48.58	52.11	49.75	55.23
TiO_2	2.51	0.18	0.23	0.62	0.39	0.87	0.40	1.01	1.29	1.23
Al_2O_3	14.74	2.13	2.66	6.10	5.69	7.39	9.50	6.44	10.54	11.70
FeO	13.25	3.67	6.82	16.78	6.93	12.95	7.86	10.61	9.60	10.35
MnO	0.18	0.08	0.14	0.19	0.24	0.24	0.17	0.22	0.20	0.18
MgO	4.63	3.54	19.19	26.30	17.59	21.13	13.96	14.93	9.77	9.15
CaO	7.66	6.27	18.35	4.91	16.40	8.92	16.94	11.70	8.99	7.16
Na_2O	3.61	1.33	0.12	0.15	0.46	0.14	1.28	1.15	2.13	2.50
K_2O	1.68	0.13	0.14	0.28	0.40	0.42	0.47	0.55	0.93	1.67
P_2O_5	0.52	0.04	0.08	0.05	0.05	0.09	0.06	0.10	0.10	0.11
FeS	0.516	0.074	1.924	0.146	2.920	0.117	0.692	0.907	5.578	0.606
CuS	0.009	0.005	0.029	0.006	0.110	0.012	0.028	0.139	0.699	0.071
NiS	0.010	0.008	0.044	0.223	0.146	0.135	0.063	0.141	0.423	0.060
TOTAL	100.00	100.00	100.00	100.00	100.00	100.00	100.00	100.00	100.00	100.00
Zn	130.90	24.10	40.10	81.10	53.80	98.50	73.00	71.90	75.40	78.10
Cu	58.90	29.70	185.00	38.80	706.40	72.50	182.10	893.50	4477.80	458.40
Ni	64.70	52.20	273.30	1338.60	906.20	820.00	399.90	886.60	2634.90	378.40
Nb	18.89	1.30	1.78	3.12	0.03	6.09	3.76	5.56	5.33	11.90
Zr	348.53	52.67	37.00	47.19	79.30	85.41	101.26	111.02	128.45	200.98
Y	52.25	7.14	12.65	8.80	10.95	15.60	23.28	25.88	21.46	26.11
Sr	347.29	26.99	70.76	22.12	144.15	30.19	283.15	107.68	368.59	242.07
Rb	51.03	4.67	5.18	11.00	14.53	16.92	9.91	17.80	26.69	62.79
Co	50.60	11.40	41.00	152.80	27.10	111.30	29.40	72.40	137.00	60.70
Cr	30.10	90.30	58.90	189.60	27.70	448.20	177.50	493.80	400.40	191.60
V	277.70	41.30	38.80	75.30	56.20	148.70	54.50	198.00	243.60	169.20
Ce	91.68	9.18	12.66	15.52	18.10	27.46	31.20	33.89	38.95	41.26
Nd	51.48	4.47	7.04	6.78	11.18	14.12	16.29	18.48	20.96	20.28
La	33.22	3.45	4.82	5.19	7.22	8.72	8.15	9.05	12.98	13.63
Ba	446.70	12.70	9.80	30.70	45.70	54.40	83.90	100.30	210.40	283.20
Sc	23.30	7.90	5.30	16.60	6.10	25.20	6.90	34.30	29.00	25.80
Th	3.94	2.48	2.24	2.25	1.27	2.33	2.43	3.11	2.35	4.69
Pb	3.14	3.86	1.49	1.38	6.74	0.57	5.08	5.66	5.61	7.79
S	1887.39	308.16	6953.43	1245.26	11100.88	884.56	2772.88	4145.25	23293.02	2573.98

Table D-7 *Whole-rock XRF analyses of borehole SH8, normalised for H2O$^-$ and LOI free.*

SAMPLE	SH8-8	SH8-9	SH8-10	SH8-11	SH8-15	SH8-16	SH8-17
Depth m	*463.34*	*465.07*	*465.97*	*466.40*	*466.73*	*468.26*	*469.86*
	Basal Gabbro	Basal Gabbro	Basal Gabbro	BG - chill	Quartzite	Dolomite	Diabase
SiO_2	49.39		54.69	53.55	97.13	32.18	51.68
TiO_2	1.37		1.96	1.76	0.02	0.31	2.71
Al_2O_3	13.21		15.38	15.14	0.71	8.08	14.99
FeO	7.38		8.65	7.44	1.23	5.86	11.30
MnO	0.15		0.14	0.12	0.02	0.42	0.34
MgO	5.16		5.39	5.99	0.33	21.43	5.06
CaO	7.60		6.46	10.22	0.25	31.18	7.06
Na_2O	2.70		3.89	3.68	0.23	0.01	3.82
K_2O	1.17		1.12	1.75	0.01	0.11	2.12
P_2O_5	0.14		0.22	0.21	0.00	0.08	0.54
FeS	9.526		1.675	0.083	0.060	0.257	0.250
CuS	1.765		0.305	0.018	0.006	0.045	0.096
NiS	0.445		0.109	0.023	0.004	0.030	0.024
TOTAL	100.00		100.00	100.00	100.00	100.00	100.00
Zn	80.10	91.00	54.90	50.20	8.80	66.10	113.00
Cu	11417.20	14335.00	1933.10	110.90	37.20	227.50	617.40
Ni	2804.20	2251.20	673.70	136.90	26.50	148.40	147.00
Nb	7.57	9.97	11.57	11.16	-0.45	3.83	20.02
Zr	146.91	142.02	149.34	127.36	51.84	47.99	394.68
Y	24.82	25.10	30.74	36.36	1.16	12.54	51.84
Sr	399.98	443.23	297.48	371.99	11.11	122.80	378.70
Rb	40.72	52.00	31.06	63.90	0.62	4.07	80.37
Co	137.10	114.90	52.30	24.30	2.80	20.30	31.70
Cr	84.30	48.80	40.50	51.40	56.90	142.90	31.90
V	220.30	233.70	230.00	224.20	8.80	41.70	278.20
Ce	57.41	55.14	46.77	48.47	2.28	15.23	90.82
Nd	27.79	26.51	23.26	30.91	1.41	8.39	47.93
La	20.31	17.71	13.70	18.43	1.52	4.97	35.55
Ba	223.00	356.90	261.80	364.00	5.30	-22.40	328.50
Sc	25.30	24.90	23.20	24.50	0.40	-0.90	24.50
Th	4.17	8.92	3.32	0.39	0.90	3.12	4.14
Pb	16.87	20.86	5.52	0.98	6.14	1.93	17.74
S	41108.18	0.00	7162.47	413.18	249.98	904.40	1269.83

Table D-7 (cont) *Whole-rock XRF analyses of borehole SH8, normalised for H2O$^-$ and LOI free.*

SAMPLE	SH10-17	SH10-18	SH10-1	SH10-2	SH10-3	SH10-4	SH10-5	SH10-19	SH10-6	SH10-7	SH10-8
Depth m	*371.70*	*386.13*	*390.45*	*393.17*	*396.89*	*398.74*	*400.16*	*400.95*	*401.09*	*403.18*	*403.49*
	Diabase	LrPXT	LrPXT	LrPXT	LrPXT	LrPXT	LrPXT	LrPXT	LrPXT	Basal Gabbro	Basal Gabbro
SiO_2	50.24	58.22	41.30	42.47	49.72	44.90	48.12	51.90	46.63	51.56	54.01
TiO_2	2.45	0.63	0.31	0.30	0.92	0.35	0.98	1.19	1.03	0.86	1.74
Al_2O_3	14.81	14.49	12.45	6.23	10.01	5.52	8.05	7.53	9.04	13.55	11.15
FeO	13.39	5.05	13.72	12.34	6.74	15.41	12.67	11.62	14.13	7.46	9.23
MnO	0.19	0.11	0.20	0.25	0.32	0.20	0.18	0.18	0.18	0.20	0.22
MgO	5.20	8.66	26.23	25.81	10.73	25.87	20.12	16.28	21.33	7.68	8.21
CaO	7.94	7.57	4.12	6.63	16.85	4.81	6.71	6.54	5.45	15.40	9.34
Na_2O	3.24	4.24	0.47	0.71	2.10	0.70	1.35	0.97	0.12	1.23	2.89
K_2O	1.52	0.81	0.58	0.37	0.56	0.22	0.49	1.33	1.03	1.35	1.13
P_2O_5	0.47	0.18	0.07	0.02	0.07	0.02	0.07	0.10	0.07	0.14	0.08
FeS	0.522	0.010	0.222	4.260	1.794	1.413	0.990	1.942	0.702	0.509	1.777
CuS	0.011	0.002	0.049	0.212	0.084	0.238	0.089	0.238	0.088	0.006	0.122
NiS	0.015	0.025	0.270	0.384	0.097	0.323	0.184	0.187	0.188	0.047	0.088
TOTAL	100.00	100.00	100.00	100.00	100.00	100.00	100.00	100.00	100.00	100.00	100.00
Zn	132.00	28.50	92.80	106.30	55.60	119.30	95.00	89.40	101.50	50.70	73.20
Cu	72.90	9.90	322.60	1389.00	550.10	1537.80	575.40	1521.70	557.90	36.00	786.10
Ni	94.90	150.10	1745.20	2454.80	617.20	2025.50	1157.00	1161.20	1153.70	296.60	553.90
Nb	16.29	11.24	2.77	1.31	2.27	1.84	5.65	5.90	5.14	5.97	11.41
Zr	329.40	384.74	43.64	31.61	74.92	36.36	74.56	98.35	59.81	110.65	164.54
Y	46.76	18.90	7.67	6.70	20.85	7.34	13.61	16.26	12.24	16.65	26.10
Sr	412.79	291.22	107.63	131.52	809.45	161.39	224.65	179.25	73.33	285.91	314.65
Rb	47.34	27.60	15.59	11.95	18.02	7.66	16.83	54.12	45.36	21.57	39.49
Co	56.50	19.50	157.50	195.70	56.70	177.50	129.50	112.50	141.20	38.50	73.00
Cr	32.80	16.40	130.60	611.00	368.90	302.10	454.50	758.90	294.80	390.30	447.40
V	275.30	56.10	47.20	73.10	224.30	68.90	136.70	186.90	109.70	127.50	232.10
Ce	74.34	21.86	21.66	16.97	26.30	18.98	23.92	31.53	22.34	35.73	41.95
Nd	44.06	12.28	11.48	6.18	14.09	8.33	12.51	16.95	8.33	18.20	22.29
La	32.66	9.64	7.73	1.97	9.92	4.88	9.37	10.78	5.91	15.45	14.46
Ba	439.70	128.20	126.00	126.70	445.40	102.20	172.30	210.80	94.90	244.60	284.10
Sc	22.60	6.50	12.50	19.70	36.50	16.40	23.10	26.00	15.90	21.90	29.50
Th	2.29	11.40	2.29	3.82	-2.38	2.16	2.33	2.65	2.17	2.62	2.33
Pb	8.89	6.34	4.31	13.98	7.66	11.86	3.96	7.22	2.32	10.67	7.82
S	1925.65	120.68	1924.30	17392.21	7028.93	6882.48	4439.01	8214.64	3341.79	1994.90	6990.33

Table D-8 *Whole-rock XRF analyses of borehole SH10, normalised for H2O^{-} and LOI free.*

SAMPLE	SH10-20	SH10-21	SH10-22	SH10-9	SH10-10	SH10-11	SH10-12	SH10-13	SH10-14	SH10-15	SH10-16
Depth m	*403.59*	*403.70*	*403.99*	*404.07*	*404.90*	*405.40*	*405.66*	*407.22*	*408.58*	*409.46*	*422.40*
	Basal Gabbro	Dolomite	Dolomite	Basal Gabbro	Basal Gabbro	Basal Gabbro	Basal Gabbro	Basal Gabbro	Basal Gabbro	BG - chill	Diabase
SiO_2	51.60	44.46	42.79	48.63	43.89	44.33	52.04	52.82	51.93	51.79	52.10
TiO_2	1.13	0.50	1.09	1.07	1.43	1.51	1.71	1.58	1.79	1.84	2.48
Al_2O_3	8.82	6.32	6.69	8.42	11.92	13.08	14.82	14.04	14.94	14.91	14.76
FeO	8.44	7.28	8.15	13.91	6.67	7.17	11.31	10.97	11.32	11.50	12.64
MnO	0.27	0.18	0.17	0.20	0.16	0.16	0.16	0.17	0.16	0.16	0.17
MgO	8.91	16.66	21.24	19.96	6.20	5.88	6.17	6.58	5.85	5.66	4.26
CaO	14.61	22.79	17.79	6.17	8.41	8.71	9.54	8.86	9.43	9.46	7.56
Na_2O	2.64	0.03	0.15	0.74	1.98	2.16	2.85	2.93	2.98	3.20	3.36
K_2O	0.50	0.02	0.13	0.46	0.53	0.64	0.75	1.12	0.90	0.71	1.65
P_2O_5	0.06	0.07	0.10	0.09	0.08	0.07	0.09	0.12	0.15	0.18	0.53
FeS	2.733	1.396	1.502	0.161	16.462	14.321	0.516	0.756	0.504	0.555	0.478
CuS	0.167	0.161	0.089	0.036	1.503	1.314	0.027	0.030	0.015	0.015	0.008
NiS	0.114	0.122	0.104	0.153	0.764	0.659	0.016	0.030	0.013	0.013	0.009
TOTAL	100.00	100.00	100.00	100.00	100.00	100.00	100.00	100.00	100.00	100.00	100.00
Zn	68.40	22.90	35.50	110.20	56.50	71.40	96.50	78.50	94.00	104.60	112.20
Cu	1073.00	1022.70	550.70	225.30	9858.70	8551.80	174.80	192.40	97.70	99.40	54.00
Ni	710.10	754.90	624.10	939.00	4878.50	4171.60	98.70	186.40	84.30	83.60	54.90
Nb	6.71	2.53	3.43	7.56	5.36	4.02	6.57	9.17	7.35	7.86	18.58
Zr	116.55	95.54	137.66	90.83	87.39	74.28	109.19	121.40	110.68	103.58	349.94
Y	32.17	19.46	27.17	16.30	18.80	19.57	22.11	24.35	24.28	25.61	52.56
Sr	361.27	58.94	68.36	240.95	361.26	442.91	473.11	416.29	481.95	485.77	354.64
Rb	10.17	1.60	4.41	17.66	20.65	22.55	27.98	40.94	31.36	23.42	56.06
Co	81.80	51.10	72.20	116.10	310.10	250.60	58.70	58.10	55.90	55.60	46.90
Cr	703.00	183.30	470.30	276.70	113.60	85.40	61.60	87.90	47.20	43.50	25.70
V	256.20	68.50	92.30	138.40	241.40	317.50	281.10	248.30	276.90	270.10	263.80
Ce	36.13	27.55	30.88	31.81	32.24	34.47	32.55	36.45	37.69	42.05	91.44
Nd	24.99	16.00	18.52	15.80	17.27	14.89	19.46	20.21	20.93	23.31	49.49
La	12.60	9.68	13.36	9.77	9.48	5.45	7.86	9.96	11.36	11.01	33.56
Ba	133.00	-8.20	29.40	165.10	198.50	279.70	251.30	220.80	234.60	250.20	457.20
Sc	30.40	7.10	18.70	19.30	26.70	26.60	26.50	27.30	26.30	25.70	21.50
Th	1.00	3.19	2.36	1.21	3.02	3.19	0.75	1.36	0.78	0.13	4.75
Pb	5.99	3.58	3.94	4.71	12.39	0.74	5.67	5.12	3.62	3.95	5.30
S	10566.08	5786.99	5694.82	1184.18	66873.45	57741.73	1985.42	2864.42	1886.33	2067.14	1734.4C

Table D-8 (cont) *Whole-rock XRF analyses of borehole SH10, normalised for H2O$^-$ and LOI free.*

SAMPLE	SH25-1	SH25-2	SH25-3	SH25-4	SH25-5
Depth m	*641.38*	*641.74*	*642.09*	*642.39*	*642.78*
	LrPXT	Basal Gabbro	Basal Gabbro	Basal Gabbro	BG - chill
SiO_2	49.01	54.12	54.81	56.27	55.47
TiO_2	0.89	0.97	1.10	1.41	1.55
Al_2O_3	8.04	15.36	14.83	15.01	15.54
FeO	15.15	8.28	8.77	9.01	9.39
MnO	0.19	0.14	0.16	0.16	0.18
MgO	17.71	6.69	6.39	5.05	5.28
CaO	6.22	8.36	7.94	6.84	6.62
Na_2O	0.25	3.10	3.73	3.75	4.58
K_2O	2.12	2.31	1.81	1.99	1.08
P_2O_5	0.10	0.11	0.13	0.17	0.16
FeS	0.144	0.500	0.279	0.290	0.123
CuS	0.013	0.032	0.028	0.035	0.020
NiS	0.151	0.027	0.017	0.012	0.013
TOTAL	100.00	100.00	100.00	100.00	100.00
Zn	99.90	75.80	73.20	60.90	46.90
Cu	79.30	208.30	181.30	224.40	125.40
Ni	928.80	167.60	103.60	74.90	81.40
Nb	4.41	7.01	5.60	10.75	8.72
Zr	68.33	115.66	119.50	182.70	81.93
Y	15.01	21.47	22.92	29.42	20.22
Sr	78.29	467.83	320.16	320.71	237.59
Rb	148.07	82.57	45.20	54.80	24.30
Co	142.00	51.40	42.00	37.10	32.00
Cr	234.20	82.00	71.00	44.10	39.20
V	134.40	164.80	174.30	197.20	227.80
Ce	26.56	36.88	35.40	51.91	29.86
Nd	12.47	19.53	20.63	27.43	17.19
La	6.98	14.19	13.98	19.53	11.03
Ba	88.40	312.90	312.30	340.00	181.70
Sc	18.80	24.30	24.30	22.70	24.00
Th	2.89	0.54	0.82	3.85	0.88
Pb	2.70	3.95	5.37	2.70	2.71
S	1045.10	1967.41	1123.53	1170.34	536.50

Table D-9 *Whole-rock XRF analyses of borehole SH25, normalised for $H2O^-$ and LOI free.*

SAMPLE	SH26-1	SH26-2	SH26-3	SH26-4	SH26-5	SH26-6	SH26-7	SH26-8	SH26-9	SH26-1C
Depth m	*491.06*	*491.68*	*492.02*	*492.58*	*493.20*	*493.46*	*494.21*	*494.88*	*496.74*	*498.97*
	LrPXT	Basal Gabbro	Basal Gabbro	Basal Gabbro	Basal Gabbro	Basal Gabbro	Basal Gabbro	Basal Gabbro	Basal Gabbro	BG - chill
SIO_2	46.82	46.36	49.39	43.82	50.12	54.87	56.34	55.67	56.61	57.41
TIO_2	1.30	1.18	1.14	1.12	1.50	1.57	1.59	1.55	0.70	1.52
Al_2O_3	7.67	9.53	11.83	9.65	13.49	14.66	14.83	14.39	17.54	14.84
FeO	13.25	15.50	8.02	6.24	6.82	8.91	7.72	9.77	5.44	7.75
MnO	0.20	0.23	0.17	0.18	0.16	0.16	0.12	0.17	0.08	0.14
MgO	21.06	15.94	7.48	7.03	4.59	4.58	5.18	5.26	3.09	4.18
CaO	8.76	9.29	8.33	7.96	8.23	7.26	7.69	7.14	4.80	6.99
Na_2O	0.13	0.58	2.65	2.00	3.97	4.10	4.06	4.08	0.49	5.25
K_2O	0.13	0.31	1.64	1.11	0.94	1.60	2.20	1.51	11.11	1.32
P_2O_5	0.11	0.21	0.30	0.13	0.17	0.20	0.20	0.19	0.12	0.19
FeS	0.382	0.723	7.892	19.304	8.724	1.807	0.046	0.228	0.027	0.396
CuS	0.040	0.010	0.743	0.216	0.839	0.206	0.011	0.021	0.002	0.007
NIS	0.157	0.142	0.416	1.245	0.451	0.079	0.011	0.013	0.008	0.009
TOTAL	100.00	100.00	100.00	100.00	100.00	100.00	100.00	100.00	100.00	100.00
Zn	84.00	88.60	46.20	59.90	24.90	49.40	36.70	69.70	29.10	45.70
Cu	249.70	65.40	4756.90	1391.50	5430.00	1330.80	68.60	132.90	9.50	43.40
NI	944.10	864.60	2594.10	7790.10	2841.40	495.20	68.60	82.60	47.20	56.10
Nb	7.63	7.03	8.73	8.11	11.03	15.25	14.27	13.49	27.45	12.90
Zr	114.53	100.70	157.97	130.64	179.67	213.08	208.49	202.42	615.08	215.25
Y	14.66	19.25	35.18	23.87	26.79	30.26	33.95	31.99	31.93	30.90
Sr	25.79	46.99	253.83	270.97	397.25	348.92	297.06	308.10	213.85	359.99
Rb	3.56	6.90	52.35	37.67	22.19	45.58	57.99	47.75	268.40	41.46
Co	93.90	76.70	180.50	426.70	164.90	56.30	19.10	37.50	12.00	32.20
Cr	277.70	193.10	192.80	231.50	51.60	45.40	34.90	70.80	6.90	37.70
V	158.80	207.40	245.20	219.20	215.40	214.20	201.30	208.50	36.90	199.90
Ce	24.19	35.11	67.80	43.40	54.05	59.10	56.49	57.12	34.59	58.00
Nd	10.48	18.42	37.68	23.42	29.33	32.45	30.64	30.53	22.60	30.37
La	10.12	11.39	25.66	19.78	22.76	23.84	21.74	24.91	15.12	23.91
Ba	6.80	54.90	372.10	286.90	255.00	398.90	654.20	374.40	3787.50	402.10
Sc	17.20	18.30	27.60	27.40	23.30	23.10	23.70	24.20	7.90	21.80
Th	3.32	4.42	5.05	6.31	5.04	4.46	3.41	4.35	16.21	3.03
Pb	3.16	5.82	5.76	6.84	5.76	5.66	1.53	4.22	1.16	2.39
S	1940.11	2980.84	31536.93	73042.96	35255.42	7350.45	235.29	915.14	124.62	1458.23

Table D-10 *Whole-rock XRF analyses of borehole SH26, normalised for H2O$^-$ and LOI free.*

SAMPLE	SH27-13	SH27-14	SH27-1	SH27-2	SH27-3	SH27-15	SH27-4	SH27-5
Depth m	*564.40*	*566.98*	*567.32*	*568.59*	*569.01*	*570.33*	*570.68*	*571.30*
	Diabase	Dia - chill	LrPXT	LrPXT	LrPXT	Dolomite	Basal Gabbro	Basal Gabbro
SiO_2	50.72	49.90	47.79	49.81	48.38	41.66	54.22	52.43
TiO_2	2.43	2.63	0.70	1.09	1.16	0.67	0.94	1.24
Al_2O_3	14.61	14.70	7.02	7.86	9.29	8.52	10.97	10.78
FeO	13.25	13.73	13.92	11.86	13.81	5.96	9.25	9.18
MnO	0.16	0.18	0.22	0.18	0.17	0.27	0.16	0.16
MgO	5.05	4.91	21.61	18.53	18.23	23.40	9.77	9.21
CaO	7.75	8.17	7.00	5.26	6.29	18.78	8.27	8.42
Na_2O	3.39	3.35	0.18	0.76	0.86	0.03	2.37	2.40
K_2O	1.66	1.33	0.83	1.26	1.11	0.01	0.98	0.99
P_2O_5	0.47	0.54	0.10	0.11	0.09	0.07	0.09	0.13
FeS	0.473	0.537	0.414	2.635	0.391	0.566	2.589	4.634
CuS	0.009	0.009	0.021	0.286	0.064	0.029	0.205	0.104
NiS	0.014	0.011	0.194	0.363	0.146	0.047	0.188	0.323
TOTAL	100.00	100.00	100.00	100.00	100.00	100.00	100.00	100.00
Zn	65.20	118.30	87.40	94.30	103.40	24.50	61.70	86.10
Cu	54.70	56.80	134.20	1809.10	408.90	178.40	1321.00	670.30
Ni	86.60	67.80	1179.90	2235.90	905.10	280.60	1177.40	2023.80
Nb	17.42	18.57	5.08	7.85	8.27	3.04	6.62	7.81
Zr	336.36	315.27	78.51	93.03	87.36	111.56	139.34	167.11
Y	48.82	52.49	15.86	15.18	16.79	20.37	21.13	25.98
Sr	370.56	368.69	62.62	157.29	222.60	15.90	271.50	268.74
Rb	57.96	39.64	41.63	57.54	40.67	0.69	37.63	39.85
Co	53.20	54.10	138.40	158.10	118.90	33.00	99.50	131.90
Cr	31.30	30.60	294.00	580.80	382.00	63.10	617.50	742.10
V	281.50	296.80	132.80	147.50	179.60	51.80	180.40	220.30
Ce	78.96	86.36	31.14	34.64	34.46	19.28	37.00	46.29
Nd	45.08	49.30	12.93	15.83	16.31	13.43	19.79	22.99
La	32.64	36.39	10.74	13.08	14.59	7.48	11.06	15.31
Ba	483.10	434.50	95.90	287.30	208.90	5.40	229.60	172.00
Sc	23.10	24.40	21.90	19.70	21.80	8.10	31.00	31.20
Th	2.91	1.93	2.85	3.32	2.97	1.14	3.61	4.13
Pb	2.47	2.09	2.05	4.15	3.97	0.83	7.72	6.69
S	1740.95	1962.66	2135.29	11289.70	2066.63	2129.14	10473.52	17822.10

Table D-11 *Whole-rock XRF analyses of borehole SH27, normalised for $H2O^-$ and LOI free.*

SAMPLE	SH27-6	SH27-7	SH27-8	SH27-9	SH27-16	SH27-10	SH27-11	SH27-12
Depth m	*572.04*	*572.82*	*573.75*	*574.58*	*575.07*	*575.72*	*576.58*	*577.56*
	Basal Gabbro	Basal Gabbro	Basal Gabbro	Basal Gabbro	Diabase	Basal Gabbro	Basal Gabbro	BG - chill
SiO_2			55.64	56.02	51.78	56.05	56.26	56.77
TiO_2			1.59	1.57	2.48	1.57	1.51	1.57
Al_2O_3			14.74	14.73	14.68	14.87	14.74	14.93
FeO			10.16	9.42	12.04	9.73	9.64	8.78
MnO			0.15	0.13	0.17	0.14	0.15	0.11
MgO			4.65	4.62	4.53	4.54	4.56	4.43
CaO			7.40	7.68	8.09	7.65	7.61	7.61
Na_2O			3.45	3.37	3.68	3.45	3.24	3.55
K_2O			1.63	1.41	1.48	1.36	1.55	1.27
P_2O_5			0.18	0.18	0.51	0.18	0.18	0.18
FeS			0.371	0.827	0.536	0.437	0.502	0.762
CuS			0.017	0.025	0.015	0.013	0.048	0.030
NiS			0.011	0.011	0.010	0.010	0.015	0.012
TOTAL			100.00	100.00	100.00	100.00	100.00	100.00
Zn	11.40	30.70	61.10	54.10	62.50	78.00	82.90	32.20
Cu	14233.10	15491.60	108.20	159.60	94.30	83.20	308.60	193.60
Ni	2217.10	4423.60	70.80	68.40	63.40	64.20	92.30	74.80
Nb	11.51	8.92	12.24	12.60	18.61	13.49	12.07	13.01
Zr	118.85	127.56	188.66	205.74	367.92	186.80	202.43	204.38
Y	25.03	22.79	19.02	30.44	52.64	28.92	30.04	30.36
Sr	278.30	460.04	404.29	401.48	358.13	415.70	390.99	366.92
Rb	31.47	41.17	52.46	51.99	53.52	51.76	56.20	46.62
Co	150.50	253.90	42.20	46.60	46.80	44.20	42.40	41.20
Cr	495.40	53.00	40.00	40.10	29.90	37.60	39.00	34.70
V	237.60	235.10	209.90	217.30	276.60	214.00	208.30	216.70
Ce	50.49	54.85	57.17	58.22	85.12	61.47	54.97	55.69
Nd	27.09	25.69	28.22	29.23	46.73	31.42	29.26	29.65
La	16.68	15.29	21.16	21.60	34.51	21.63	22.20	21.81
Ba	156.50	252.80	347.30	288.70	467.60	352.90	371.30	230.30
Sc	29.10	22.80	23.10	22.90	23.50	22.80	22.30	23.10
Th	3.54	7.01	3.37	3.74	3.30	3.05	3.87	4.34
Pb	4.96	14.94	3.35	4.45	2.30	6.09	4.75	2.75
S	0.00	0.00	1409.72	3043.91	1979.60	1631.02	1985.16	2831.29

Table D-11 (cont) *Whole-rock XRF analyses of borehole SH27, normalised for H2O$^-$ and LOI free.*